UC Berkeley
UC Berkeley Electronic Theses and Dissertations

Title

Forelimb and hindlimb bone growth and development in human infants and children

Permalink

https://escholarship.org/uc/item/5z40f3vg

Author

Taylor, Catherine

Publication Date

2022

Peer reviewed|Thesis/dissertation

eScholarship.org Powered by the California Digital Library
University of California

Forelimb and hindlimb bone growth and development in human infants and children

By

Catherine Elizabeth Taylor

A dissertation submitted in partial satisfaction of the

requirements for the degree of

Doctor of Philosophy

in

Integrative Biology

in the

Graduate Division

of the

University of California, Berkeley

Committee in charge:

Professor Leslea J. Hlusko, Chair
Professor Tim D. White
Professor Z. Jack Tseng

Spring 2022

Forelimb and hindlimb bone growth and development in human infants and children
Copyright © 2022
by
Catherine E. Taylor

Abstract

Forelimb and hindlimb bone growth and development in human infants and children

by

Catherine Elizabeth Taylor

Doctor of Philosophy in Integrative Biology

University of California, Berkeley

Professor Leslea J. Hlusko, Chair

Evolutionary changes in locomotion modify the way an organism interacts with its environment. Changes in locomotion coincide with changes in various other features, including procurement of both food and mates. Beginning roughly 7 million years ago, a major shift in hominid locomotion began, resulting in the obligate bipedality of *Homo sapiens*. Humans today exhibit a unique shift in locomotion throughout ontogeny, from a locomotor form that requires use of an individual's forelimbs and hindlimbs to full bipedality that appears around 1 year of age. To date, it is unclear whether this ontogenetic shift in how infants move originated with the beginnings of hominid bipedality, or began later in evolutionary history. This dissertation offers insight into how growth in human limb bones correlates with ontogenetic shifts in locomotion and provides a framework for understanding the skeletal morphology preserved in the fossil record of human evolution.

This dissertation uses a newly published dataset of medical CT scans of recently deceased humans from the New Mexico Decedent Imaging Database (NMDID) to study long bone growth qualitatively and quantitatively in human infants and children. Results are correlated with relative onset of locomotor development such as crawling, bipedal standing and walking, and development of hand preference.

Each chapter focuses on a different aspect of skeletal growth. Chapter 3 examines intra-element growth and variation by comparing growth rates and patterns of growth at multiple different positions along each long bone diaphysis. Chapter 4 explores inter-element growth by comparing growth at homologous positions on different skeletal elements (e.g., the proximal humerus and the proximal femur). Chapter 5 investigates the development and variation in bilateral asymmetry between paired right and left elements. Each chapter focuses on one broad hypothesis with two or three subsequent questions outlined in each chapter.

Results of Chapter 3 show that there are differences in growth patterns and rates of growth at different positions along the same skeletal elements, but only in the humerus. Results from Chapter 4 show different rates of growth between the humerus and femur at different ontogenetic stages. These changes in growth rates and bone strength broadly correlate with the onset of locomotor developments such as crawling and walking. Results from Chapter 5 indicate that asymmetry in long bone length is present at birth, but does not follow the same pattern of asymmetry as is seen in adults or expected from hand-preference data. As individuals get older, they are more likely to exhibit asymmetries that align with an overall populational right-hand

preference. Asymmetries in the femur are also present at birth, but patters of asymmetry do not change with age to the same extent as the humerus.

This dissertation expands current knowledge of variation in human ontogenetic long bone growth and acts a preliminary study on the growth, development, and variation in growth of human long bones. Future research will focus on increasing sample sizes of human individuals, as well as investigating long bone ontogenetic growth in non-human primates, with the eventual goal of understanding the evolution of crawling throughout human evolution.

I dedicate this dissertation to my grandmothers,

Erzsébet Papp and Dorris Taylor

Table of contents

Dedication....i
Table of Contents....ii
List of Figures and Tables....vi
Acknowledgements....viii

Chapter 1: Introduction and Background....1
1.1 | Introduction....1
1.2 | Fetal Limb Development....1
1.2.1 | Early Embryology....1
1.2.2 | Genetic Patterning....1
1.2.3 | Mineralization....3
1.2.4 | Timing and pattern of limb growth and ossification....4
1.2.5 | Postnatal Limb Development....6
1.2.5.1 | Catch-up growth....6
1.2.5.2 | Growth spurts....6
1.2.5.3 | Hormonal influences....7
1.3 | Biomechanical Influences on Bone Growth....8
1.3.1 | Response mechanisms to loading....8
1.3.2 | Evidence of response to load variation in human infants....9
1.3.3 | Research Methodologies on Bone Growth and Biomechanics....9
1.3.3.1 | Cross-sectional data....10
1.3.3.2 | Computed Tomography (CT) scan data....10
1.3.3.3 | Bilateral asymmetry....11
1.4 | Human Infant Behavior and Cultural Contexts....13
1.5 | Non-Human Primate Limb development....14
1.5.1 | Chimpanzees....14
1.5.2 | Gorillas....15
1.6 | Evolution of Limb Development....16
1.6.1 | Fossil evidence of infants and young children....16
1.6.2 | Growth and development of hominids....18
1.6.2.1 | Prenatal growth....18
1.6.2.2 | Postnatal growth....19
1.7 | Hypotheses and Study Design of this Project....20
1.7.1 | Hypotheses....21

Chapter 2: Materials and methods....23
2.1 | Introduction....23
2.2 | Materials....23
2.2.1 | CT Scans....23
2.3 | Data Collection Methods....23
2.3.1 | Manual measurements....24
2.3.2 | Segmenting bones....24
2.3.3 | Moments of area....24
2.3.4 | Error Calculations....25
2.3.5 | Data analysis....25

Chapter 3: Intra-element growth and development.....29
3.1 | Introduction.....29
3.2 | Materials and Methods.....30
3.2.1 | Materials.....30
3.2.2 | Data Collection Methods.....31
3.2.3 | Analytical Methods.....31
3.3 | Results.....32
3.3.1 | Humerus.....32
3.3.1.1| Length.....32
3.3.1.2 | Diaphyseal circumference.....32
3.3.1.3 | Cortical Area.....32
3.3.1.4 | Medullary Area.....33
3.3.1.5 | Second moments of area.....33
3.3.1.6 | Polar second moments of area.....34
3.3.2 | Femur.....34
3.3.2.1 | Length.....34
3.3.2.2 | Diaphyseal circumference.....34
3.3.2.3 | Cortical area.....35
3.3.2.4 | Medullary Area.....35
3.3.2.5 | Second moments of area.....35
3.3.2.6 | Polar second moments of area.....35
3.4 | Discussion.....36
3.5 | Conclusions.....37

Chapter 4: Inter-element growth and development.....59
4.1 | Introduction.....59
4.2 | Materials and Methods.....60
4.2.1 | Materials.....60
4.2.2 | Data Collection Methods.....60
4.2.3 | Analytical Methods.....61
4.3 | Results.....61
4.3.1 | Length.....61
4.3.2 | Comparison of Proximal Ends of the Humerus and Femur.....61
4.3.2.1 | Diaphyseal circumference.....61
4.3.2.2 | Cortical Area.....62
4.3.2.3 | Medullary Area.....62
4.3.2.4 | Second moments of area.....62
4.3.2.5 | Polar second moments of area.....63
4.3.3 | Comparison of Humeral and Femoral Midshaft.....63
4.3.3.1 | Diaphyseal circumference.....63
4.3.3.2 | Cortical Area.....63
4.3.3.3 | Medullary Area.....63
4.3.3.4 | Second moments of area.....64
4.3.3.5 | Polar second moments of area.....64
4.3.4 | Comparison of Distal Ends of the Humerus and Femur.....64

4.3.4.1 | Diaphyseal circumference....64
4.3.4.2 | Cortical Area....65
4.3.4.3 | Medullary Area....65
4.3.4.4 | Second moments of area....65
4.3.4.5 | Polar second moments of area....65
4.4 | Discussion....66
4.5 | Conclusions....68

Chapter 5: Bilateral Asymmetry....94
5.1 | Introduction....94
5.2 | Materials and Methods....95
5.3 | Results....95
5.3.1 | Clavicle....95
5.3.1.1 | Clavicular Length....95
5.3.1.2 | Clavicular midshaft circumference....96
5.3.1.3 | Clavicular cortical area....96
5.3.2 | Humerus....96
5.3.2.1 | Humeral Length....96
5.3.2.2 | Humeral diaphyseal circumference....96
5.3.2.3 | Humeral cortical area....96
5.3.2.4 | Humeral second moment of area....97
5.3.2.5 | Humeral polar moment of area....97
5.3.3 | Femur....97
5.3.3.1 | Femoral Length....97
5.3.3.2 | Femoral diaphyseal circumference....97
5.3.3.3 | Femoral cortical area....98
5.3.3.4 | Femoral second moment of area....98
5.3.3.5 | Femoral polar moment of area....98
5.4 | Discussion....98
5.5 | Conclusions....99

Chapter 6: Conclusions....112
6.1 | Introduction....112
6.2 | Context....112
6.3 | Chapter 3: Intra-element growth and development....112
6.3.1 | Question 1....112
6.3.2 | Question 2....113
6.3.3 | Question 3....114
6.4 | Chapter 4: Inter-element growth and development....114
6.4.1 | Question 1....114
6.4.2 | Question 2....114
6.5 | Chapter 5: Bilateral Asymmetry....115
6.5.1 | Question 1....115
6.5.2 | Question 2....115
6.6 | Variability throughout ontogeny....116
6.7 | Limitations....116

6.8 | Future directions..... 117
6.9 | Conclusions.....118

References.....122

List of figures and tables

Chapter 2

Figure 2.1....27
Figure 2.2....27
Table 2.1....28
Table 2.2....28

Chapter 3

Figure 3.1....39
Figure 3.2....40
Figure 3.3....41
Figure 3.4....42
Figure 3.5....43
Figure 3.6....44
Figure 3.7....45
Figure 3.8....46
Figure 3.9....47
Figure 3.10....48
Figure 3.11....49
Figure 3.12....50
Figure 3.13....51
Figure 3.14....52
Figure 3.15....53
Figure 3.16....54
Figure 3.17....55
Figure 3.18....56
Figure 3.19....57
Figure 3.20....58

Chapter 4

Figure 4.1....69
Figure 4.2....70
Figure 4.3....71
Figure 4.4....72
Figure 4.5....73
Figure 4.6....74
Figure 4.7....75
Figure 4.8....76
Figure 4.9....77
Figure 4.10....78
Figure 4.11....79
Figure 4.12....80
Figure 4.13....81
Figure 4.14....82

Figure 4.15....83
Figure 4.16....84
Figure 4.17....85
Figure 4.18....86
Figure 4.19....87
Figure 4.20....88
Figure 4.21....89
Figure 4.22....90
Figure 4.23....91
Figure 4.24....92
Figure 4.25....93

Chapter 5

Figure 5.1....100
Figure 5.2....100
Figure 5.3....101
Figure 5.4....101
Figure 5.5....102
Figure 5.6....102
Figure 5.7....103
Figure 5.8....103
Figure 5.9....104
Figure 5.10....104
Figure 5.11....105
Figure 5.12....105
Figure 5.13....106
Figure 5.14....106
Figure 5.15....107
Figure 5.16....107
Figure 5.17....108
Figure 5.18....108
Figure 5.19....109
Figure 5.20....109
Figure 5.21....110
Figure 5.22....110
Figure 5.23....111
Figure 5.24....111

Chapter 6

Figure 6.1....119
Figure 6.2....120
Figure 6.3....121

Appendix 1: List of individuals....148

Acknowledgements

I thank my dissertation committee for their guidance, support, and encouragement throughout this process, as well as for their patience and constructive comments over the last few years. I am profoundly thankful to my advisor, Leslea Hlusko, and her continuous support throughout my graduate career. She has been a steadfast mentor and supporter and is responsible for much of my development as a researcher and as a person. I am also deeply grateful to Tim White, who has helped me hone my skills as a scientist and encouraged me to think critically. I also thank Jack Tseng, who has broadened my analytical mind and provided sound advice and invaluable feedback on my work.

I also thank Tom Carlson and Jun Sunseri for their mentoring throughout my qualifying exam preparation, and for the conversations that helped me discover where my research interests lie. Their positivity and encouragement helped me discover passion for this area of research. I am also deeply thankful to Yohannes Haile-Selassie for the inspiration to pursue this graduate degree and his unwavering mentorship throughout the years. Without Yohannes, I would certainly not be where I am today. I also thank Denise Su, Scott Simpson, and Darin Croft, for providing me with a roadmap to graduate school, and without whom I would never have found passion for research in evolutionary biology.

I thank Heather Edgar and the staff and researchers at the New Mexico Decedent Imaging Database, without whom I would not have data for this dissertation. I am also sincerely grateful to the National Science Foundation for providing funding to support this work (DGE 1752814).

This dissertation exists because of the many conversations had with friends and collaborators over the years. I am especially appreciative of the members of the Hlusko lab and Human Evolution Research Center for the kindness, intellectual stimulation, and deep sense of community they have provided over the years. Marianne Brasil has been an unfaltering collaborator and friend, and has always provided me with productive discussion, advice, and laughs. I also thank Peter Kloess for his kindness and willingness to be a sounding board for research projects, and also for his immense help with CT software and analyses. I thank Joshua Carlson for providing advice and much needed human interaction throughout the isolation of the last two years. I also thank Laura Sánchez-Romero, Tara Lepore, and Tesla Monson for keeping morale high, and I thank Lewis Bartlett for his friendship and analytical help throughout my graduate career.

I attribute the success I have had in my life to my parents, Cyrus and Elizabeth Taylor. I would not be here without their unwavering support and encouragement to follow my passions. My mother has been a constant and uplifting source of motivation. My father has been an incredible and compassionate mentor, always providing sound advice and intellectually rigorous conversation. I am also grateful to my many wonderful friends for supporting me through this journey and helping me slow down and enjoy the little things in life, including Cassie Torrence, Giovanna Figueroa, and Maryam Sedaghatpour. I must also thank Mooshka and Finn, who always help me relax and smile during stressful times. And of course, I am forever grateful to my partner, Mahya Krouse, for the love, support, and grounding that she has given me.

Chapter 1: Introduction and Background

1.1 | Introduction

One of the most distinctive features unique to humans compared to other primates is the way that we use our limbs: from human bipedality, to right-biased hand preference, we also have unique ontogenetic changes in locomotion. Fortunately, evidence of these behaviors is preserved in skeletal morphology.

The modern human skeleton is the product of the intricate amalgamation of embryology, genetics, prenatal development, postnatal growth and senescence, hormone, nutritional, and environmental influences that have all been modified over time by evolutionary forces. To fully understand how the human skeleton responds to changes in locomotion and limb use throughout ontogeny, we first need to understand the underlying mechanisms that form the human skeleton and the forces that act on it throughout an individual's life. This chapter begins with an overview of embryonic bone growth and ossification and its genetic underpinnings, followed by a discussion of postnatal bone growth, bone biomechanics, human infant behavior, non-human primate ontogeny, and the evolution of human ontogeny. This literature review provides the framework of this dissertation research. It concludes with the articulation of 3 hypotheses that will be tested in the subsequent chapters.

1.2 | Fetal Limb Development

The publication of Hippocrates' works in the 5th century BCE titled "On Generation", "Nature of the Child" and "On Bones" constitute the earliest written record of embryological research (Dunn, 1993; Craik, 2008). Throughout the subsequent thousands of years of investigation, each study has brought us closer to understanding the extremely complex series of events that constitute human embryology and skeletal development. What follows is an overview of the current state of the science on fetal limb development, combining evidence from a range of disciplines.

1.2.1 | Early embryology

At the start of the fourth week postfertilization (Carnegie stage 9), the human embryo undergoes the process of neurulation (O'Rahilly & Muller, 2007). The neural plate folds inward to form the neural groove. The lateral margins of the neural groove form the neural crest cells, which eventually detach and migrate into the embryonic mesoderm (Cunningham, Scheuer, & Black, 2016). As the neural plate begins to fold inwards, mesoderm alongside the notochord differentiates into several different types. This lateral plate mesoderm eventually gives rise to elements of the postcranial skeleton and some aspects of the skull (O'Rahilly & Gardner, 1975; Lovejoy, Cohn, and White, 1999; O'Rahilly & Muller, 2007). By the end of the fourth week *in utero*, limb buds are present and visible. The appearance of the upper limb bud usually precedes that of the lower limb bud by 1-2 days (Lewis, 1902; O'Rahilly & Gardner, 1975).

1.2.2 | Genetic patterning

Genetic patterning of skeletal development is a complex field of study, and understanding normal development of the skeleton often requires investigation of skeletal diseases. Through the study of skeletal diseases, researchers have identified several important genes that are essential

for normal skeletal development. Here, I provide a very brief overview of six genes/gene pathways that have major effects on skeletal development.

Cleidocranial dysplasia (CCD) is an autosomal dominant skeletal dysplasia that causes clavicular hypoplasia, skull deformities such as midface hypoplasia and brachycephaly, as well as dental malformations and overall short stature (Cooper et al., 2001; Karagüzel et al., 2010; Pan, Tseng, Lan, & Chang, 2017; Farrow et al., 2018). It has now been determined that CCD is caused by mutations of *CBFA1*/*Runx2* gene, located on the short arm of chromosome 6 (Mundlos et al., 1997; Komori, 2010; Bufalino et al., 2012). This gene encodes a transcription factor that is necessary for normal activation of osteoblast differentiation (Ducy et al., 1997; Komori et al., 1997; Ooki et al., 2020). Researchers have identified single nucleotide polymorphisms (SNPs) in the polyalanine tract of *CBFA1/Runx2* that cause missense or nonsense mutations responsible for one non-functional *CBFA1/Runx2* gene (Mundlos et al., 1997; Lee et al., 1997; Motaei et al., 2021). Additionally, mouse studies have shown that at least one functional copy of the *CBFA1/Runx2* gene is necessary for any bone formation at all, with $CBFA1^{-/-}$ mice showing no bone formation and $CBFA1^{-/+}$ mice exhibiting cleidocranial dysplasia (Otto et al., 1997).

Research on campomelic dysplasia, a lethal skeletal malformation syndrome, has shed light on the important role that the *SOX9* protein coding gene plays in cartilage formation (Lefebvre et al., 1997; Bi et al., 1999; Lefebvre, Angelozzi, & Haseeb, 2019). *SOX9* induces chondrogenic differentiation from mesenchyme and remains expressed in adult chondrocytes in articular cartilage (Lefebvre & Dvir-Ginzberg, 2016). It is also critical for chondrogenesis, and thus directly affects endochondral bone formation. $SOX9^{+/-}$ mice die perinatally and exhibit extreme malformation in skeletal structures formed via cartilaginous precursors (Bi et al., 2001; Song & Park, 2020).

Bone morphogenic proteins (BMPs), a group of signaling molecules belonging to the transforming growth factor-β (TGF-β) superfamily of proteins, are also necessary for normal skeletal patterning and bone formation, and malfunctions of BMPs cause skeletal diseases in humans (Wang et al., 2014). BMPs have diverse functions and are active in many different tissues. They play a complex role in chondrocyte and osteoblast differentiation (Cao & Chen, 2005; Rahman et al., 2015). This group of signaling molecules regulates mesenchymal stem cell differentiation throughout embryogenesis and regulates bone formation and maintenance during postnatal growth (Wu, Chen, & Li, 2016). These molecules are also of vital importance during healing after skeletal injury and are applied in a clinical context to promote bone formation during healing from surgery or bone injury (Wu, Chen, & Li, 2016). Additionally, BMP signaling is a necessary part of mechanosensation and mechanotransduction in bone, because they contribute to bone's resorption or expansion as a result of loading (da Silva Madaleno, Jatzlau, & Knaus, 2020).

Studies on the underlying mechanisms behind other bone diseases have led to further research on the role of the Wnt-signaling pathway, although its exact function(s) in endochondral bone development are not well understood (Mak et al., 2006; Kim et al., 2013; Monroe et al., 2012) Recent studies suggest that Wnt signaling stimulates bone formation in response to mechanical loading (Baron & Rawadi, 2007; Lawson et al., 2022). Disruption of Wnt signaling from a mutation in *CBFA1*/*Runx2* prohibits mesenchymal proliferation at the site of cranial sutures and causes the lack of fusion of cranial vault bones seen in people with cleidocranial dysplasia (Motaei et al., 2021). Disruption of normal Wnt signaling can lead to osteoporosis, sclerosteosis,

and overproduction of bone tissue (Ellwanger et al., 2008; Wang et al., 2014). Abnormal activation of the Wnt pathway also plays a role in carcinogenesis and is often targeted during cancer treatments (Chen et al., 2009; Zhan, Rindtorff, & Boutros, 2017; Zhang & Wang, 2020).

Additionally, the Sonic Hedgehog (*Shh*) signaling pathway is important for limb bud patterning early in development (Yang, Andre, Le, & Yang, 2015). Indian hedgehog (*Ihh*) controls osteoblast differentiation during endochondral ossification by controlling the expression of *CBFA1/Runx2* and is also important in controlling chondrocyte proliferation (St-Jaques, Hammerschmidt, & McMahon, 1999; Karp et al., 2000; Yang et al., 2015).

Additional factors that affect bone formation and resorption include platelet-derived growth factor (PDGF), fibroblast growth factors (FGFs) and insulin-like growth factors (IGF) (Henriksen et al., 2009; Teti, 2011). PDGF is involved in several steps in bone formation, regulates osteogeneisis and is released at bone injury sites to promote fast bone proliferation (Caplan & Correa, 2011; Zhang et al., 2021). The 22 FGFs are involved in bone formation in numerous different ways. For example, FGF 2 mediates osteoblast mineralization, FGF 8 is necessary for normal limb formation, FGF18 regulates autophagy of chondrocytes in the growth plate, and FGF23 regulates bone mineralization by mitigating metabolism of Vitamin D and phosphorous (Wesseling-Perry, 2010; Cinque et al., 2015; Shahi et al., 2017). IGF-1 is necessary for the differentiation of osteoprogenitors and is directly correlated with bone strength (Crane et al., 2013; Crane & Cao, 2014; Locatelli & Bianchi, 2014).

1.2.3 | Mineralization

I will refer to endochondral bone growth as derived from lateral plate mesoderm and intramembranous bone growth as derived from neural crest cells. While this is an overgeneralization (Matsuoka et al., 2005), the division is sufficient for the purposes of my discussion here.

The skeleton comprises of two main tissues – cartilage, and bone. Chondrocytes, the cells that form cartilage, are mesodermal in origin and derive from a multipotent embryonic progenitor cell type called an osteochondroprogenitor (Karsenty & Wagner, 2002; Karsenty, 2003). Each chondrocyte cell is isolated from nearby cells within an extracellular matrix lacking innervation and vascularization (Archer & Francis-West, 2003). Cartilage is an important tissue in both the fetal and immature organism, where it acts as a template for bone growth, and in the adult, where it is necessary for the normal function of joints, allows for smooth articulation of skeletal elements, and provides support for structures like the trachea and external ear (Archer & Francis-West, 2003; Cunningham, Scheuer, & Black, 2016). Chondrocyte differentiation is largely stimulated by bone morphogenic proteins (BMPs) which are also necessary for other aspects of skeletal development (Long & Ornitz, 2013).

Bone comprises 90% collagen (organic protein) and 10% hydroxyapatite, a dense, inorganic form of calcium phosphate (White, Black, & Folkens, 2012). Bone tissue is made of up three different types of cells –osteoblasts, osteocytes, and osteoclasts (White et al., 2012). Like chondrocytes, osteoblasts derive from embryonic osteochondroprogenitor cells. Osteoblasts are bone-forming cells that deposit osteoid, an unmineralized pre-bone matrix that can become mineralized to form bone. Osteocytes are essentially osteoblasts that have been embedded in bone matrix, although the exact mechanisms of the differentiation of osteocytes are still poorly

understood (Dallas, Prideaux, & Bonewald, 2013; Franz-Odendaal, Hall, & Witten, 2005; Bonewald 2010).

Roughly 10-20% of osteoblasts will differentiate into osteocytes (Aubin & Turksen, 1996). These immobilized cells imbedded in bony matrix compose up to 95% of bone cells in adult humans, and each osteocyte can live for decades (Bonewald, 2010). Osteocytes, surrounded by their bony matrix, are housed in small cavities called lacunae, connected to each other by tiny fluid filled channels known as canaliculi. The arrangement of lacunae and canaliculi into concentric circles of lamellar bone with a blood vessel in the center are known as haversian systems (White et al., 2016). Osteocytes also serve an important role in controlling osteoblastic bone deposition and osteoclastic bone resorption (Bonewald, 2010; Noble, 2008; Bellido, 2014, Klein-Nulend & Bonewald, 2020).

Osteoclasts are multi-nucleated, tissue-specific macrophages that are responsible for bone resorption (Boyle, Simonet, & Lacey, 2003; Väänänen, Zhao, Mulari, & Halleen, 2000). They differentiate from embryonic hematopoietic stem cells and are similar to other types of macrophage cells (Boyle et al., 2003; Noble, 2008). Adult bone is constantly remodeling, and about 10% of adult bone content is replaced annually (Alliston & Derynck, 2002). The cytokine receptor activator of nuclear factor kappa B ligand (RANKL) is necessary for normal formation and function of osteoclasts, and is primarily produced in osteocytes (Boyle, Simonet, & Lacey, 2003; Väänänen et al., 2000; Bellido, 2014; Xiong et al., 2015). Osteocytes also secrete osteoprotegerin (OPG), a cytokine receptor that prevents the binding of RANKL on osteoclasts and thus inhibits bone resorption (Pneumaticos et al., 2013).

1.2.4 | Timing and pattern of limb growth and ossification

There are two distinct ways that bone grows: endochondral ossification and intramembranous ossification. Intramembranous ossification occurs when osteoblasts develop directly from mesenchymal cells, with no cartilaginous precursor. This can occur in two different ways – dermally, as in cranial bones and the lateral clavicle, and periosteally. Periosteum is a tissue on the surface of every bone, and is developed intramembranously even in long bones where the rest of the bone develops through endochondral ossification (Cunningham et al., 2016). In endochondral bone development, which is responsible for longitudinal growth of long bones, a cartilaginous pre-bone scaffolding is eventually replaced by bone. Mesenchyme from the lateral plate mesoderm condense into individual elements between the 5^{th} and 7^{th} weeks *in utero* (Provot & Schipani, 2004; Burr & Organ, 2017). Proliferating chondrocytes in the center of the cartilage analgen trigger a mesenchymal condensation on the perimeter of the analgen that forms the perichondrium (Burr & Organ, 2017).

During the 8^{th} week in utero, the analgen undergoes vascularization, which supports the differentiation of osteoblasts and the beginnings of ossification. Ossification begins at the nutrient artery and extends in both directions of what will eventually become the diaphysis (Bruder & Caplan, 1989; Reddi, 1981). Cartilage continues to ossify through a process of apposition and resorption that occurs at a growth plate. At growth plates, chondrocytes continue to proliferate and are gradually replaced by osteoblasts (Cunningham et al., 2016). Eventually, as skeletal growth ceases, the terminal plate is formed and trabeculae of the diaphysis and epiphysis fuse to form a complete element (Weinmann & Sicher, 1947). Woven bone, or immature bone, forms rapidly and has much less structural integrity than lamellar, or adult bone (Turner,

Forwood, Rho, & Yoshikawa, 1994; Hernandez, Majeska, & Schaffler, 2004). Woven bone mostly forms during embryonic growth, but is also formed at fracture sites, and contains a higher concentration of osteocytes than lamellar bone (White et al., 2016).

The clavicle develops from two ossification centers that have different embryonic origins (Matsuoka et al., 2005). The lateral clavicle originates from the embryonic neural crest and develops via intramembranous ossification, whereas the medial clavicle originates from embryonic mesoderm and ossifies endochondrally (Ogata & Uhthoff, 1990). While most endochondral bones develop from cartilage formed by primary chondrocytes (deriving from embryonic mesoderm), clavicular chondrocytes also arise from the periosteum and may be able to respond to mechanical stimuli (Hall & Miyake, 2000). In the 6th week of gestation (stage 17), membranous ossification begins at both ends of the fetal clavicle. By 7 weeks, the two ends fuse, and the bone forms its classic sinusoidal shape by the end of the 8th week (Gardner, 1968; Ogata & Uhthoff, 1990).

Humeral mesenchyme is visible by stage 16 (~5 weeks of gestation), and chondrification begins by the 6th week in utero. The bony collar forms around the cartilaginous diaphysis by week 8, followed by the appearance of the diaphyseal ossification center and vascular nutrient foramen by week 10 (O'Rahilly & Gardner, 1975). The proximal epiphysis usually comprises three separate ossification centers (one for the humeral head, greater trochanter, and usually the lesser tubercle). Carnegie stages are often used to refer to stages of embryonic development based on external features (numbered 1 to 23; DiCaglio, 2017). At Carnegie stage 16 (37-40 days postfertilization), the chondrogenic anlage of the humeral head can be seen in serial dissections, and begins ossification around or shortly after birth (Cunningham et al., 2016; Hita-Contreras et al., 2017). The other two ossification centers that contribute to the proximal epiphysis vary considerably in their timing of appearance, from ~3 months to 3 years postpartum, and timing of the coalescence of the separate ossification centers is not well established (Cunningham et al., 2016). The distal epiphysis forms from four separate centers (one each for the capitulum, medial epicondyle, trochlea, and lateral epicondyle), the first three of which fuse together just before fusing to the diaphysis. The capitular ossification center appears within the first year or so of life, and the others begin to appear around ages 8-10. The lateral epicondyle remains unfused until later. The fusion of epiphyses to the diaphysis varies considerably. The proximal epiphysis fuses between ages 14-19 in females and 16-21 in males, while the distal epiphysis (including the lateral epicondyle) fuses between the ages of 11-15 in females and 14-18 in males (Cunningham et al., 2016).

Femoral chondrification in the embryo begins a few days later than that of the humerus, usually at Carnegie stage 17 (end of the 5th week), following the delayed appearance of the hind limb bud by about 2 days earlier in development (Lewis, 1902; O'Rahilly & Gardner, 1975). The bony collar around the cartilaginous diaphysis is visible by ~8 weeks post-conception. The proximal epiphysis of the femur consists of multiple (and somewhat variable) centers of ossification. The femoral head is the first to condense from the mesenchyme in the months after birth, and appears in female infants roughly two months before male infants (Garn, Rohmann, Wagner, & Ascoli, 1967). The greater trochanter and lesser trochanter grow from their own ossification centers, which are highly variable in timing of appearance and fusion (Cunningham et al., 2016). Some individuals exhibit a fourth proximal femoral growth center at the proximal end of the gluteal ridge (Dixon, 1896). The distal femoral ossification center is large and is often considered the fastest growing epiphysis in the human body (Cunningham et al, 2016). This

ossification center is present before birth (Gardner & Gray, 1970) and is responsible for about 66% of the total longitudinal growth of the femur (Sissons & Kember, 1977).

Maternal biology can impact fetal and infant growth in many ways. Vitamin D and calcium are both necessary nutrients for normal skeletal growth. Mothers deficient in vitamin D are more likely to give birth to infants who will be born with or develop rickets or osteomalacia, among a plethora of other developmental abnormalities (Weinert & Silveiro, 2015; Fiscaletti, Stewart, & Munns, 2017). Maternal stress, and its timing, can affect an offspring's birthweight and rates of bone formation (Amugongo & Hlusko, 2014). Postnatally, early cessation of breastfeeding without providing a formula alternative can cause impairment of osteogenesis in rats (Albuquerque Maia et al., 2013).

1.2.5 | Postnatal Limb Development

Human infants are born with a partially ossified, partially cartilaginous skeleton. During post-natal skeletal growth, the skeleton is susceptible to the influences of many endogenous and exogenous factors, some of which can affect an individual's adult bone morphology (Gluckman & Hanson, 2006; Javaid et al., 2006). Although some bones begin developing as early as six weeks post-fertilization, much of fetal bone growth occurs during the third trimester (Namgung & Tsang, 2003). In this section, I focus on postnatal limb growth but need to begin by characterizing growth across the timing of birth.

1.2.5.1 | Catch-up growth. Infants who are born prematurely are susceptible to osteopenia of prematurity, a metabolic bone disease that is caused by the early removal of maternal nutrient supply as well as lack of biomechanical loading due to immobilization of pre-term infants in the hospital (Bozetti & Tagliabue, 2009; Harrison & Gibson, 2013; Rehman & Narchi, 2015). Overall, the lack of normal loading results in a failure or malfunction of the ossification process, and can cause premature ossification and decreased cortical thickness and cortical area (Rodriguez et al., 1988).

Several studies show that there is a strong relationship between infant/childhood height, weight, and activity patterns and adult bone strength and bone mineral content (e.g. Cooper et al., 1995; Javaid & Cooper, 2002; Cooper et al., 2005; Gluckman et al., 2008). Longitudinal studies have concluded that infants who were small at birth reach pubertal milestones, including the pubertal growth spurt, earlier on average than infants that were an average weight at birth (Hvidt, Brix, Earnst, Lauridsen, & Ramlau-Hansen, 2019).

1.2.5.2 | Growth spurts. Human infant and childhood growth is nonlinear growth velocities oscillate throughout infancy and childhood (Lampl, 1993; Thalange et al., 1996; Hermanussen, 1998; Caino et al., 2010; Lejarraga, 2002). Growth spurts are a period of increased growth velocity throughout infancy, childhood, and adolescence. Several growth spurts of various magnitudes have been described. Infants grow relatively fast during the first year of life (Lejarraga, 2002). The infancy-childhood growth spurt is a period of increased growth velocity that typically ceases by 3 years (Karlberg, 1990). Some children also experience a preadolescent growth spurt between 6.5 and 8 years of age (Molnari, Largo, & Prager, 1980; Dandurand & Shultz, 2010). Data from the Edinburgh Longitudinal Growth Study and the Fels Longitudinal study suggest the presence of up to four prepubertal growth spurts (Butler, McKie, & Ratcliffe, 1990;

Bock, 2003). Individual variation in number of growth spurts and growth velocity is considerable and influenced by a number of variables such as nutritional status, hormonal influences, and environmental factors, among others (Bock, 2003). The pubertal, or adolescent growth spurt is the most well-studied, as it coincides with the beginnings of skeletal maturation and sexual development. The adolescent growth spurt is a period of markedly increased growth rate, which also correlated with sexual maturation (including menarche in females and spermarche in males) as well as the beginning of skeletal maturation (Brown & Grave, 1976; Taranger & Hägg, 1980; Hägg & Taranger, 1982).

1.2.5.3 | Hormonal influences. Throughout childhood and adolescence, there are numerous hormones that influence skeletal growth and the timing of growth spurts. The relationship between timing of pubertal onset and adult height in normally maturing children is not settled. Some research shows that timing of pubertal onset does not have any effect on adult height (Marshall & Tanner, 1986; Vizmanos et al., 2001), whereas others have established a correlation between earlier onset of puberty and shorter adult stature (Bourguignon, 1988; Tanaka et al., 1998; Karlberg et al., 2003; Limony, Koziel, & Friger, 2015). The importance of estrogen in normal skeletal development is well established (Cutler, 1997). Research on individuals with complete androgen insensitivity syndrome (CAIS) shows that XY individuals with androgen insensitivity exhibit a normal growth spurt, and those with partial androgen insensitivity syndrome (PAIS) and CAIS grow taller than average females but not as tall as average males (Danilovic et al., 2007). The difference in height suggests that androgen has some effect on achieving taller height in males, but there is likely to be an additional effect from genes on the Y chromosome (Zachmann et al., 1986).

Males with various types of estrogen insensitivity exhibit abnormal skeletal growth, and have a bone age of 14 or 15 well into adulthood. The growth plates on their long bones do not fuse appropriately, and thus these individuals continue to grow throughout adulthood and often attain heights of well over 6’6” (Frank, 2003). Females tend to start and end their pubertal growth spurt on average 2 years earlier than males, and thus reach skeletal maturity before males of the same age. In a male/female co-twin study, Iuliano-Burns et al. (2009) suggested that the taller average height of males is likely due to their elongated period of skeletal growth, influenced in part by the later onset of male puberty and adrenarche. They also found that pre-pubescent males had slightly thicker diaphyses than their female twins by about 4-7% (Iuliano-Burns, et al., 2009). Additionally, females with aromatase deficiency (resulting an in an inability to synthesize endogenous estrogens) do not exhibit any growth spurts and have a bone age roughly ~4 years younger than their actual age (Jones et al., 2007).

1.2.5.3 | Hormonal influences. Data from the Fels Longitudinal study show that timing of epiphyseal fusion has been decreasing over the last century (Boeyer et al., 2018). This coincides with the decreasing age at menarche in populations around the world (e.g., Harris, Prior, & Koehoorn, 2008; Cho et al., 2010; Sohn, 2015; Márvan et al., 2016). These are likely caused by a combination of better infant and childhood nutrition, fewer severe childhood illnesses, and increased access to regular visits with a medical professional. Exposure to exogenous estrogens and hormone mimics through diet or

environment may also play a role in earlier growth plate fusion (Weise et al., 2001; Boeyer et al., 2018).

1.3 | Biomechanical Influences on Bone Growth

The influence of biomechanical loading on bone morphology is the topic of much debate. While correlations between increased loading and increased bone strength have been established, partially with the aid of *in-vivo* experiments on mice and rats, the mechanisms behind bone response to mechanical loading are not well understood (Raab-Cullen, Akhter, Kimmel, & Recker, 1994; Forwood, Owan, Takano, & Turner, 1996; Akhter et al., 1998; Cullen, Smith, & Akhter, 2000; De Souza et al., 2005; Sugiyama, Price, & Lanyon, 2010). The concept of bone adapting to mechanical loads by altering rates of osteoblastic bone formation and osteoclastic bone resorption is known as "Wolff's Law", although Wolff (1892) originally established this as an explanation for orientation of trabeculae. Bones experience a variety of mechanical forces, including the pull from muscles and external forces like gravity (Currey, 2012). Typically, there are several types of mechanical loads that act upon a bone: 1) axial compression, like the force of gravity, 2) bending, 3) twisting, and 4) shear and can be either compressive or tensile. In order for a bone to function, it needs to be strong enough and pliable enough to resist the forces of mechanical loading without failing. In the paragraphs below, I provide an overview of the current understanding about how bone responds to mechanical loading and the research related to bone loading and growth.

1.3.1 | Response mechanisms to loading

Osteocytes are believed to be a mechanosensor responsible for sensing mechanical load and regulating osteoblastic and osteoclastic activity in response to mechanical loads (Cowin et al., 1991; Forwood, Kelly, & Worth, 1998; You, Weinbaum, Cowin, & Schaffler, 2004; Yavropoulou & Yovos, 2016). Osteocytes, trapped in their three-dimensional network of immobilized cells, are restricted in their motion and thus dependent on other molecules for cell signaling. The complex network of fluid-filled lacunae and canaliculi are likely responsible for some portion of osteocyte response to loading. The fluid within these tiny channels moves during loading and transports metabolites and signaling molecules to and from osteocytes (Lewis et al., 2017; Klein-Nulend & Bonewald, 2020).

Osteocytes also produce intra-cellular calcium (Ca^{2+}) that is used in signaling, the magnitude and duration of which responds to magnitude and duration of mechanical loading (Pearson & Lieberman, 2004; Lewis et al., 2017). The *Sost* gene, which encodes the protein Sclerostin (an inhibitor of bone formation) is found exclusively in osteocytes and has been demonstrated to exhibit reduced expression during mechanical loading in living rats, as well as increased expression that is correlated with loss of bone during periods of disuse (Robling et al., 2006; Galea, Lanyon, & Price, 2017; Uda, Azab, Sun, Shi, & Pajevic, 2017). Osteoclasts are also known to increase resorption in areas of the bone where osteocytes are underloaded, while osteoblasts are recruited to increase bone formation in regions where osteocytes are sufficiently loaded (Smit & Burger, 2000). Essentially, as bone undergoes loading, the bone responds by adding or redistributing bone (Kimura & Takahashi, 1982; Ruff & Hayes, 1982; Ruff and Hayes, 1983; Pearson & Lieberman, 2004; Cowgill, 2010; Yavropoulou & Yovos, 2016).

1.3.2 | Evidence of response to load variation in human infants

Although the mechanisms for bone's response to loading are not yet fully understood, the effect of mechanical loading on skeletal elements is well documented. Human infants have similar humeral:femoral strength proportions to quadrupedal baboons prior to the onset of bipedal walking (Ruff, 2003a). Preterm infants who are immobilized are at risk of low bone mineral density and reduced bone strength (Moyer-Mileur et al., 2000), and spontaneous activity of limbs is important for normal bone mineralization and strength (Eliakim et al., 2002).

Furthermore, inducing physical activity in infants with very low birth weights and preterm infants results in an increase in bone strength (Litmanovitz et al., 2003; Chen et al., 2010; Litmanovitz et al. 2016). Individuals who had decreased fetal movement are more likely to experience bone fractures as infants, suggesting that decreased biomechanical loading on the fetal skeleton may impact a bone's second moments of area and polar second moments of area (Miller, 2005). Ruff (2003b) found a rapid increase in polar section moduli in the humeri of individuals 6 months to one year old. It has also been established that certain types of exercise can increase bone strength and induce osteogenesis (Turner & Robling 2005; Boreham & McKay, 2011). There is also evidence that femoral neck trabeculae exhibit adaptation to the onset of walking by reorganizing and depositing bone in the medial femoral neck, which is heavily loaded during typical walking (Milovanovic et al., 2017). Studies on macaques show that locomotor changes in ontogeny are reflected in ontogeny of the musculoskeletal system (Turnquist & Wells, 1994).

1.3.3 | Research Methodologies on Bone Growth and Biomechanics

Research on skeletal growth and biomechanics has utilized numerous different methodologies across taxa. Early research relied heavily on destructive methods like sectioning to visualize internal structured of bones (Brash, 1934; Thigpen, 1941; Olsen & Whitmore, 1944). As technology improved, radiography became a prominent method of visualizing the internal structure of bones to study biomechanics and growth (Garn et al., 1967; Alexander & Vernon, 1975). While less destructive than physically sectioning bones for cross-sectional investigations, radiography may distort bone images (O'Neill & Ruff, 2004). However, x-ray radiography is often not suitable for dense, highly mineralized fossil material (DeBeer, Prevec, Cisnaros, & Abdala, 2006). Before micro-CT scanners became more widely available, x-rays and low-resolution CT scans were both used in tandem (Runestad et al., 1993). Today, many researchers are using the non-destructive micro-CT approach to produce scans of impressive resolution that works well on fossils and very small bony structures (eg. Lovejoy, Suwa, Spurlock, Asfaw, & White, 2009; Kono, Zhang, Jin, Takai, & Suwa, 2014; Tseng & Flynn, 2015; de León et al., 2018; Prybyla, Tseng, & Flynn, 2018; Morimoto et al., 2020).

Inferences made about activity patterns and biomechanical loading have relied on measurements of diaphyseal circumference, cortical thickness, cortical area, etc. Measurements of cortical area can provide insight into a bone's resistance to axial loading (Levenston, Beaupre, & Van Der Meulen, 1994; Trinkaus & Ruff, 1999). While it does not necessarily reflect overall bone strength, relative cortical area or relative medullary cavity size can be used as an indication of robusticity and periosteal/endosteal bone formation or resorption. Periosteal bone expansion decreases drastically after skeletal maturity, so individuals who experience more mechanical loading in adulthood are able to increase bone strength only by adding bone or reducing bone

resorption endosteally, resulting in a smaller overall increase in bone strength than if the bone was deposited periostially (Schoenau, Neu, Rauch, & Manz, 2001; Bass et al., 2002; Pearson & Lieberman, 2004). In general, thicker cortices are correlated with higher body mass and relatively more or higher mechanical loading, smaller medullary cavities are associated with higher loading and more overall bone strength throughout infancy and childhood until skeletal maturity.

1.3.3.1 | Cross-sectional data. Although simple measurements of cortical thickness, medullary cavity size, cross sectional area, and/or cross-sectional shape can be moderately useful and have been frequently utilized in past studies, more recent investigations of bone strength rely on second moments of area (SMA) usually denoted by I_x, I_y, or I_{xy}. If, for example, we take x and y as coordinates in a plane transverse to the axis of a long bone and perpendicular to each other, then

$$I_x = \int\int x^2 dA,$$

$$I_y = \int\int y^2 dA,$$

$$I_{xy} = \int\int xy\, dA,$$

where in each case the integral is over the region where there is bone. While these moments are defined with respect to a particular choice of direction for the x axis (and hence also for the y axis, which is perpendicular to the x axis, which is done automatically based on axes during scanning by the Dragonfly software), one can always rotate the axes so that I_{xy} vanishes. This defines the principal axes; the two remaining area moments will take on the maximum and minimum possible values, I_{max} and I_{min}. These values are not dependent on the orientation of a bone in the CT scanner, but rather on the distribution of bone around the central point. I_{max} and I_{min} are essentially measuring the bone's resistance to bending at that particular point along the diaphysis. Also of interest is the polar moment of area, denoted by J and defined by

$$J = \int\int r^2\, dA$$

where the integral is again taken over the area where there is bone. Since $r^2 = x^2 + y^2$,

$$J = I_x + I_y.$$

Thus, J is measuring the bone's resistance to torsion at a specific slice along the diaphysis.

In practice, these values are calculated by taking a 2-dimensional image of bone in a plane transverse to the long axis of a bone and dividing the cortical area into small uniform squares (in this case pixels) of area $\Delta A = \Delta x\, \Delta y$, where $\Delta x = \Delta y$ = the length of a sides of the pixel. The coordinates of each pixel are calculated as the distance in the x- and y- directions from the center of the pixel to the origin, or the center of the medullary cavity. SMA calculations are often simplified in bone literature to the following:

$$\mathrm{I} = \int_{-y_{max}}^{+y_{max}} y^2\, dA$$

A = area

y = perpendicular distance to an axis through the centroid

Polar second moments of area are calculated as the sum of two perpendicular measurements (ie. $I_{max} + I_{min}$).

1.3.3.2 | Computed Tomography (CT) scan data. Medical CT scanners, invented in 1971, have revolutionized many scientific fields (Bhattacharyya, 2016). The ability to visualize the interior morphology of a bone without creating a physical section has opened the door for minimally invasive research on the inner mechanisms of bone and soft tissue. By the 1980's, the first micron-level CT scanner had been developed. While much lower resolution, medical CT scanners are more widely available, less time consuming to use, and safe to use on living organisms (McCollough, Bushberg, Fletcher, & Eckel, 2015).

The application of medical CT scans in investigating bone properties is well established (Kaneko et al., 2003; van Eijnatten et al., 2017). Due to the number of CT analysis software programs and the lack of standardization for analyzing CT scans, there are numerous ways to accomplish the same task when working with CT scans (e.g., DeVries et al., 2008; Gassman, Nicole, Kiran, Austin, & Nicole, 2008; Rathnayaka, Sahama, Scheutz, & Schmutz, 2010; van Eijnatten et al., 2017). Segmentation is the process of isolating the desired object (in this case, a single bone) from the scan as a whole. To separate a region of interest (ROI) from the rest of a scan, various segmentation methods may be employed, including manual thresholding, intensity thresholding, edge detection, and a plethora of automated techniques.

Each method has its own set of pros and cons. Manual thresholding can have higher inter- and intra-observer error, but is useful for segmenting bones from individuals of different ages with varying bone densities (Argüello, Acevedo, & Gonzáles-Estrada, 2019). Intensity thresholding uses a single threshold level for segmentation of a region, and does not work well for the segmentation of whole elements or elements from different anatomical regions (Rathnayaka et al., 2011). Edge detection is fast and highly repeatable, but may mistakenly include artefacts or find edges where they shouldn't be (Testi, Zannoni, Cappello, & Viceonti, 2001). Many non-manual techniques also require some form of manual segmentation to bridge gaps or remove artifacts. Even with manual segmentation, sub-voxel accuracy is possible, though special care should be taken when working with cortical bone less than 1mm thick (DeVries et al., 2008; Rathnayaka et al., 2010; Treece et al., 2010; Nauer et al., 2011).

1.3.3.3 | Bilateral asymmetry. Bilateral asymmetries are very common in the human body. Everything from the placement of organs, development of muscles and limbs, and brain morphology have some asymmetry. Thus, it is not surprising that asymmetries appear in the skeleton as well. *In utero*, bilateral asymmetries in brain development, gene transcription, and cortical folding are common (Wada, Clarke, & Hamm, 1975; Chi, Dooling, & Gilles, 1977; Hering-Hanit, Achiron, Lipitz, & Achiron, 2001; Sun et al., 2005; Kasprian et al., 2011). Humans also exhibit lateralized behavior, with the majority of modern humans favoring their right hand for manual tasks over their left. Lateralized behavior in fetuses can be observed as early as 12 weeks, and right-dominant arm movements occur at rates similar to adults (McCartney & Hepper, 1999).

Fetuses have been observed preferring to suck one thumb over the other *in utero*, which is apparently related to postnatal hand preference (DeVries et al., 2001; Hepper, Wells, & Lynch, 2005; Boschetto et al., 2010; Hepper, 2013). Newborn infants often show a bias in head orientation and limb motion (Churchill, Igna, & Senf, 1962; Goodwin & Michel, 1981; Trevarthen, 1996). Some infants also have stronger arm and hand reflexes on one side than the other, although this may be dependent on which limb they can see better (Grattan, De Vos, Levy, & McClintock, 1992; Tan & Tan, 1999; Ocklenberg et al., 2010).

Studies on bilateral asymmetries of bone properties in athletes of lateralized sports, like tennis, opened the study of skeletal bilateral asymmetries to inferences about activity. In tennis players, bone strength and muscle size are larger in the primary racket arm (Ducher et al., 2004; Ducher et al., 2011; Ireland et al., 2014; Chapelle et al., 2021). Pre-pubertal tennis players showed less asymmetry than pubertal players, suggesting that the pubertal spurt in bone growth plays a role in the development of asymmetry in these athletes (Palaiothodorou, Antoniou, & Bagenas, 2020). Asymmetries are not affected by length of playing time, but there are significant correlations between age at which the individual started playing and magnitude of bilateral asymmetry (Ruff, Walker, & Trinkaus, 1994).

The scientific interest in the underlying reasons for hand preference in modern humans stems from the observation that up to 90% of individuals prefer to use their right hand for complex tasks (Cashmore, Uomini, & Chapelain, 2008; McManus, 2019;). While there is some geographic variation in hand preference, cross-cultural studies show that right hand dominance during complex tasks is seen in 75-95% of people regardless of geographic ancestry or culture (Raymond & Pontier, 2004; Cavanagh, Berbesque, Wood, & Merlowe, 2016). Many invertebrates and non-human vertebrates exhibit some lateralization in limb preference as well, though the magnitude of their lateralization seems smaller (Frasnelli, Vallortigara, & Rogers, 2012; Güntürkün & Ströckens, 2020). Although individual great apes exhibit lateralization in hand preference during complex tasks, their preference often varies depending on the task and they do not show the same species-wide hand preference that is seen in humans (McGrew & Marchant, 1997). Hypotheses on the evolutionary forces driving a right-bias in human hand preference have variously suggested that the trait evolved with tool-use (Cavanagh et al., 2016), language (Corballis, 2003; Cashmore et al., 2008), or even bipedality (Osborn & Homberger, 2015).

Biomechanical forces acting upon muscle and bone in repetitive, lateralized behaviors causes increased loading on one limb over the other and produces bilateral asymmetries in bone (Mays, Steele, & Ford, 1999; Lazenby, 2002; Auerbach & Raxter, 2008). Bilateral asymmetries in the element length, cortical thickness, bone strength, etc. are of particular interest to researchers trying to understand the activities of past populations. Right-biased upper limb asymmetries have been found in the limbs of Holocene humans, with pre-industrial groups exhibiting more asymmetry than industrial groups, as well as more dimorphism in asymmetry (Auerbach & Ruff, 2006). Asymmetries have often been used to estimate activity patterns and hand preference in archaeological populations (eg. Ruff & Jones, 1981; Trinkaus, Churchill, & Ruff, 1994 Mays, 2002; Stock & Pfeiffer,

2004; Wescott & Cunningham, 2006; Maggiano et al., 2008; Battles, 2009; Cashmore & Zakrzewski, 2009). Investigations of paleo-hand preference have also examined stone tool morphology to determine which hand was the dominant hand during knapping (Toth, 1985; Westergaard & Suomi, 1996; Cashmore, Uomini, & Chapelain, 2008; Uomini & Ruck, 2018, but see Pickering & Hensley-Marschand, 2008 for critique of some methods). Striations on incisors are also often used to interpret hand preference in hominids and archaeological populations (e.g. Bermúdez de Castro, Bromage, & Fernandez-Jalvo, 1988; Lozano-Ruiz, Bermúdez de Castro, Carbonell, & Arsuaga, 2008; Uomini, 2011; Volpato et al., 2012; Lozano-Ruiz et al., 2017).

Several studies have interpreted evidence from tool use, skeletal asymmetry, and scratches on teeth to suggest that Neanderthals and *Homo heidelbergensis* exhibited a right-dominant hand preference similar to that seen in humans today (eg., Bermúdez de Castro, Bromage, & Fernandez-Jalvo, 1988; Lozano-Ruiz et al., 2008; Cashmore et al., 2008; Lozano et al., 2009; Frayer et al., 2012; Uomini, 2011; Volpato et al., 2012; Estalrrich & Rosas, 2013). An investigation of flaking patterns consistent with right-hand dominance places the origins of handedness in human evolution at 1.4 to 1.9 Ma (Toth, 1985), while preserved lateralized striations on the incisors of OH 65 suggest that right-handedness was present in at least one individual by 1.8 Ma (Frayer et al., 2016).

1.4 | Human Infant Behavior and Cultural Contexts

Infant development is often tracked in developmental milestones. At birth, human infants are usually alert, and most are capable of following people or objects with their eyes. They also have several adaptive reflexes, including the moro (startle) reflex, stepping reflex, grasping reflex, rooting reflex, and sucking reflex. The grasp reflex and moro reflex are both present by 25 weeks post-conception and can be observed in fetuses as well as pre-term infants, whereas the stepping reflex is not present until 29 to 32 weeks post-conception (Allen & Capute, 1986). Prior to the development of whatever initial mode of locomotion a baby uses, all typical infants are doing relatively the same things with their limbs. At birth, neonates typically have the ability to move their limbs and grasp objects with their hands. Regardless of cultural background, the grasping reflex and purposeful movement of an infant's arms are typical among newborns (van der Meer, van der Weel, & Lee, 1995; Futagi, Toribe, & Suzuki, 2012). There are two types of reflexes found in human infants: postural reflexes (righting reflex, tonic neck reflex) and primitive reflexes (rooting reflex, sucking reflex). Primitive reflexes are present at birth and decrease in frequency and magnitude after about 3 months, whereas postural reflexes begin to emerge at around 3 months (Malina, 2004). The stepping reflex, while not functional for locomotion, are important for the infant's motor development (Forssberg, 1985). Infants who are placed in a sling to be easily carried may use their postural reflexes to reposition themselves to more comfortable positions or grasp onto their mother's clothing while nursing (Goldberg, 1972).

Infant care varies widely around the world. While many cultural anthropological and historical studies on infant motor and locomotor development group individuals based on perceived race, they often overlook other, perhaps more important variables such as culture and socioeconomic status (Kuchirko & Tamis-LeMonda, 2019). For example, in Hopi culture, a cradleboard has been often used to restrain infants for up to 14 months, although there is no correlation with duration of cradleboard use and onset of walking (Dennis & Dennis, 1991). On the opposite end of the spectrum, some mothers in Uganda actively encourage their infants to sit as early as three

months of age by propping them up (Ainsworth, 1967). Ugandan infants in one study spent significantly less time on their backs than American infants, which may contribute to their earlier onset of crawling and walking (Cintas, 1989). Jamaican mothers expect their infants to sit, crawl, and walk earlier than their English or Indian counterparts, which was reflected in their infant's behavior (Hopkins & Westra, 1990). This suggests that mothers who encourage sitting, crawling, and walking have offspring who reach those developmental milestones earlier on average than mothers who actively discourage such behavior.

In a cross-cultural study of 5-month-old babies sitting, mothers in the United States, South Korea, Argentina, and Italy would not leave their babies unattended while sitting independently, while mothers from Cameroon and Kenya were more likely to do so. The infants who were briefly left unattended were more likely to sit independently for longer periods of time – although the mother's willingness to briefly leave them unattended may reflect their knowledge that their infants would be able to sit unattended without falling (Karasik et al., 2015). Cultures that do not encourage crawling show large proportions of infants that skip crawling altogether (Hopkins & Westra, 1989). Overall, infants that are encouraged to move in some fashion tend to hone their motor skills earlier than infants that are actively restricted (Karasik et al., 2010).

Most human babies employ some form of pre-walking locomotion such as crawling, scooting, or rolling (Robson, 1970; Robson, 1984; Largo et al., 1985; Bottos et al., 1989; Fox, Palmer, & Davies, 2002; Patrick, Noah, & Yang, 2012). About 85% of infants utilize a "hands and knees" crawling strategy prior to the onset of walking (Robson, 1984; Størvold, Aarethun, & Bratberg, 2013). Pre-walking, intermediate forms of locomotion are highly variable, and the time of onset often has a cultural component to it (Super, 1976; Hopkins & Westra, 1989; Adolph, Vereijken, & Denny, 1998; Karasik et al., 2015;). For example, infants growing up in urban China begin crawling and walking 6-8 weeks after their American counterparts, on average (Chen et al., 1998; Jia, Zhang, Trindade, & Sobko, 2013; Zhang, Li, Wu, & Zong, 2018). There is some evidence that some aspects of the cross-cultural variation in onset of crawling and walking stems from variation in things like nutritional variation or diaper difference between different cultural groups (Angulo-Barroso et al., 2011; Cole, Lingeman, & Adolph, 2012). Atun-Einy, Cohen, Samuel, & Scher (2013) also found that season of birth may affect motor development in infants, including onset of walking.

1.5 | Non-Human Primate Limb development

A thorough understanding of the evolution and growth of the human skeleton necessitates an understanding of our closest living relatives. Research on *Pan* and *Gorilla* not only increases our comprehension about how other species evolve and function, but also helps place human evolution and variation into a wider context. It is impossible to fully understand what it means to be human without appreciating the things that make us unique amongst animals. Therefore, I provide a brief background on the ontogeny of chimpanzees and gorillas.

1.5.1 | Chimpanzees

An observation of a wild chimpanzee shows visible labor lasting just under two hours (Goodall & Athumani, 1980). There have been multiple observations of apes giving birth in captivity (e.g., Lotshaw, 1971; Fisher, 1972; Beck, 1984), although caution should be used in considering the behavior of captive mothers as typical for their wild conspecifics. In captive chimpanzees, pregnant females will reportedly avoid strenuous activity in the last two months of pregnancy

(Yerkes & Elder, 1943). While wild chimpanzees do not appear to share this avoidance behavior, they will reportedly leave their group for a few weeks before birth until after the infant has been born (Goodall, 1977). There are also reports of captive chimpanzee mothers exhibiting fear towards their infant immediately after birth (Coe, Connolly, Kraemer, & Levine, 1979) or failing to recognize the act of birth and allowing the newborn to fall from a high platform to its death (Budd & Smith, 1943).

While there is some variation in the ability of infant chimpanzees to grasp onto their mother's fur immediately postnatally, it is generally noted that healthy infants grasp onto their mothers shortly after birth. Still, most ape mothers support their infants either with their arms or with their legs for the first few months of life. Goodall (1967) found that chimpanzee mothers would cradle with hands, feet, or thighs almost constantly for the first three months of the infant's life. She also notes that chimpanzee mothers would alert their infants if they were to rise from a sitting position to move, thus that the infant could grasp the mother's fur more tightly and avoid falling from their mother's stomach.

There is quite a bit of variation regarding maternal and infant behavior both within and between primate species. While there are numerous studies on infant and maternal behavior in captive chimpanzees and gorillas (Ueno & Matsuzawa, 2004; Hayashi & Matsuzawa, 2017), it is markedly more difficult to study behavior of wild primate groups. Throughout her extensive fieldwork, Goodall observed the perinatal behavior of multiple mother-infant pairs in the Gombe Stream Chimpanzee Reserve. For the first few months of an infant's life, the baby will cling to its mother in a ventro-ventral position. As the baby gets older and its locomotor skills develop, it will begin climbing around on the mother's body, sometimes riding on her back, or otherwise climbing around her. Beginning between 3 and 6 months after birth, the baby will begin attempting to leave its mothers body, which the mother often actively restricts for a few weeks following the onset of the desire to leave the mother. For the first 3 to 6 months of an infant chimpanzee's life, it will be in constant physical contact with its mother.

Fieldwork on the Ngogo population of chimpanzees has provided important information on the ontogenetic changes of posture and locomotion in wild chimpanzees. Sarringhaus (2014) and Doran (1992) both found that infant chimpanzees spent the majority of their time moving arboreally (under-branch swinging) compared to quadrupedally locomoting. As the infants grew, they spent increasingly more of their time moving quadrupedally. Goodall (1967) observed that infants kept in constant physical contact with their mothers for the first three months after birth, before becoming more independent and walking/climbing near their mother.

1.5.2 | Gorillas

In gorillas, parturition usually occurs with the mother in a squatting position. Visible labor is short, lasting only a few minutes to an hour (Stewart, 1977). When the infant is delivered, the mother reaches back to catch the infant while it exits the birth canal.There are multiple cases of captive gorillas failing to care for infants immediately after birth (Carmichael et al., 1962; Reed & Gallagher, 1962; Lotshaw, 1971). In most cases, mothers seek solitude for the days or weeks before giving birth, however, the observation of a wild mountain gorilla birth suggests that the mother was in constant close proximity to the group leading up to the delivery (Stewart, 1977).

After parturition, typical gorilla and chimpanzee mothers will hold their newborn to their abdomen in a ventro-ventral position. Almost immediately after birth, gorilla infants actively grasp onto their mother's fur. While typical mothers will cradle their infant almost constantly for a few months, the ability of the infant to firmly grasp onto their mother is extremely important. The act of cradling allows the infant to sleep and relax its grip enough that it would likely fall without the mother's additional support.

Ruff et al. (2013) investigated the skeletal changes that occur in young mountain gorillas (*Gorilla beringei beringei*) from birth to full locomotor independence. In this study, they looked at diaphyseal areas, second moments of area, and section moduli to determine the relative strength of long bones. They found that infants younger than 2 years old have relatively stronger arms than legs, which reflects their largely arboreal mode of locomotion. Around the age of 2, there is a steep change in the relative strength of the hind limbs as the juveniles commit to largely terrestrial locomotion. The arboreal infants had interlimb strength ratios closest to the more arboreal Western Lowland Gorillas (*Gorilla gorilla gorilla*). Young mountain gorillas exhibit scapular morphology that is consistent with a high frequency of arboreal locomotion, and the ontogenetic shape changes of scapulae reflect the ontogenetic changes in locomotion (Taylor, 1995).

1.6 | Evolution of Limb Development

Human limb function is unique among mammals. As adults, our hindlimbs are generally used for locomotion and our forelimbs are used for a variety of tasks, from object manipulation to communication. As infants, our forelimbs are often engaged in both locomotor and object manipulation tasks. The multiple uses of our forelimbs are not unique – other primates use their forelimbs for both locomotion and object manipulation as well. However, the intermediate form of locomotion that humans exhibit during infancy and early childhood is unique to humans, as is the accuracy and precision with which we can use our hands. Discerning the emergence of crawling in human evolutionary history would not only answer the question of why we crawl, but may also provide insight into social structures and parental care in past populations. Here, I will provide an overview of the research regarding juvenile hominid fossils and the evidence for the evolution of ontogeny.

1.6.1 | Fossil evidence of infants and young children

Hominids are relatively rare in the fossil record. Remains of juvenile individuals are even less common, especially postcrania. Juvenile skeletal elements are not only smaller than those of adults, but juvenile bone is also more porous, less mineralized, and more susceptible to weathering and taphonomic damage (Currey & Butler, 1975; Specker et al., 1987). Misidentification of juvenile skeletal material due to lack of knowledge of juvenile morphology may also be a factor (Saunders, 2008). Here, I present an overview of the more complete specimens of juvenile postcranial remains known from the hominid fossil record outside of *Homo sapiens*.

The 3.3-million-year-old (Ma) Dikika child (DIK-1-1) is one of the oldest partial juvenile skeletons of a hominid currently published, and one of the most complete Pliocene partial skeletons to date (Alemseged et al., 2006). The juvenile *Australopithecus afarensis* preserves the cranium and mandible, as well as numerous postcranial elements including the scapulae, hyoid,

clavicles, femora, tibia, humeri, radii, ulnae, multiple vertebrae, and several manual and pedal elements (many of these elements are fragmentary, with fracture patterns indicative of non-recovery post-fossilization and post exposure). Using an African ape dental model based on the work of Dean & Wood (2003), Alemseged et al., determined that DIK-1-1 was approximately three years old at death, though DeSilva, Gill, Prang, Bredella, & Alemseged (2018) suggest an age of 4.5 to 6 years old may be more accurate. Alemseged et al. (2006) also suggest that, while the hind limb exhibits morphology consistent with other bipedal *A. afarensis*, the scapula is more ape-like and suggests that arboreal locomotion was important in the lives of *A. afarensis* (Alemseged et al., 2006; DeSilva et al., 2018). This assertion has been hotly debated.

Slightly younger than DIK-1-1, the AL333 assemblage preserves multiple immature postcranial elements and is dated to 3.2 Ma (Behrensmeyer, 2008). Immature individuals in this assemblage include AL 333-95, a right proximal femur; AL 333-110, a left distal femur; AL 333-111, a right distal femur; AL 333-39, a left tibia; AL 333w-43, a left distal tibia; and AL 333-120, a left distal fibula, and AL 333-?, an infant first metatarsal that was apparently accidentally misidentified and forgotten about in the CMNH collection for over 30 years (Lovejoy, Johanson, & Coppens, 1982; Hillenbrand, 2009).

Perhaps the most well-known hominid juvenile partial skeleton is KNM-WT-15000, a ~1.53-million-year-old *Homo erectus* individual. Age at death for KNM-WT 15000 ranges from 8-13 years (e.g. Dean, 2007; Dean & Smith, 2009). Dean & Smith (2009) suggest a bone age of ~13 years old, and ~11 based on dental age. Studies using chimpanzee models for growth trajectory place KNM-WT 15000 at 7 to 9 years old at death and dental histology suggests an age at death between 7 and 9 (Smith, 1993; Dean et al., 2001; Dean, 2007; Dean & Smith, 2009; Schwartz, 2012). Analyses of the postcranial robusticity in KNM-WT 15000 suggest femoral strength comparable to modern *Homo sapiens* of the same age, but lower than the Teshik-Tash 1 and La Ferrassie 6 Neanderthal individuals (Ruff et al., 1994).

MH1 is the ~1.9-million-year-old juvenile type specimen for *Australopithecus sediba*. This individual has all second molars erupted and in occlusion, and is estimated to have attained at least 95% of its adult brain size (Berger et al., 2010). Subsequent research by Kimbel & Rak (2017) assert that a fully grown MH1 would closely resemble *Au. africanus*, and thus *Au. sediba* is unlikely to be a legitimate species. Using a human model, the skeletal maturation of MH1 suggest an age at death of 12-15 years, while a chimpanzee model suggests an age at death of 9-11 years (Cameron, Bogin, Bolter, & Berger, 2017). Cameron et al. (2017) also assert that MH1's growth is most consistent with an ape-like pattern of maturity, and thus suggests that a delayed postcranial growth pattern evolved after 1.53 million years ago.

Sites in the Sierra de Atapuerca have yielded several juvenile skeletal elements, including several partial crania, mandibles, and postcrania (including humeri, clavicles, and scapulae) from Sima de los Huesos, mandibular and postcranial elements (including a clavicle) from Gran Dolina, etc. (Arsuaga et al., 1993; Carretero, Arsuaga, & Lorenzo, 1997; Pérez, Gracia, Martínez, & Arsuaga, 1997; Carretero, Lorenzo, & Arsuaga, 1999; Garcia-González et al., 2009; Bermúdez de Castro et al., 2010; Pablos et al., 2013; Pablos et al., 2014; Bermúdez de Castro et al., 2017). Dental eruption and tooth development in *H. antecessor* have been established to fall within the ranger of *H. sapiens* (Bermúdez de Castro et al., 2010). Additionally, two well preserved juvenile *H. antecessor* scapulae from the TD6.2 level of Gran Dolina imply a postcranial ontogenetic growth pattern similar to that of modern *H. sapiens* (Bermúdez de Castro et al., 2020). There are also

immature modern human skeletal elements from nearby Huérmeces consisting of a mandible, some deciduous teeth, a phalanx, and a metatarsal (Quam et al., 2001).

Neanderthal fossils are better represented in the fossil record in terms of juveniles. There dozens of juvenile Neanderthals known to science, and even several infant partial skeletons and isolated elements. Amud has yielded multiple partial skeletons, ranging from newborns to 1 year at death (Rak, Kimbel, & Hovers, 1994). There is also a juvenile Neanderthal from Spy represented by two mandibular corpus fragments with associated teeth (Crevecoeur et al., 2010). Five immature partial skeletons, including fetuses, have been recovered from La Ferrassie (Heim, 1976; Heim 1982; Gómez-Olivencia, Crevecoeur, & Balzeau, 2015; Balzeau et al., 2020). A study on a juvenile partial skeleton from El Sidrón, Spain, suggests a growth rate in Neanderthals very similar to that of modern humans (Rosas et al., 2017). Still, most research on Neanderthal ontogeny focuses on crania, mandibles, and dentition, with a relative paucity of research on the postcranial skeleton.

1.6.2 | Growth and development of hominids

Growth and development in human evolution is an active area of research. With relatively few juvenile hominids preserved in the fossil record, many of the inferences about hominid life history relies on the available fossil remains and studies of extant primates to form an understanding of how birth and juvenile growth have evolved throughout human evolution.

1.6.2.1 | Prenatal growth. In comparison with our extant relatives, humans have a slightly longer gestational period (~ 8 months in chimpanzees and ~8.5 months in gorillas, compared to ~9 months in humans), and give birth to babies that are sometimes referred to as "under-developed" compared to the infants of extant non-human primates. Non-human primate infants are born with the ability to cling to their mothers shortly after birth and gain the ability to locomote independently shortly after, a trait notably not found in human infants (Portmann, 1969). While people frequently refer to human infants as "under-developed" or "born too soon", Dunsworth (2012) shows that human gestation length is not shorter than expected for a human-sized primate.

Although humans are born with the absolutely largest brains of any primate, we are also born with only about 30% of our adult brain size, compared to 40% in chimpanzees (DeSilva & Lesnik, 2006; Dunsworth, 2012). Humans are also one of the few primates that experiences a highly difficult and painful labor where the infant head has to rotate through the birth canal, caused by a tight fit between fetal size and female pelvic dimensions. Humans are also the only living bipedal primates, which has led to the idea that the energetics of bipedal walking have limited the maximum width of female pelves, thus pushing humans to give birth to "underdeveloped" infants "earlier" than we would otherwise. This is known as the "obstetrical dilemma" – our pelves cannot get wider because they would be inefficient for walking, so we give birth to more helpless babies instead. This idea, first promoted by Sherwood Washburn in 1960, is ubiquitous in biological anthropology, but has recently been revisited by deliberation on the validity of the obstetrical dilemma (Dunsworth, 2018; Haeusler et al., 2021; DeSilva, 2022). Warrener (2015) found that individuals with wider hips use energy as efficiently as those with narrower hips when walking. Additionally, research has shown that individuals with wider hips are actually more efficient walkers when they are carrying objects, are more

energy efficient when changing speeds, and have longer stride lengths (Wall-Scheffler & Myers, 2007; Wall-Scheffler, 2012; Whitcome, Miller, & Burns, 2017). The metabolic hypothesis for human altriciality suggests that constraints on gestation length and fetal growth are limited not by pelvic size, but instead by maternal metabolism – a mother's body can simply not provide enough energy to a growing fetus (and its large brain) past a certain point (Dunsworth et al., 2012).

Reconstructions of hominid birth canals vary. It was speculated that the ARA-VP-6/500 anteroposteriorly expanded birth canal would have allowed for *Ardipithecus ramidus* to have given birth to a small-brained infant without rotation (DeSilva, 2011). Birth canal reconstructions of AL 288-1 suggest that infant head size (assuming it was about the size of a modern chimpanzee newborn) would not require rotation during birth (Tague & Lovejoy, 1986). However, other reconstructions of *Australopithecus* pelves suggest that AL 288-1 is the earliest preserved pelvis to have morphology suggestive of fetal rotation during birth, which is also observed in many later *Australopithecus* fossils including Sts 14, Sts 65, and MH2, and the rotational aspect is likely driven by fetal shoulder breadth as opposed to fetal head size (Berge, Orban-Segebarth, & Schmid, 1984; Claxton et al., 2016; DeSilva, Laudicina, Rosenberg, & Trevathan, 2017; DeSilva, 2022). Thus, neonatal shoulder breadth may have provided more of a constraint during earlier hominid births than cranial size (Rosenberg & Trevathan, 2002). The discovery of a 1.8-million-year-old female *Homo erectus* pelvis from Gona, Ethiopia, exhibits a wide pelvis and relatively short stature, suggesting that the delivery of relatively helpless babies was present by this time (Simpson et al., 2008).

1.6.2.2 | Postnatal growth. The few fossils of hominid juveniles known to science allow for inferences of growth rates in hominid infants and children. Research on two of the best-preserved juvenile *Australopithecus afarensis* crania (DIK-1-1 and AL 333-103) in comparison with *A. afarensis* adults suggest that *A. afarensis* juvenile brains grew more slowly and for a longer period of time than modern chimpanzees (Gunz et al., 2020). There is also evidence from KNM-WT 15000, who has a young dental age compared to bone age, that *Homo erectus* and earlier hominids experienced a shorter adolescent growth period than modern humans (Tardieu, 1998) and either an earlier adolescent growth spurt or no adolescent growth spurt at all (Zollikofer & Ponce de Léon, 2010). The latter is most likely, given that the morphology of KNM-WT 15000's femora are very similar to humans during or shortly after the adolescent growth spurt (Tardieu, 1998), and given that chimpanzees and gorillas also exhibit an adolescent growth spurt (Leigh & Shea, 1995; Bellisari et al., 2001; Leigh, 2001; Hamada & Udono, 2002; Walker, Hill, Burger, & Hurtado, 2006).

The age at weaning throughout human evolution is also an active area of research (e.g., Lee, 1996; Robson & Wood, 2008; Van Noordwijk, Kuzawa, & Van Chaik, 2013; Tacail et al., 2017; Smith et al., 2018. etc.). Great apes tend to wean their young relatively late, usually between 4 and 5 years for chimpanzees and gorillas and up to 8 years in orangutans (Kennedy, 2005; Smith et al., 2017; Dettwyler, 2017; Robbins & Robbins, 2021). Breastfeeding primates have very low levels of luteinizing hormone, which actively prevents pregnancy while an individual is lactating (sometimes called

'lactational infecundibility'; McNeilly, 1979). Modern human infants are usually weaned by 3 years of age (Locke & Bogin, 2022; Hrdy & Burkhart, 2022). Analyses of dental wear in hominid juveniles suggest that LH 2 (*A. afarensis*) showed a deciduous molar wear pattern similar to nursing great apes, while Taung 1, Sts 24 and StW 59 have sufficiently worn deciduous molars to suggest reliance on solid foods (Aiello, Montgomery, & Dean, 1991). Smith (2017) cautions against using dental wear as a proxy for introduction of solid food.

Investigations of calcium isotopes in hominid enamel suggest that early *Homo* babies were reliant on breast milk for longer than infant *Australopithecus africanus* and *Australopithecus (Paranthropus) robustus* individuals (Tacail et al., 2017; Tacail et al., 2019). Additionally, barium isotopes in dental enamel show that Neanderthal infants were introduced to solid foods around 2.5 years of age (Austin et al., 2013; Smith et al., 2018). There is also some evidence that Neanderthals had a shorter period of dental development than modern humans (Ramirez Rozzi & Bermúdez de Castro, 2004; Smith et al., 2007a). These differing growth trajectories and the presence of conflicting hypotheses make it difficult to compare postcranial ontogeny in hominids and modern humans when dental eruption is used to determine age (Cowgill, 2010). Additionally, extant dental development can be affected by environmental factors such as socioeconomic status and childhood illness (Cardoso, 2007). Relatively stronger tibiae in Neanderthal children than modern human children may suggest that Neanderthals started walking earlier than industrialized modern humans, but a better understanding of modern human strength ratios is necessary to reach a firm conclusion (Cowgill & Johnston, 2018).

Overall, there are numerous hypotheses on the life histories of hominids throughout evolutionary history. By ~315,000 years ago, dental development was very similar to modern *Homo sapiens* (Smith et al., 2007b; Hublin et al.,2017). Juvenile *H. erectus* may have reached skeletal maturity earlier and exhibited an adolescent growth spurt earlier than modern humans. Pre-*Homo* species may have relied on maternal breast milk for a shorter period of time than modern humans, and likely began to exhibit some form of fetal rotation during birth. Large neonatal brains and wide female pelves were present in *Homo erectus*, suggesting that their early life history may have been very similar to that of extant *H. sapiens*. Further evidence from *H. antecessor* suggests that ontogeny was nearly modern by 0.89 Ma (Garcia-Martinez et al., 2021).

1.7 | Hypotheses and Study Design of this Project

My over-arching research aim was to examine the relationship between ontogenetic locomotion and skeletal properties in humans in order to improve our understanding of juvenile hominid fossils. Previous researchers Ruff (2003a, 2003b), Cowgill (2008), and Sumner & Andriacchi (1996) found that the humerus and femur are relatively similar in strength within the first year of life, followed by the femur increasing in relative strength compared to the humerus. However, these studies rely either on small sample sizes (Ruff, 2003b), estimated age and sex (Cowgill, 2008), or very few individuals in wide age categories. Each limitation lowers the validity of results (Sumner & Andriacchi, 1996).

I overcome these hurdles by utilizing data from the New Mexico Decedent Imaging Database (NMDID). This research resource includes the medical CT scans of 100 infants and children aged 0-14 years. Ages are determined in months from known birthdates, providing a much higher-resolution understanding of growth within the first few years than studies that bin individuals into yearly age groups or use age estimations. I assess bone properties including length, diaphyseal circumference, medullary cavity size, cortical thickness, second moments of area, and polar second moments of area. Data collection related to this project is ongoing, and thus, this thesis represents a preliminary study addressing the hypotheses outlined below.

Based on the literature review provided above, I identified three hypotheses to test using the NMDID population:

1.7.1 | Hypotheses

Hypotheses for each chapter are outlined below. Each overarching hypothesis is investigated in two or three specific questions in each chapter. Each hypothesis builds on previous work and uses this new sample to provide evidence on the validity of conclusions from previous studies.

1) The proximal and distal diaphyses will mature more quickly than the midshaft. Proximal and distal diaphyseal cross sections and relative strength will begin to level out earlier in maturation than midshaft diaphyseal cross sections and relative strength. Sex differences in growth patterns will be minimal **(Investigated in Chapter 3).**

Hypotheses investigated in this chapter build on previous work showing that the proximal humerus and distal femur contribute disproportionately to longitudinal growth, distal segments grow faster than proximal segments, and endosteal bone formation is important during ontogenetic cortical bone growth (Moss, Noback, & Robertson, 1955; Ogden, Conlogue, & Jensen, 1978; Ozonoff, 1979; Pritchett, 1991; Gosman et al., 2013; Maggiano et al., 2015; Cunningham, Scheuer, & Black, 2016).

2) The relative strength of the clavicle, humerus, and femur, will change throughout the first few years of life. Within the first year, the humerus and femur will be more similar in relative strength. The femur will increase in relative strength compared to the humerus after ~ 1 year of age. This correlates with the onset of bipedal walking as the main form of locomotion. **(Investigated in Chapter 4).**

This chapter uses a large sample with accurate ages to corroborate results from Ruff (2003a, 2003b) and Cowgill et al. (2010). Previous studies found that humeral to femoral strength proportions change throughout early childhood, and children learning to walk experience unique biomechanical loading patterns on their long bones.

3) Bilateral asymmetry of the clavicle, humerus, and femur will increase with age. The humerus and clavicle will exhibit relatively more bilateral asymmetry in length and robusticity than the femur. Infant individuals will be more symmetrical in length, cross sectional properties, and relative strength than older children. Emergence of bilateral asymmetry will correlate with the relative onset of developmental milestones such as increased manual manipulation and emergence of the use of a dominant hand. **(Investigated in Chapter 5)**.

Studies on the development of bilateral asymmetry in human children have reached conflicting conclusions. Schultz (1926) found that fetal humeri already exhibit bilateral asymmetry, with

most individuals having a longer right humerus than left humerus. Conversely, Blackburn (2011) found that infants and young children do not exhibit any significant asymmetry in humeral length, midshaft diameter, or epicondylar breadth. This chapter uses the NMDID sample to better understand perinatal asymmetry and how asymmetry develops throughout ontogeny.

The materials and methods of the research are described in detail in Chapter 2. Chapters 3-5 report on the tests of each of these three hypotheses, and Chapter 6 provides a discussion of results, conclusions, and areas of interest for future research.

Chapter 2: Materials and methods

2.1 | Introduction

The goal of this PhD thesis is to expand the current knowledge of bone properties throughout human ontogeny and human evolution. The New Mexico Decedent Imaging Database provides a unique dataset of recently deceased individuals of known age, measured in months (Edgar et al., 2019). This dataset allows for an increase in knowledge of how the human clavicle, humerus, and femur, grow throughout infancy and adolescence, and thus provides a framework from which to view hominid fossil evidence.

2.2 | Materials

2.2.1 | CT Scans

Whole body medical CT scans used in Chapters 3-5 of this thesis were downloaded with permission from the New Mexico Decedent Imaging Database (NMDID; Edgar et al., 2020). The NMDID is a database containing whole body medical CT scans of over 15,000 people who died in New Mexico between 2010 and 2017. Each individual is scanned by the New Mexico Office of the Medical Examiner (OMI), a centralized medical examiner for the state of New Mexico. Any individual who dies in the state of New Mexico of a sudden, violent, or unexpected death is sent to the OMI for autopsy. In 2015, about 35% of deaths in the state went through the OMI (Edgar, 2016). Consent and information on the decedent's medical history are acquired from next of kin. All individuals included in the NMDID are CT scanned at the OMI's central Albuquerque facility using a Philips Brilliance Big Bore 16 CT scanner following a standard protocol (protocol can be found at https://nmdid.unm.edu/resources/data-information). Individuals whose body is less than 36 inches in length are scanned in a single acquisition, and taller individuals are scanned in three acquisitions (head/neck/upper extremity, torso, and lower extremity). All CT scans included in this study have slice thickness of 1 mm with 0.5 mm overlap. For each individual, NMDID provides reconstructions for optimal brain, soft tissue, lung, and bone visualization. The bone reconstructions were used in this study. All individuals included in this study are listed in Appendix 1.

The NMDID contains CT scans of 714 individuals aged 0-14 that were screened for this study. Individuals were excluded from this sample for a variety of reasons, including a recorded history of broken bones (provided by NMDID), congenital deformity of any part of the postcranial musculoskeletal system, moderate to severe decomposition, incomplete preservation, or circumstances of death that caused skeletal trauma (ie. automobile accidents, severe burns, head and neck injuries, etc.). While all individuals in the database up to age 15 were screened for inclusion, individuals were only included until the eruption of their second molars (determined by eruption from the crypt by CT scan). All individuals included in this study were scanned within 48 hours of death. There is a male skew in these data, with 60 males (age 0-174 months of age) and 40 females (age 0-158 months of age) included.

2.3 | Data Collection Methods

ORS Dragonfly imaging software v. 2020.2.0.941 was used to visualize scans and collect data. DICOM images from NMDID were loaded into the Dragonfly imaging software and x, y and z axes defined (x = 1mm, y = 1mm, z = 0.5mm) to match scanning protocols. All measurements and their definitions are listed in Table 2.1. I collected all metric data used in these analyses.

2.3.1 | Manual measurements

All measurements excluding second moments of area and polar second moments of area were taken from 2D images from the scans. Right and left humeri and femora were measured in two different ways. Total bone length was measured, including all secondary ossification centers that were more than 1mm x 1mm in dimension. Diaphyseal bone length was measured using only the humeral and femoral shafts and excluding secondary ossification centers and epiphyseal growth plates. In individuals that exhibited some fusion of epiphyseal growth plates, diaphyseal length was measured based on the maximum length from one growth plate to another (Figure 2.1). Clavicular length was measured as the maximum length of the bone. All length measurements were measured in two planes and averaged, and any discrepancies of more than 2mm were investigated and remeasured. Due to the variation in cadaver orientation during scanning, axes were manually established for length measurements. Axes were adjusted thus that the total length of the bone was visible in two planes.

Cross-sectional measurement positions on the humerus and femur were established at 25%, 50%, and 75% of the diaphyseal bone length as well as 50% of total bone length. Both 50% of total bone length and 50% of diaphyseal length were measured to analyze the utility of using total bone length vs. diaphyseal bone length when studying juveniles. Only one measurement position was established on the clavicle, at 50% total bone length. Axes were adjusted such that the x axis runs through the long axis of the bone, the y axis runs perpendicular through the diaphysis, and the z axis runs perpendicular to the x and y axes. At each measurement position, diaphyseal circumference and medullary cavity circumference were measured using the ruler tool (Figure 2.1). This tool also calculated area two area measurements – total cross-sectional area (subperiosteal area), and medullary area. Cortical area was calculated by subtracting medullary area from total cross-sectional area.

2.3.2 | Segmenting bones

Segmentation is the process of isolating a particular region (in this case, a single skeletal element) from the rest of the scan. Manual thresholding was used to segment individual bones in this study (see Chapter 1 section 3.2.2 for background on thresholding methods). Manual thresholding was chosen to better accommodate the wide range of bone densities found in individuals aged 0-14 years old. For each individual, a threshold was chosen based on the minimum density of the humeral cortex, thus that a Region of Interest (ROI) would include the humeral cortical bone and not humeral trabeculae. Once threshold was established, the entire skeleton was segmented into a single ROI, then separated into individual elements using the multi-ROI 26-connected tool. Each bone of interest was manually selected into its own ROI, then re-sampled in 1 x 1 x 0.5 mm slices into a derived ROI based on the correct axes.

2.3.3 | Moments of area

With axes adjusted for cross-sectional measurement as described above, ROIs were selected and isolated. The slice number of each measurement position was recorded. Second moment of area (SMA) measurements including I_{xx}, I_{yy}, I_{max}, I_{min}, J, and the number of Voxels per slice were measured using Dragonfly's slice analysis tool. Moment measurements were then exported to Microsoft Excel. The Dragonfly slice analysis tool measured the selected variables at every 0.5mm slice along the bone, and SMA measurements were taken on slices corresponding to the measurement positions discussed above.

2.3.4 | Error Calculations

Percent error was calculated by remeasuring a subset of 10 (5 males, 5 females) of varying ages. There are no statistically significant measurement errors in clavicular (mean = 0.9%), humeral (mean = 0.5%), or femoral length (mean = 1.3%). Measurement error was highest in the medullary area measurement, for which there is an average error of 6.5% in the humerus and 4.6% in the femur. Error in clavicular medullary area was consistently over 10% due to poor resolution, and thus these measurements are not included in any analyses. Measurement error for all other manually collected measurements is below 5% (range = 1.21 – 4.6%).

Second moment of area percent errors were calculated following the same protocol as manual measurements. I_{max} measurements have an average of 4.9% error and J has an average error of 8.1%. The relatively high error in measurement of J has not been accounted for in analyses and should be noted by the reader. SMA were only measured for the humerus and femur, as error calculations for clavicular measurements were over 20%, likely due to a combination of thin cortical bone characteristic of juvenile clavicles and poor scan resolution.

The smaller overall size of younger individuals results in lower resolution scans. The same protocol was used for measuring all individuals regardless of age and scan resolution. Scans of 10 older individuals were then re-measured using lower resolution of the original scans. To reduce the resolution of higher quality scans, the import settings on the Dragonfly CT software were set such that the program sampled only every third pixel. Figure 2.2 shows the change in resolution on the same midshaft slice of the right femur from a 13-year-old female (158 months) with a femoral midshaft slice at normal resolution from a newborn female (0 months). Scans of older individuals were reduced in resolution and re-measured following standard protocols described in Section 3. Reduced resolution measurements of older individuals were compared to original measurements from the higher resolution scans. Results of error calculations show that there is no statistically significant difference between length or diaphyseal circumference measurements (p= 0.01 – 2.14%). Medullary area measurements are the most affected by poor resolution, with an average of 10.4% error in the humerus and 6.0% error in the femur. This error is exacerbated when calculating the percent of the total area is represented by the medullary cavity ((medullary area / total area)*100). On average, the poor resolution scans of smaller children produce an overestimation of the relative size of the medullary cavity by ~10%, with a range of 6.54-12.5% error. To compensate for less accurate measurements on smaller individuals, measurements have been adjusted by 10% on all individuals 0-12 months to compensate for the poor resolution of scans. Moment measurements are also consistently overestimated in lower resolution scans by an average of 15.4% (range – 11.5 to 20.9%). Thus, SMA data has been adjusted by 15% in individuals under 12 months of age to account for the 15% overestimation of SMA measurements.

2.3.5 | Data analysis

All analyses are done in the in the R statistical environment v3.6.1 (R Core Team, 2021). Results reported in Chapters 3, 4, and 6 are from measurements taken from the right side of each individual. Figures were made using *ggplot2* (v3.3.0; Wickham, 2016) in the R statistical environment v3.6.1 (R Core Team, 2021) and compiled in Adobe Illustrator CC 2020 (Adobe, Inc). Error calculations and descriptive statistics are performed in Excel, and tests of significance are done in R. Descriptions of analyses and analytical methods are included in Chapters 3-6,

because analyses used in each chapter vary. Age groups used for statistical analyses are listen in Table 2.2.

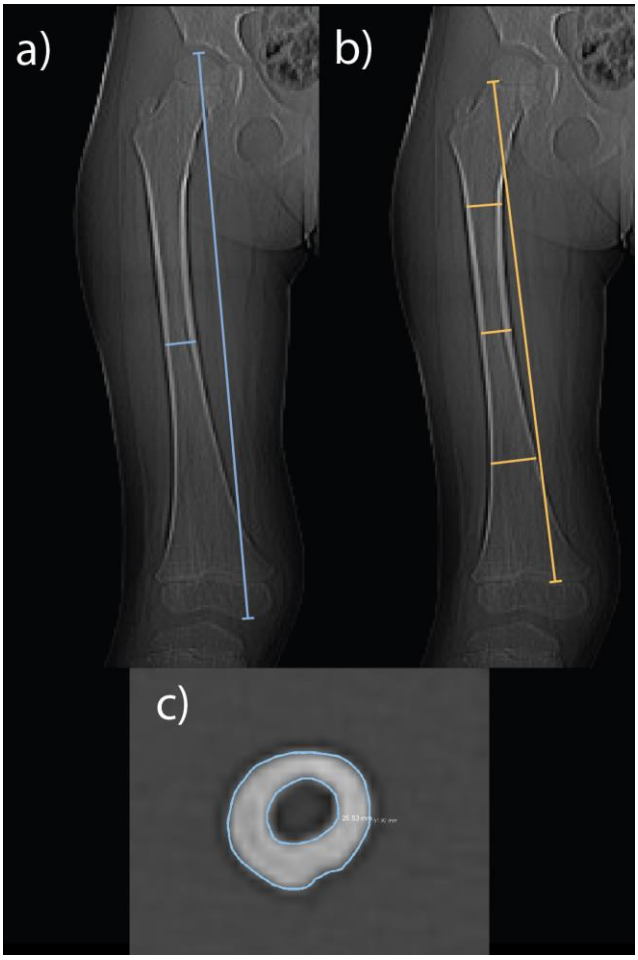


Figure 2.1. Measurement methodology for long bone measurements. a) Total element length including epiphyses and cross-sectional midshaft measurement at 50% total element length. b) Diaphyseal element length and cross-sectional measurement positions at 25%, 50%, and 75% diaphyseal length. c) Illustration of cross-sectional measurements. Outside circle represents diaphyseal circumference and inside circle represents medullary circumference. Area measurements are calculated in Dragonfly from the circumferential measurements.

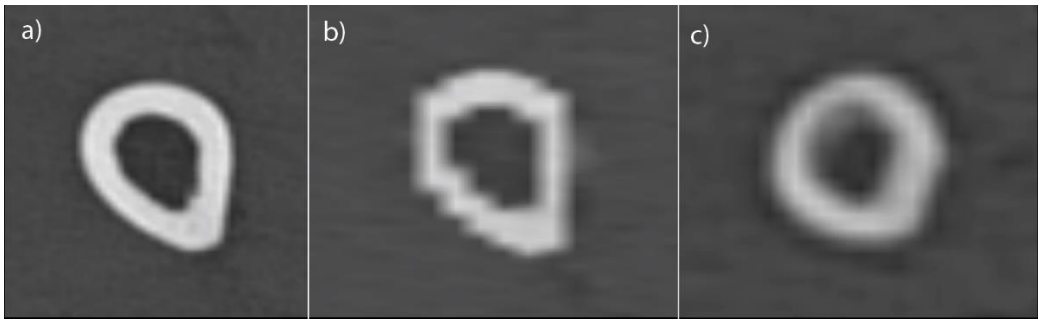


Figure 2.2. Resolution of scans. a) Femoral cross-section of a female age 158 months prior to resolution reduction. b) Femoral cross-section from frame a) with reduced resolution for infant error calculation. c) femoral cross-section of a female age 0 months.

Measurement	Definition	Measurement position
Total length	Maximum length from the proximal most point (proximal epiphysis, if present) to the distal most point on the medial side (distal epiphysis, if present)	-
Diaphyseal length	Maximum length of the diaphysis from the proximal most point to the distal most point on the medial aspect of the diaphysis	-
Diaphyseal circumference	Total bone circumference of the diaphysis in a cross-sectional view	25%, 50%, 75% diaphyseal length
Medullary circumference	Circumference of the medullary cavity in cross-sectional view	25%, 50%, 75% diaphyseal length
Diaphyseal cross-sectional area	Total area of both cortical bone and medullary cavity	25%, 50%, 75% diaphyseal length
Medullary cross-sectional area	Total area of the medullary cavity in cross-sectional view	25%, 50%, 75% diaphyseal length
Cortical area	Diaphyseal cross-sectional area - medullary cross-sectional area	25%, 50%, 75% diaphyseal length
Relative medullary cavity size	((medullary area / total area) x 100)	25%, 50%, 75% diaphyseal length
Min second moment of area (I_{min})	Minimum resistance to bending	25%, 50%, 75% diaphyseal length
Max second moment of area (I_{max})	Maximum resistance to bending	25%, 50%, 75% diaphyseal length
Polar second moment of area (J)	Resistance to torsion	25%, 50%, 75% diaphyseal length

Table 2.1. Measurement definitions.

Group	Age	*n*
Group 1	0-6 months	33
Group 2	7-10 months	7
Group 3	11-36 months	26
Group 4	36+ months	33

Table 2.2. Age groups used for statistical analyses.

Chapter 3: Intra-element growth and development

3.1 | Introduction

Long bone growth is a complex topic that has been studied for centuries (Hales, 1733; Ollier, 1867; Compere & Adams, 1937; Buschang, 1982; Mays, 1985; Smith & Buschang, 2005; Cambra-Moo et al., 2012). Early work established that long bones grew from their epiphyses via experimental drilling of holes into the tibiae of growing chickens and measuring the distance between the holes throughout growth (Hales, 1733). An investigation of bone growth in children with elbow and knee injuries showed that proximal and distal segments of long bones grow at different rates and have varying contributions to overall bone length (Ollier, 1867). From there, much of the research on long bone ontogeny stemmed from investigations of pathologies and skeletal injuries (e.g., Compere & Adams, 1937). The Fels Longitudinal Study, which began in 1929, and other longitudinal studies utilized anthropometry and x-ray radiography to track longitudinal growth in cohorts of people from birth throughout their lives (Roche, 1992). Radiographs remain a common source of ontogenetic data, and have even been used to calculate second moment of area measurements using a latex cast method (LCM; Ruff, 1989; Cowgill et al., 2010). In this dissertation, the recent publication of the New Mexico Decedent Imaging database now provides a new dataset of medical CT scans from which to collect cross-sectional data on long bone ontogeny.

Growth rates along a single long bone vary. For example, the proximal humeral epiphysis is responsible for about 80% of growth in humeral length (Ozonoff, 1979; Ogden et al., 1978; Ogden, 1984; Pritchett, 1991; Cunningham et al., 2016). Conversely, it is the distal femur that is responsible for the majority of growth in femoral length, contributing about 66% of total longitudinal growth (Sissons & Kember, 1977). Additionally, rates of growth differ between the humerus and the femur. The osteological length of human femora is already greater than that of the humerus in fetuses 14 weeks post-conception, despite the fact that the forelimb develops ~2 days before the hindlimb (Bareggi et al., 1994; 1996). Moss et al., (1955) found that distal segments of all long bones grew relatively faster than the proximal segments in human fetuses.

Similarly, there is evidence that pre-pubertal midshaft humeri grow primarily due to periosteal and medullary expansion whereas distal humeri grow from periosteal expansion alone (Bass et al., 2002). There is some debate on the role of periosteal expansion vs endosteal contraction in humeral bone growth. In several studies, the humeral endosteum showed reduced or no response to biomechanical loading when compared to the periosteum (Meade et al., 1984; Lee, Maxwell, & Lanyon, 2002; Srinivasan et al. 2013). These studies are focused on *in vivo* investigations of non-human mammals including dogs and mice, and thus caution should be used when applying these principles to human bones because canine and murine bone growth is somewhat different from that of humans (Jilka, 2013).

Human studies have suggested that the humeral endosteum is nearly as osteogenic as the periosteum, and that endosteal growth is responsible for distal humeral cortical growth (Bass et al., 2002; Maggiano et al., 2015). Maggiano et al. (2015) also found that endosteal primary tissue was found only in the anterolateral aspect of the midshaft and distal humerus, but wrapped around nearly the entire endosteal surface of the proximal humerus.

Intra-element variation in growth patterns in the femur have also been studied. Unlike the humerus, the distal femur exhibits the most activity from endosteal tissue, followed by the

midshaft and then the proximal femur (Maggiano et al., 2015). Rate of growth in the femoral midshaft is the highest during toddlerhood (2-3 years) and the pubertal growth spurt, and slows down during mid-childhood and late adolescence (Goldman et al., 2009; Gosman et al., 2013). Further, the proximal and distal femur are both more responsive to mechanical loading than the midshaft during ontogeny, especially in infants and toddlers (0-2 years) (Gosman et al., 2013). Some research has shown that net endosteal bone formation (and thus, medullary contraction) increases in later adolescence (Garn et al., 1970; Chevalley, Bonjour, Ferrari, & Rizzoli, 2008; Goldman et al., 2009). This finding was contradicted by those of Gosman et al. (2013) who found no medullary contraction in adolescence. Several authors have also noted the absence of sex differences in endosteal apposition (Kontulainen et al., 2005; Goldman et al., 2009; Gosman et al., 2013). The relative size of a long bone's medullary cavity also exhibits changes throughout ontogeny, Perinatal and postnatal infants have a proportionally wide cortex that narrows throughout childhood in combination with a medullary cavity that gradually reduces over time (Cambra-Moo et al., 2007).

This review of the literature raises three questions about intra-element development of the humerus and the femur in human infants and children:

> *Question 1:* Are there measurable differences in cortical properties in the portions of the humerus and femur that contribute the most to longitudinal growth (i.e., the proximal humerus and the distal femur)?
>
> *Question 2:* Is there any evidence from cross-sectional properties that endosteal bone formation is contributing to cortical growth?
>
> *Question 3*: Are there any sex differences in the growth of the humerus and femur along the diaphysis?

Many of the studies discussed above rely on incomplete age data, small sample sizes, or large age categories that span many years of development. As a consequence of using a securely aged population, I am able to employ a more nuanced analysis of ontogenetic development to investigate how different areas of a single skeletal element grow and change throughout infancy and childhood using cross-sectional measurements from three different positions on the humerus and femur.

3.2 | Materials and Methods

3.2.1 | Materials.

This study uses data collected from 100 infants and children ranging in age from third trimester (pre-natal) to 14 years old. The upper limit of age was determined by the eruption of the second molar (i.e., none of the individuals included have erupted second molars, determined by eruption from the crypt by CT scan). Scans of all individuals were downloaded from the New Mexico Decedent Imaging Database (Edgar et al., 2019). All individuals included in this study died in New Mexico between 2010 and 2017 and are listed in Appendix 1 by their unique anonymizing-identification number. Individuals were excluded if they had a recorded history of bone fracture, musculoskeletal disease or deformation, or traumatic circumstances of death that would distort their bones (i.e., car accidents, skeletal trauma). This research was approved by the New Mexico Decedent Imaging Database and the University of New Mexico. The Free Access Decedent Database funded by the National Institute of Justice grant number 2016-DN-BX-0144.

3.2.2 | Data Collection Methods.

Measurements at each measurement position (25%, 50%, and 75% of diaphyseal length) were collected for each individual and are described in Chapter 2. CT scans were downloaded from the NMDID (Edgar et al., 2019) and imported into Dragonfly 2020.1 beta (Dragonfly 2020.1). Linear measurements of total bone and diaphyseal lengths were taken from the right side of the body.

Long bones were segmented manually. Density thresholds for cortical bone were determined based on the cortical bone of the right humerus. Segmented long bones were then resampled individually. Maximum and minimum second moments of area (I_{min} and I_{max}, respectively), polar second moments of area (J), and Ixx and Iyy were calculated by the Dragonfly software from the resampled segmented bones using the Slice Analysis tool.

Collecting data from medical CT scans raises the possibility that the quality of the scan could differentially introduce bias based on the size of the person. The smaller overall size of younger individuals results in lower resolution medical CT scans. See Chapter 2 for description of how poor resolution affects measurement error. The same protocol was used for measuring all individuals regardless of age and scan resolution. Scans of older individuals were then re-measured using lower resolution of the original scans. To reduce the resolution of higher quality scans, the import settings on the Dragonfly CT software were set such that the program sampled only every third pixel. Figure 2.2 shows the change in resolution on the same midshaft slice of the right femur from a 13-year-old female (158 months) with a femoral midshaft slice at normal resolution from a newborn female (0 months). Linear and area measurements of older individuals were reduced in resolution and re-measured following standard protocols described in Chapter 2. Reduced resolution measurements of older individuals were compared to original measurements from the higher resolution scans. Results of error calculations show that there is no statistically significant difference between length or diaphyseal circumference measurements ($p= 0.003 – 0.5$). Medullary area measurements are the most affected by poor resolution, with an average of 5.6% error in the humerus and 6.0% error in the femur. This error is exacerbated when calculating the percent of the total area is represented by the medullary cavity ((medullary area / total area)*100). On average, the poorer resolution of the scans of smaller children produces an overestimation of the relative size of the medullary cavity by ~10%, with a range of 8.9-12.3% error. Thus, measurements have been adjusted (decreased by 10%, described in detail in Chapter 2) on all individuals 0-12 months to compensate for the poor resolution of scans.

3.2.3 | Analytical Methods

Statistics were calculated in the R statistical environment v3.6.1 (R Core Team, 2019). Correlation coefficients were calculated using Pearson's correlations. Welch two sample t-tests were used to calculate significance of difference between age groups. For statistical analyses, individuals were divided into three groups: 6 months and under (when individuals are most likely to be pre-locomotion), 7 to 10 months (when individuals are most likely to utilize a pre-walking form of locomotion), and 11+ months (when individuals are most likely to begin walking bipedally). Linear regressions on log-transformed values were used to calculate growth rates for cortical area, second moments of area (SMA) and polar second moments of area, as modified from Ruff (2003a). Tests for difference of means were calculated from natural log-transformed

growth rates. Bivariate plots were made using *ggplot2* (v3.3.0; Wickham, 2016) in the R statistical environment v3.6.1 (R Core Team, 2019) and compiled in Adobe Illustrator CC 2020 (Adobe, Inc). For statistical analyses of growth rates derived from linear regressions on natural log-transformed values, individuals are split into three age groups that correspond to likelihood of utilization of a certain locomotor type. Individuals younger than 6 months of age are the first group and most likely to be pre-locomotion. Individuals 7-10 months are grouped into the second group, and are most likely to be utilizing some pre-walking form of locomotion such as walking and scooting. Individuals 11 months and older make up the third group, and are most likely to be walking bipedally some to all of the time (Malina, 2004; Adolph, Berger, & Leo, 2011; CDC, 2022). Pairwise comparisons were done between different measurement positions within an age group, and between the same measurement position in different age groups. Figures depicting bivariate plots of measurements against age visually represent growth rate, but figures showing linear regressions quantify growth rates.

A change point detection analysis was performed using the changepoint package in the R statistical environment (Killick et al., 2022). Results indicate that there is a change in variance of cross-sectional properties around 70 months, which indicates that individuals less than 70 months of age have similar variance, which changes in those over 70 months of age.

3.3 | Results

Bivariate plots are presented in Figures 3.1 – 3.18. For relevant figures, I also standardized by length to better visualize the data. I present the results for intra-element growth and development on an element-by-element basis. Results for each measurement are reported for all three measurement positions (proximal, midshaft, and distal) together.

3.3.1 | Humerus

3.3.1.1| Length. Humeral diaphyseal length is very tightly correlated with age (r^2 = 0.98 Figure 3.1). Female newborns (<1 month) have slightly shorter humeri than male newborns, but the difference is not statistically significant (p=0.90). All individuals aged 4 months or older exhibit proximal and/or distal epiphyses large enough to be measured (>1mm). Of the 26 individuals aged less than 4 months, 7 exhibit proximal and/or distal epiphyses large enough to be measured.

3.3.1.2 | Diaphyseal circumference. Humeral diaphyseal circumference (DC) increases at roughly an equal rate at the proximal, midshaft, and distal humerus (Figure 3.2). Growth rate in humeral diaphyseal circumference is the highest in the first 12 months, after which it levels out and then increases again at all three measurement positions around 4 years of age. Diaphyseal circumference then plateaus through late childhood. Compared to longitudinal bone growth, the proximal, midshaft, and distal humerus are growing more quickly in circumference than in length in the first 6 months, after which the humerus is growing faster in length than in circumference throughout the remainder adolescence (Figure 3.2, right panel).

3.3.1.3 | Cortical Area. There is quite a bit of variation in cortical area (CA) throughout childhood, resulting in complete overlap in the 95% confidence intervals for the three measurement positions. All three positions on the humerus exhibit a steep

increase in total cortical area in the first 6 months, followed by a series of ups and downs throughout infancy and early childhood (Figure 3.3). Proximal, midshaft, and distal cortical area all increase in parallel. CA shows some leveling off around 30-40 months of age, followed by another relatively rapid increase in cortical size that continues into late childhood and early adolescence. Relative to growth in humeral length, CA increases faster than humeral length for the 5 months, after which the increase in length is greater than the increase in cortical area. This is shown in the top right panel of Figure 3.3, where the trend lines decrease with age because the humeral diaphysis (denominator in the standardization equation) is increasing faster than cortical area (numerator in the standardization equation). Linear regression on natural log-transformed values are shown in Figure 3.4. Within each age group, there are no statistically significant differences in the rates of growth at different measurement positions. Between <6 month old individuals and 7-10-month-old individuals, there is only a statically significant difference in the cortical area growth rate of the midshaft ($p = 0.035$), with the younger individuals exhibiting a faster rate of growth than the intermediate individuals. Between the intermediate (7-10 month) and oldest (11+ month) age group, the proximal, midshaft, and distal humerus all have statistically different rates of growth ($p < 0.004$ for each measurement position). Rate of growth in cortical area decreases in the 11+ age group at all three measurement positions.

3.3.1.4 | Medullary Area. Relative medullary area (MA) is distinct at each of the three measurement positions along the humerus with very little overlap of the 95% confidence intervals (Figure 3.5). Throughout infancy, relative medullary area increases across the length of the bone, most notably in the distal humerus. Ups and downs in the first ~9 months are followed by a steep increase in relative medullary cavity size between 10 and 24 months, most notably in the midshaft. There is a peak in relative medullary cavity size in all three positions along the humerus around 25 months. This peak is followed by a steady decline in MA. When standardized against humeral diaphyseal length, the proximal, midshaft, and distal humeral MA are distinct. In the proximal humerus, longitudinal growth is greater than MA growth in infants and young children. At midshaft, MA increases slightly faster than length for the first~2 years. For the distal humerus, the two are about the same, with MA increasing more quickly than diaphyseal length for the first ~10 months. At all three measurement positions, the rate of MA increase compared to diaphyseal length increase decreases drastically just before 2 years and continues throughout adolescence.

3.3.1.5 | Second moments of area. Maximum second moments of area increase quickly in infants along the humerus and reach a peak around 6 months (Figure 3.6). Between 6 and 12 months, SMA decrease across the humerus, followed by an increase between ~12 months and ~24 months. Throughout the rest of ontogeny, SMA at the proximal, midshaft, and distal femur grow in parallel to each other, with a few peaks throughout later childhood and early adolescence. There is a trough just prior to 50 months, followed by another increase. Linear regressions on log-transformed SMA values show that there is a statistically significant difference between the SMA growth rates between the <6-month-old and 7-10-month-old age groups (Figure 3.7). Between these two age groups, the proximal ($p = 0.009$), midshaft ($p < 0.00001$), and distal

humerus ($p = 0.0028$) increases in resistance to bending more quickly in younger, pre-crawling individuals than in those who are most likely to be crawling.

3.3.1.6 | Polar second moments of area. Polar second moments of area at all three measurement positions increase steadily with age for the first ~6 months of life (Figure 3.8). Proximal and midshaft second moments of area exhibit a peak around 7 months, followed by a decline until about 13 months. The distal humerus exhibits a similar peak a few months later, around 10 months, after which polar second moment of area declines for several months. Polar second moment of area then increases across the humerus after 12 months and decreases in rate of growth throughout toddlerhood. All three measurement positions converge between 32 and 50 months as polar second moment of area increases. Polar second moment of area levels off in the midshaft first at around 75 months, followed by the distal humerus and then the proximal humerus. Resistance to torsion is highest in the proximal humerus for the majority of individuals included in this study regardless of age. Similar to Imax, growth rates of J are similar across the three measurement positions in each age group (Figure 3.9). The only statistically significant difference is between the proximal and midshaft humerus in <6-month-old individuals ($p = 0.0018$). There are also statistically significant differences in growth rates between the youngest and intermediate age groups in the proximal ($p = 0.0077$), midshaft ($p < 0.00001$), and distal humerus ($p = 0.0029$).

3.3.2 | Femur

3.3.2.1 | Length. Femoral length for the NMDID sample follows the same pattern as CDC reference data from childhood growth (Figure 3.10). Total femoral length and diaphyseal length are very tightly correlated with age ($r^2 = 0.96$ for both total and diaphyseal length; Figure 3.11). Notably, femoral length is less tightly correlated with age in infants less than 12 months old ($r^2 = 0.74$). Additionally, correlation between femoral length and body weight increases through ontogeny, with infants(<12mo) showing a loose correlation between femoral diaphyseal length and weight ($r^2 = 0.46$), toddlers showing a tighter correlation ($r^2 = 0.69$), and older children showing a tight correlation ($r^2 = 0.93$). There is a statistically significant difference in femoral diaphyseal length between male and female newborns (<1 month, $p = 0.017$), but not for any other age group. Female femora grow in length more quickly in the first 10 months, after which male and female femoral lengths are very similar (Figure 3.12). These sexually dimorphic characteristics may be an artifact of poor sample sizes for female newborns, so additional research is warranted. Length increases more quickly within the first ~15 months, then decreases in rate of growth. Only one individual (age 1 month) exhibited proximal and distal epiphyses too small to be measured (<1mm). All other individuals had at least one secondary growth center present and large enough to be measured.

3.3.2.2 | Diaphyseal circumference. Femoral diaphyseal circumference in the proximal, midshaft, and distal femur develop in parallel throughout infancy, childhood, and adolescence (Figure 3.13). At all ages, distal femoral circumference is greatest, following by the proximal femur and then the midshaft. Diaphyseal circumference at all three positions increases quickly for the first 6 months, levels out for about 10 months, then increases again for all three measurement positions between 15 and 24 months. Over

the course of the rest of childhood and early adolescence, femoral diaphyseal circumference increases with age before leveling off around 125 months. Diaphyseal circumference continues to increase throughout childhood.

3.3.2.3 | Cortical area. Cortical area increases with age, height, and weight (r^2 = 0.59, 0.59, 0.66, respectively). Cortical area in infants and toddlers increases and exhibits multiple peaks in the first two years of life (Figure 3.14). Cortical area continues to increase at varying rates until ~140 months. Total cortical areas across the three femoral measurement positions are mostly similar and follow similar growth patterns, and the 95% confidence intervals overlap almost entirely throughout ontogeny. Overall, females have smaller cortical areas than males across the femur for the first year of life, after which female cortical area overtakes that of the males throughout the rest of childhood, although differences are not statistically significant. Cortical area increases throughout childhood and peaks between 125 and 150 months of age. There are no significant differences in growth rate between proximal, midshaft, and distal cortical area in any of the three age groups (Figure 3.15). There are no significant differences between the growth rate of the two youngest groups, but all three measurement positions show significantly faster growth rate in the youngest group compared to the 11+ month old group ($p < 0.0001$ for all).

3.3.2.4 | Medullary Area. Relative medullary cavity size is significantly lower in the midshaft than the proximal and distal femur ($p < 0.001$; Figure 3.16). Distal femoral medullary area increases at a steadier rate in infants younger than 6 months than proximal or midshaft medullary area. In older children, distal medullary cavity area remains relatively large while midshaft and proximal medullary cavity area decrease over time in older individuals.

3.3.2.5 | Second moments of area. Contrary to the growth pattern seen in the humerus, the distal femur has the greatest resistance to bending and overall strength in infants, though 95% confidence intervals overlap considerably (Figure 3.17). The proximal femur is the next strongest in the early months of life, followed by the midshaft. Natural log-transformed growth rates show no significant differences between growth rates within an age group. 11+ month old individuals have significantly slower I_{max} growth rates than the <6-month-old group, but there are no significant differences between the oldest or youngest group and the intermediate group (Figure 3.18). This may be due to small sample sizes of individuals 7-10 months of age.

3.3.2.6 | Polar second moments of area. Polar second moments of area increase with age at all three measurement positions between 0 and 10 months of age (Figure 3.19). At 50 months, resistance to torsion begins to increase notably, which continues throughout the rest of ontogeny. The 95% confidence intervals overlap almost entirely throughout ontogeny. The femoral midshaft *J* increases at a significantly faster rate than the distal femur, in the youngest group ($p = 0.0001$) and in the 11+ month-old group ($p = 0.017$). Growth rate in midshaft J is significantly higher in the 7-10 month-old-group than the <6-month-old group ($p = 0.03$). While there are no other significant differences between adjacent groups, all three measurement positions grow more quickly in the

youngest group compared to the oldest group ($p < 0.05$ for all measurement positions; Figure 3.20).

3.4 | Discussion

Human long bones are known to grow at different rates at different positions along each bone, both *in utero* and throughout postnatal ontogenetic growth (Moss et al., 1955; Gray and Gardner, 1969; Bass et al., 2002; Cunningham, Scheuer, & Black, 2016). Moss et al. (1955) first established that long bone distal limb segments grow relatively faster than the proximal segments, though this observation was based on diaphyseal length and not cross-sectional properties.

> *Question 1:* Are there measurable differences in cortical properties in the portions of the humerus and femur that contribute the most to longitudinal growth?

Yes, there are measurable differences in the proximal humerus but not the distal femur, though there is a notable amount of overlap in almost all of the 95% confidence intervals from this data set. While this indicates that many patterns are undetectable in this sample, there are a few patterns that are clear. Future work should focus on increasing sample sizes to better understand variation and overall patterns, especially in infants.

Results from the humerus show measurable differences in the cortical properties of the proximal humerus, which contributes more to longitudinal growth than the distal humerus. The proximal portion of the bone grows significantly faster in I_{max} and J than the midshaft (Figures 3.4 and 3.5). Of particular interest is the growth in MA in the proximal humerus. While the slower rate of growth in MA is visible in the left panel of Figure 3.3, the difference between the proximal, midshaft, and distal humerus in the relative size of the medullary cavity is notable in the right panel of Figure 3.3. Relative medullary cavity size is distinct in the three sections of the humerus, but when standardized against humeral length, the proximal humerus is the only one that is increasing in relative size more slowly than the bone is growing in length. In other words, the humerus is getting longer faster than the proximal medullary cavity is growing. This may be because the proximal epiphysis is responsible for a disproportionate amount of growth in the length of the humerus, though it may also be impacted by loading from shoulder musculature.

The distal femur, which is responsible for the majority of longitudinal growth of the femoral diaphysis, does not exhibit any cross-sectional properties that distinguish that region from the midshaft or proximal femur. The distal femur does however show the most overall resistance to bending and torsion (Figures 3.15 – 3.18). This is likely because the distal femur undergoes the largest mean loading during running of any part of the femur (Edwards, Gillette, Thomas, & Derrick, 2008). Since the resistance to bending and torsion of the distal femur is already greater than the midshaft and proximal femur perinatally, it is unlikely a direct response to biomechanical loading from the knee musculature, but may indicate an evolutionary adaptation to obligate bipedality.

Future investigations of this question should increase sample sizes and explore the cortical properties of non-human primates to elucidate the effect of bipedalism on cross-sectional properties across the humerus and femur.

Question 2: Is there any evidence from cross-sectional properties that endosteal bone formation is contributing to cortical growth?

Yes, most notably in the proximal humerus. Crawling stance in children is usually accompanied by a relatively stiff elbow and more engaged, mobile shoulder (Rightetti, Nylen, Rosander, & Ijspeert, 2015), which results in more loading from the shoulder musculature than the elbow musculature. Thus, during crawling, the proximal humerus is undergoing more biomechanical loading from the shoulder musculature than the distal humerus. This loading pattern may also explain the pattern of decrease and increase in MA in the proximal humerus (as well as the midshaft and distal humerus) around 10 months of age, when babies typically begin standing and walking bipedally (Figure 3.3). Leading up to this locomotor development, relative MA decreases as the shoulder is loaded during crawling and scooting, whereas MA begins to increase again around 10 months when the arm begins to undergo less loading from crawling. The relatively slow growth of the proximal medullary cavity (Figure 3.3, right panel) also suggests that there endosteal bone formation is taking place, and supports the findings of Maggiano et al. (2016).

Though the results of Moss et al. (1995) are based on diaphyseal lengths and not cross-sectional properties, their conclusions appear to be supported by the data presented here in multiple cross-sectional properties of the femur. Relative medullary cavity area reaches a trough around 10 months of age, which correlates with the onset of bipedal standing and walking. This suggests that there is either a slowdown in the rate of endosteal resorption or an increase in endosteal formation during this time, which is potentially impacted by the mechanical loading of femora during the beginnings of bipedal locomotion. Notably, there is also a change in femoral length around 10 months of age. Infants younger than 10 months show very little correlation between standardized femoral length (femoral diaphyseal length / body length) and age, weight, and length (r^2 = 0.19, 0.006, and 0.18, respectively). In the entire sample, the correlation between standardized femoral length and age, weight, and length, are much higher (r^2 = 0.82, 0.78, and 0.83, respectively).

Question 3: Are there any sex differences in the growth of the humerus and femur along the diaphysis?

While there is no statistically significant sexual dimorphism in most of the traits investigated in this study, there are a few traits that stand out. The humerus shows no statistically significant differences between males and females in any trait investigated. However, perinatal females have significantly shorter femora than males. When standardized for body length, this dimorphism is clearly visible (Figure 3.12), as is the relatively faster rate of femoral growth in females than males in the first ~7 months. While the dimorphism gradually disappears during early ontogeny, female femora grow more quickly than male femora between 50 and ~100 month. Beyond 100 months, sample sizes for females are very small, so the effect of sex is not clear in older children and adolescents. Females also have smaller cortical areas than males around birth, but surpass males at all three measurement positions by ~15 months. Increasing sample sizes of younger individuals will add clarity and determine if this pattern is a result of sampling.

3.5 | Conclusions

The results presented here show that there are some cross-sectional and longitudinal length changes within the humerus and femur around the onset of crawling and walking. The proximal

humerus appears to be more affected by endosteal bone formation than other parts of the humerus, which may be due to increased loading from shoulder musculature during crawling. The femur also shows some changes around the average onset of walking, particularly in standardized femoral length and medullary area. Most sex differences are miniscule, especially in the humerus.

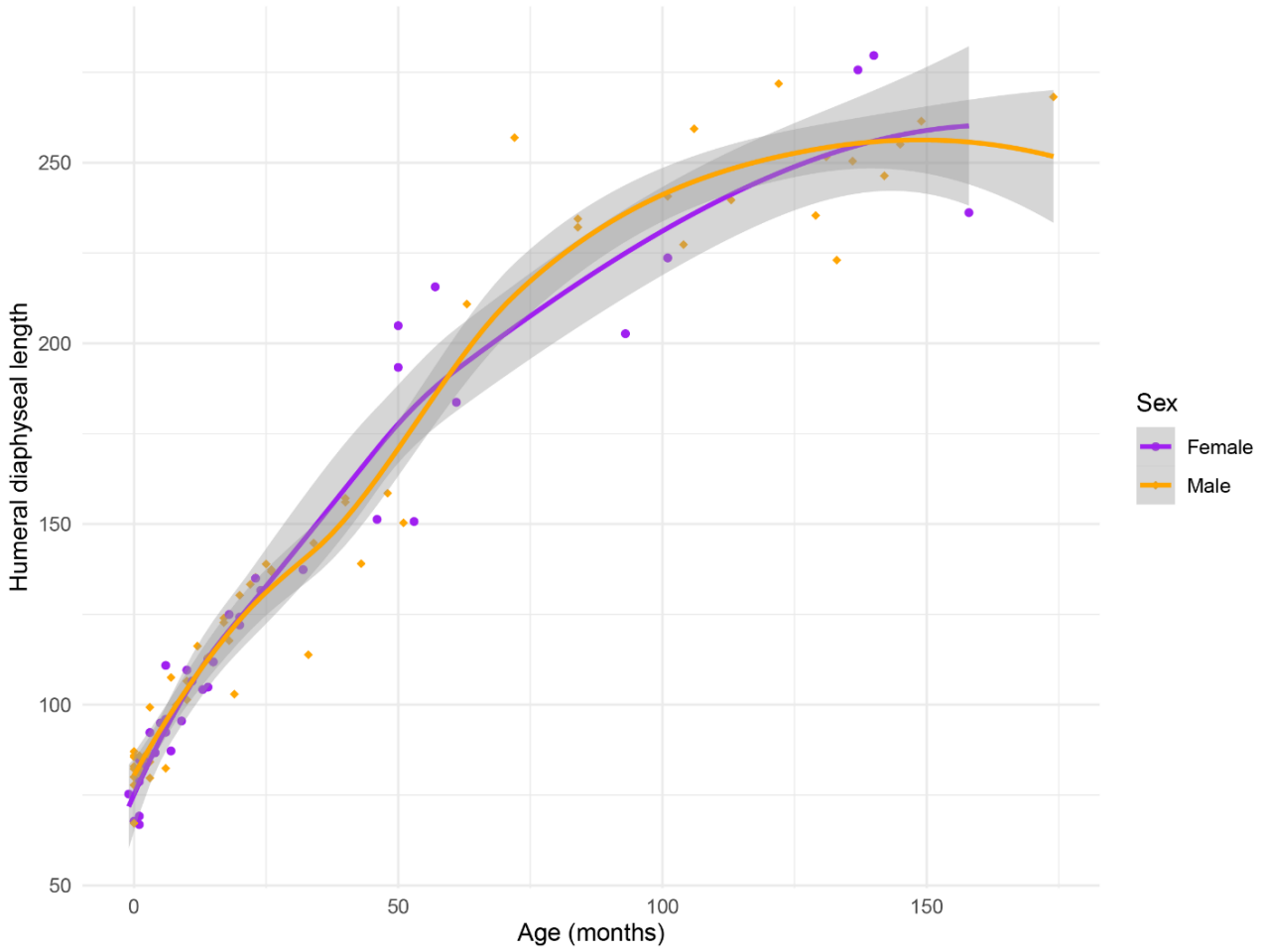


Figure 3.1. Humeral diaphyseal length (mm).

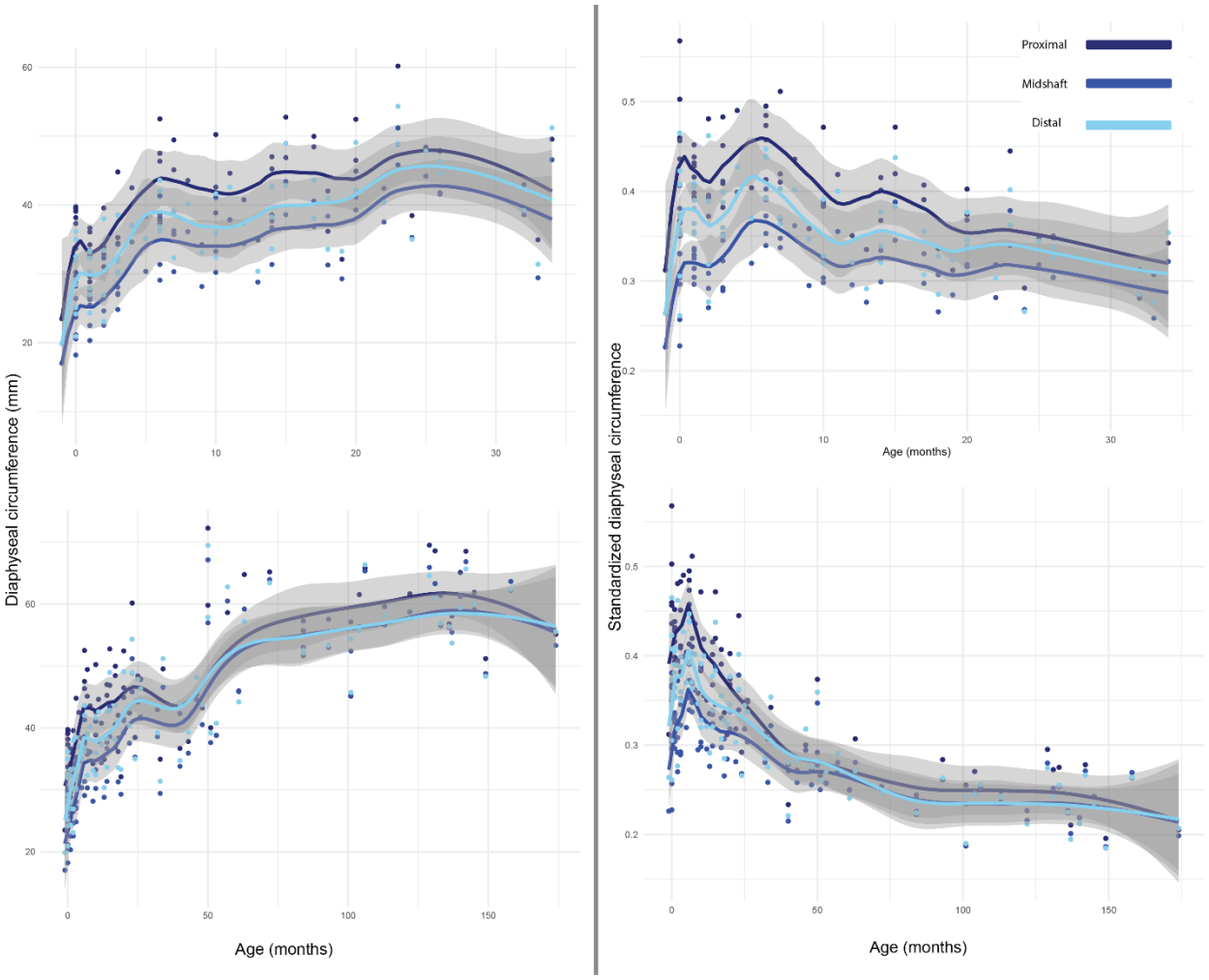


Figure 3.2. Humeral diaphyseal circumference. Top panels - infants aged 0 – 40 months. Bottom panels - All individuals. Left side shows absolute measurements (in millimeters), right side shows measurements standardized by humeral length. Grey areas indicate a 95% confidence interval.

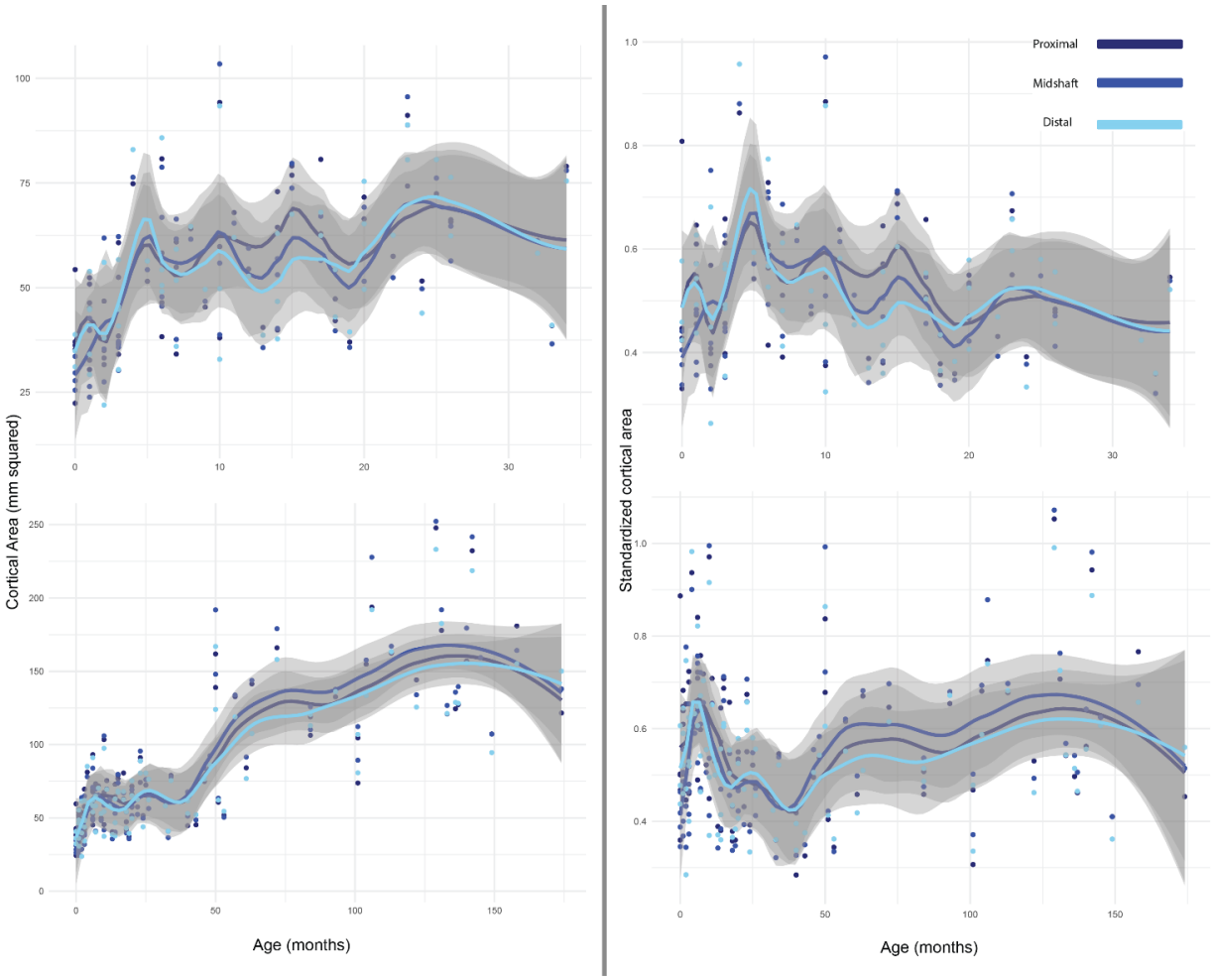


Figure 3.3. Humeral cortical area. Top panels - infants aged 0 – 40 months. Bottom panels - All individuals. Left side shows absolute measurements, right side shows measurements standardized by humeral length. Grey areas indicate a 95% confidence interval.

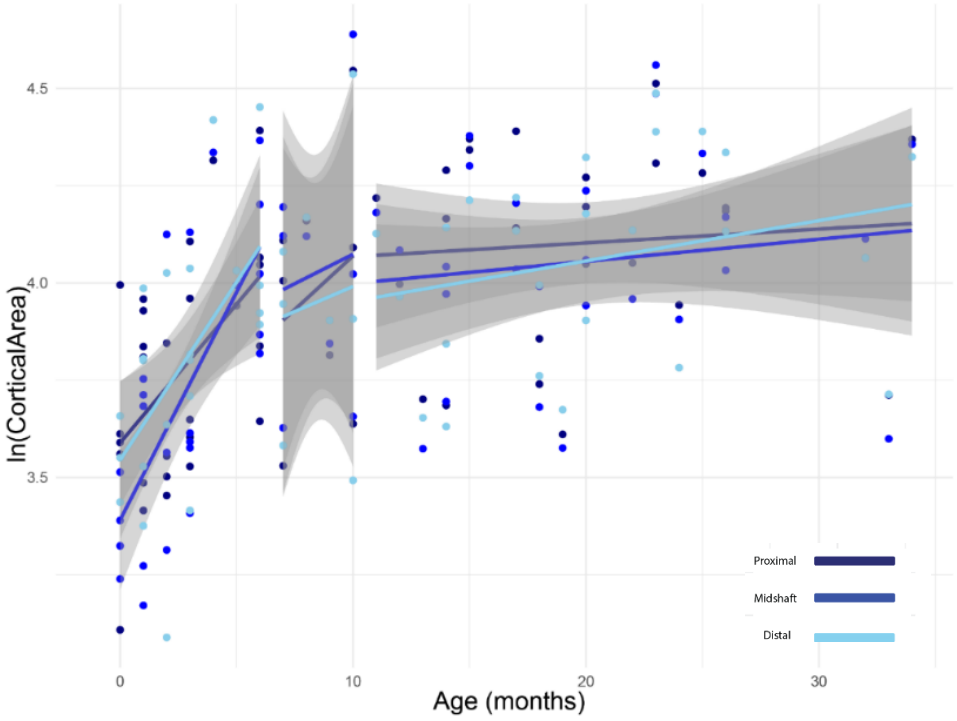


Figure 3.4. Linear regression on natural log-transformed values of cortical area in infants (0-6 months), 7–10-month-old individuals, and 11+ month old.

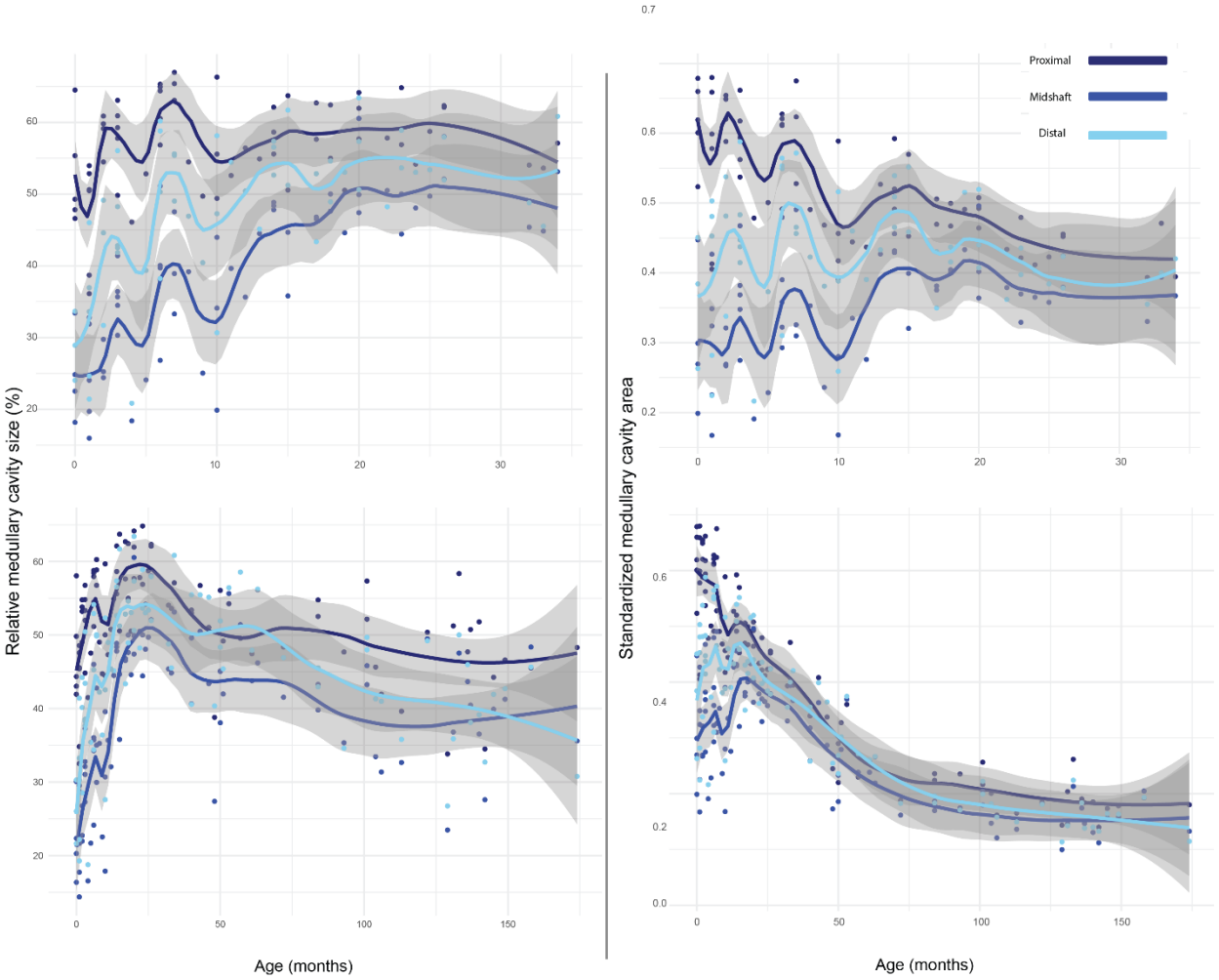


Figure 3.5. Humeral relative medullary cavity area. Top panels - infants aged 0 – 40 months. Bottom panels - All individuals. Left side shows absolute measurements, right side shows measurements standardized by humeral length. Grey areas indicate a 95% confidence interval.

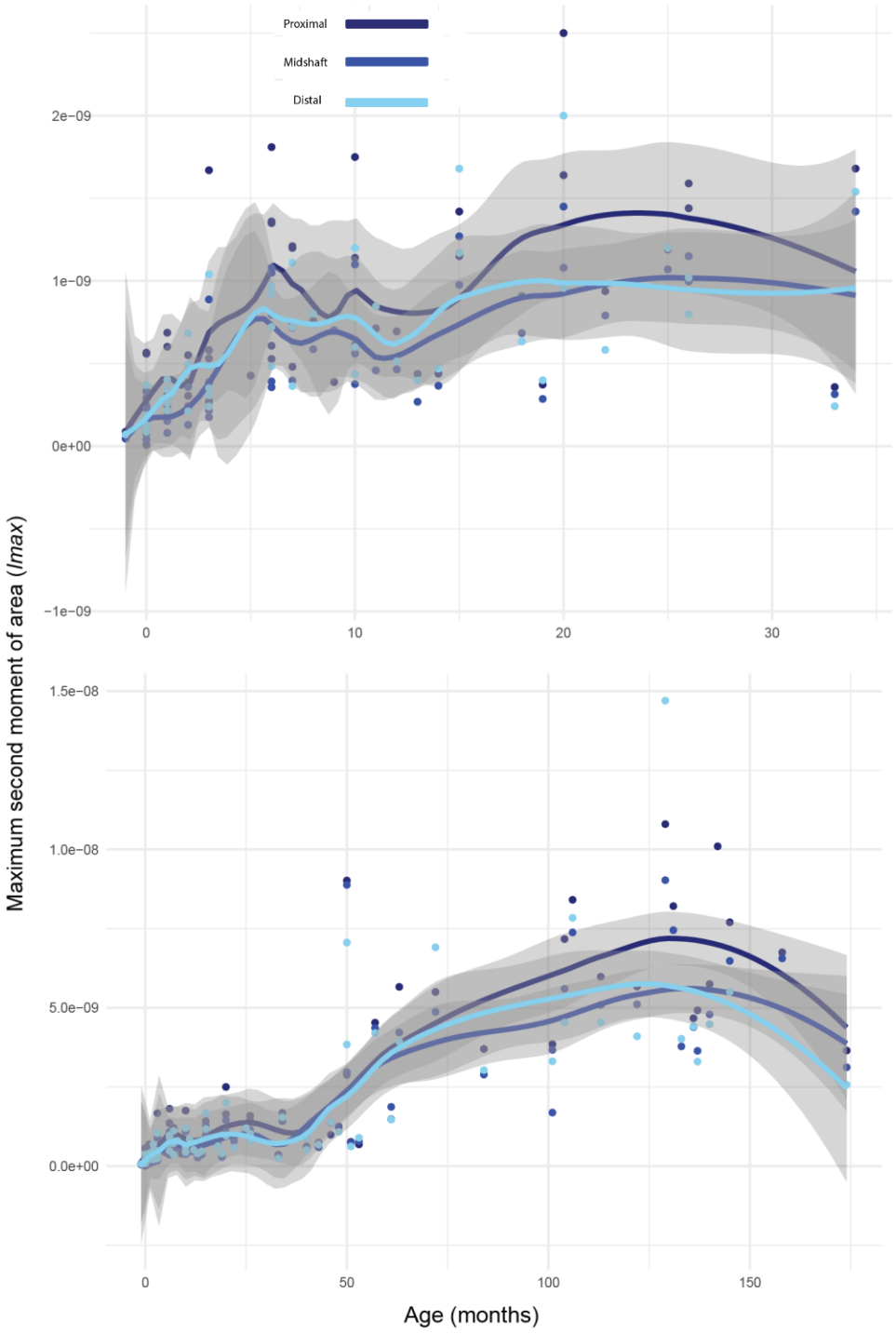


Figure 3.6. Humeral maximum second moment of area (resistance to bending). Top: infants aged 0 – 40 months. Bottom: all individuals. Grey areas indicate a 95% confidence interval.

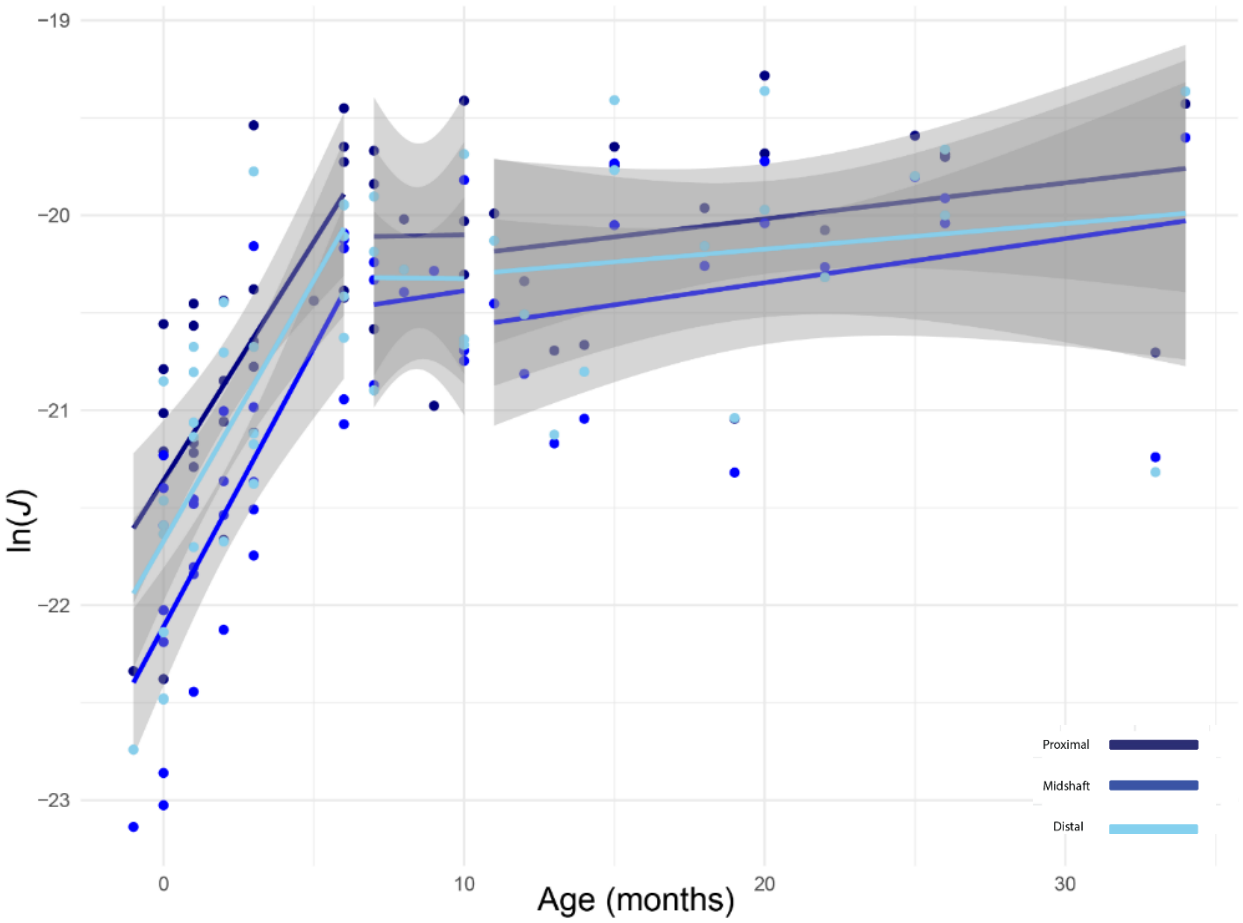


Figure 3.7. Linear regression on natural log-transformed humeral polar second moment of area (resistance to torsion). Grey areas indicate a 95% confidence interval.

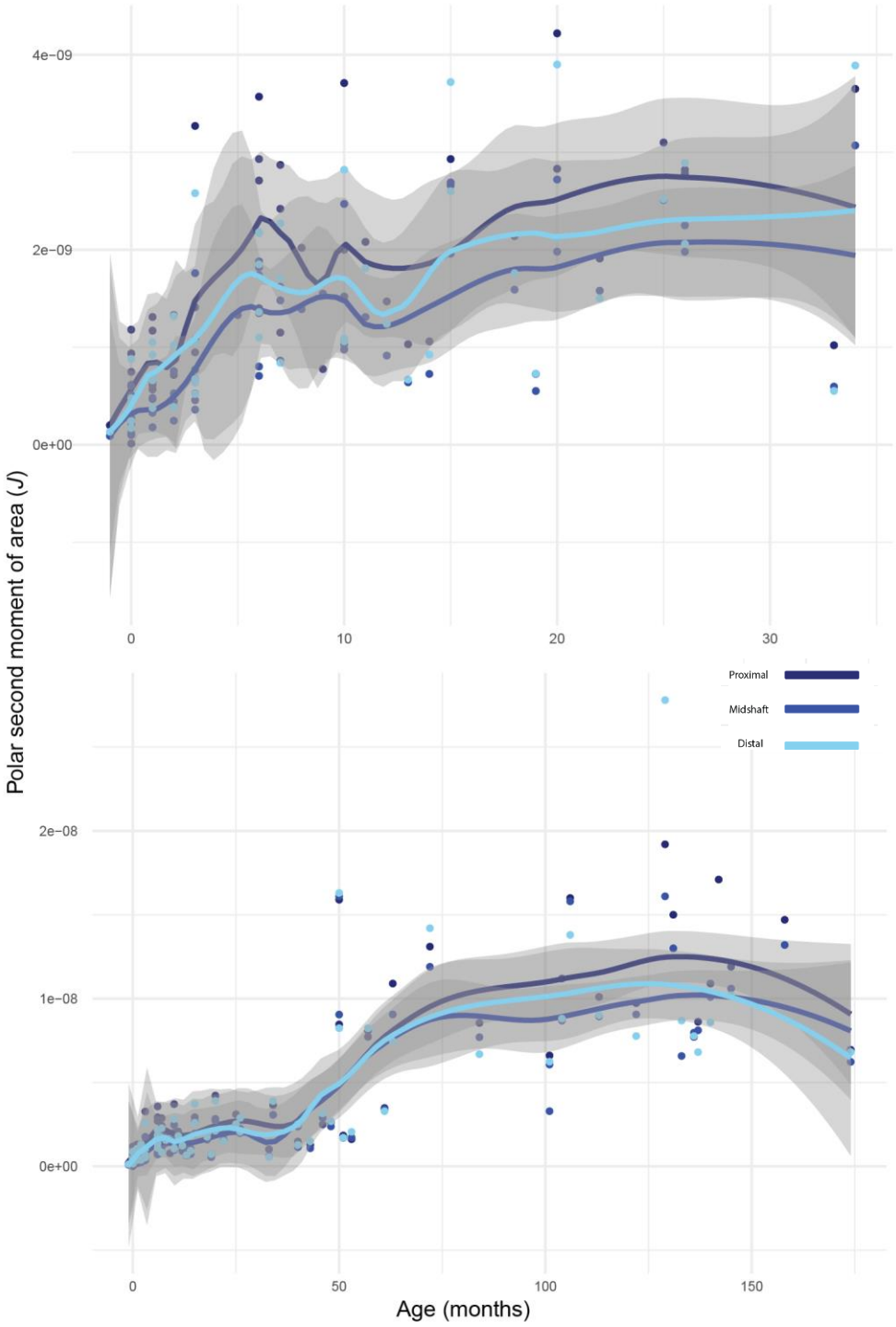


Figure 3.8. Humeral polar second moment of area (resistance to torsion). Top: infants aged 0 – 40 months. Bottom: all individuals. Grey areas indicate a 95% confidence interval

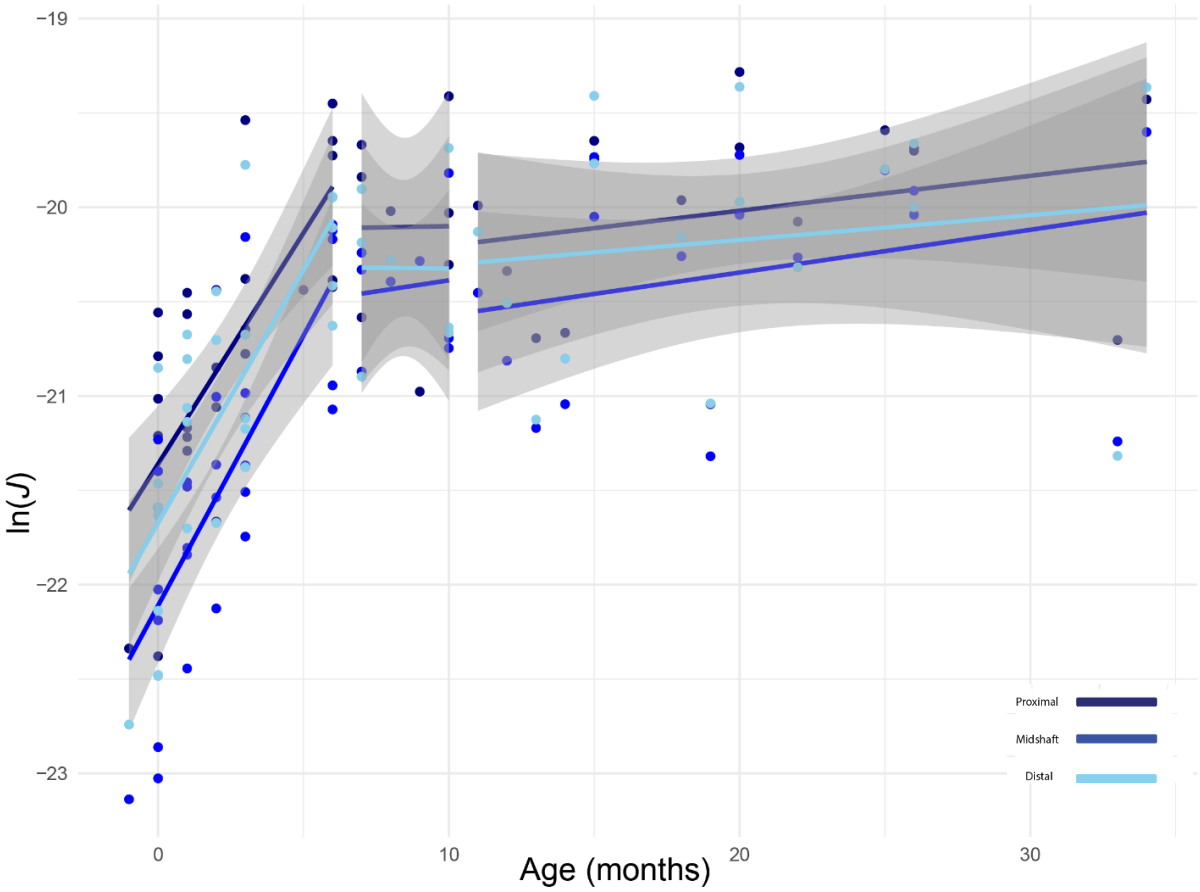


Figure 3.9. Linear regression on natural log-transformed humeral polar second moment of area (resistance to torsion). Grey areas indicate a 95% confidence interval.

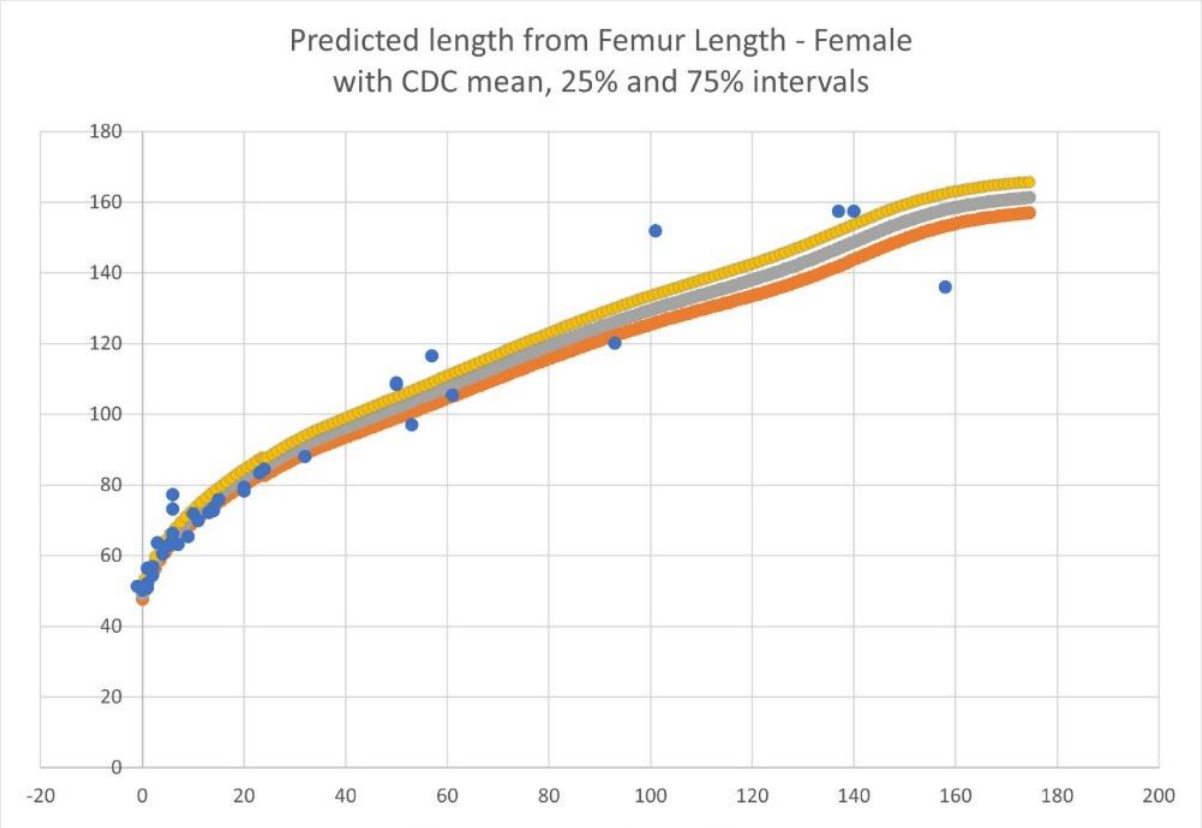


Figure 3.10. NMDID individuals (blue dots) plotted on CDC growth chart. Yellow is 25%, grey is 50%, and orange is 75% intervals.

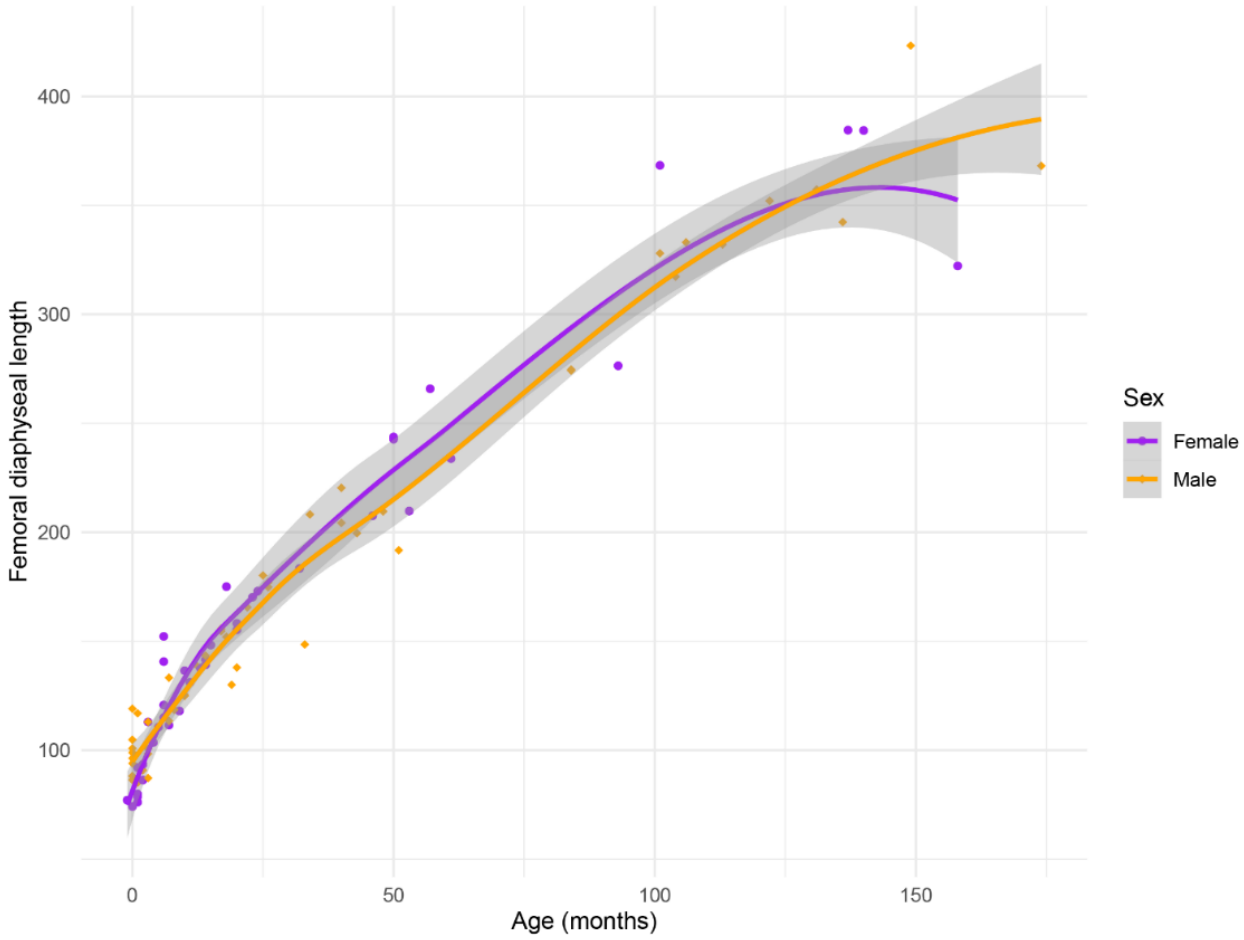


Figure 3.11. Femoral diaphyseal length in millimeters.

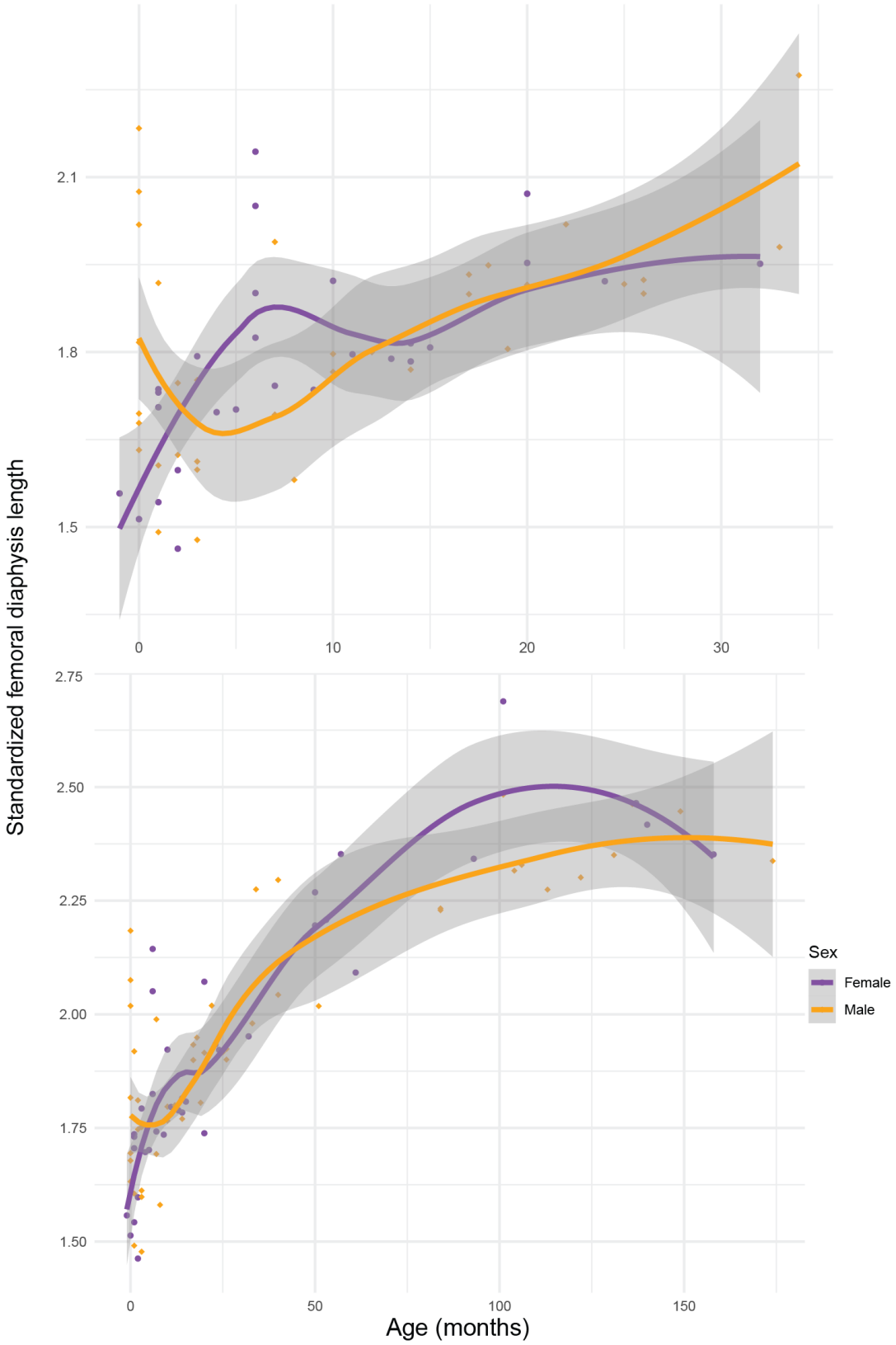


Figure 3.12. Standardized femoral diaphysis length in babies (top) and all individuals (bottom). Femoral diaphysis length was standardized by cadaver length.

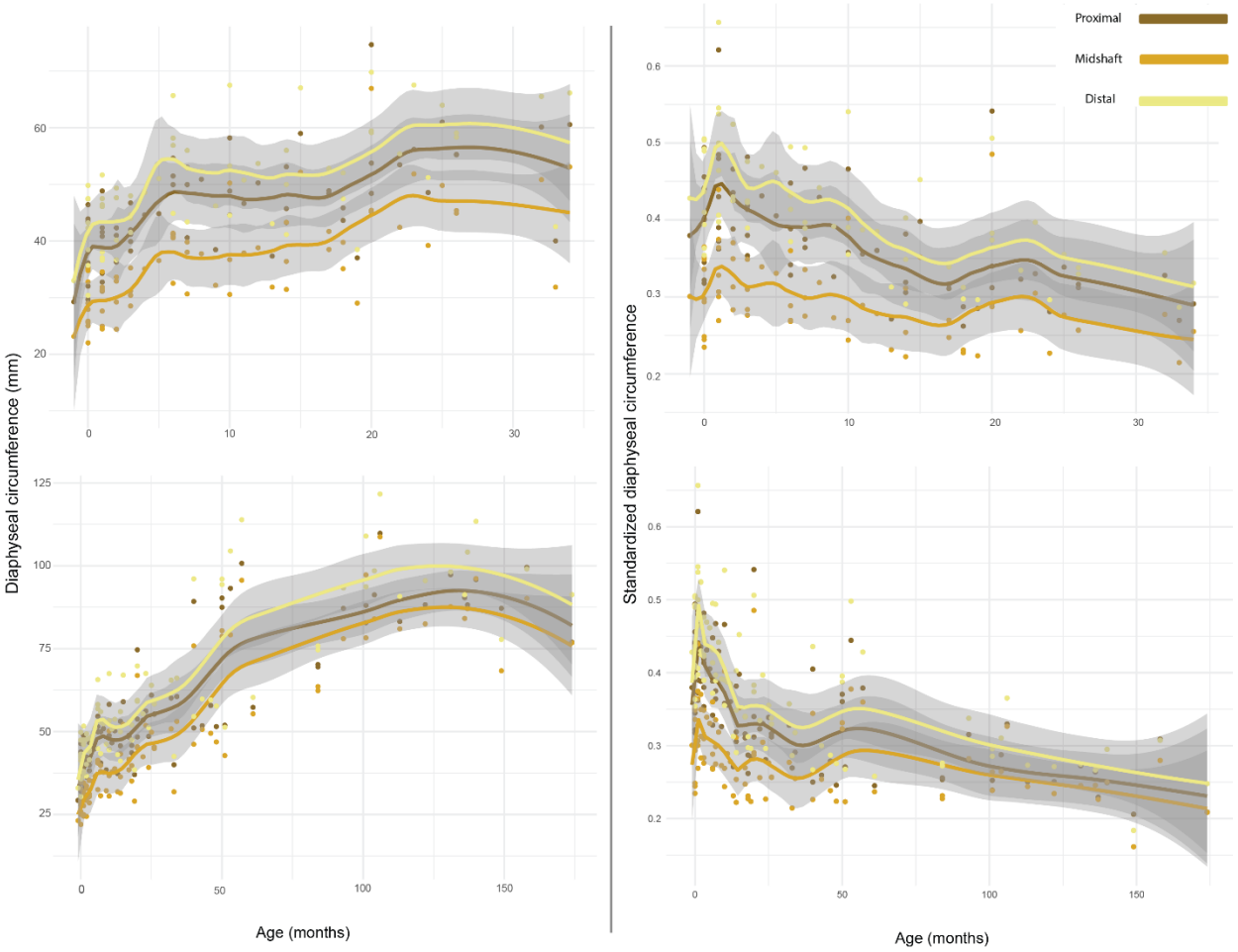


Figure 3.13. Femoral diaphyseal circumference. Top panels - infants aged 0 – 40 months. Bottom panels - All individuals. Left side shows absolute measurements, right side shows measurements standardized by femoral length. Grey areas represent a 95% confidence interval.

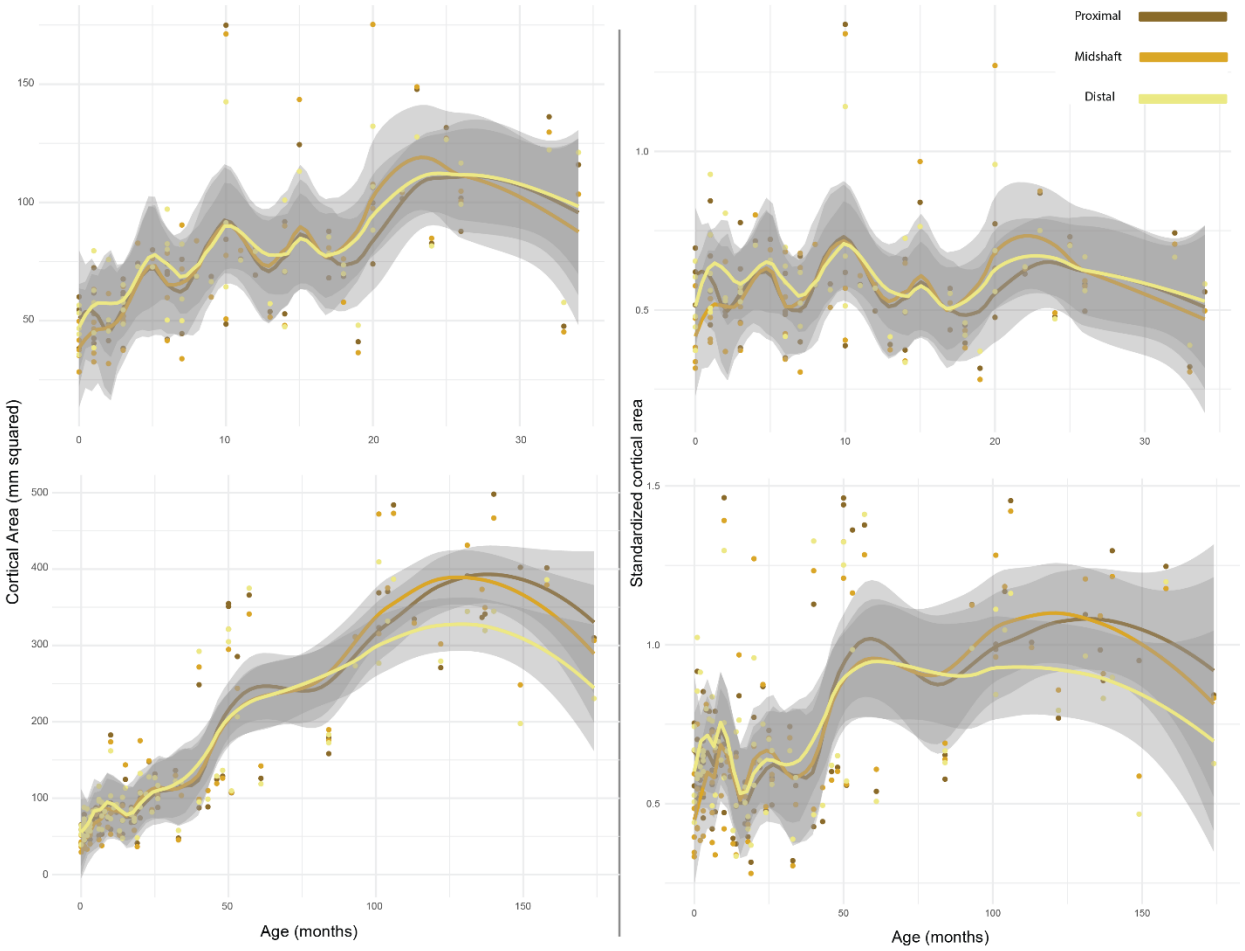


Figure 3.14. Femoral cortical area. Top panels - infants aged 0 – 40 months. Bottom panels - All individuals. Left side shows absolute measurements, right side shows measurements standardized by femoral length. Grey areas represent a 95% confidence interval.

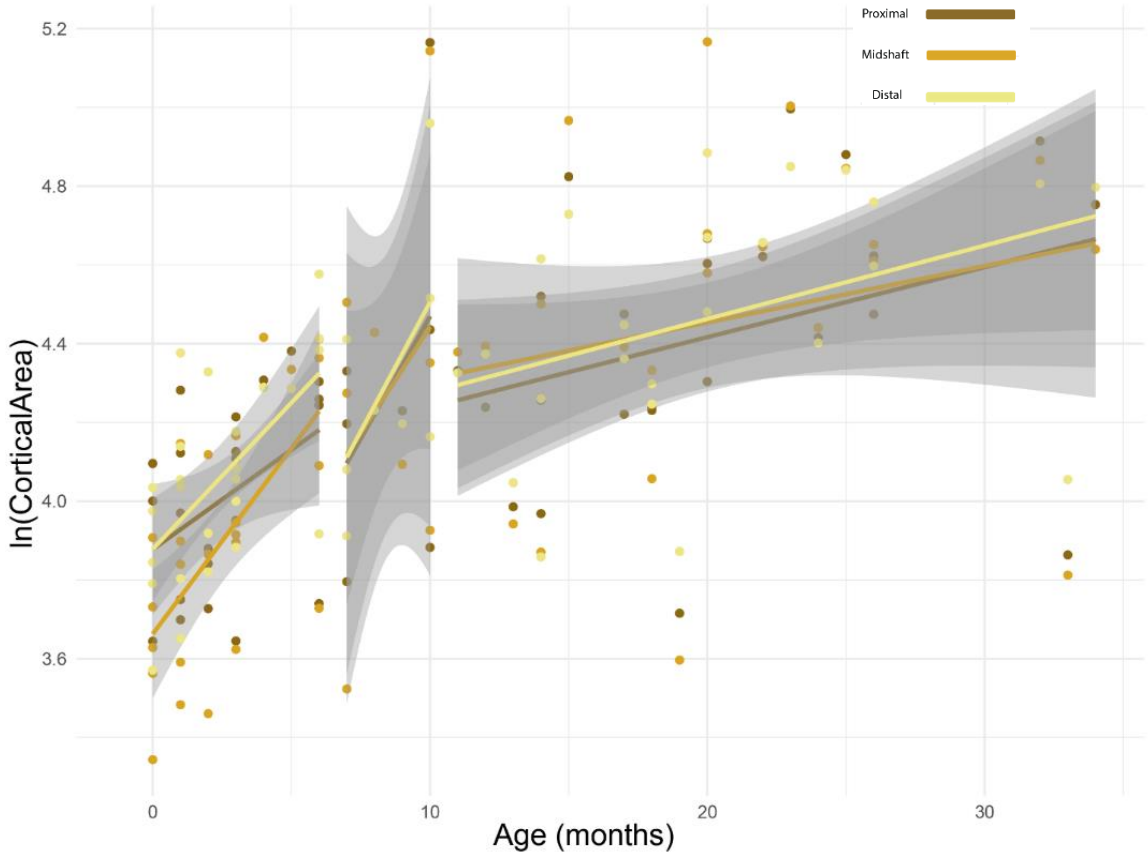


Figure 3.15. Linear regression on natural log-transformed values of femoral cortical area in infants (0-6 months), 7–10-month-old individuals, and 11+ month old individuals. Grey areas indicate a 95% confidence interval.

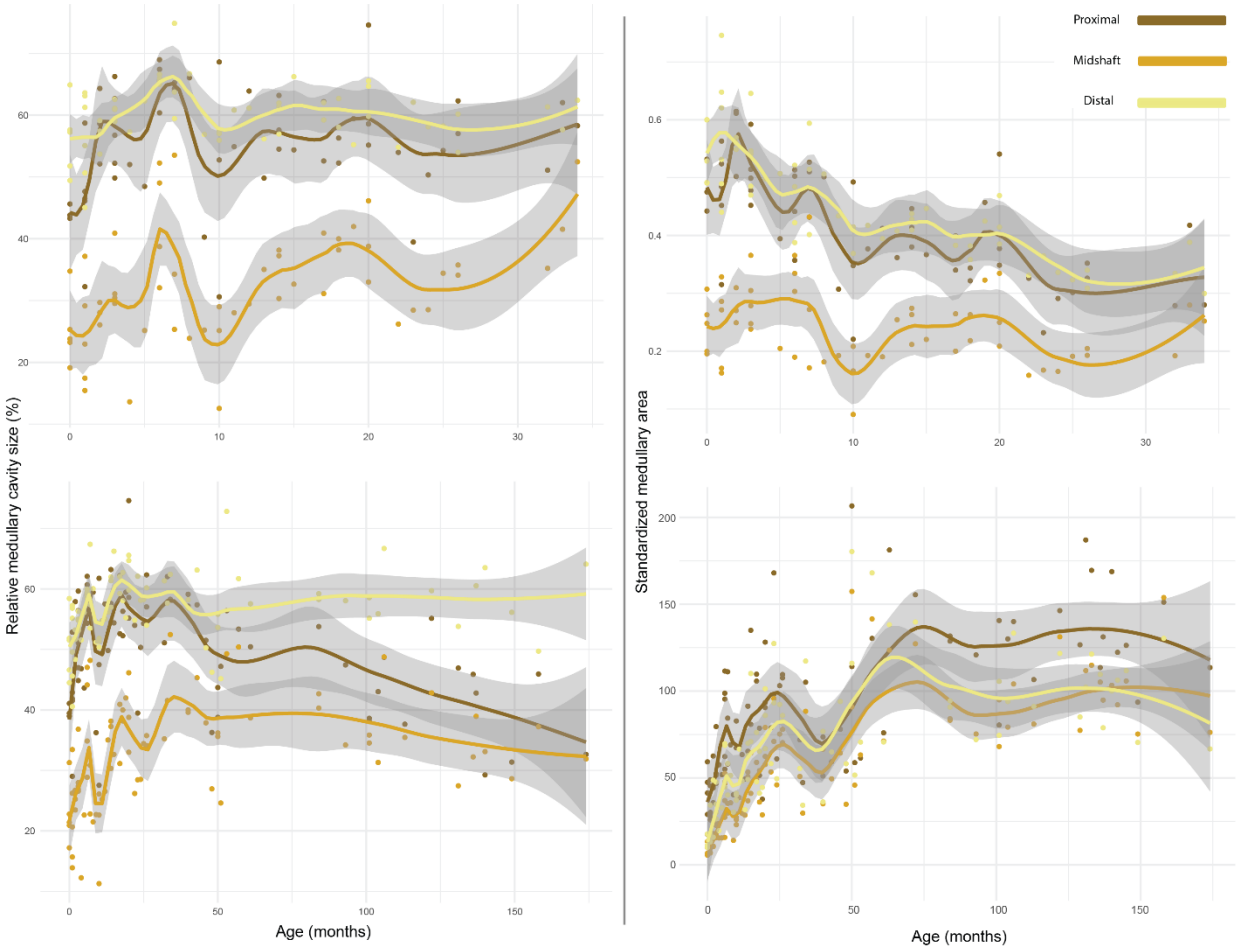


Figure 3.16 Femoral medullary area. Top panels - infants aged 0 – 40 months. Bottom panels - All individuals. Left side shows absolute measurements, right side shows measurements standardized by femoral length. Grey areas represent

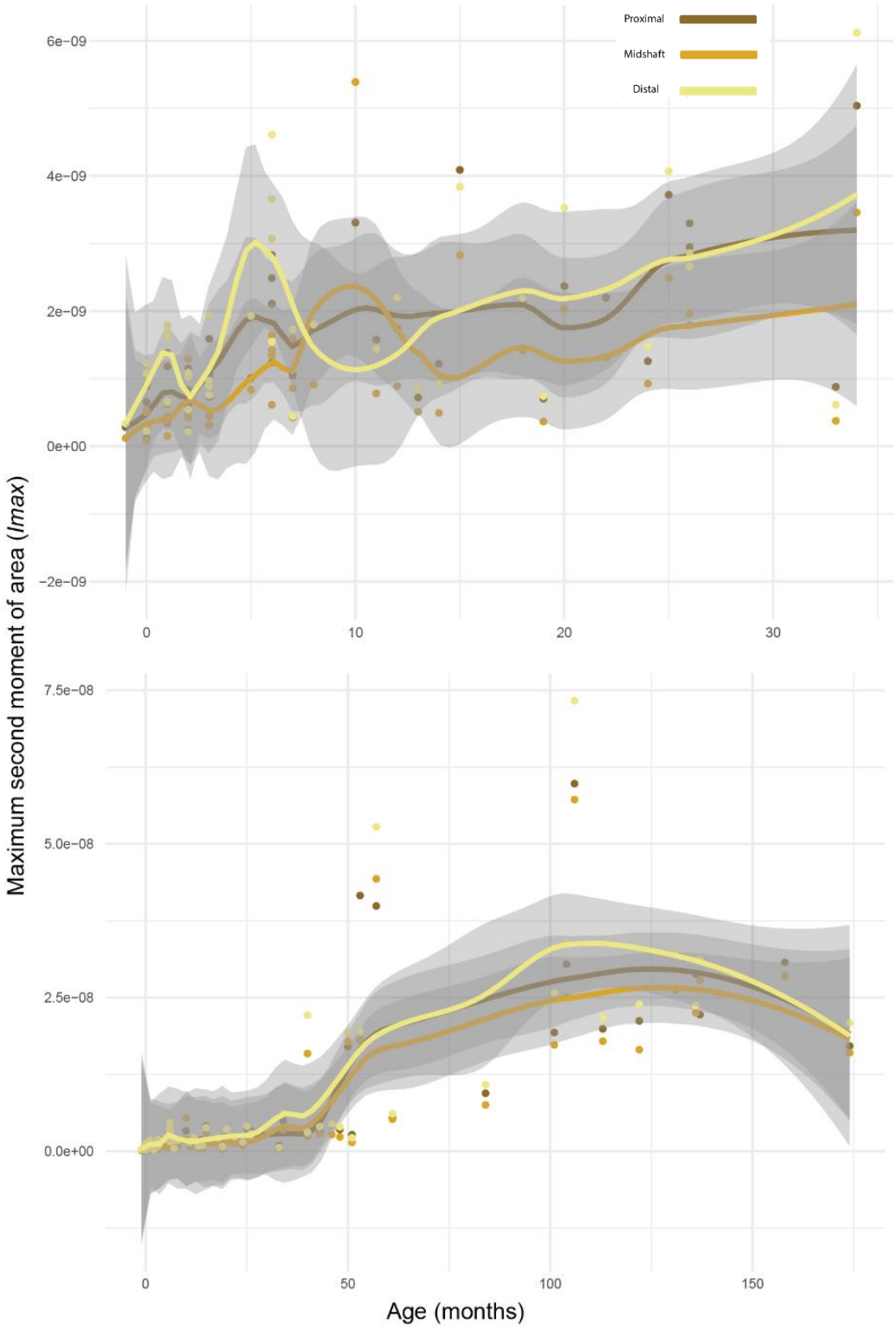


Figure 3.17. Femoral maximum second moment of area (resistance to bending). Top: infants aged 0 – 40 months. Bottom: all individuals. Grey areas represent 95% confidence intervals.

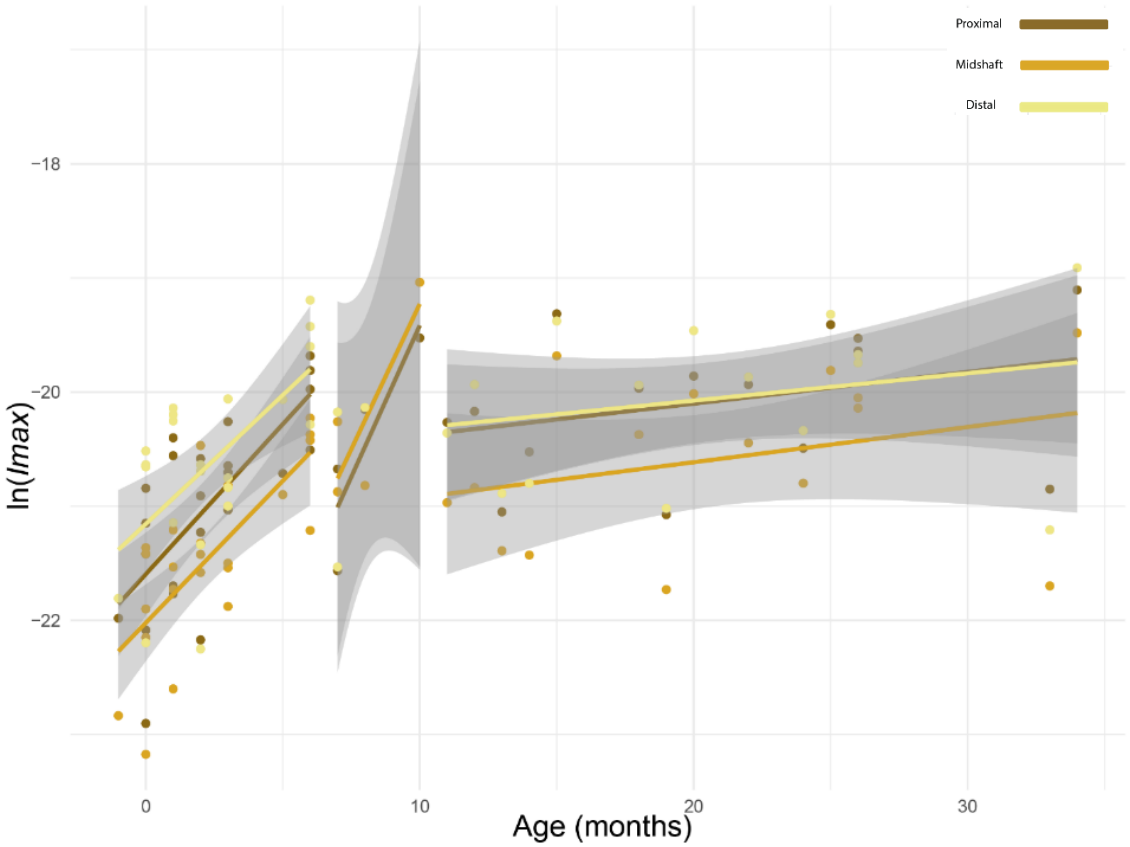


Figure 3.18. Linear regression on natural log-transformed values of femoral second moments of area in (0-6 months), 7–10-month-old individuals, and 11+ month old individuals. Grey areas indicate

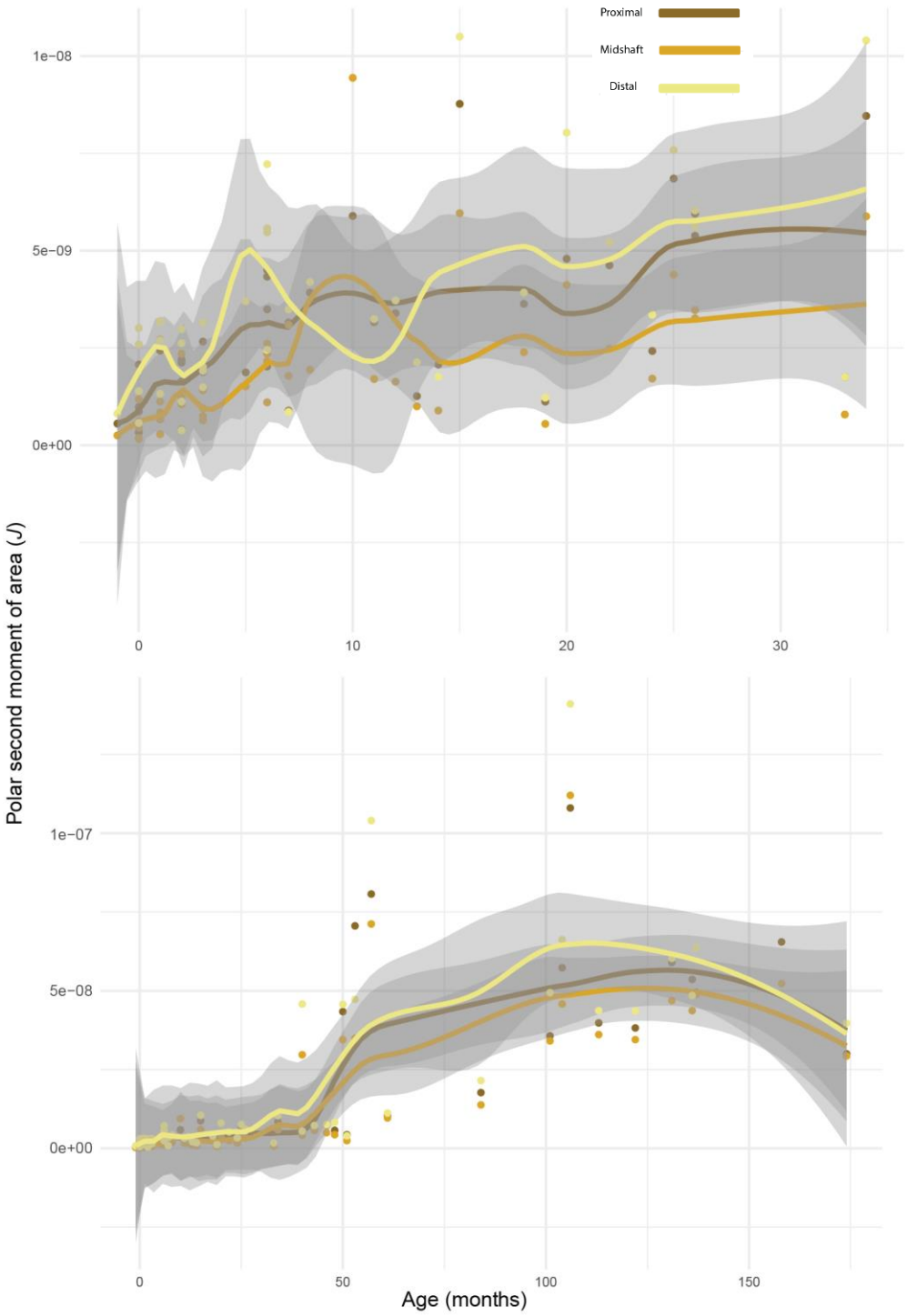


Figure 3.19. Femoral polar second moment of area (resistance to bending). Top: infants aged 0 – 40 months. Bottom: all individuals. Grey areas indicate a 95% confidence interval.

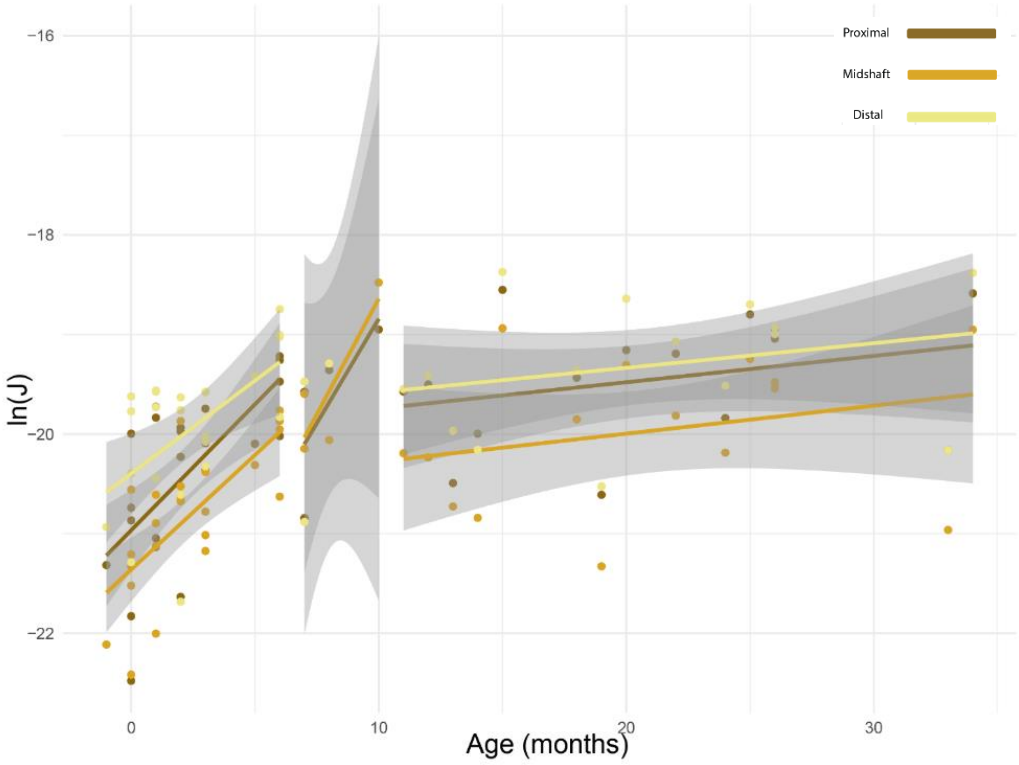


Figure 3.20. Linear regression on natural log-transformed values of femoral polar second moments of area in (0-6 months), 7–10-month-old individuals, and 11+ month old individuals. Grey areas indicate a 95% confidence interval.

Chapter 4: Inter-element growth and development

4.1 | Introduction

The humerus and femur are central to an understanding of locomotion, even for bipedal humans due to the involvement of both the fore and hind limbs in the early stages of childhood locomotion. Most human babies employ some form of prewalking mobility such as crawling, scooting, or rolling (Robson, 1970; Robson, 1985; Largo et al., 1985; Bottos et al., 1989; Fox et al., 2002; Patrick et al., 2012). About 85% of infants utilize a "hands and knees" crawling strategy prior to the onset of walking (Robson, 1984; Størvold, Aarethun, & Bratberg, 2013).

These prewalking, intermediate forms of locomotion are highly variable, and the time of onset often has a cultural component to it (Super, 1976; Hopkins & Westra, 1989; Adolph, Vereijken, & Denny, 1998; Karasik et al., 2015). For example, infants growing up in urban China begin crawling and walking 6-8 weeks after their American counterparts, on average, likely because of cultural differences around allowing toddlers to roam freely (Chen et al., 1998; Jia, Zhang, Trindade, & Sobko, 2013; Zhang, Li, Wu, & Zong, 2018). Infants in rural Papua New Guinea spend up to 86% of their time being held or carried in the first 12 months of life and rarely exhibit a hands-and-knees crawling behavior, but often scoot instead (Tracer & Wyckoff, 2020). Infants who are encouraged to walk through gentle postural training or daily encouragement to stand exhibit an earlier onset of independent walking (Zelazo, Zelazo, & Kolb, 1972; Lobo & Galloway, 2012). This is likely why cultures that actively encourage infant mobility have babies that start walking earlier, on average (Adolph et al., 2019).

There is some evidence that aspects of the cross-cultural variation in the onset of crawling and walking stems from variation in things like nutritional variation or diaper practice among different cultural groups (Angulo-Barroso et al., 2010; Cole, Lingeman, & Adolph, 2011). Atun-Einy et al. (2013) also found that season of birth may affect motor development in infants, including onset of walking. Prior to the development of whatever initial mode of locomotion a baby uses, all infants are doing relatively the same things with their limbs. At birth, neonates typically have the ability to move their limbs and grasp objects with their hands. Regardless of cultural background, the grasping reflex and purposeful movement of an infant's arms are typical among newborns (van der Meer et al. 1995; Futagi et al., 2011).

The CDC places the onset of crawling in US babies between 6 and 9 months of age, with most babies exhibiting the ability to stand bipedally and begin walking by 12 months of age (CDC, 2022). These data are supported by outside studies that indicate that crawling on stomach or hands and knees usually begins between the 6^{th} and 9^{th} month, cruising usually in the 9^{th} month, and bipedal walking in the 11^{th} month (Malina, 2004; Adolph, Berger, & Leo, 2011).

The relative strength and growth trajectories of different bones are key parts of understanding overall bone growth and locomotor development in infants. In typical hands and knees crawling, the humerus and femur are both contributing to locomotion and undergoing biomechanical loading from body weight. In a longitudinal study of 20 children, Ruff (2003a) found that humeral to femoral length proportions in infants are close to those of adults, but humeral to femoral strength proportions change throughout early childhood. Ruff (2003a, 2003b) also found that adult femoral/humeral strength proportions were not seen in children less than 1 year of age, but adult-like strength proportions seem to develop after the onset of bipedal walking. However, none of the individuals included in the study were measured prior to 6 months of age. There is

also evidence that toddlers have significantly higher mediolateral forces acting upon their femora than adults, which is correlated with the biomechanical influences of the "waddling" that is classic of an immature bipedal gait (Cowgill et al., 2010).

Although these previous studies suggest a change in fore- and hind-limb strength during the transition from prewalking locomotion to bipedal walking, some gaps in knowledge remain. In this study, measurements from the humerus and femur are compared to better understand the similarities and differences in growth patterns of these two long bones. Comparisons are made between homologous positions on the two bones (e.g., the proximal measurement position on both bones). The NMDID dataset is used to answer the following questions:

> *Question 1:* Are there statistically significant differences between humeral and femoral growth throughout infancy and childhood?
>
> *Question 2:* Do the observed growth patterns broadly correlate with the onset of crawling and walking?

These questions are investigated using humeral and femoral cross-sectional measurements from 100 individuals from birth to 14 years of age.

4.2 | Materials and Methods.

4.2.1 | Materials. This study uses data collected from 100 infants and children ranging in age from third trimester (pre-natal) to 14 years old. The upper limit of age was determined by the eruption of the second molar (i.e., none of the individuals included have erupted second molars). Scans of all individuals were downloaded from the New Mexico Decedent Imaging Database. All individuals included in this study died in New Mexico between 2010 and 2017 and are listed in Appendix 1. Individuals were excluded if they had a recorded history of bone fracture, musculoskeletal disease or deformation, or traumatic circumstances of death that would distort skeletal material (i.e., car accidents, skeletal trauma).

4.2.2 | Data Collection Methods. CT scans were downloaded from the NMDID (Edgar et al., 2019) and imported into Dragonfly 2020.1 beta (Dragonfly 2020.1). Linear measurements of total bone and diaphyseal lengths were taken from the right side of the body. Measurements at each measurement position (25%, 50%, and 75% of diaphyseal length) were collected for each individual and are described in Chapter 2.

Long bones were segmented manually. Density thresholds for cortical bone were determined based on the cortical bone of the right humerus. Segmented long bones were then resampled individually. Maximum and minimum second moments of area (I_{min} and I_{max}, respectively), polar second moments of area (J), and Ixx and Iyy were calculated by the Dragonfly software from the resampled segmented bones using the Slice Analysis tool.

Collecting data from medical CT scans raises the possibility that the quality of the scan could differentially introduce bias based on the size of the person. The smaller overall size of younger individuals results in lower resolution medical CT scans. See Chapter 2 for description of how poor resolution affects measurement error. The same protocol was used for measuring all individuals regardless of age and scan resolution. Scans of older individuals were then re-measured using lower resolution of the original scans. To reduce the resolution of higher quality

scans, the import settings on the Dragonfly CT software were set such that the program sampled only every third pixel. Figure 2.2 shows the change in resolution on the same midshaft slice of the right femur from a 13-year-old female (158 months) with a femoral midshaft slice at normal resolution from a newborn female (0 months). Linear and area measurements of older individuals were reduced in resolution and re-measured following standard protocols described in Chapter 2. Reduced resolution measurements of older individuals were compared to original measurements from the higher resolution scans. Results of error calculations show that there is no statistically significant difference between length or diaphyseal circumference measurements ($p = 0.003 – 0.5$). Medullary area measurements are the most affected by poor resolution, with an average of 5.6% error in the humerus and 6.0% error in the femur. This error is exacerbated when calculating the percent of the total area is represented by the medullary cavity ((medullary area / total area) x 100). On average, the poorer resolution of the scans of smaller children produces an overestimation of the relative size of the medullary cavity by ~10%, with a range of 8.9-12.3% error. The over-estimation of medullary area gradually reduces with age with no clear change point, and error in individuals over 12 months is within expected ranges. Thus, measurements have been adjusted (decreased by 10%, described in detail in Chapter 2) on all individuals 0-12 months to compensate for the poor resolution of scans.

Additionally, change point detection analyses indicate that there is a change in variance of cross-sectional properties around 70 months. This indicates that individuals less than 70 months of age have similar variance, which changes in those over 70 months of age. This might be an effect of small sample sizes in individuals over 70 months of age, and thus no adjustments have been made.

4.2.3 | Analytical Methods. Statistics were calculated in the R statistical environment v3.6.1 (R Core Team, 2019). Welch two sample t-tests were used to calculate significance of difference between age groups. For statistical analyses, individuals were divided into three groups: 6 months and under (when individuals are most likely to be pre-locomotion), 7 to 10 months (when individuals are most likely to utilize a pre-walking form of locomotion), and 11+ months (when individuals are most likely to begin walking bipedally). Linear regressions on log-transformed values were used to calculate growth rates for cortical area, second moments of area (SMA) and polar second moments of area, as modified from Ruff (2003a). Bivariate plots were made using *ggplot2* (v3.3.0; Wickham, 2016) in the R statistical environment v3.6.1 (R Core Team, 2019) and compiled in Adobe Illustrator CC 2020 (Adobe, Inc).

4.3 | Results

4.3.1 | Length. Both humeral and femoral diaphyseal length increase with age (Figure 4.1). Femoral diaphyseal length is greater than that of the humerus.

4.3.2 | Comparison of Proximal Ends of the Humerus and Femur

4.3.2.1 | Diaphyseal circumference. Diaphyseal circumference increases with age and body weight. For individuals aged 0-25 months, the increase in diaphyseal circumference in the proximal humerus and femur occur at relatively similar rates. After 25 months, the rate of growth in the humerus decreases until the proximal humeral circumference plateaus around 50 months. Proximal femoral diaphyseal circumference continues to increase until about 125 months (Figure 4.2).

4.3.2.2 | Cortical Area. In infants 0-5 months old, humeral and femoral cortical area overlap entirely and increase in parallel (Figure 4.3). Around 7 months, femoral cortical area begins to increase at a faster rate than humeral cortical area at the same relative position (Figure 4.4). Around 20 months, humeral and femoral proximal cortical area decouple as femoral cortical area continues to increase and humeral cortical area plateaus. There is a notable increase in humeral cortical area around 40 months of age, after which the humeral growth rate slows and plateaus. This spurt of increase in cortical area is also present in the proximal femur. Proximal femoral cortical area continues to increase with age but appears to plateau around 125 months. By 72 months, femoral cortical area has completely surpassed that of the humerus, and no overlap is seen for the rest of childhood and adolescence (Figure 4.3). Linear regression on natural log-transformed cortical area values show that rates of growth differ in different age groups (Figure 4.4). In individuals less than 6 months old, humeral cortical area grows significantly faster than femoral cortical area ($p = 0.0024$). In individuals between 7 and 12 months of age, proximal femoral cortical area grows more quickly than proximal humeral cortical area, but the difference is not statistically significant, possibly due to small sample sizes and increased variation during that period. In older children (greater than 1 year of age), proximal femoral cortical area grows at a significantly faster rate than proximal humeral cortical area ($p = 0.0005$).

4.3.2.3 | Medullary Area. Humeral and femoral relative medullary area are very similar in magnitude and increase with age at similar rates. Both humeral and femoral proximal medullary area peak around 6 months, after which they both exhibit a decline followed by increases in medullary area after 10 months (Figure 4.5). There is another, larger peak in relative medullary area around 25 months, after which both the proximal humerus and the proximal femur decrease in relative medullary area throughout childhood and adolescence. When standardized against diaphyseal length, both humeral and femoral relative medullary area decrease quickly between 6 and 10 months, indicating that cortical bone is being formed faster than longitudinal growth is occurring during this time period.

4.3.2.4 | Second moments of area. From birth, femoral maximum second moment of area is larger than the humeral second moment of area. Both humeral and femoral maximum second moments increase throughout infancy, with femoral I_{max} increasing quickly for the first 5 months. Proximal I_{max} in the femur continues increasing throughout toddlerhood, while I_{max} plateaus in the humerus around the same time. After ~25 months, femoral proximal I_{max} remains much higher than that of the humerus. At 50 months, both humeral and femoral proximal area begin to increase, after which the humeral maximum second area plateaus for a second time while the femoral maximum second area continues to increase for another 50 months (Figure 4.6). Growth rates of the proximal humerus and femur are derived from linear regressions on log-transformed values and show that differences in SMA growth rate between the proximal humerus and proximal femur are statistically significant in individuals under 6 months ($p = 0.0093$) and in individuals older than 11 months ($p = 0.0031$; Figure 4.7). In the first 6 months, humeral SMA increases at a faster rate than femoral SMA, which is reversed in individuals over 11 months. Individuals between 7 and 10 months exhibit faster rates of growth in femoral SMA compared to humeral SMA, but the difference is not statistically

significant and increased sample sizes are needed to better understand the growth pattern during this period.

4.3.2.5 | Polar second moments of area. Perinatal infants have relatively lower humeral resistance to bending than femoral resistance to bending at the proximal measurement position. The humeral polar second moments of area increase quickly in months 2-7. Between 10 and 20 months, humeral *J* mostly plateaus, while femoral *J* continues to increase (Figure 4.8). Linear regression on logged J values show a similar growth pattern in torsional strength as bending strength (Figure 4.9). In the first 6 months, humeri are increasing in their resistance to torsion faster than femora ($p = 0.047$).

4.3.3 | Comparison of Humeral and Femoral Midshaft

4.3.3.1 | Diaphyseal circumference. At midshaft, infants are born with overlapping but offset humeral and femoral diaphyseal circumferences (femoral circumference is larger than humeral circumference). Within the first six months, the overall circumference of the two bones becomes more similar before diverging around 2 years of age. For the rest of childhood and adolescence, there is very little overlap in humeral and femoral midshaft circumference (Figure 4.10). Femoral midshaft circumference increases more quickly than that of the humerus in children aged 25 – 50 months.

4.3.3.2 | Cortical Area. Similar to overall diaphyseal circumference, there is some overlap between the humeral and femoral midshaft cortical areas present at birth, with the femoral cortical areas on average larger than those of newborn humeri (Figure 4.11). By 4 months, humeral midshaft cortical area is nearly equal to that of the femur. In infants aged 6-10 months, humeral cortical area is equal to or greater than that of the femur. Humeral cortical area remains relatively stagnant between 10 and 20 months, while femoral cortical area increases during this period. Around 16 months, femoral cortical area exhibits a notable increase, with humeral midshaft exhibiting a smaller increase in cortical area. Beginning around 22 months, the cortical areas of the two midshafts diverge, with more cortical area in the femoral midshaft than the humeral midshaft. Linear regression on log-transformed cortical area values indicate that there is only a statistically significant difference between humeral and femoral cortical area growth rates after 11 months of age ($p = 0.0002$; Figure 4.12), where femoral midshaft cortical area increases at a faster rate than humeral midshaft cortical area. The rate of increase in femoral midshaft cortical area is greater than that of the humerus in the 7-10 month age group, but larger sample sizes are needed to better understand the growth rate during this time period.

4.3.3.3 | Medullary Area. At birth, relative medullary cavity size at midshaft in the humerus and femur are nearly identical (Figure 4.13). The notable overlap continues until roughly 6 months of age, when medullary area in the femur decreases quickly until 10 months of age. Between 10 and 20 months, the medullary area in the femoral midshaft increases. Both values continue to increase until they both peak in relative size in individuals around 25 months of age. Following this peak, both humeral and femoral relative medullary cavity size at midshaft decrease for the remainder of childhood and adolescence. Humeral relative medullary cavity size exhibits a higher overall peak than

that of the femur before decreasing in relative size and overlapping entirely with femoral relative medullary cavity size in individuals over 50 months of age.

4.3.3.4 | Second moments of area. Femoral maximum second moment of area is slightly higher than that of the humerus in premature and perinatal individuals (Figure 4.14). The maximum resistance to bending in both the humerus and femur steadily increases for the first 6 months of life. Humeral maximum resistance to bending increases at a decreasing rate after 12 months of age, whereas the same measurement in the femur continues to increase and exhibits much variation between individuals. There is a slight increase in maximum second moment of area in both the humerus and femur of individuals that begins around 50 months old, after which the humerus remains relatively stable in maximum second moment of area while the femur continues to increase and shows significantly more variation. Linear regression on log-transformed values show that growth rates in humeral and femoral midshaft SMA are statistically significant only in individuals 6 months and younger ($p = 0.001753$), with humeral midshaft SMA increasing at a faster rate than femoral midshaft SMA (Figure 4.15). Between 7 and 10 months, femoral midshaft SMA appears to increase at a much faster rate than humeral midshaft SMA, but larger sample sizes are needed to statistically evaluate rate of growth during this time period. After 11 months, humeral and femoral midshaft SMA are increasing at similar rates.

4.3.3.5 | Polar second moments of area. Around birth, humeral and femoral midshaft resistance to torsion are very similar, with the femur exhibiting slightly higher resistance to torsion than the humerus. Resistance to torsion in both bones increases for the first 10 months at roughly similar rates. At 10 months, individuals begin to show increased variation in resistance to torsion in both bones. At this point, the humerus begins to decrease in rate of increase and levels off by 20 months. The femur continues to exhibit quite a bit of variation in resistance to torsion. Both bones show an increase in resistance to torsion beginning at about 50 months, followed by a much higher resistance to torsion in the femur than the humerus for the rest of the examined period (Figure 4.16). Humeral and femoral growth rates in resistance to torsion are only significantly different in individuals 6 months and younger, where humeral midshaft *J* increases at a faster rate than femoral midshaft *J* ($p = 0.0036$; Figure 4.17).

4.3.4 | Comparison of the Distal Ends of the Humerus and Femur

4.3.4.1 | Diaphyseal circumference. At the distal measurement position on the humerus and femur, infants show a significant difference in diaphyseal circumference between the humerus and femur from birth (Figure 4.18). Diaphyseal circumference increases quickly in the first few months of life, with the velocity of growth peaking at around 6 months in both the humerus and the femur. After 6 months, diaphyseal circumference continues to increase with age at a slower pace until ~50 months, whereas femoral growth velocity increases and eventually levels out at around 100 months. The humerus exhibits a similar growth spurt at around 50 months, but of a smaller magnitude.

4.3.4.2 | Cortical Area. Peri-natal infants have relatively larger cortical areas in the distal femur than the distal humerus. Both bones exhibit a steep increase in cortical area in the first 6 months after birth, but the humerus adds cortical area at a faster rate

than the femur in this time period. Distal humeral cortical area peaks at 10 months, then begins to decline a bit until early childhood. Distal femoral cortical area continues to increase and gradually levels out closer to 20 months. Individuals between 40-50 months old begin to show an increase in distal femoral cortical area and an increase in variation. Distal humeral cortical area increases quickly slightly later, starting at 50 months and slowly leveling out (Figure 4.19). Linear regressions on natural logged cortical area values indicate that rates of growth in distal cortical area between the humerus and femur are statistically significant in all three age groups ($p > 0.05$; Figure 4.20). In infants 6 months and younger, the distal humeral cortical area increases faster than distal femoral cortical area, whereas distal femoral cortical area increases more quickly than that of the humerus in the two older age groups.

4.3.4.3 | Medullary Area. The relative medullary cavity in the humerus is significantly smaller than that of the femur perinatally. Femoral relative medullary cavity size increases slightly during the first 6 months of life, but humeral medullary cavity size increases at a much faster rate. By about 10 months, increase in humeral distal medullary cavity size begins to slow and levels off around 20 months. Femoral medullary cavity size increases quickly in the first few months after birth and levels off closer to 7 months. Distal humeral medullary cavity size exhibits an overall maximum peak at around 2 years of age, then declines throughout childhood and adolescence. Distal femoral medullary cavity size peaks around the same time as the humerus, but mostly plateaus in older kids rather than decreasing as the humerus does (Figure 4.21).

4.3.4.4 | Second moments of area. In infants 0-6 months old, maximum second moments of area in the distal humerus and femur are relatively similar, with the femoral measurements being slightly higher than the humeral measurements. Both increase within the first 6 months. At around 6 months, the measurements in the two bones seem to decouple, with the humerus increasing in maximum second moment of area at a decreasing rate between 6 and 20 months. After 20 months, the humeral distal maximum second moment of area begins to decrease slightly. Femoral maximum second moments have a bit more variation than those of the humerus, and continue to increase for the first few years of life. After 50 months, humeral maximum second moments level out while femoral second moments continue to increase, with a lot of variation (Figure 4.22). Growth rates based on linear regressions of log-transformed values show that the difference in growth rates is statistically significant in individuals younger than 6 months and older than 11 months ($p = 1.495e\text{-}06$ and 0.00043, respectively). Intermediate aged children (7-10 months) have poor representation in this measurement and results from this age group are therefore inconclusive (Figure 4.23).

4.3.4.5 | Polar second moments of area. The distal polar second moment of area already shows significant differences between the humerus and femur at birth. Femoral polar second moment of area is significantly greater than that of the humerus even prior to full gestation. Between birth and 6 months, distal polar second moments of area increase for both the humerus and the femur. Humeral values are overall lower and level off between 10 and 20 months, whereas femoral polar second moment of area shows an increase between 6 and 10 months, followed by increases at a decreasing rate until 30 months. Older children have much more variation in femoral polar second moments of area than humeral polar second moments of area (Figure 4.24). Results of differences in

growth rates between the distal humerus and distal femur mirror those of SMA (described above; Figure 4.25).

4.4 | Discussion

The proximal humerus and femur provide muscle attachment for many of the muscles used during crawling. The results of this ontogenetically cross-sectional data analyzed here indicate that the humerus and femur grow at different rates during different locomotor regimes. At birth, most measurements are slightly smaller in the humerus than the femur, which is unsurprising given that humeri are typically smaller than femora in adults. Individuals exhibit an impressive increase in humeral diaphyseal circumference and significant increase in cortical area within the first 6 months after birth. The period of growth between 7 and 10 months, when babies are most likely to be crawling, scooting, and beginning to stand bipedally shows much in this sample. This is likely due to the amount of variation in locomotor styles observed in individuals of these ages, as well as the relatively small sample sizes. A larger sample of crawling-age individuals is needed to provide a clearer understanding of growth patterns in this period of development. However, results from this preliminary study provide some insight into the developmental patterns and rates of growth in infants and children.

> *Question 1:* Are there statistically significant differences between humeral and femoral growth throughout infancy and childhood?

Results described above show that there are statistically significant differences between humeral growth and femoral growth throughout infancy and childhood. In the proximal portions of the humerus and femur, humeral growth rates exceed that of the femur in cortical area, second moments of area, and polar second moments of area during the first six months. After 11 months, the pattern is reversed, and these dimensions of the femur grow relatively more quickly than they do in humeri. In the midshaft, humeri grow more quickly than femora. In the midshaft, the same three cross-sectional properties increase more quickly in the humerus than the femur for the first 6 months. In individuals over 11 months of age, the growth rates between the humeral and femoral midshaft are nearly exactly the same (Figures 4.2, 4.15, 4.17). In the distal portions of the bones, results mirror that of the proximal portion in terms of differences between the humerus and femur. The lack of clarity and significant differences between humeral and femoral growth rates in the 7–10-month-old age group is likely caused by a combination of factors. First, sample sizes for this age group are relatively small. Additionally, type and timing of each individual's development of a locomotor repertoire exhibit a notable amount of variation that complicates the understanding of humeral and femoral growth rates in individuals of this age.

> *Question 2:* Do the observed growth patterns broadly correlate with the onset of crawling and walking?

The rates and patterns of growth in the humerus compared to the femur change throughout infancy and childhood and correlate broadly with the timing of locomotor milestones. In infants 6 months of age and younger, humeri grow faster in most properties than femora. In individuals that are likely standing and walking bipedally as their main form of locomotion (11+ months), results show a different growth pattern between the humerus and femur than in pre-locomotion infants. This suggests that the onset of crawling and walking does correlate with changes in the growth and development of the humerus and femur. Around the onset of crawling (7-10 months),

the results from this study are unclear and more research should be done to investigate growth patterns in this time period.

There is substantial variation in growth rate and timing of developmental milestones in infants. For the purposes of clarity, we can break down infant motion into two categories: internal motion and external motion. Internal motion is any limb motion that does not involve some other object or substrate (e.g., grasping at air or startle reflex, etc.). External motion is any limb motion that involves an object or substrate (e.g., grasping an object, crawling, etc.). While perinatal infants typically already possess the motor skills to grasp an object (often referred to as the "grasping reflex"), it is commonly referred to as an involuntary reflex. By about 2-3 months after birth, limb movements are smoother and infants typically begin using their arms to push themselves up when placed on their stomachs and touch objects within their reach (Fiorentino, 2014; van der Meer et al., 1995). Sheridan (2002) notes that arm movements tend to be symmetrical at this stage of development, while leg movements are often independent. By 4 months, most infants can support their bodyweight with their arms when placed on their stomachs. At roughly 5 months, infants are often grasping things within their reach, sitting mostly independently, and using their arms to pull themselves into a seated position. This is also around the time that infants become more exploratory with their hands and can often reach for objects with each hand independently of the other. Between 6 and 7 months, babies often begin using an army-crawl locomotor pattern to move independently. Anytime around 6-9 months, babies may move from the army-crawl method to a classic hands and knees crawling pattern. Between 9 and 13 months, babies begin to walk – first dependent on objects to stabilize them, such as furniture or assistance from an adult – then independently for short periods of time (Adolph et al., 1997).

As described above, the arms are relatively more active during the pre-crawling baby's life than the legs. Infants acquire motor control of their arms weeks before their legs. This developmental pattern identified in infant behavior is mirrored in their limb development. While humeral values for most measurements reported here are often lower at birth, they grow relatively more quickly than the femur in the first 6 months of life. This is especially noticeable in measurements of second moments of are and cortical area. Humeral second polar moments of area, a measure of the bone's resistance to torsion, increases relatively more quickly during the first ~6 months than the humeral second moments of area, that measure resistance to bending.

Humeral diaphyseal circumference is slightly smaller than femoral diaphyseal circumference at birth. After 1 year of age, the two are quite similar in diaphyseal circumference. However, the two bones exhibit differences in cortical bone and medullary cavity size at midshaft. Despite having overall similar diaphyseal circumferences after ~1 year of age, femoral cortical area tends to be larger on average than that of the humerus. While diaphyseal circumference is slightly different between the humerus and femur at birth and the two converge around one year of age, cortical area and medullary area have the opposite pattern. These cross-sectional properties are very similar between the humerus and femur at birth and begin to diverge around 1 year of age. This suggests that external diaphyseal properties at midshaft can be misleading when trying to infer relative strength from diaphyseal circumference alone. Having a detailed understanding of the typical patterns of growth in human infants is an integral part to reconstructing infant and toddler behavior in archaeological or paleoanthropological populations.

4.5 | Conclusions

The overall humeral to femoral growth patterns are directly correlated with the expected onset of crawling and walking. Around the 11-month mark, nearly all humeral measurements begin to slow their rate of growth as femoral growth accelerates. Humeral bone properties grow at a slightly accelerated rate compared to femoral bone properties at the same measurement position within the first six months. Additional studies that include more individuals in the 7-to-10-month age group should be done to better elucidate the effect of intermediate locomotion in infants. Although patterns are detected in individuals younger than 1 year old, larger sample sizes would add clarity and robusticity to these conclusions.

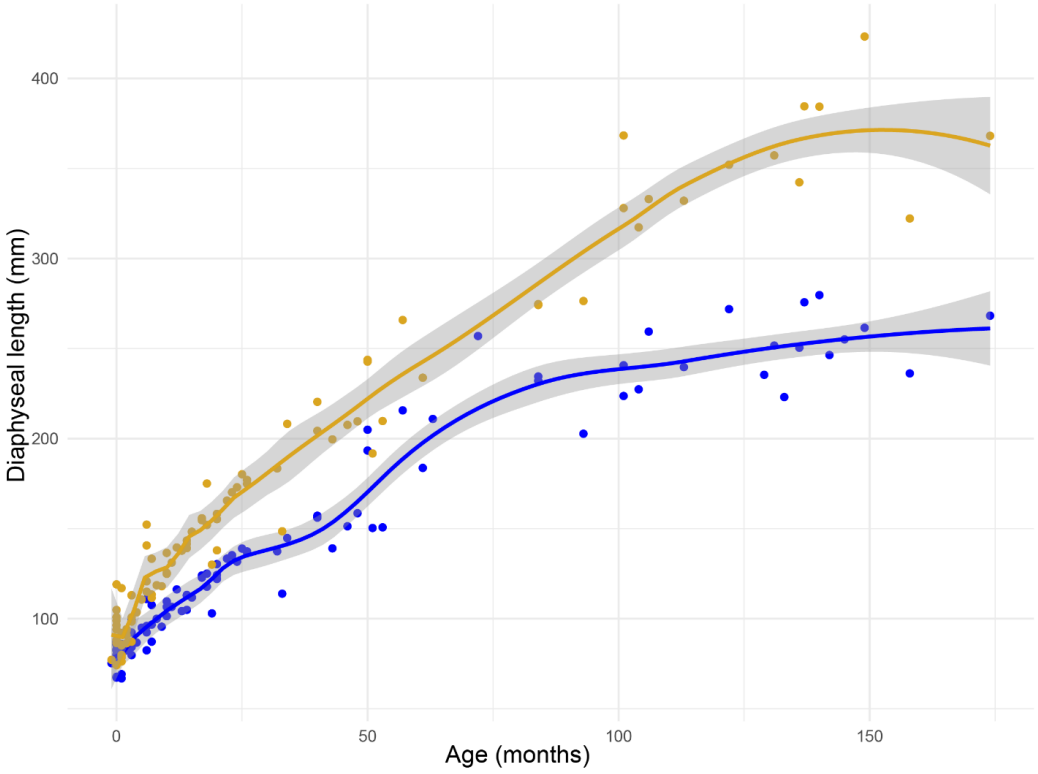


Figure 4.1. Diaphyseal bone length (mm) vs age. Gray shaded areas indicate a 95% confidence interval. Femora are in gold and humeri are in blue.

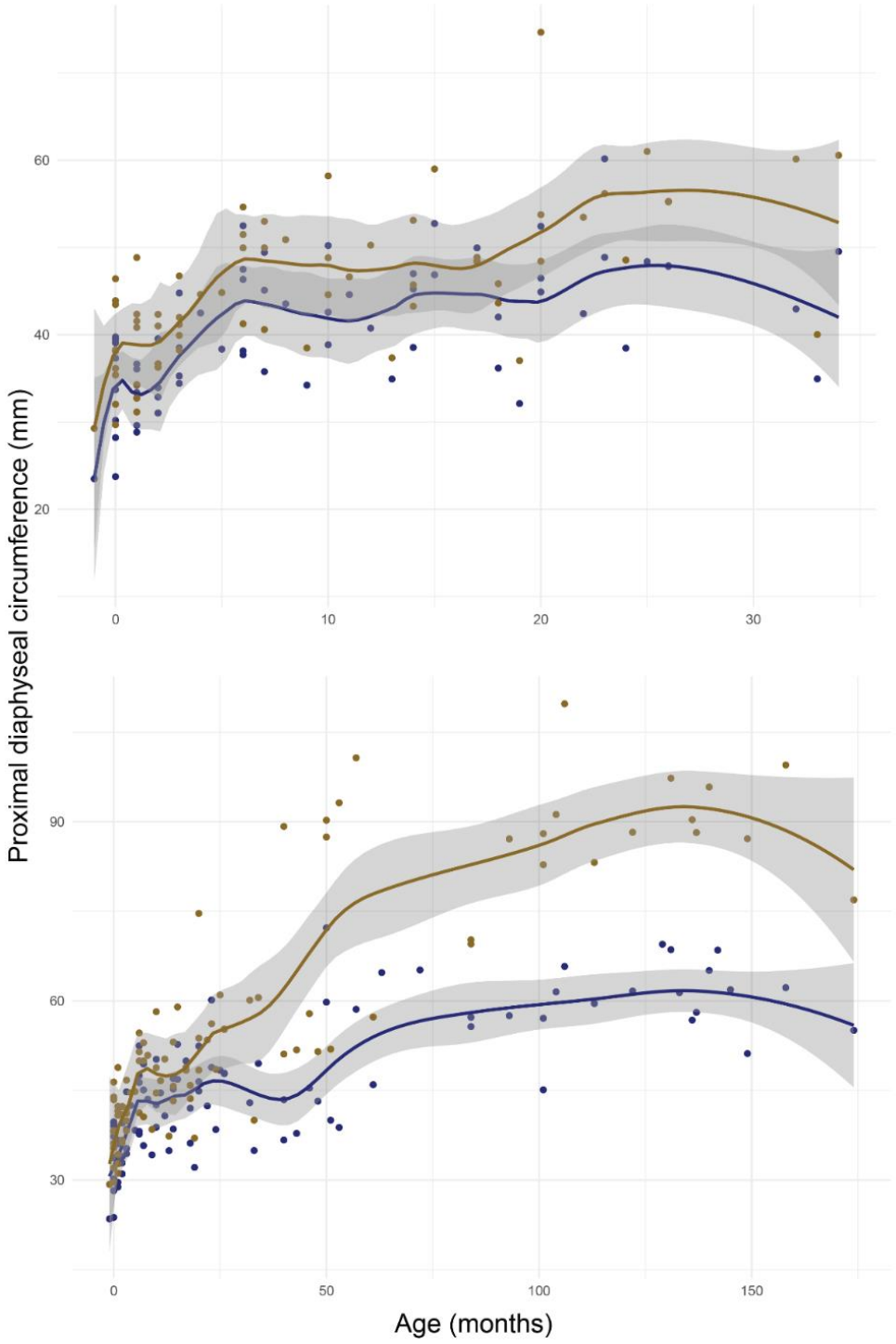


Figure 4.2. Proximal diaphyseal circumference (mm) vs. age. Femora are in gold and humeri are in blue. Top panel – babies aged 0 – 36 months. Bottom panel – all individuals. Gray shaded areas indicate a 95% confidence interval.

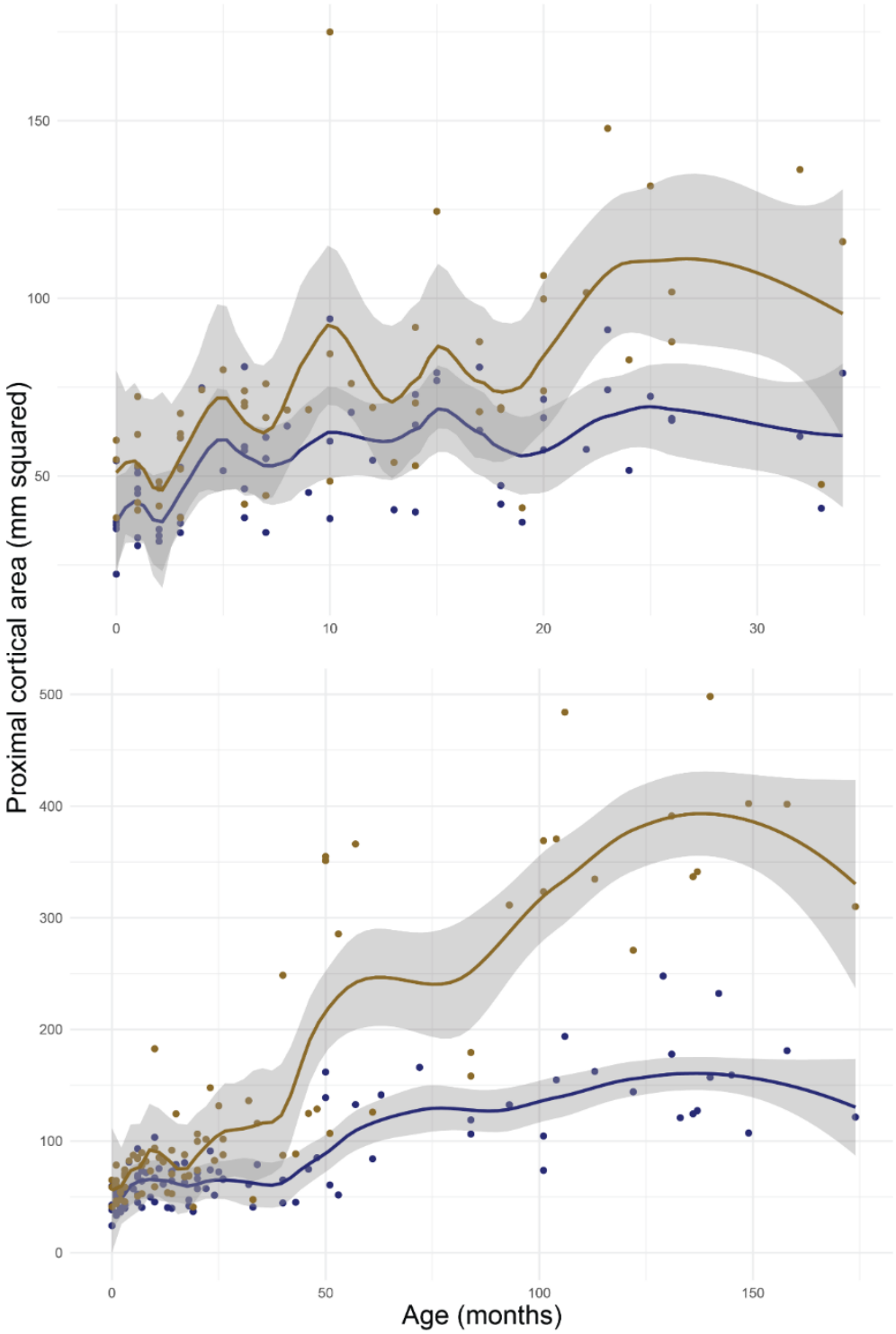


Figure 4.3. Proximal cortical area (mm^2). Femora are in gold and humeri are in blue. Top panel – babies aged 0 – 36 months. Bottom panel – all individuals. Gray shaded areas indicate a 95% confidence interval.

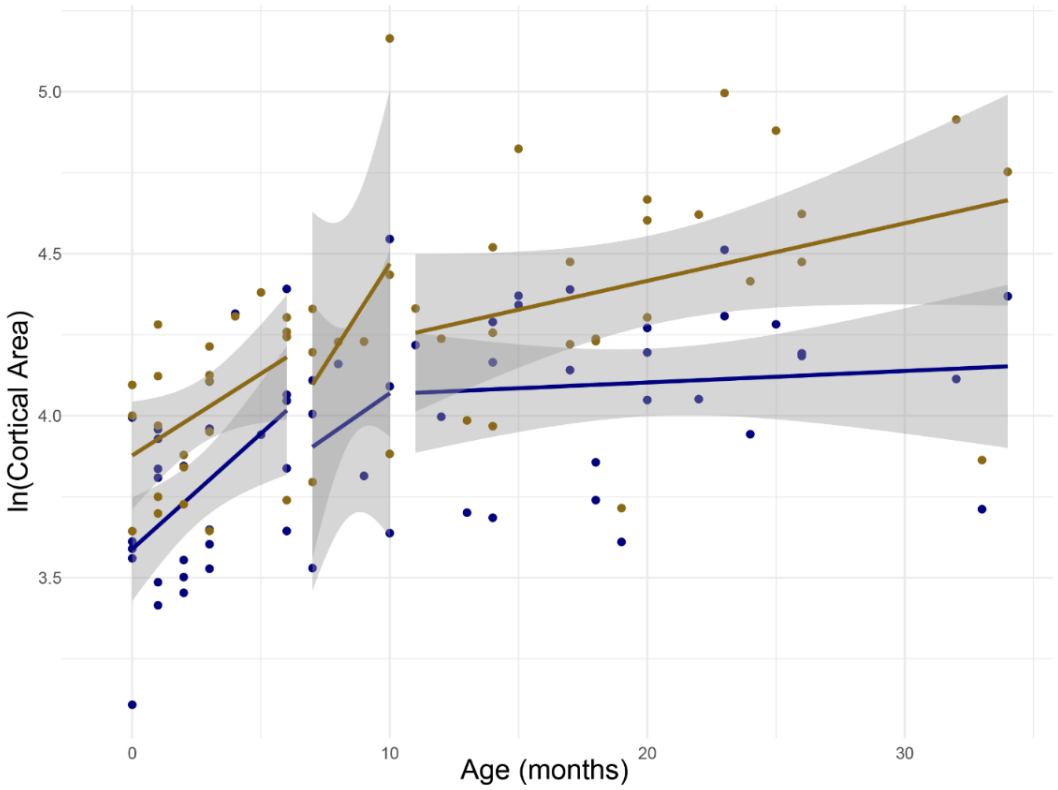


Figure 4.4. Linear regression on natural log-transformed values of proximal cortical area. Femora are in gold and humeri are in blue. Slopes are divided into three age groups: pre-locomotion (0-6 months), intermediate locomotion (7-10 months), and bipedal (11+ months). Gray shaded areas indicate a 95% confidence interval.

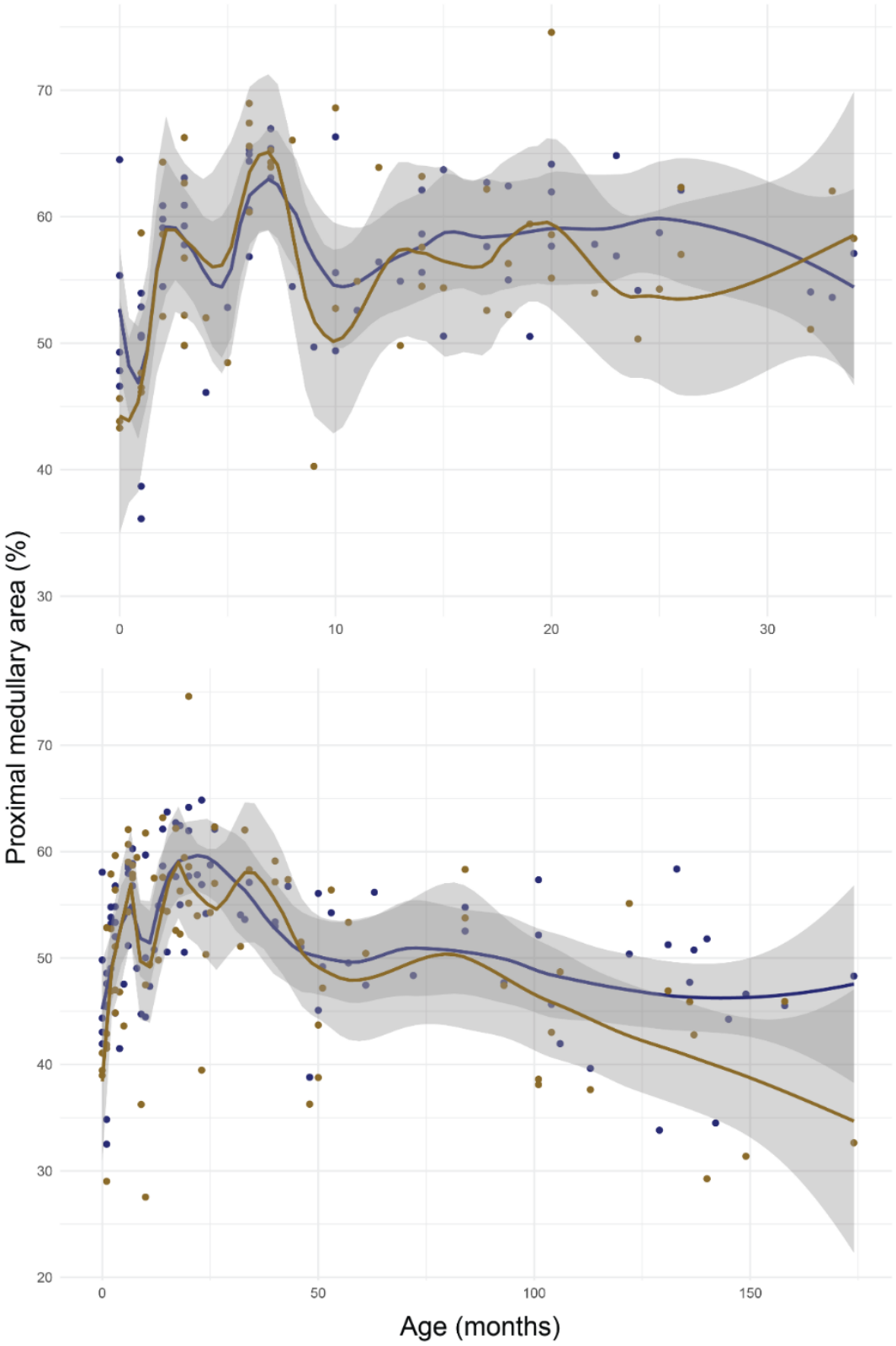


Figure 4.5. Proximal relative medullary cavity size (as a percent of the total diaphyseal area). Femora are in gold and humeri are in blue. Top panel – babies aged 0 – 36 months. Bottom panel – all individuals. Gray shaded areas indicate a 95% confidence interval.

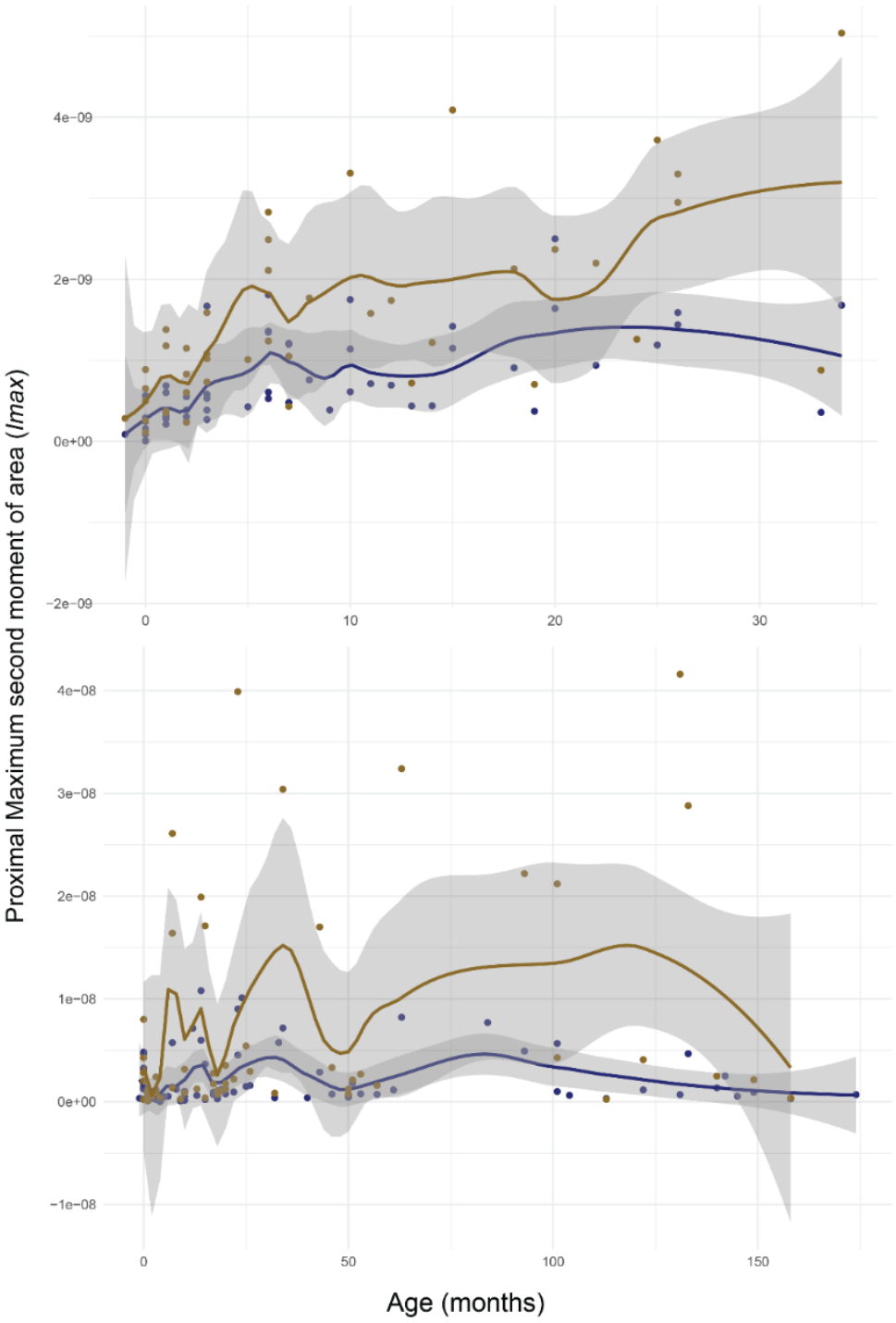


Figure 4.6. Proximal maximum second moments of area (*Imax*). Femora are in gold and humeri are in blue. Top panel – babies aged 0 – 36 months. Bottom panel – all individuals. Gray shaded areas indicate a 95% confidence interval.

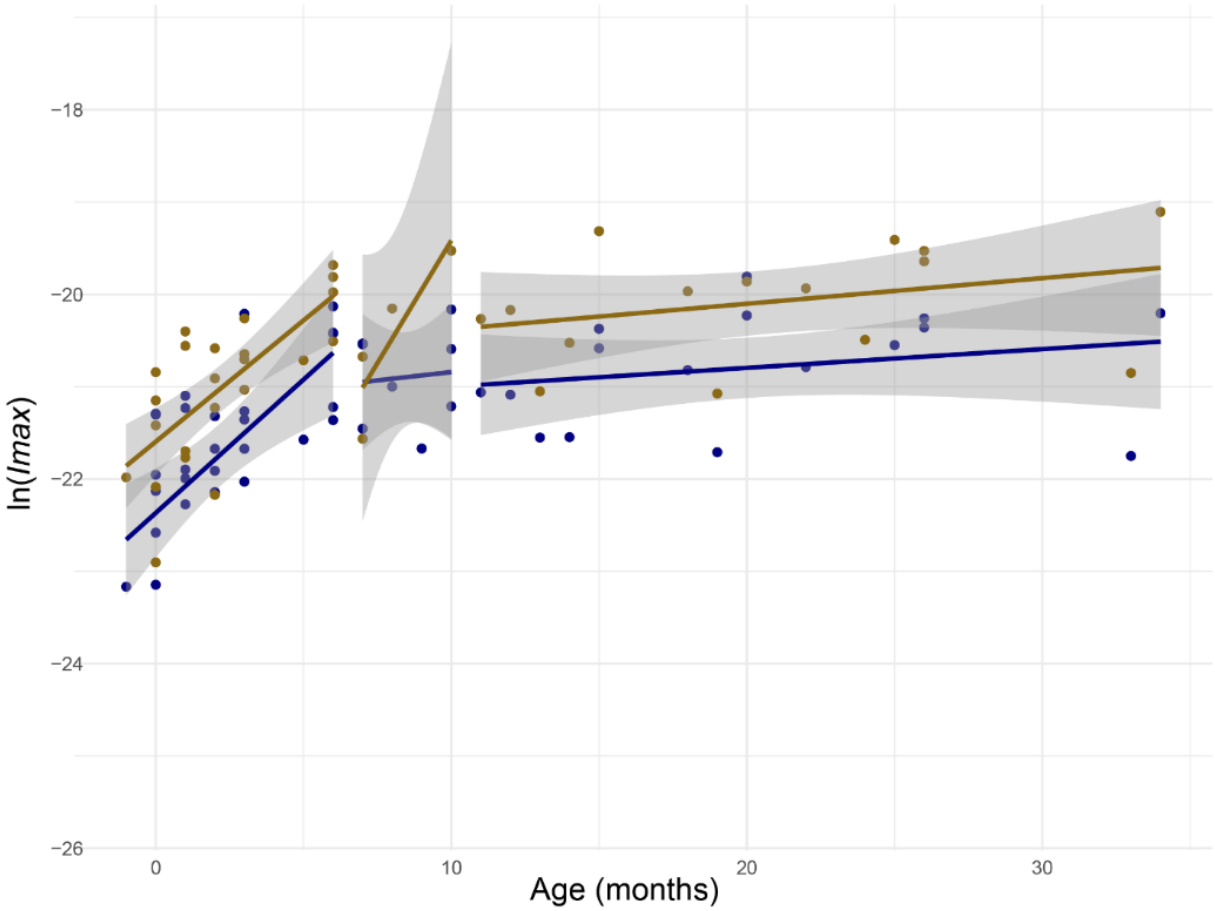


Figure 4.7. Linear regression on natural log-transformed values of proximal maximum second moment of area. Femora are in gold and humeri are in blue. Slopes are divided into three age groups: pre-locomotion (0-6 months), intermediate locomotion (7-10 months), and bipedal (11+ months). Gray shaded areas indicate a 95% confidence interval.

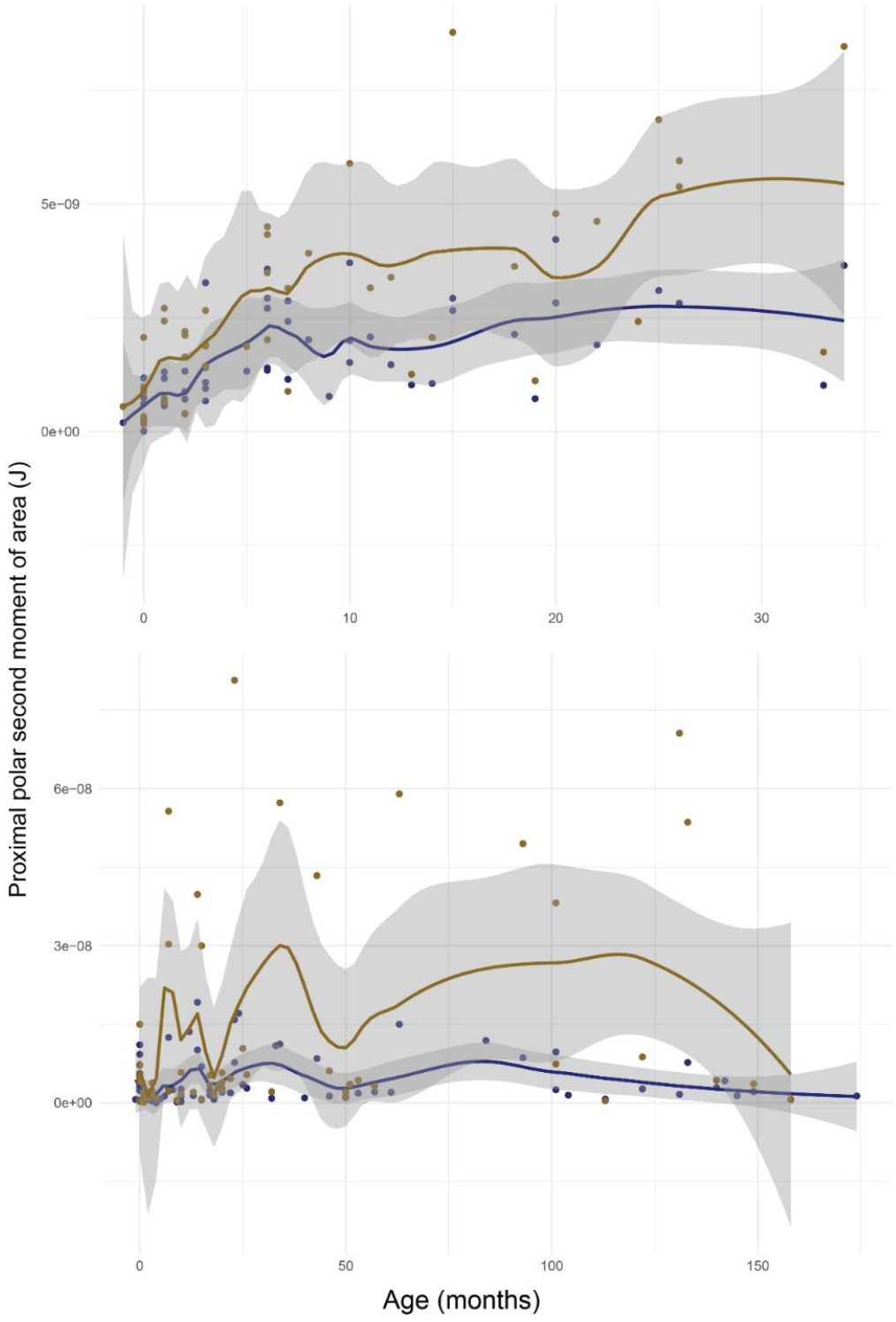


Figure 4.8. Proximal polar second moments of area (*J*). Femora are in gold and humeri are in blue. Top panel – babies aged 0 – 36 months. Bottom panel – all individuals. Gray shaded areas indicate a 95% confidence interval.

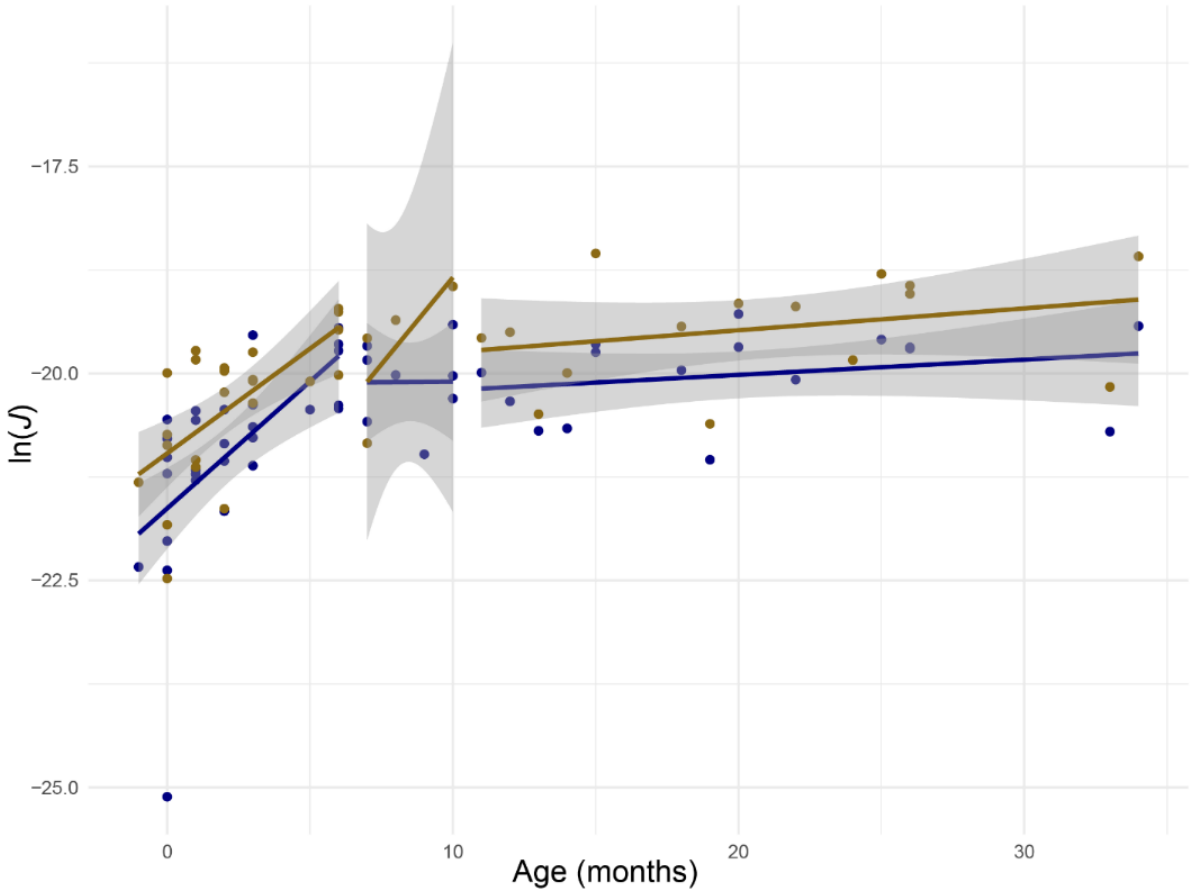


Figure 4.9. Linear regression on natural log-transformed values of proximal cortical area. Femora are in gold and humeri are in blue. Slopes are divided into three age groups: pre-locomotion (0-6 months), intermediate locomotion (7-10 months), and bipedal (11+ months). Gray shaded areas indicate a 95% confidence interval.

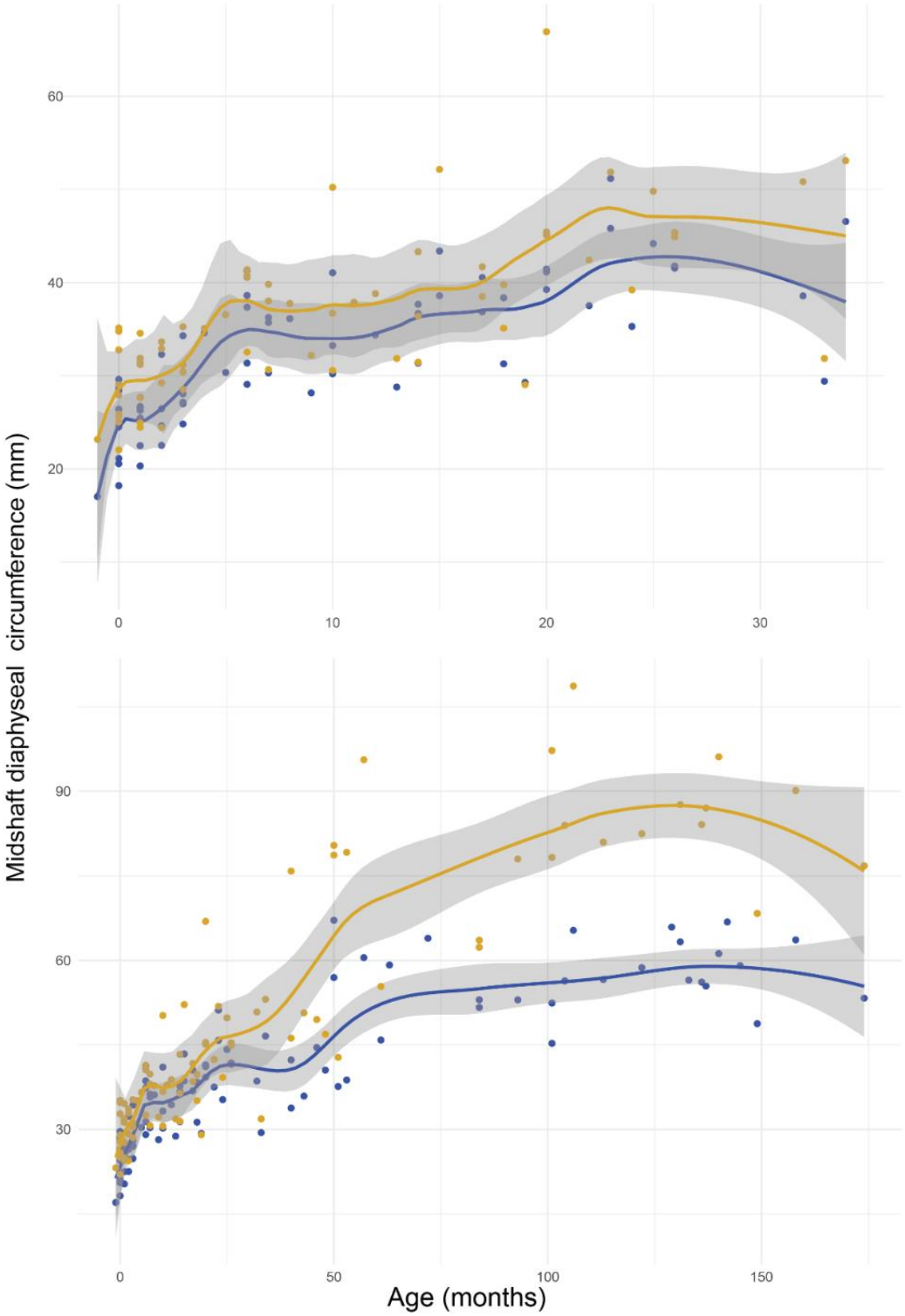


Figure 4.10. Midshaft diaphyseal circumference (mm) vs. age. Femora are in gold and humeri are in blue. Top panel – babies aged 0 – 36 months. Bottom panel – all individuals. Gray shaded areas indicate a 95% confidence interval.

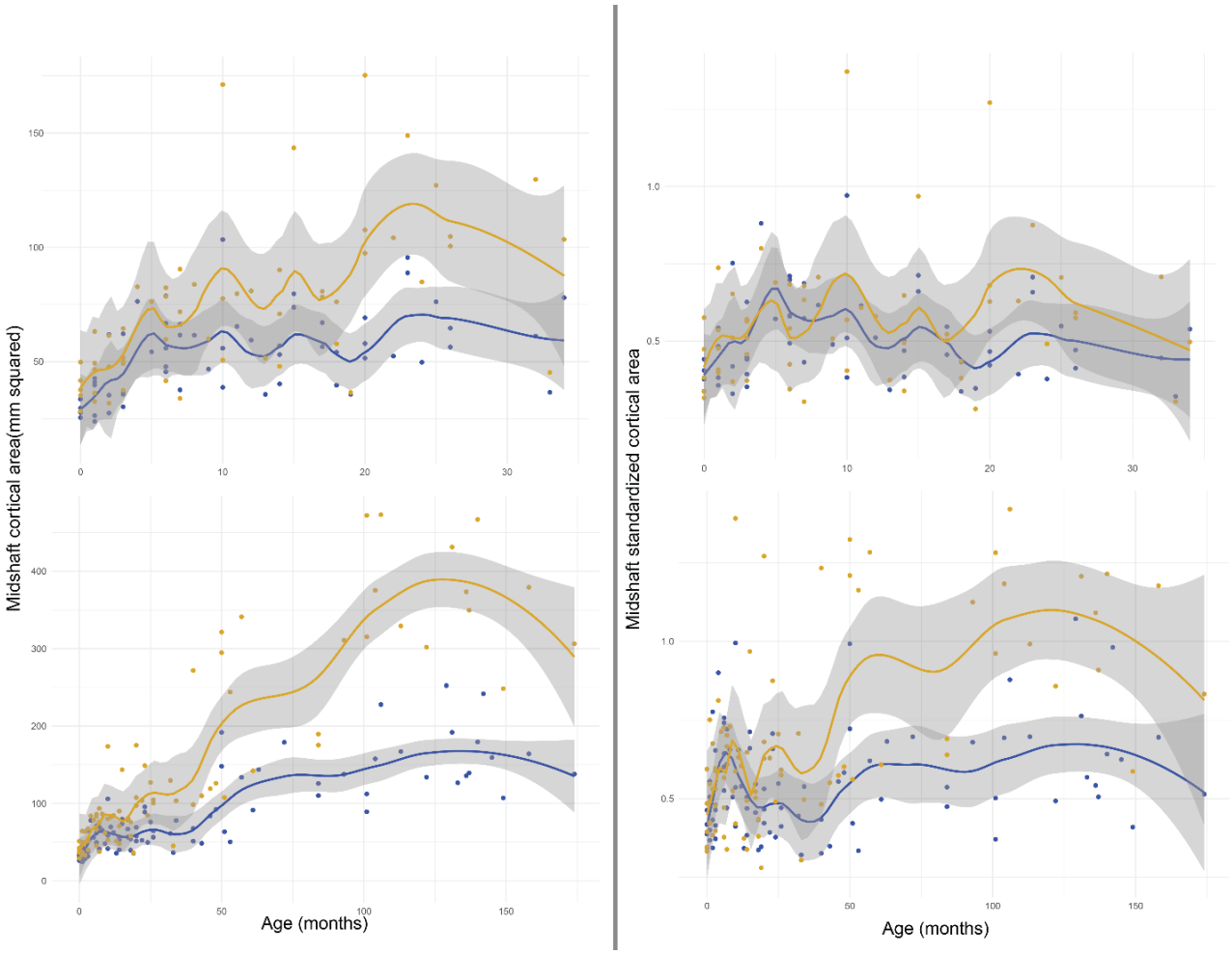


Figure 4.11. Midshaft cortical area (mm^2) vs. age. Femora are in gold and humeri are in blue. Top panels – babies aged 0 – 36 months. Bottom panels – all individuals. Left panel shows raw measurements. Right panel shows cortical area standardized against femoral length. Gray shaded areas indicate a 95% confidence interval.

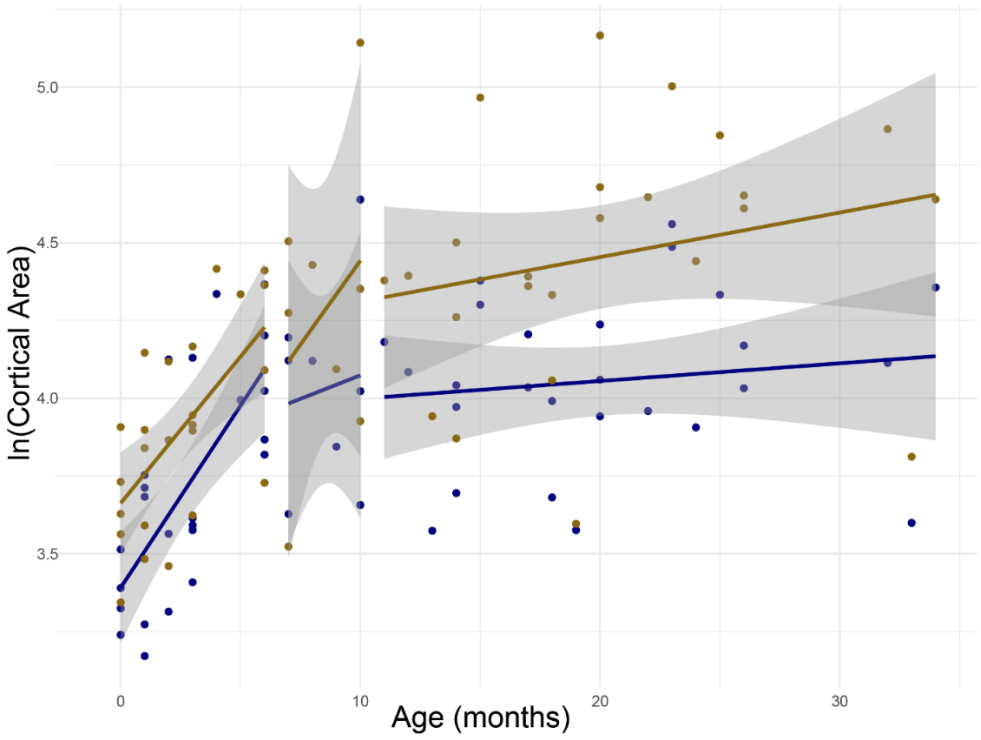


Figure 4.12. Linear regression on natural log-transformed values of midshaft cortical area. Femora are in gold and humeri are in blue. Slopes are divided into three age groups: pre-locomotion (0-6 months), intermediate locomotion (7-10 months), and bipedal (11+ months). Gray shaded areas indicate a 95% confidence interval.

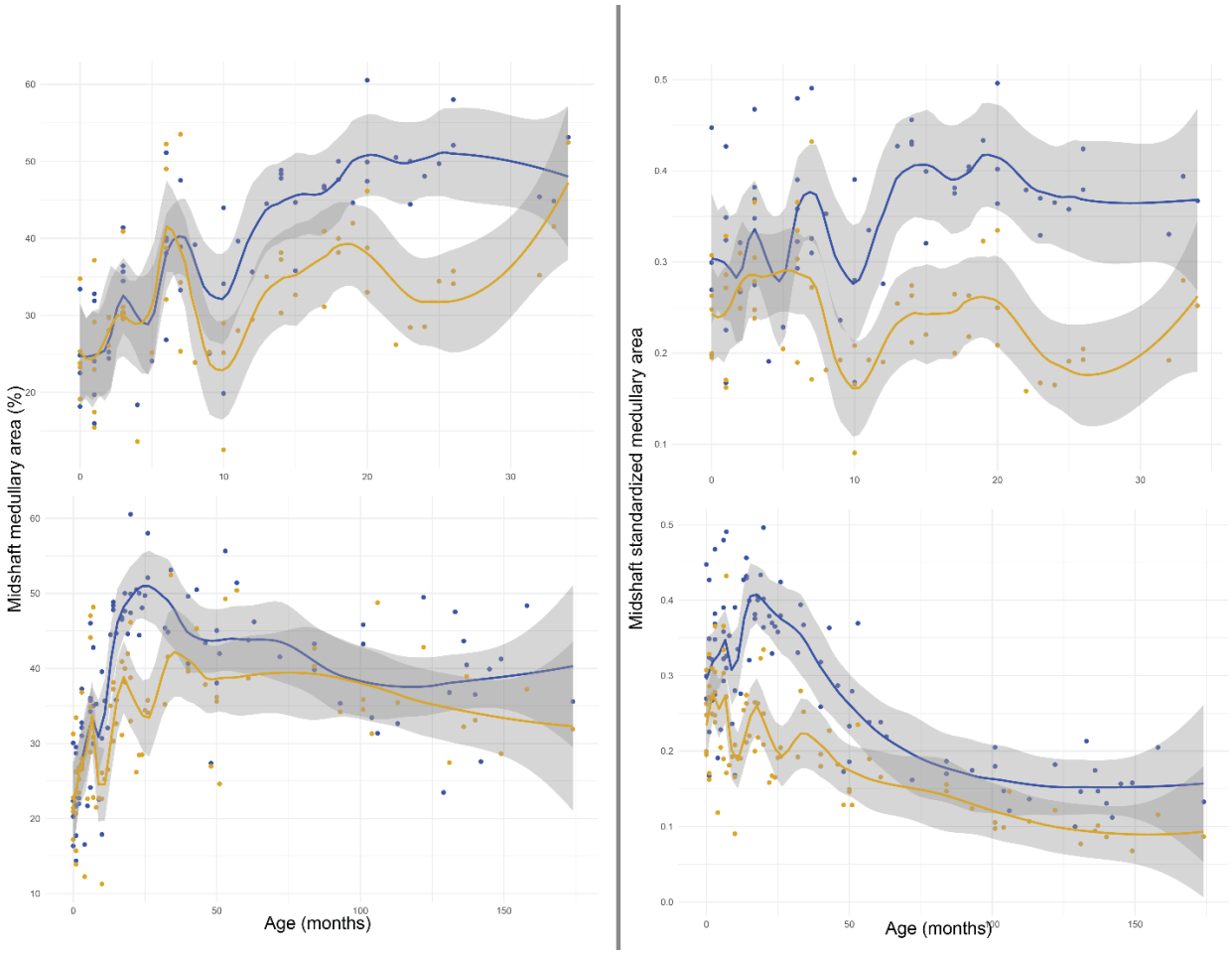


Figure 4.13. Midshaft medullary area (%) vs. age. Femora are in gold and humeri are in blue. Top panels – babies aged 0 – 36 months. Bottom panels – all individuals. Left panel shows raw measurements. Right panel shows cortical area standardized against femoral length. Gray shaded areas indicate a 95% confidence interval.

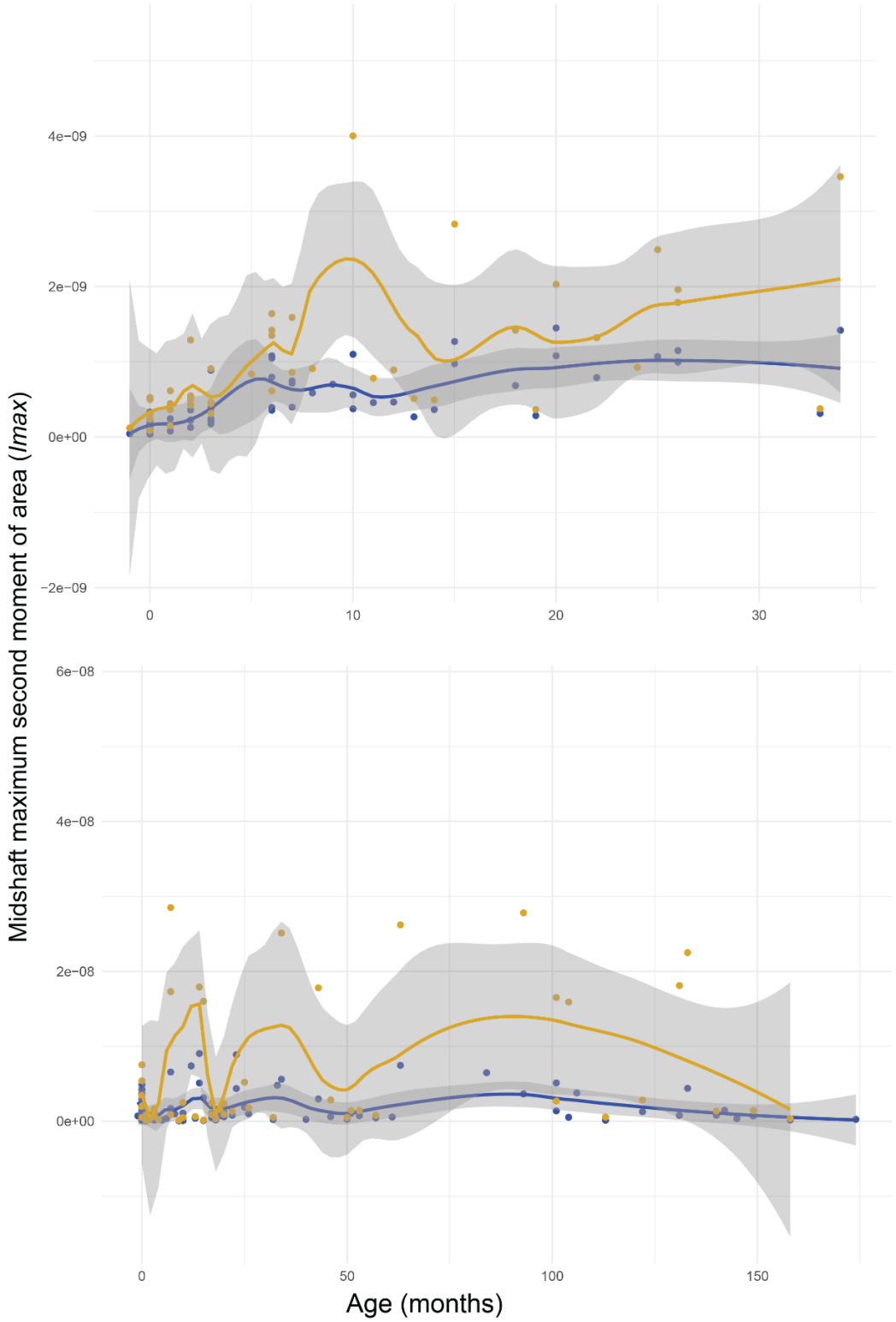


Figure 4.14. Midshaft maximum second moments of area (*Imax*). Femora are in gold and humeri are in blue. Top panel – babies aged 0 – 36 months. Bottom panel – all individuals. Gray shaded areas indicate a 95% confidence interval.

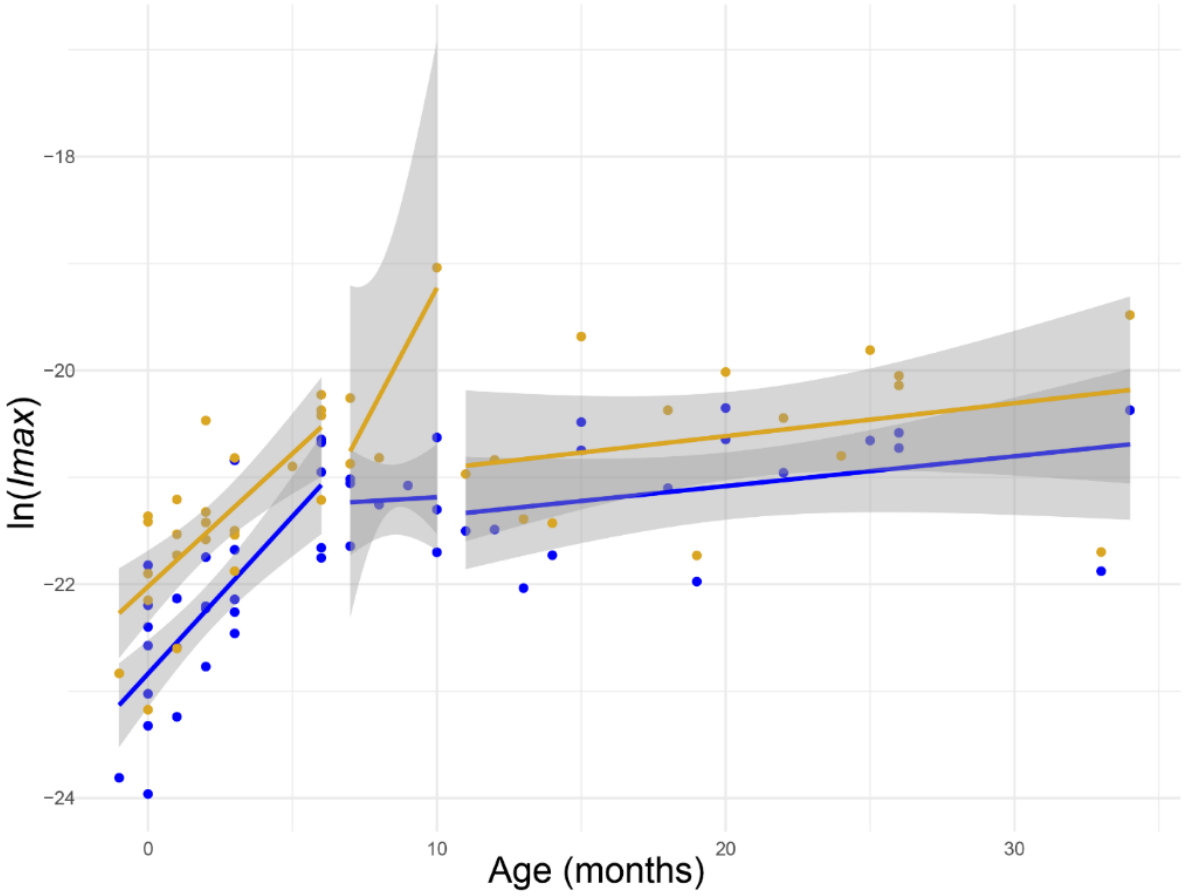


Figure 4.15. Linear regression on natural log-transformed values of midshaft maximum second moment of area. Femora are in gold and humeri are in blue. Slopes are divided into three age groups: pre-locomotion (0-6 months), intermediate locomotion (7-10 months), and bipedal (11+ months). Gray shaded areas indicate a 95% confidence interval.

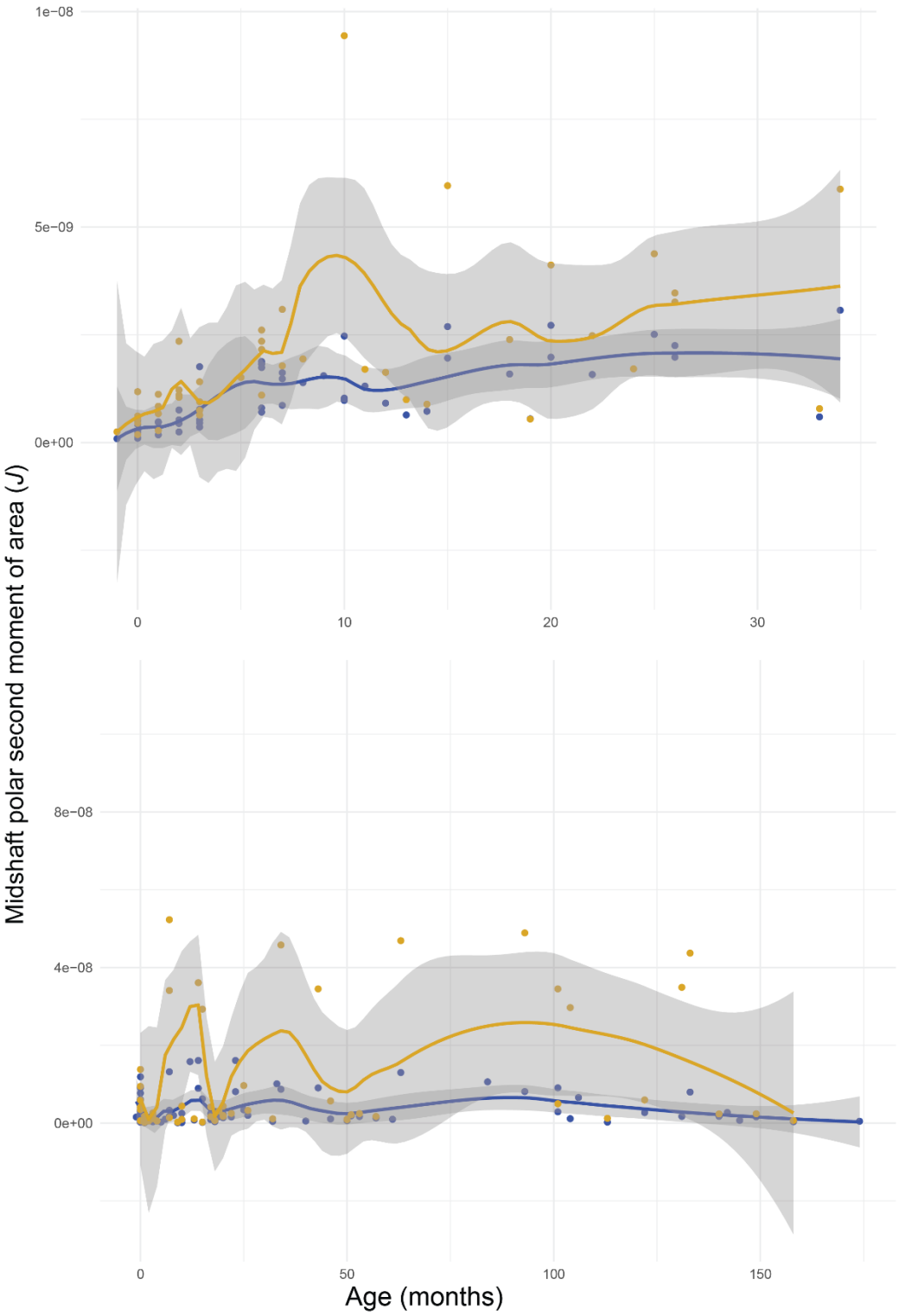


Figure 4.16. Midshaft polar second moments of area (*J*). Femora are in gold and humeri are in blue. Top panel – babies aged 0 – 36 months. Bottom panel – all individuals. Gray shaded areas indicate a 95% confidence interval.

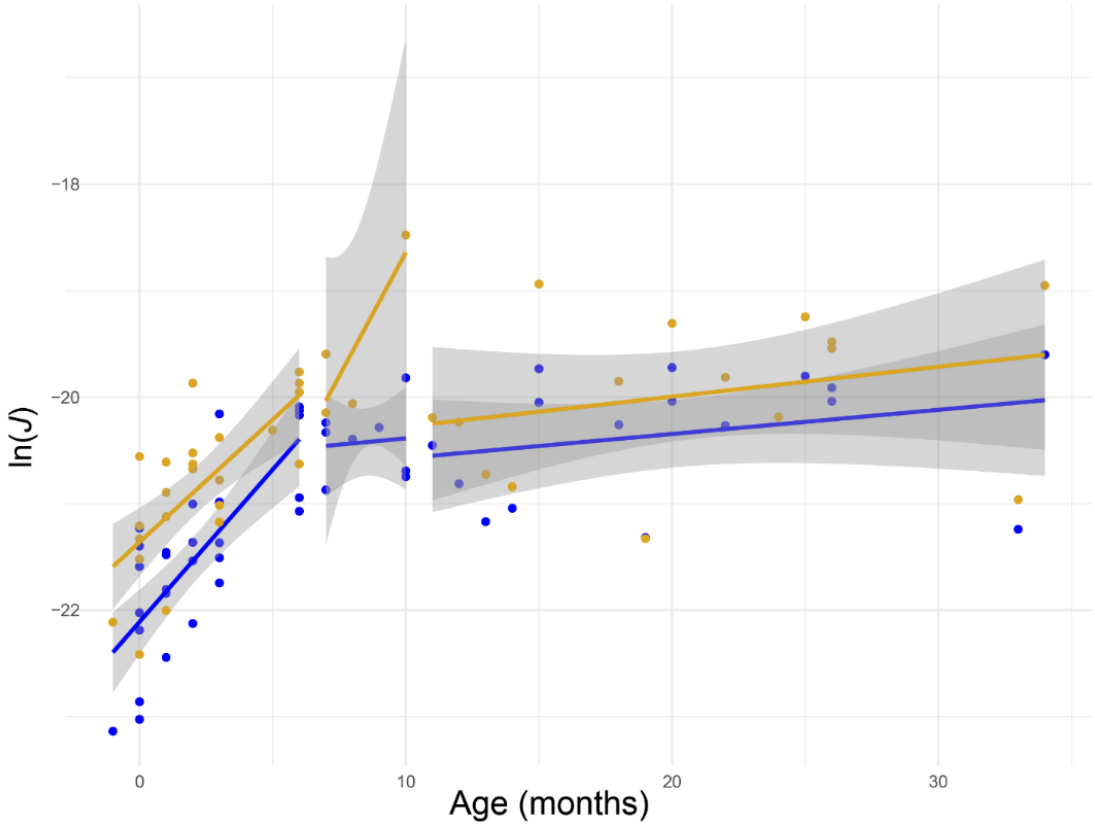


Figure 4.17. Linear regression on natural log-transformed values of midshaft polar second moments of area (*J*). Femora are in gold and humeri are in blue. Slopes are divided into three age groups: pre-locomotion (0-6 months), intermediate locomotion (7-10 months), and bipedal (11+ months). Gray shaded areas indicate a 95% confidence interval.

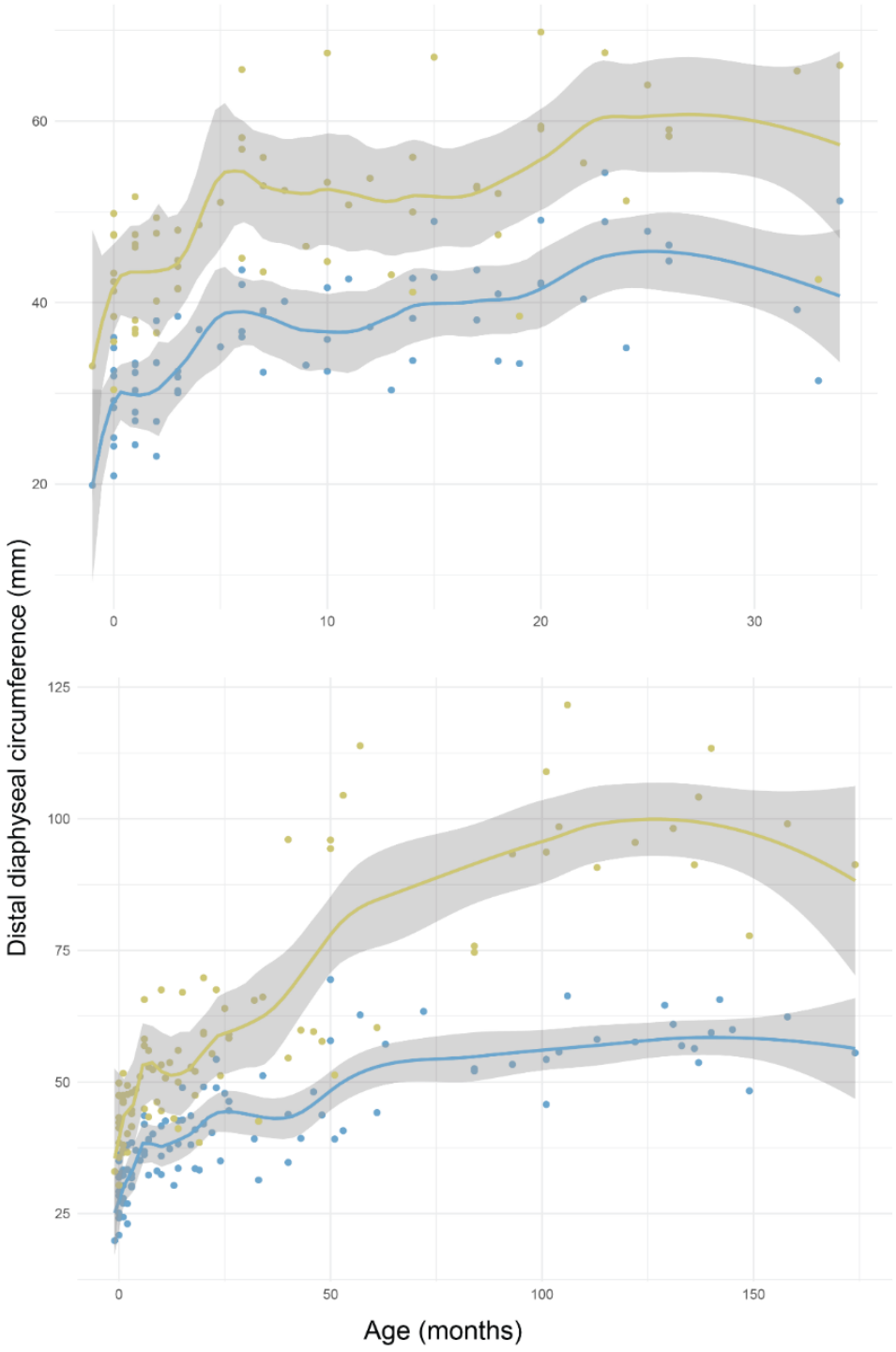


Figure 4.18. Distal diaphyseal circumference (mm) vs. age. Femora are in gold and humeri are in blue. Top panel – babies aged 0 – 36 months. Bottom panel – all individuals. Gray shaded areas indicate a 95% confidence interval.

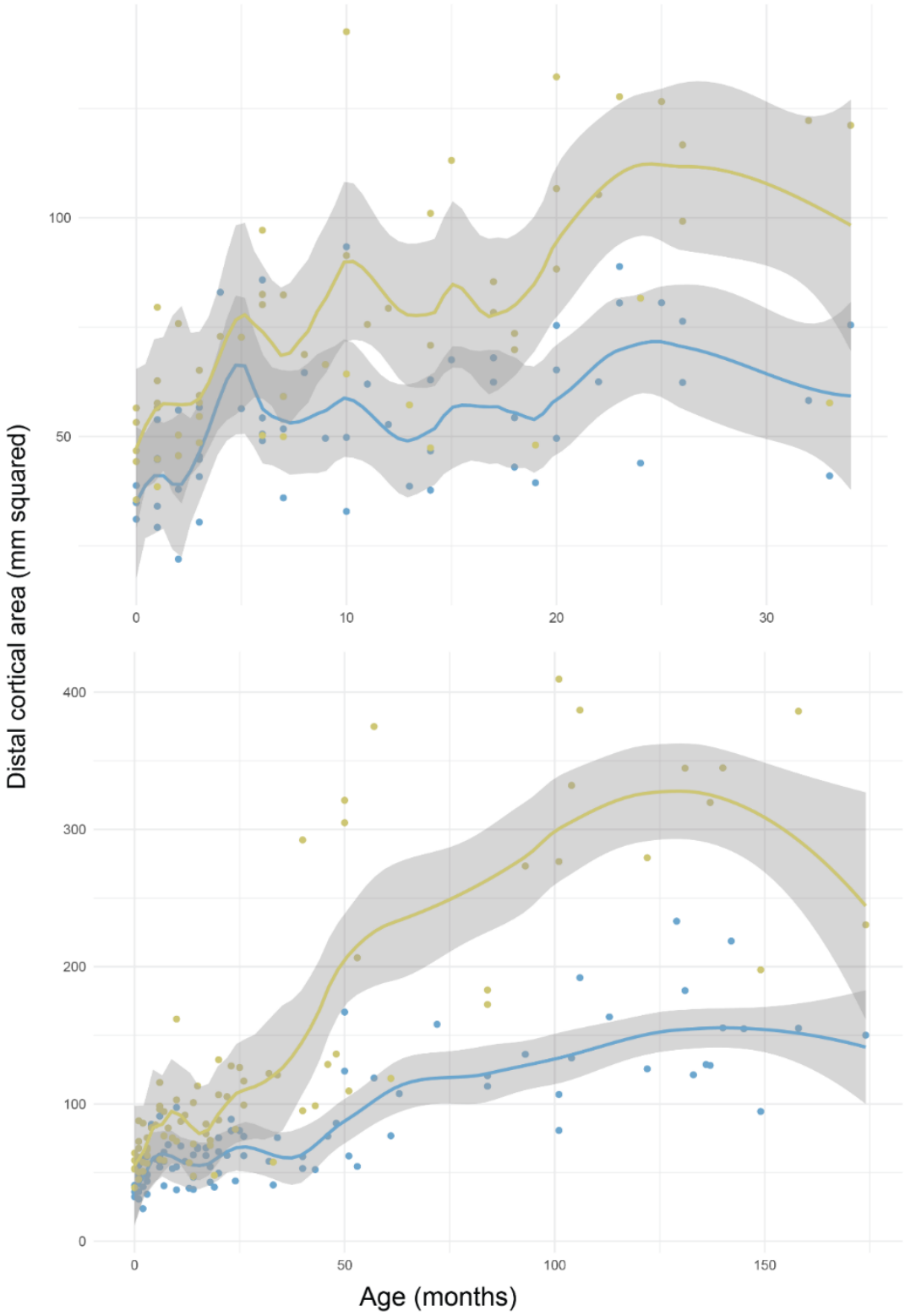


Figure 4.19. Distal cortical area (mm^2) vs. age. Femora are in gold and humeri are in blue. Top panels – babies aged 0 – 36 months. Gray shaded areas indicate a 95% confidence interval.

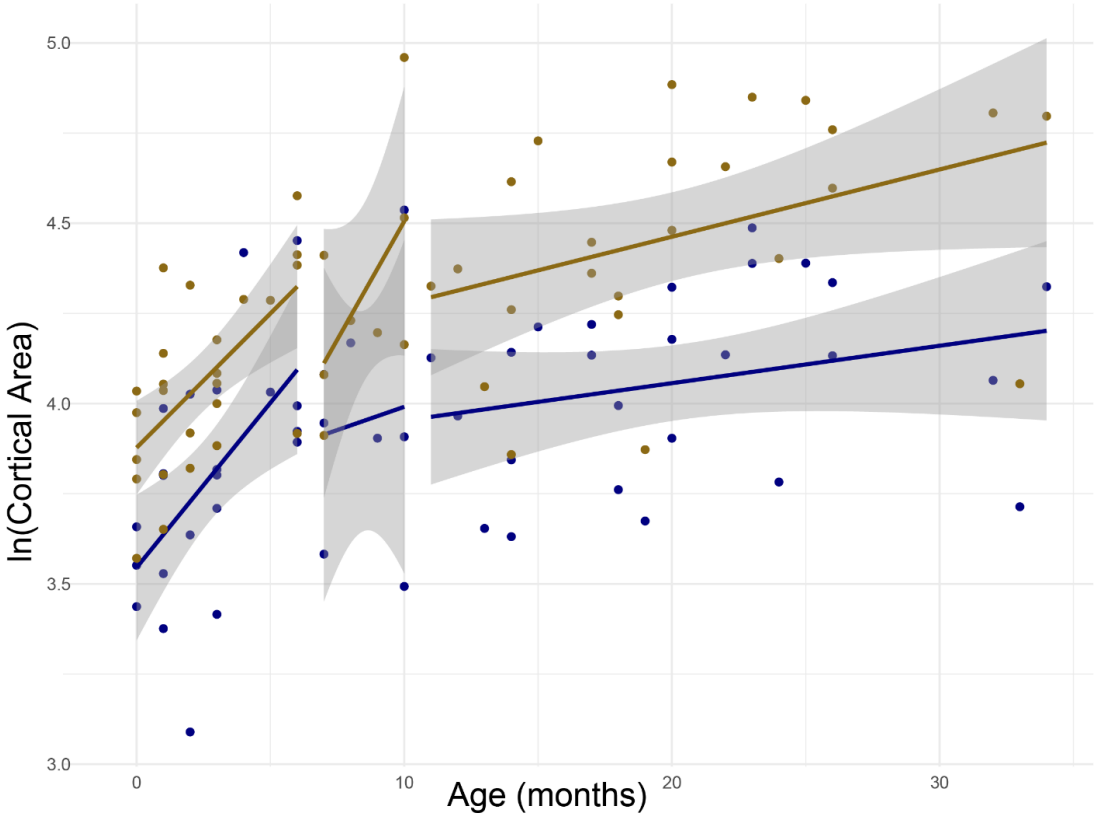


Figure 4.20. Linear regression on natural log-transformed values of distal cortical area. Femora are in gold and humeri are in blue. Slopes are divided into three age groups: pre-locomotion (0-6 months), intermediate locomotion (7-10 months), and bipedal (11+ months). Gray shaded areas indicate a 95% confidence interval

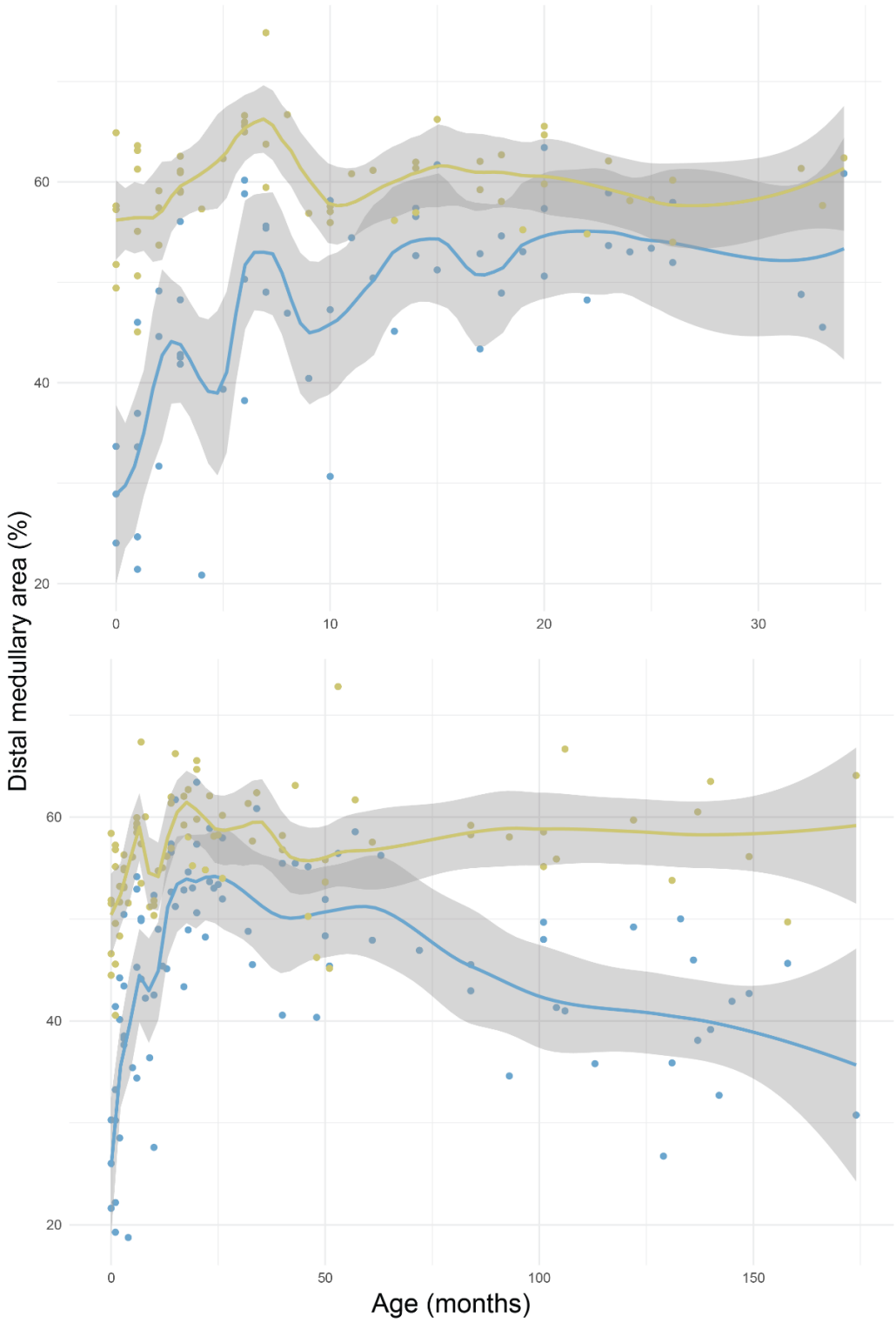


Figure 4.21. Midshaft medullary area (%) vs. age. Femora are in gold and humeri are in blue. Top panels – babies aged 0 – 36 months. Bottom panels – all individuals. Left panel shows raw measurements. Right panel shows cortical area standardized against femoral length. Gray shaded

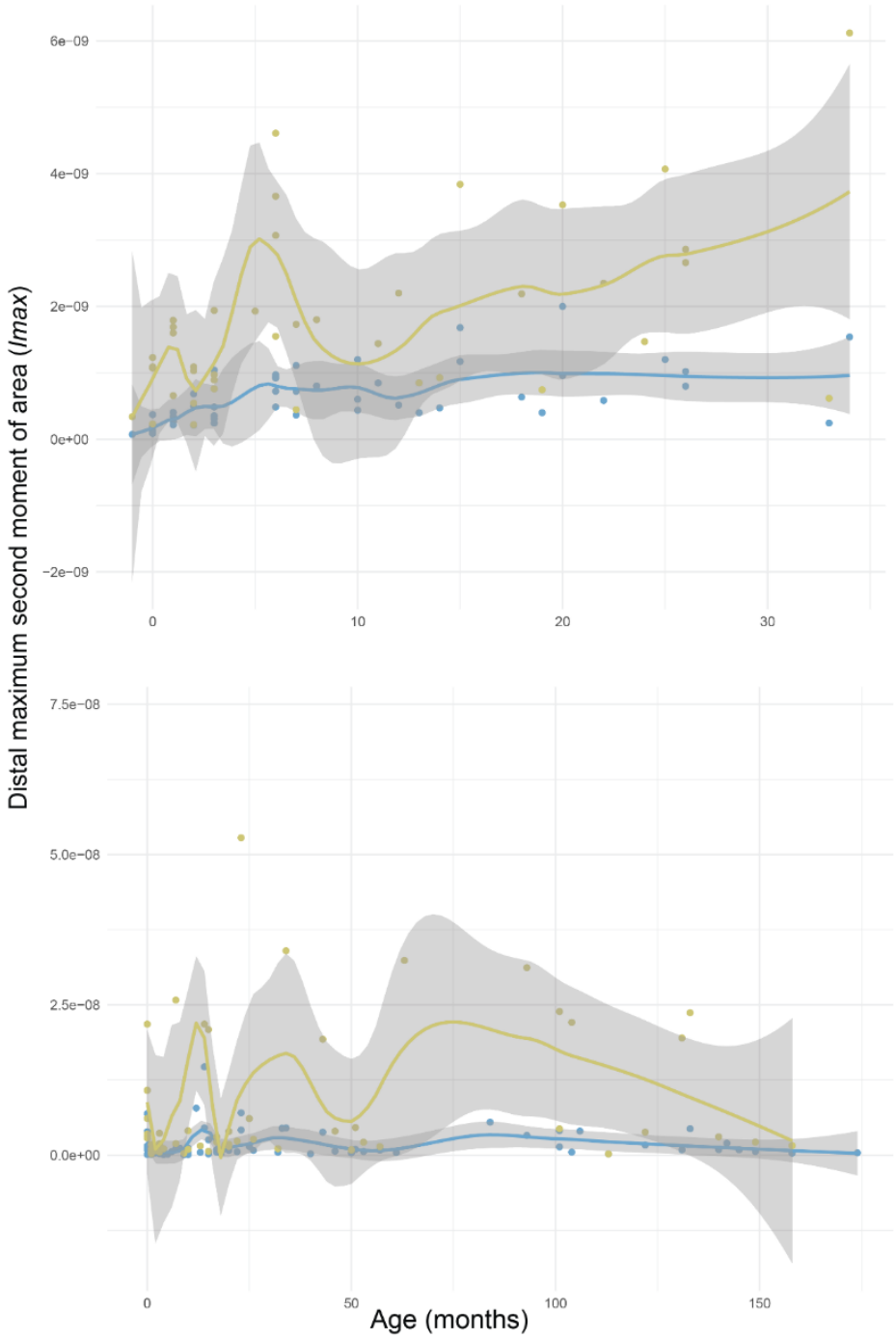


Figure 4.22. Distal maximum second moments of area (*Imax*). Femora are in gold and humeri are in blue. Top panel – babies aged 0 – 36 months. Bottom panel – all individuals.

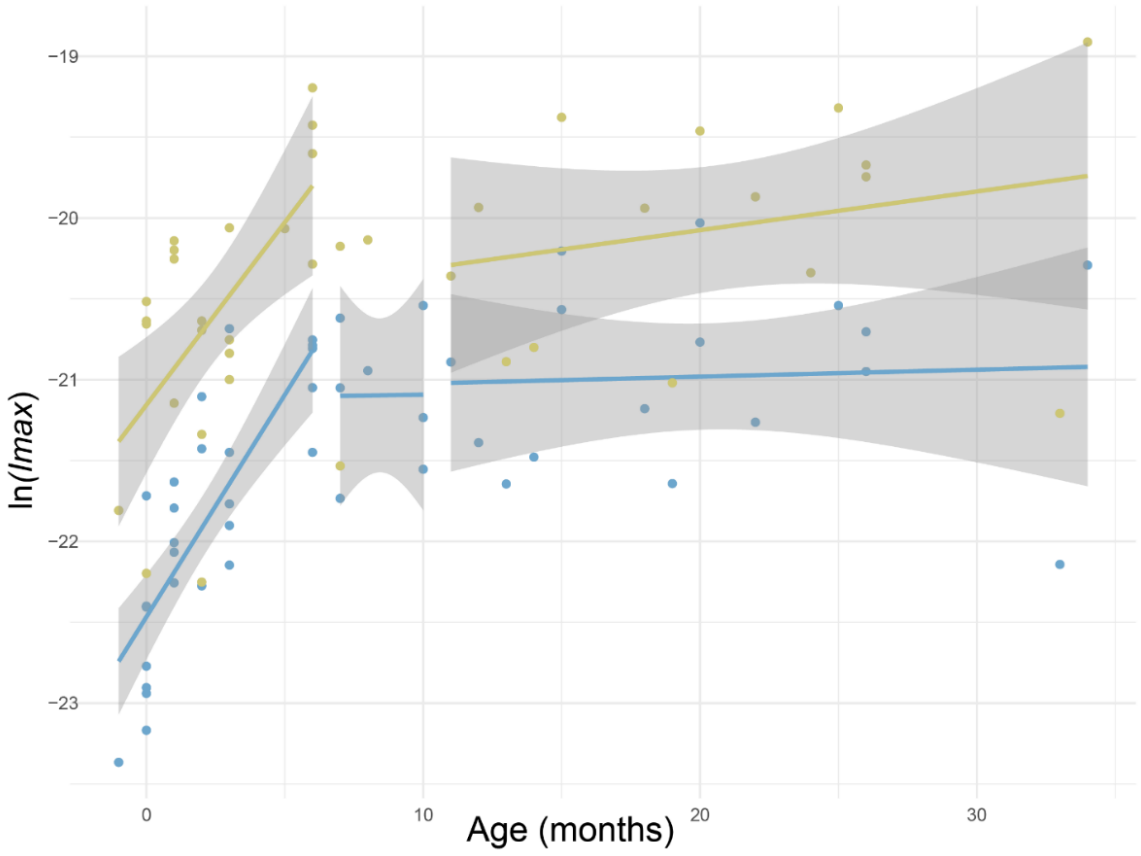


Figure 4.23 Linear regression on natural log-transformed values of distal maximum second moment of area. Femora are in gold and humeri are in blue. Slopes are divided into three age groups: pre-locomotion (0-6 months), intermediate locomotion (7-10 months), and bipedal (11+ months). Gray shaded areas indicate a 95% confidence interval.

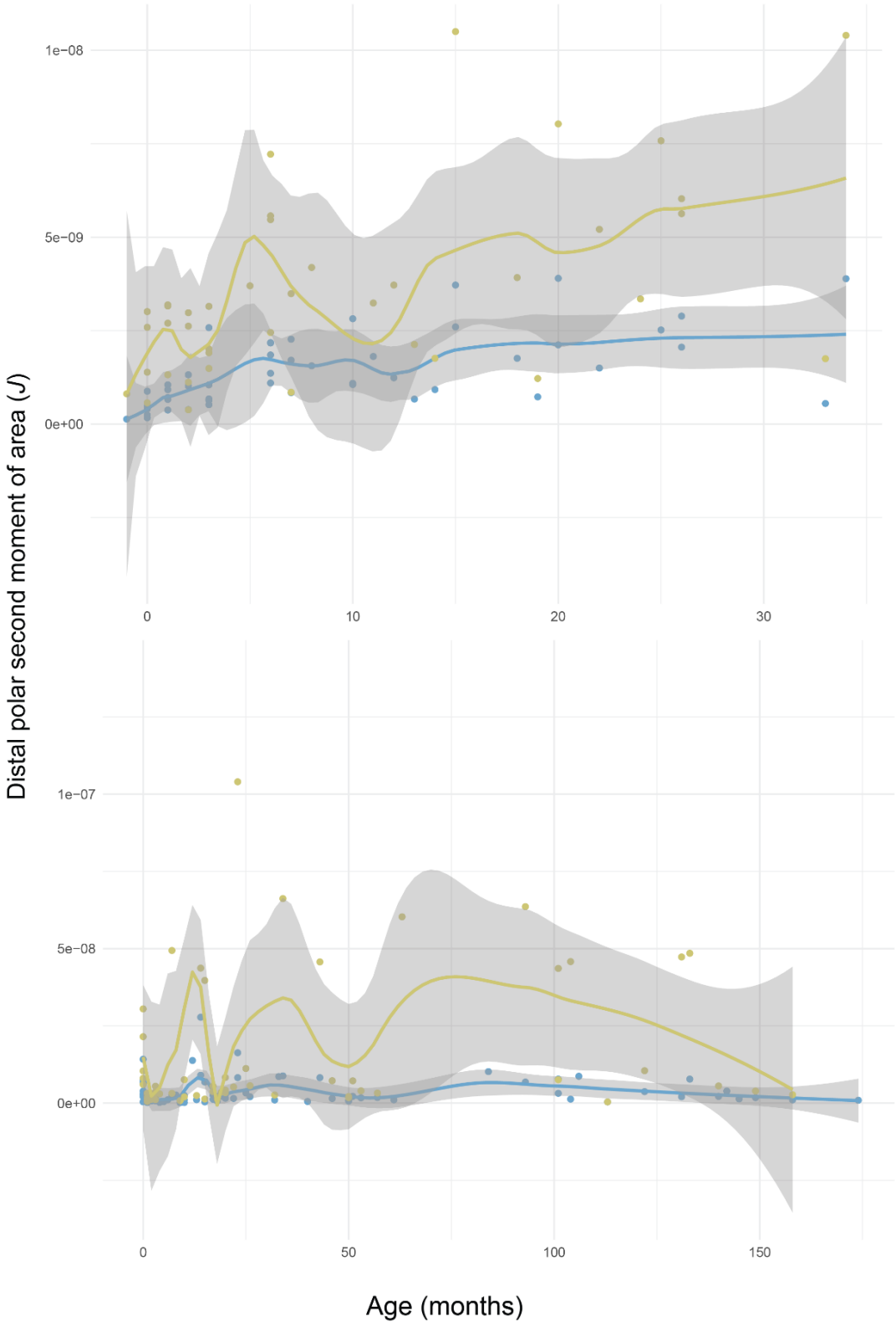


Figure 4.24. Distal polar second moments of area (*J*). Femora are in gold and humeri are in blue. Top panel – babies aged 0 – 36 months. Bottom panel – all individuals. Gray shaded areas indicate a 95% confidence interval.

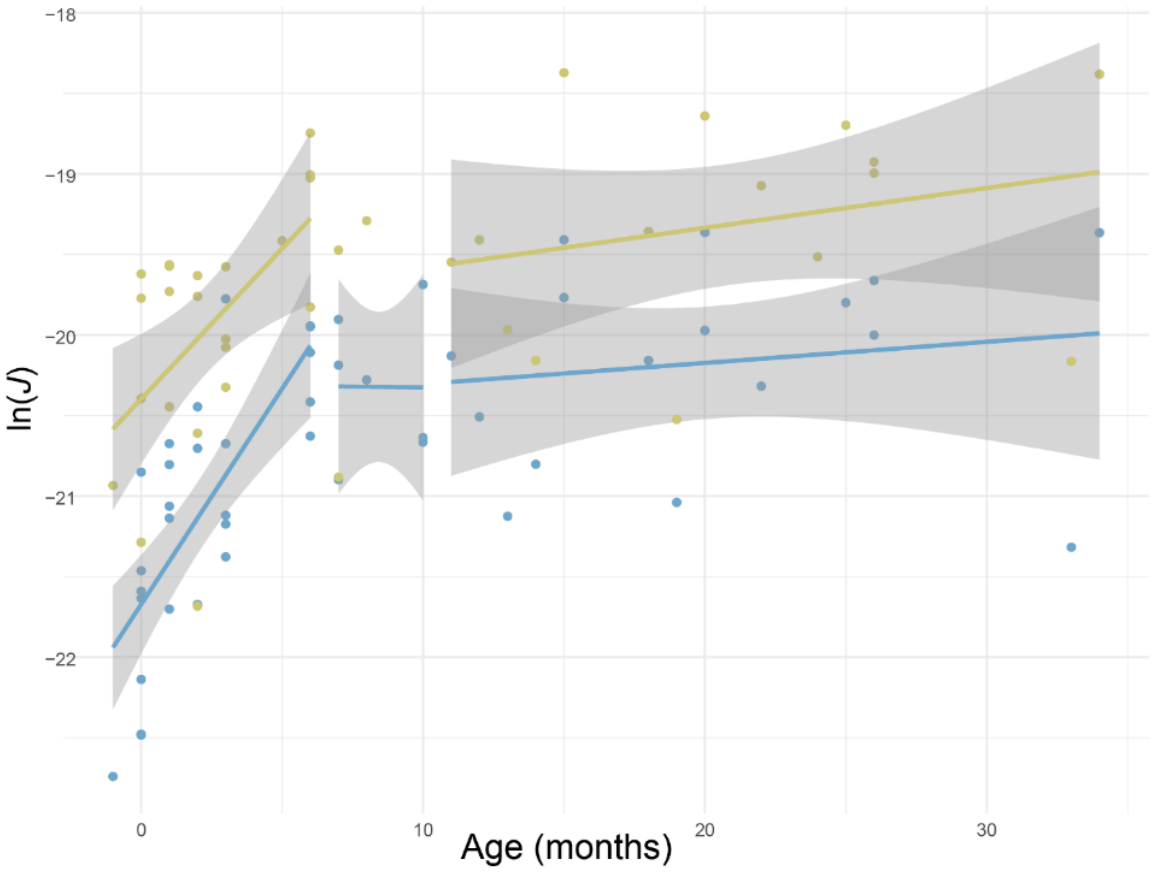


Figure 4.25 Linear regression on natural log-transformed values of distal polar second moments of area (*J*). Femora are in gold and humeri are in blue. Slopes are divided into three age groups: pre-locomotion (0-6 months), intermediate locomotion (7-10 months), and bipedal (11+ months). Gray shaded areas indicate a 95% confidence interval.

Chapter 5: Bilateral asymmetry

5.1 | Introduction

Anatomical asymmetry is a biological phenomenon found in vertebrates and invertebrates alike. Flatfish are born with bilaterally symmetrical crania, and undergo a stage of ontogeny in which both eyes migrate to one side of the skull, giving them their lateralized swimming posture and morphological asymmetry. Which side the eyes end up on is influenced by both genetic and environmental factors (Palmer, 2004; Schreiber, 2013). In some species of asymmetrical snails, the direction of shell coiling is determined by the orientation of embryonic cells (Patel, 2009). Many vertebrate organs are asymmetrical, most notably the heart and brain. Asymmetry in brain development is present in human fetuses at 12 to 14 weeks (Sun et al., 2005).

Several studies have focused on understanding the genetic and developmental underpinnings of vertebrate organ asymmetries and have identified genetic mutations that can lead to reversed symmetries in humans and mice, where organ placement is essentially mirrored (Chen et al., 1998; Schneider & Brueckner, 2000; McDowell, Rajadurai, & Levin, 2016). There are two major types of biological asymmetry: fluctuating asymmetry and directional asymmetry. Fluctuating asymmetry is essentially a random deviation from perfect symmetry (i.e., the right and left sides are exact mirrors of eachother), and is normally distributed around a mean of zero. Directional asymmetry is characterized by a directional bias and is often not centered around zero.

Skeletal asymmetry is common in vertebrates and can have several underlying causes, including developmental variation, adaptation, and function. Forelimb asymmetries in rats are typical and partially caused by small developmental variations, but are also influenced by loading patterns (Fox, Kimura, Plato, & Kitagawa, 1995). Additionally, high levels of prenatal stress can increase fluctuating asymmetry in the skeletons of rats (Mooney, Siegel, & Gest, 1985). In macaques, age, sex, and hand preferences are understood to impact directional asymmetry of the forelimb bones (Helmkamp et al., 1990). There is also a correlation between environmental stress and increased asymmetry in growth plate fusion and diaphyseal growth in these primates (Albert & Greene, 1999).

The causes of bilateral asymmetry in the human skeleton have largely been attributed to biomechanical influences caused by asymmetrical use of the right and left appendages. Lateralization of human behavior is present *in utero*. Hepper, Shahidullah, & White, (1991) observed that fetuses sucked their right thumb more frequently than their left, beginning at 15 weeks in utero, and that fetuses that sucked their right thumb were more likely to be right-handed, whereas fetuses that sucked their left thumb were more likely to be left-handed. Thus, hand preference in infants may contribute to the development of handedness in older children and adults (Hinojisa, Sheu, & Michel, 2003). Additionally, self-reported asymmetries are correlated with asymmetry in the lower limb elements, where the opposite lower limb is dominant (Carpes, Mota, & Faria, 2010; Erikson & Cramon-Taubadel, 2020). Studies of hand preference have utilized many different methods, and the use of skeletal elements to determine hand preference is somewhat controversial. Some pQCT analyses on individuals who were polled about their hand preference show very low error in determining handedness based upon humeral and ulnar asymmetries, suggesting that estimations of hand preference can be determined from skeletal anatomy (Shaw, 2011). On the other hand, an extensive literature

review suggests that quantitative measurements and qualitative observations cannot determine handedness with a sufficient degree of confidence (Ubelaker & Zarenko, 2012).

Schultz (1926) found that over 50% of fetuses studied exhibited a significantly longer right humerus than left humerus, with differences in length up to 7.5%. However, other investigations on asymmetry of the humerus have found that infants and young children do not exhibit any significant asymmetry in humeral length, midshaft diameter, or epicondylar breadth, but older children (5-17 years) do (Blackburn, 2011). The contradictory conclusions of these studies and others may stem from the varied techniques employed to study skeletal asymmetry (Cashmore, 2009).

Two questions relating to bilateral asymmetry will be addressed in this chapter.

Question 1: Are there statistically significant differences between the lengths and cross-sectional properties of the clavicle, humerus, and femur in infants and children?

Question 2: Does the pattern of asymmetry change throughout ontogeny?

These two questions are investigated using paired right and left side measurements from a sample of 100 individuals aged 0-14 years from the New Mexico Decedent Imaging Database (NMDID). See Chapter 2 for a detailed description of the sample and data collection methods.

5.2 | Materials and Methods

All individuals were measured following the same methodology on the right and left sides. Asymmetry as used here is the difference between dimensions of the left and right paired elements. Here, asymmetry is standardized by converting it into two percentages, following previous work on the topic (Steele & Mays, 1995; Mays, 2002; Auerbach & Ruff, 2006; Auerbach & Raxter, 2008; Waidhofer & Kirchengast, 2015). For each measurement, the percentage directional asymmetry (%DA) is calculated as follows:

$$\%DA = \frac{right-left}{average\ (right+left)} \text{ x } 100$$

Thus, positive %DA values indicate a right-bias (the right measurement is larger than the left) and negative values indicate a left-bias.

Absolute asymmetry was also calculated to show the directional asymmetry in each given measurement regardless of directional bias. %AA was calculated as follows:

$$\%AA = \frac{|right-left|}{average\ (right+left)} \text{ x } 100$$

Individuals are placed into one of the four age groups, shown in Chapter 2 Table 1.

5.3 | Results

5.3.1 | Clavicle

5.3.1.1 | Clavicular Length. All newborns studied have at least a slight directional asymmetry in clavicular length (Figure 5.1). For newborns with a right-sided bias, all right clavicles are less than 2.5% longer than their antimeres. For individuals with a left sided bias, directional asymmetry is higher on average, with a maximum left

biased asymmetry of over 5%. Overall, infants (12 months old and younger) have longer left clavicles than right clavicles, on average, with an average absolute asymmetry of 1.27%. Asymmetry in clavicular length decreases in toddlers, who have an average absolute asymmetry of 0.98%, then increases again in older children and adolescence, who have an average absolute asymmetry of 1.49%. Beyond 100 months of age, the majority of individuals have longer left clavicles than right clavicles (Figures 5.1 and 5.2).

5.3.1.2 | Clavicular midshaft circumference. There is roughly an even number of newborns with right and left size biases in clavicular midshaft circumference (Figures 5.3 and 5.4). Group 1 individuals have an average of 2.7% absolute asymmetry in clavicular circumference, which remains relatively stable throughout the rest of childhood and adolescence.

5.3.1.3 | Clavicular cortical area. Most infant clavicular medullary cavities are too small for accurate measurements to be taken, but there are nearly even numbers of older children who exhibit left and right sided biases. The overall average in absolute asymmetry in clavicular cortical area at midshaft is 5.48%.

5.3.2 | Humerus

5.3.2.1 | Humeral Length. At birth, neonates exhibit asymmetry in humeral diaphyseal length (Figures 5.5 and 5.6). Every newborn included in this study exhibits some exhibit asymmetry, and most individuals have a left biased DA. The average AA in newborns is 2.29%. The majority of infants have left-biased directional asymmetry, meaning that their left humerus is longer than their right. The overall DA decreases after birth until 25 months, after which it increases again. Children 100-150 months old, on average, have left humeri that are 1.3% longer than their right humeri. None of the differences between right and left humeral length are statistically significant.

5.3.2.2 | Humeral diaphyseal circumference. Of the 100 individuals included in this study, 74 have a thicker proximal humeral diaphysis on the shorter humerus (Figures 5.7 and 5.8). This trend is also true in the midshaft and distal humerus, where individuals have thicker diaphyseal circumferences on their shorter humerus (most often on the right side). The highest amount of variation in asymmetry of the humeral diaphyseal circumference at all three measurement positions is around birth, which may be an effect of a larger sample size of newborns than older infants and children. Overall, diaphyseal circumference at the proximal and midshaft measurement positions have a relatively stable amount of absolute asymmetry throughout infancy and childhood. Absolute asymmetry in the distal humerus shows a slight decline throughout childhood. In the youngest age group (<6 months), the distal humerus shows statistically significant differences between right and left, with most individuals exhibiting a larger circumference on the right humerus ($p = 0.0013$). In the oldest age group (3 years and older), there is a statistically significant difference in midshaft circumference ($p = 0.029$), but nothing else.

5.3.2.3 | Humeral cortical area. In the proximal humerus, the majority of individuals have thicker cortical bone on their left side (average = 0.64% left bias). This is primarily driven by older children, but a weak bias to thicker cortical bone in the

proximal humerus is also found in infants and toddlers (0.11% left bias in infants 0-12 months old). In the midshaft and distal humerus, the right humerus, on average, has thicker cortical bone (Figures 5.9 and 5.10). In the midshaft, infants aged 0-11 months show a right bias in cortical bone, with the right humeral midshaft cortical area being an average of 2.5% larger than the left. In older children (>12 months), the average shifts to a very slight left bias (0.01%, with an AA of 4.69%), suggesting that there is more variation in left/right biases in older children. There is a significant difference in right and left humeral cortical area only on the midshaft of the youngest group (<6 months; $p = 0.0148$) and the 1-3 year old group ($p = 0.0456$).

5.3.2.4 | Humeral second moment of area. In infants (1 year of age or less), the majority of individuals (27 of the 43 individuals) exhibit a higher average resistance to bending in the right humerus than the left humerus (Figures 5.11 and 5.12). 64% of the 1-3 year old individuals also exhibit right biased asymmetry at the three measurement positions. Absolute asymmetry increases with age. Children older than 2 years old have the highest amount of asymmetry in the humeral midshaft (average 10.92%). There are no significant differences between left and right in any of the four age groups.

5.3.2.5 | Humeral polar moment of area. All individuals have the same side bias in polar second moment of area as maximum second moment of area. Results of polar moments of area are very similar to the results from section 3.2.4, which is unsurprising and suggests that individuals grow at a similar rate in their humeral resistance to bending and resistance to torsion (Figures 5.13 and 5.14). Individuals 6 months and younger exhibit a statistically significant difference between left and right *J* at the humeral midshaft ($p = 0.0091$).

5.3.3 | Femur

5.3.3.1 | Femoral Length. Femoral diaphyseal length shows overall less directional asymmetry at birth than the humerus (Figures 5.15 and 5.16). Of the 43 infants (12 months or younger) included here, only 5 have an absolute asymmetry in femoral diaphyseal length of more than 2.5%. The other 38 individuals show less than 2.5% absolute asymmetry. The majority of infants (27 of the 43) have a longer right femur than left femur. Infants and toddlers less than 2 years old have an average of 1.99% absolute asymmetry. Children above 2 years old have an average of less than 1% absolute asymmetry in femoral diaphyseal length. There are no statistically significant differences between left and right femoral length.

5.3.3.2 | Femoral diaphyseal circumference. At the proximal, midshaft, and distal measurement positions, infants have an overall average left bias in femoral diaphyseal circumference. Infant midshafts have the greatest amount of absolute asymmetry, with an average of 2.5% (Figures 5.17 and 5.18). In individuals aged 12-24 months, the distal femur shows the greatest absolute asymmetry at 2.7%. Children older than 24 months have an average of 1.4% absolute asymmetry in the proximal femur, 0.8% in the midshaft, and 1.4% in the distal femur. There are no statistically significant differences between left and right femoral circumference.

5.3.3.3 | Femoral cortical area. Of the four age groups (0-6 months, 7-10 months, 11-36 months, and 36+ months), individuals 6 months and under have the greatest directional and absolute asymmetry in femoral cortical area in the proximal femur and at midshaft (Figures 5.19 and 5.20). Toddlers (age 11-24 months) have the greatest directional asymmetry in the distal femur, with an average absolute asymmetry of 3.95%. In the proximal femur, groups 1 and 2 are significantly different on the left and right sides ($p = 0.037$ and 0.044, respectively).

5.3.3.4 | Femoral second moment of area. 19 of the 28 individuals age 0-11 months individuals for whom femoral cross-sectional properties could be calculated exhibit higher resistance to bending in their left femur than their right, with an average absolute asymmetry of 12.9% in the proximal femur, 11.6% in the femoral midshaft, and 12.8% in the distal femur. Over 50% of children older than 2 years exhibit a left bias in the midshaft and distal femur (60% in the midshaft, 50% at the distal femur), while only 35% of children exhibit the left side bias in the proximal femur. In children older than 2 years, the proximal femur also has the lowest average absolute asymmetry (Figures 5.21 and 5.22).

5.3.3.5 | Femoral polar moment of area. Femoral resistance to bending follows the same growth pattern as second moments of area (Figures 5.23 and 5.24). Additional samples of older individuals are necessary to better understand femoral polar second moments of area. Overall, 67% of individuals aged 3 and under exhibit left-side bias in *J*.

5.4 | Discussion

Directional asymmetry in the clavicle, humerus, and femur derives from a complex combination of genetic, environmental, and behavioral factors. Bilateral asymmetry in brain development, organ placement, and movement of fetal limbs is apparent early in pregnancy. The numerus and contradictory studies on bilateral asymmetry in fetal and infant growth have left many questions about the causes of skeletal asymmetry unanswered. The data presented here support the previous hypotheses that skeletal asymmetry is present at birth.

For the vast majority of measurements examined in this study, there are no significant differences between the left and right measurements. Results show weak patterns in directional asymmetry throughout ontogeny.

Question 1: Are there statistically significant differences between the lengths and cross-sectional properties of the clavicle, humerus, and femur in infants and children?

There are very few statistically significant differences between left and right-side measurements. Most notably, age Group 1 (individuals 0-6 months of age) shows humeral midshaft cortical area and *J* are significantly different within an individual, with 50% exhibiting larger right-side values and 50% exhibiting larger left side values.

Question 2: Does the pattern of asymmetry change throughout ontogeny?

Yes, to a certain degree. Although many differences between right and left side measurements are statistically insignificant, there are some weak qualitative patterns visible in the data. In the clavicle, 60% of Group 4 individuals have longer left clavicles than right clavicles, whereas 53%

of individuals younger than 3 years have longer left clavicles. Similarly, 41% of kids under 3 years of age have a larger clavicular circumference on the left than the right, compared with 39% of individuals aged 3 and up.

The pattern is also present in the humerus, with 55% of group 1, 37% of Group 2, 42% of Group 3, and 36% of Group 4 exhibiting longer right humeri than left humeri. Group 1 measurement show about 50% of individuals showing right side bias in every single measurement taken. Group 4 individuals are more likely to have shorter right humeri, thicker midshaft circumference (60% right-bias), more midshaft cortical area (63% right-biased), and higher resistance to bending (73% right-bias). Groups 2 and 3 fall in between 1 and 2 in terms of likelihood of right-biases. As age increases, so does the likelihood of an individual having a shorter, thicker, and stronger right humerus. In the femur, on the other hand, all four groups exhibit about 50% of individuals with right or left biases in all measurements investigated, regardless of age.

While asymmetries are ubiquitous at birth, younger individuals show about a 50% chance of being right or left biased in measurements across all three bones. As age increases, the pattern shifts, and right humeri are more likely to be shorter, broader, and stronger, while femora maintain a roughly 50/50 split. In the clavicle, the pattern follows that of the humerus in terms of length, but not circumference. This may be due to error and low accuracy in measuring the clavicles of very small infants using medical CT scans. In right-handed individuals, the right humerus and clavicle tend to be shorter with thicker diaphyses compared to the left side, while the left femur is often shorter and thicker than the right (Auerbach & Ruff, 2006). This is likely because right-handed individuals tend to be left-leg dominant (Carpes et al., 2010). The patten of femoral length and robusticity is not demonstrated in this sample, but larger sample sizes would be helpful. This result mirrors the findings of Jacobsohn et al. (2012), who found that infants up to 9 months of age lack lateral manual asymmetries, but individuals 9 months and older begin to develop the group-level right-bias that forms gradually throughout ontogeny.

5.5 | Conclusions

The results presented here show that bilateral asymmetries in long bone length and circumference are present at birth. However, the proportion of right and left biases in infants and young children are not consistent with the proportion of right-hand dominant adults. The increase in proportion of older individuals with right-biased humeral circumference suggest that asymmetry changes with age, as the proportion of individuals with a thicker right humerus nears the proportion expected based on right-handedness in humans by about 8 years of age. While directional asymmetry does not increase with age, results presented here suggest that it does change the magnitude and direction of the asymmetry.

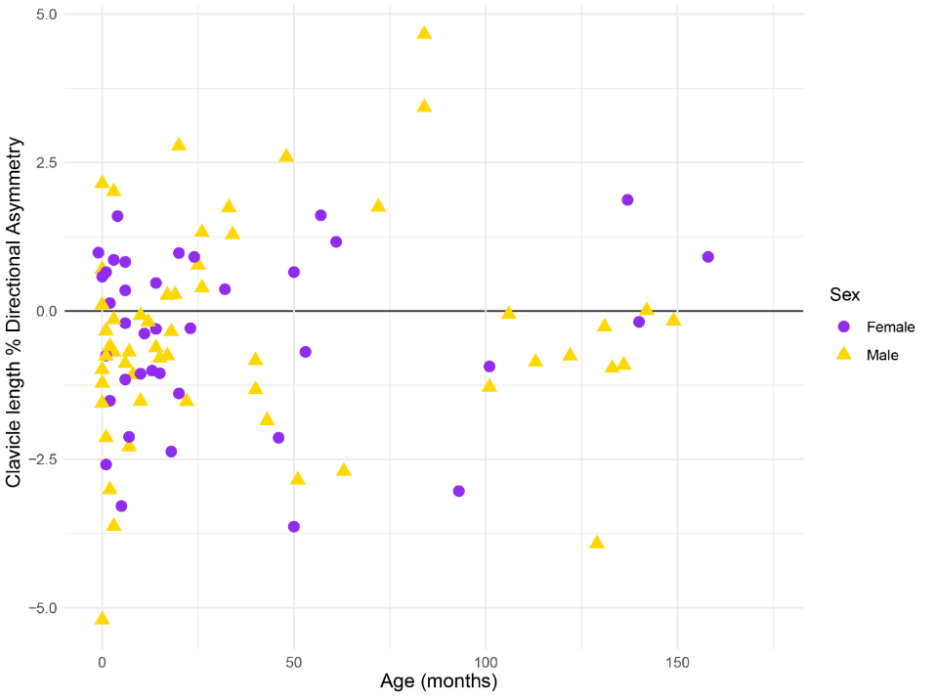


Figure 5.1. Directional asymmetry in clavicle length (%). Positive values indicate a right-side bias (right measurement is larger), negative values indicate a left-side bias (left measurement is larger).

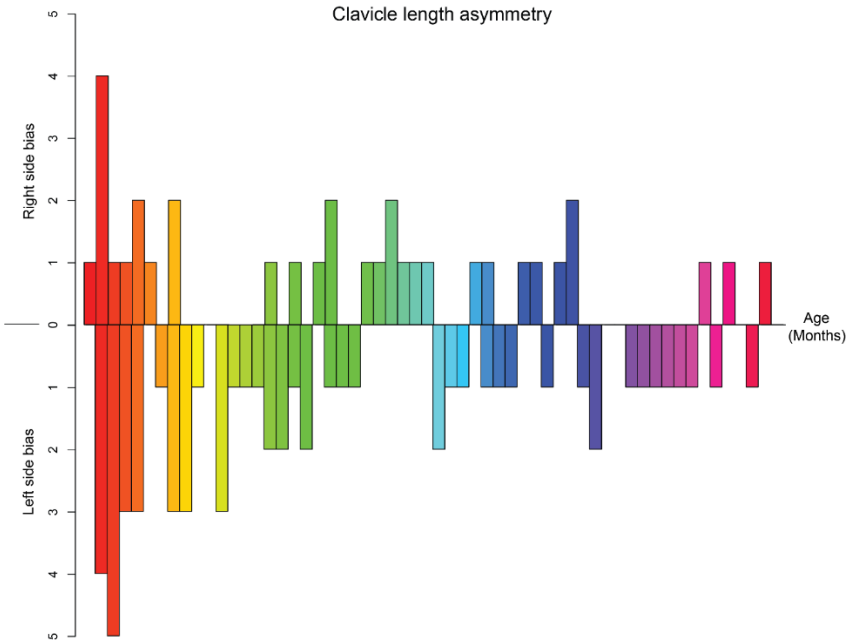


Figure 5.2. Clavicular length bar plot showing the number of individuals of each age (in months) with right-side and left-side biases.



Figure 5.3. Directional asymmetry in clavicle midshaft circumference (%). Positive values indicate a right-side bias (right measurement is larger), negative values indicate a left-side bias (left measurement is larger).

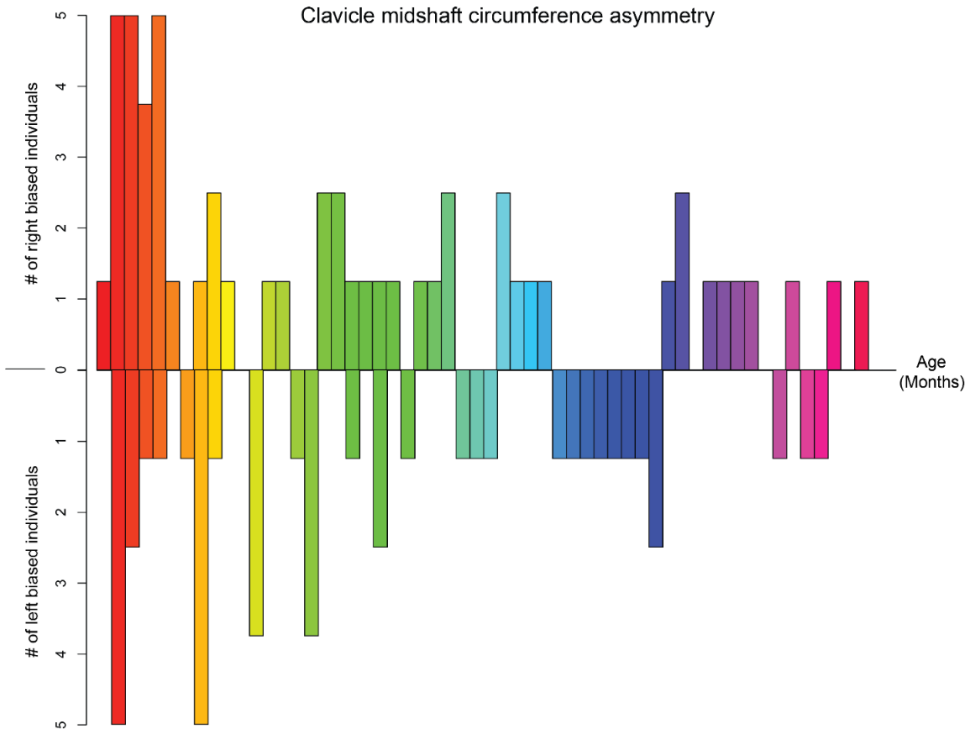


Figure 5.4. Clavicular midshaft circumference bar plot showing the number of individuals of each age (in months) with right-side and left-side biases.

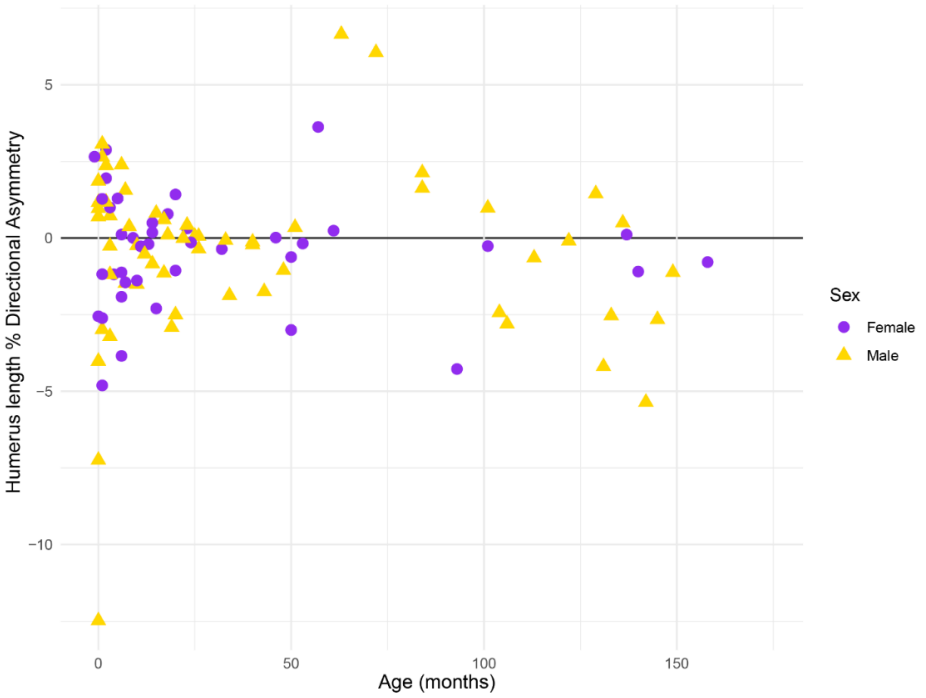


Figure 5.5. Directional asymmetry in humerus diaphyseal length (%). Positive values indicate a right-side bias (right measurement is larger), negative values indicate a left-side bias (left measurement is larger).

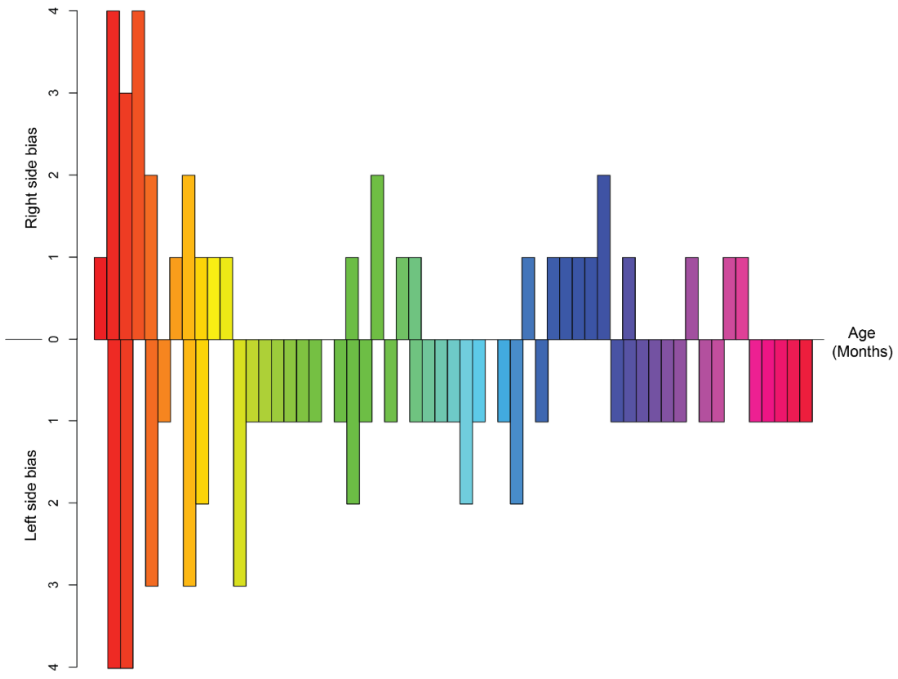


Figure 5.6. Humeral length bar plot showing the number of individuals of each age (in months) with right-side and left-side biases.



Figure 5.7. Directional asymmetry in humerus midshaft circumference (%). Positive values indicate a right-side bias (right measurement is larger), negative values indicate a left-side bias (left measurement is larger).

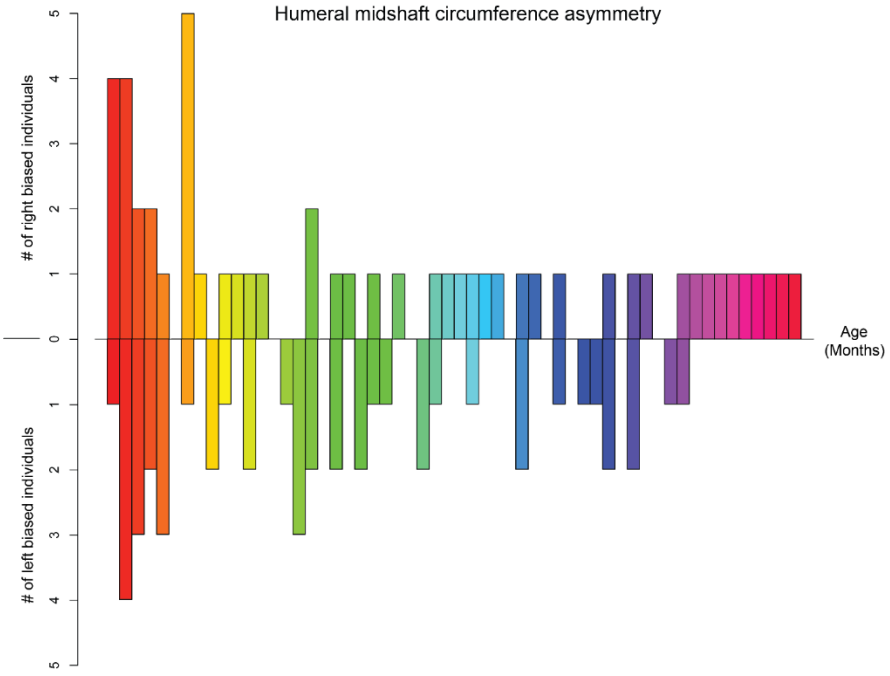


Figure 5.8. Humeral midshaft circumference bar plot showing the number of individuals of each age (in months) with right-side and left-side biases.

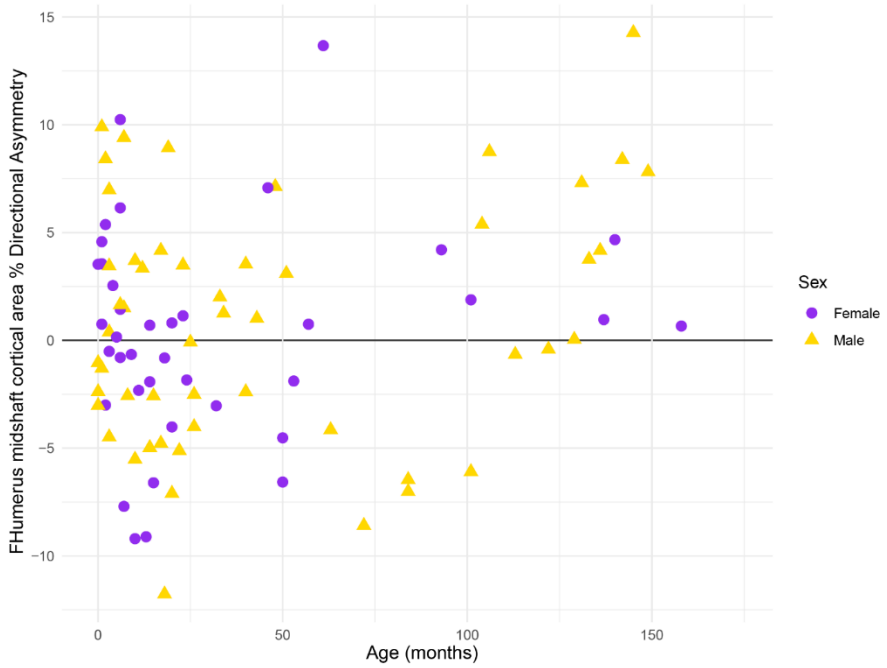


Figure 5.9. Directional asymmetry in humerus midshaft cortical area (%). Positive values indicate a right-side bias (right measurement is larger), negative values indicate a left-side bias (left measurement is larger).

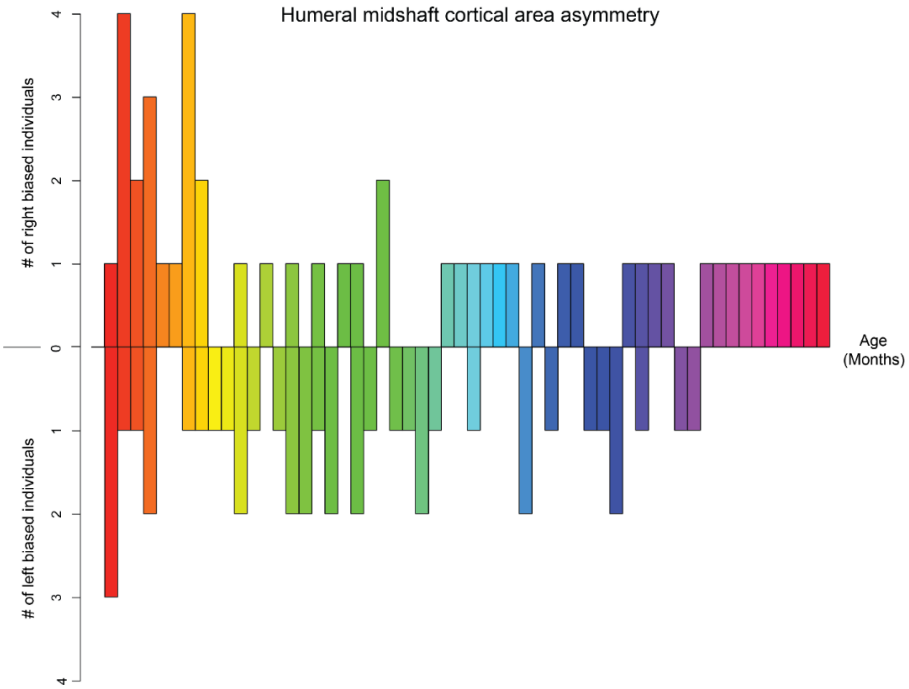


Figure 5.10. Humeral midshaft cortical area bar plot showing the number of individuals of each age (in months) with right-side and left-side biases.

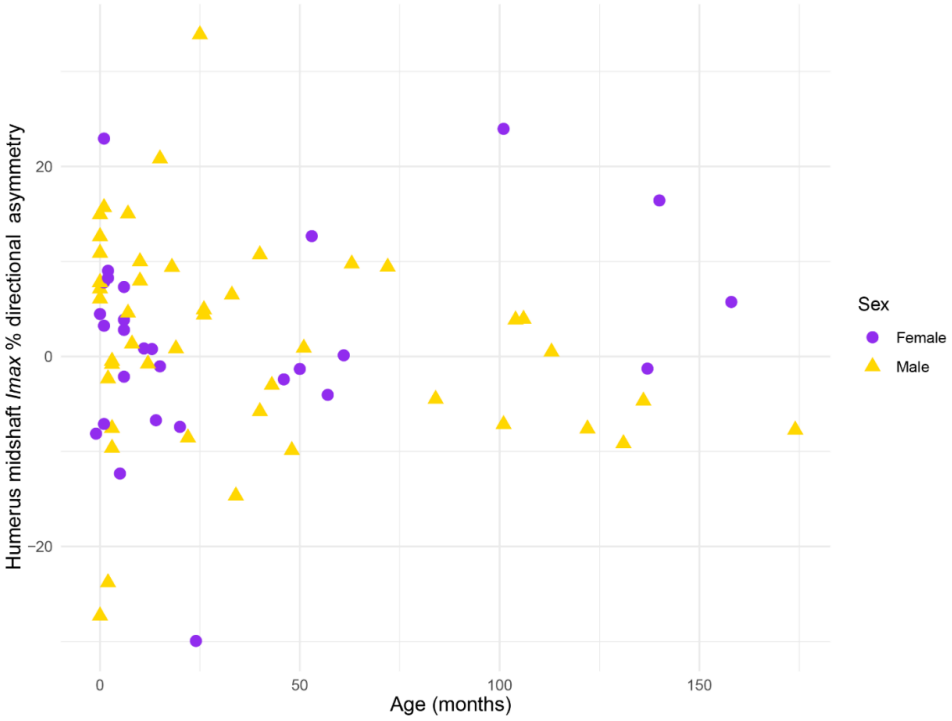


Figure 5.11. Directional asymmetry in humerus I_{max} (%). Positive values indicate a right-side bias (right measurement is larger), negative values indicate a left-side bias (left measurement is larger).

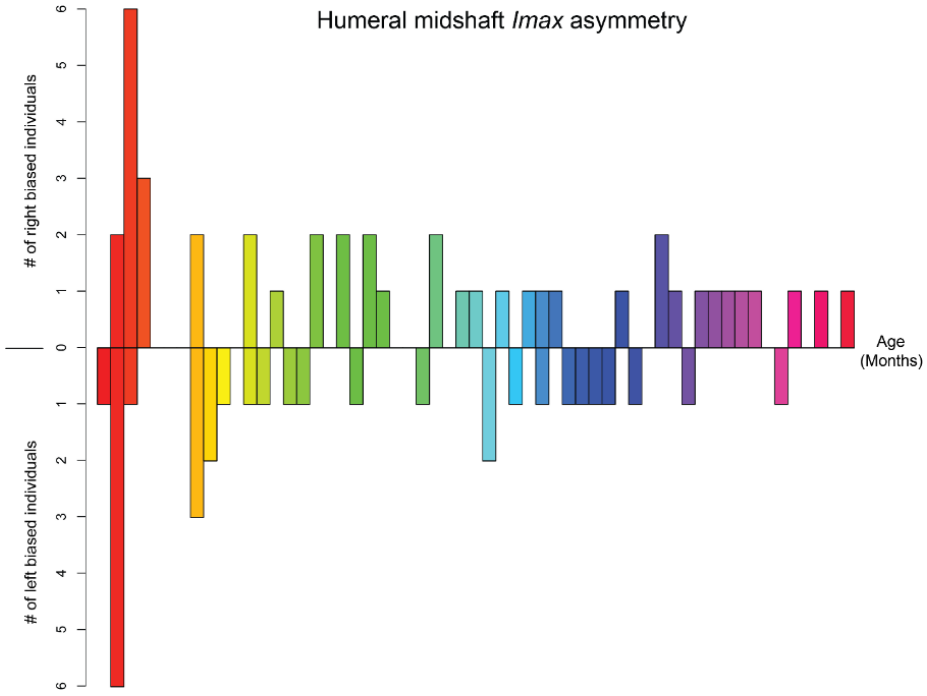


Figure 5.12. Humeral midshaft I_{max} bar plot showing the number of individuals of each age (in months) with right-side and left-side biases.

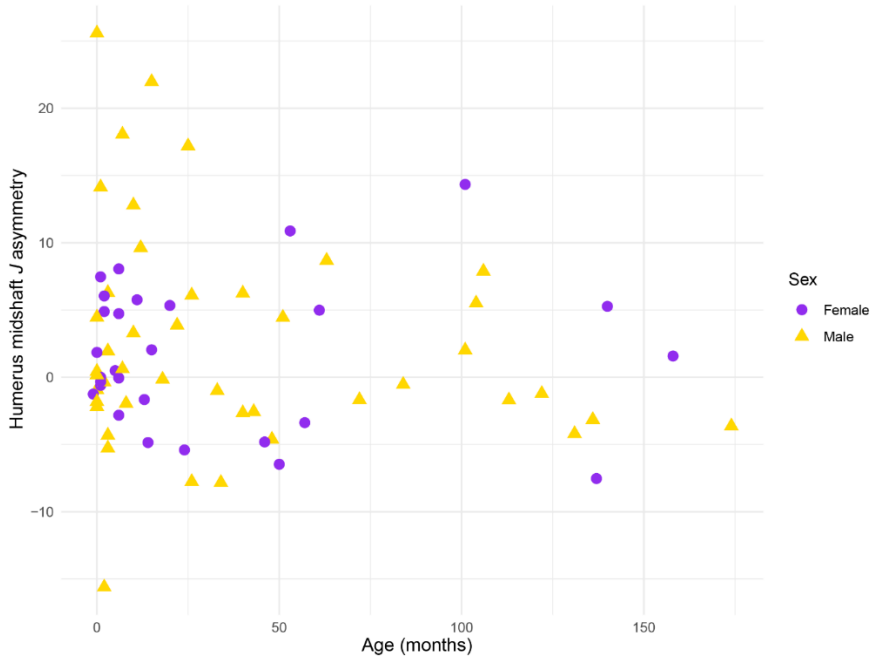


Figure 5.13. Directional asymmetry in humerus *J* (%). Positive values indicate a right-side bias (right measurement is larger), negative values indicate a left-side bias (left measurement is larger).

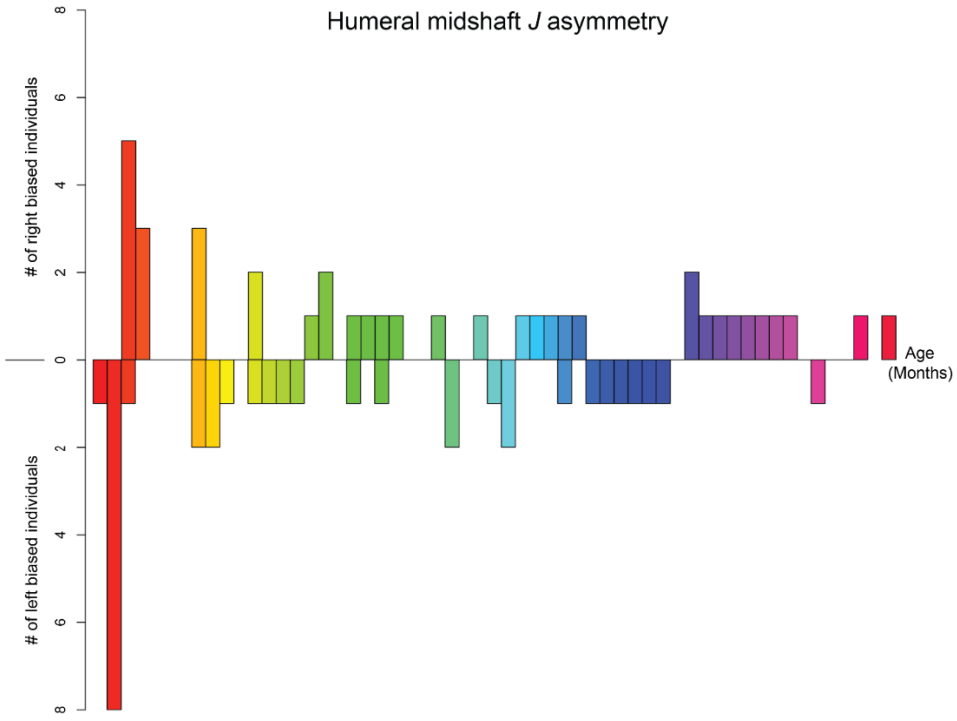


Figure 5.14. Humeral midshaft *J* bar plot showing the number of individuals of each age (in months) with right-side and left-side biases.

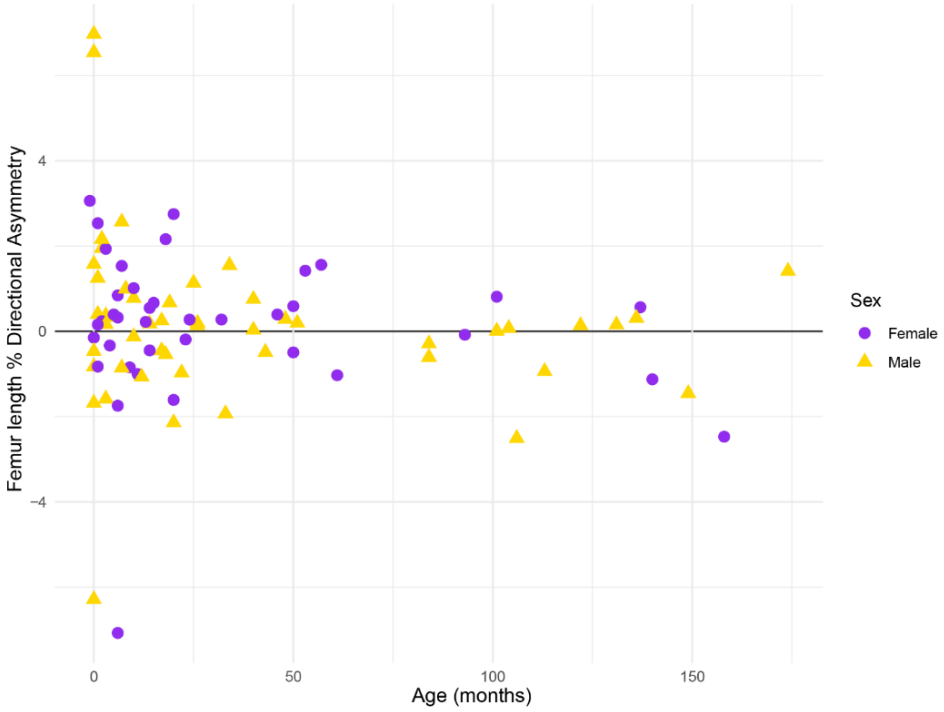


Figure 5.15. Directional asymmetry in femur diaphyseal length Positive values indicate a right-side bias (right measurement is larger), negative values indicate a left-side bias (left measurement is larger).

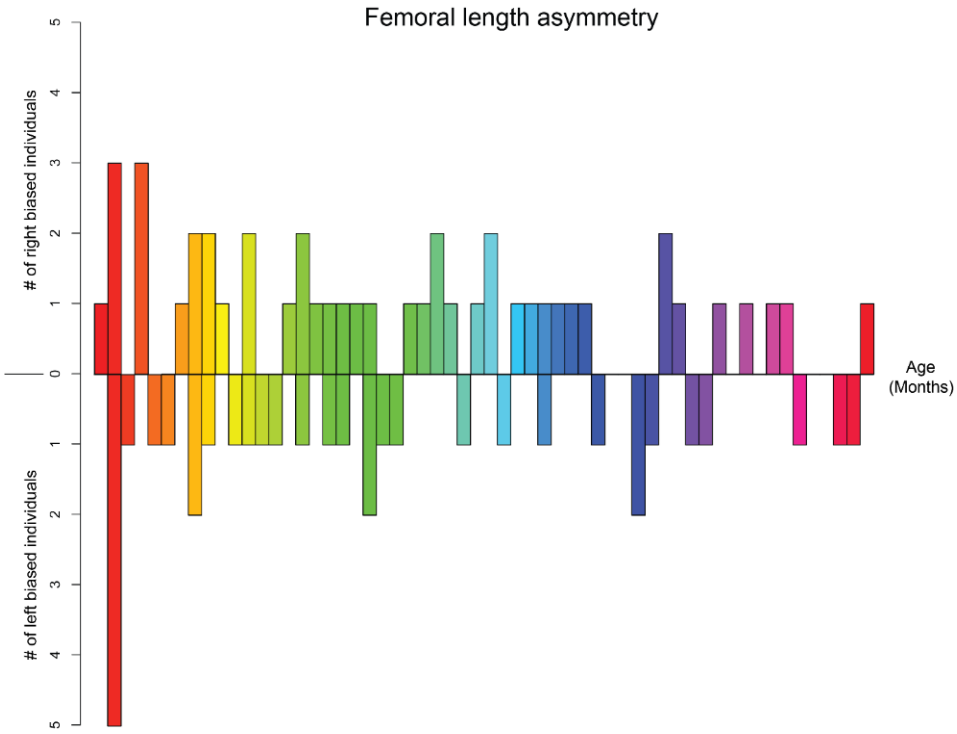


Figure 5.16. Femur diaphyseal length bar plot showing the number of individuals of each age (in months) with right-side and left-side biases.

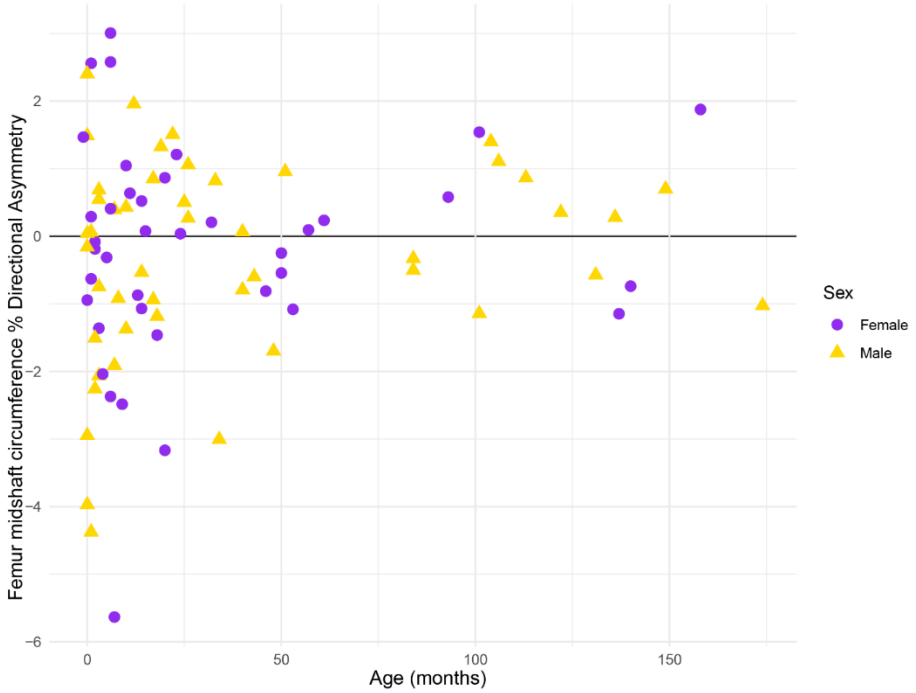


Figure 5.17. Directional asymmetry in femur midshaft circumference (%). Positive values indicate a right-side bias (right measurement is larger), negative values indicate a left-side bias (left measurement is larger).

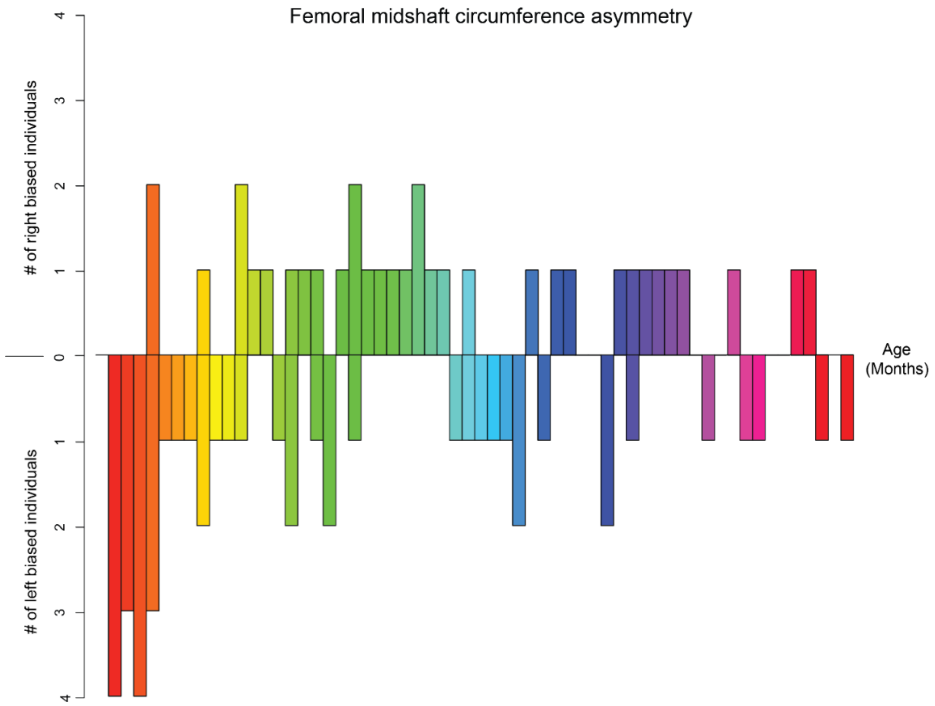


Figure 5.18. Femur midshaft circumference bar plot showing the number of individuals of each age (in months) with right-side and left- side biases.

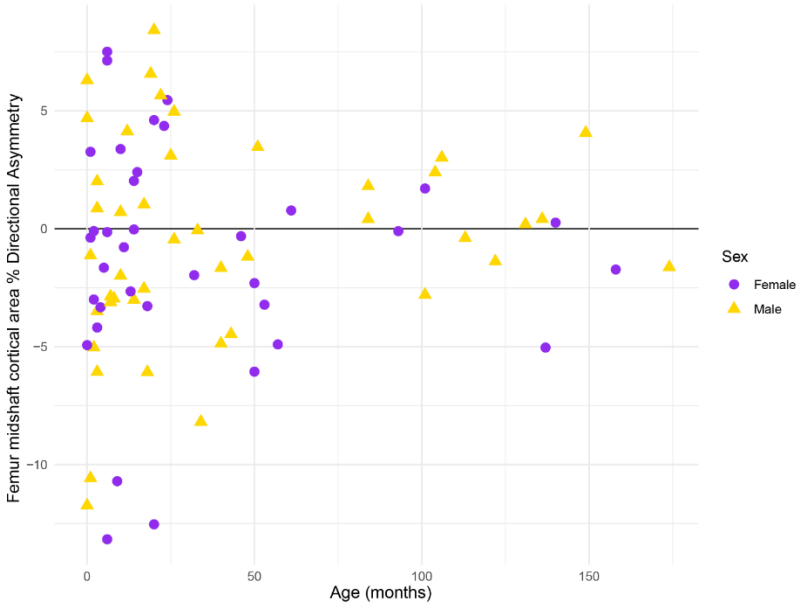


Figure 5.19. Directional asymmetry in femur midshaft cortical area (%). Positive values indicate a right-side bias (right measurement is larger), negative values indicate a left-side bias (left measurement is larger).

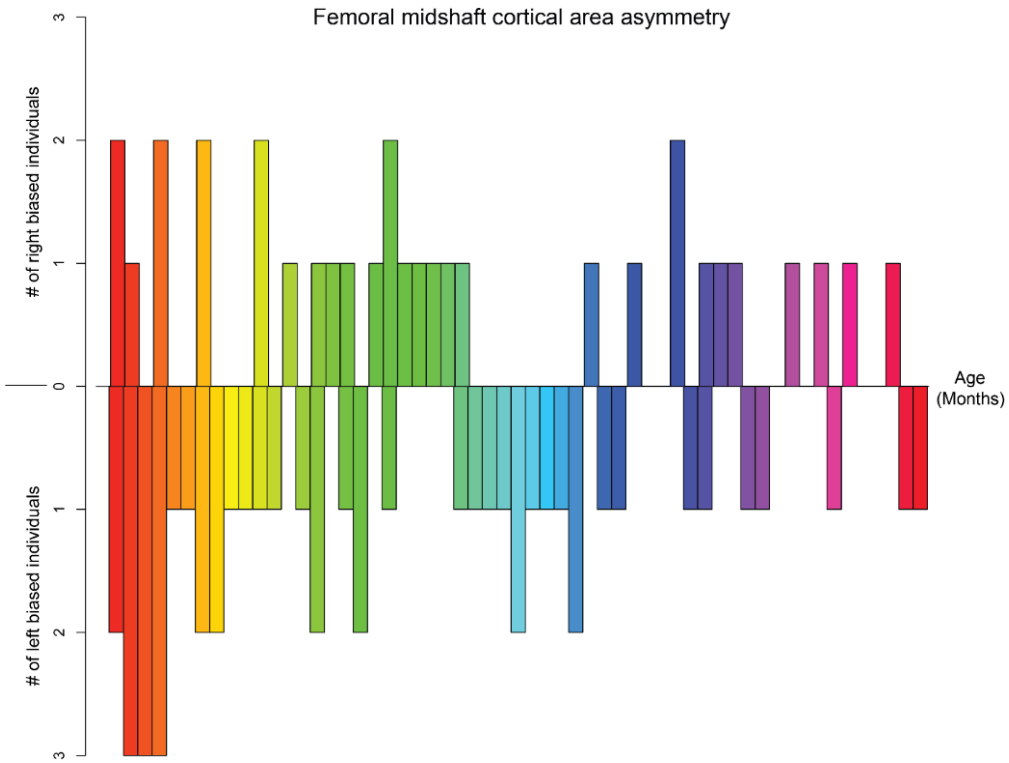


Figure 5.20. Femur midshaft cortical area bar plot showing the number of individuals of each age (in months) with right-side and left-side biases.

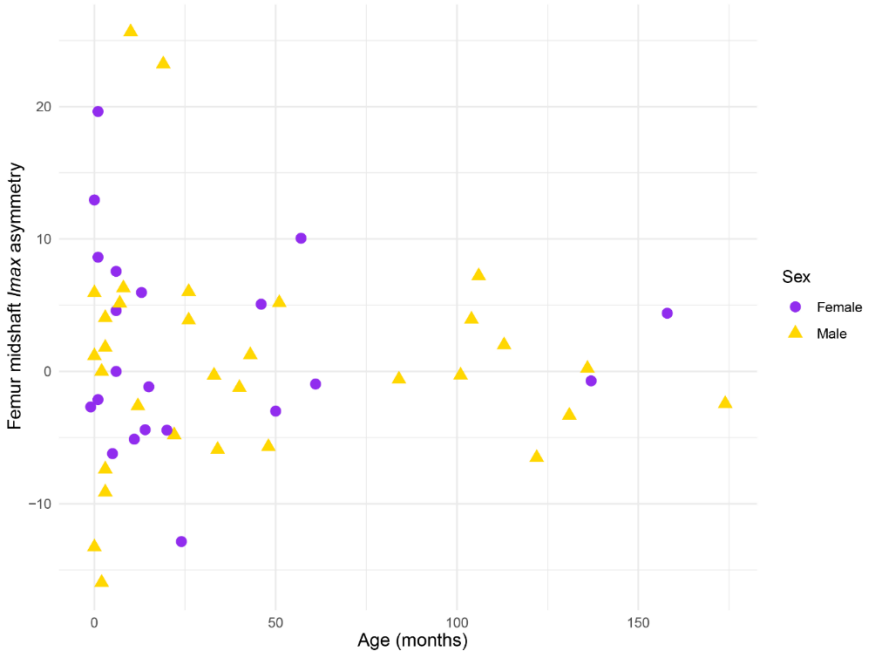


Figure 5.21. Directional asymmetry in femur midshaft I_{max} (%). Positive values indicate a right-side bias (right measurement is larger), negative values indicate a left-side bias (left measurement is larger).

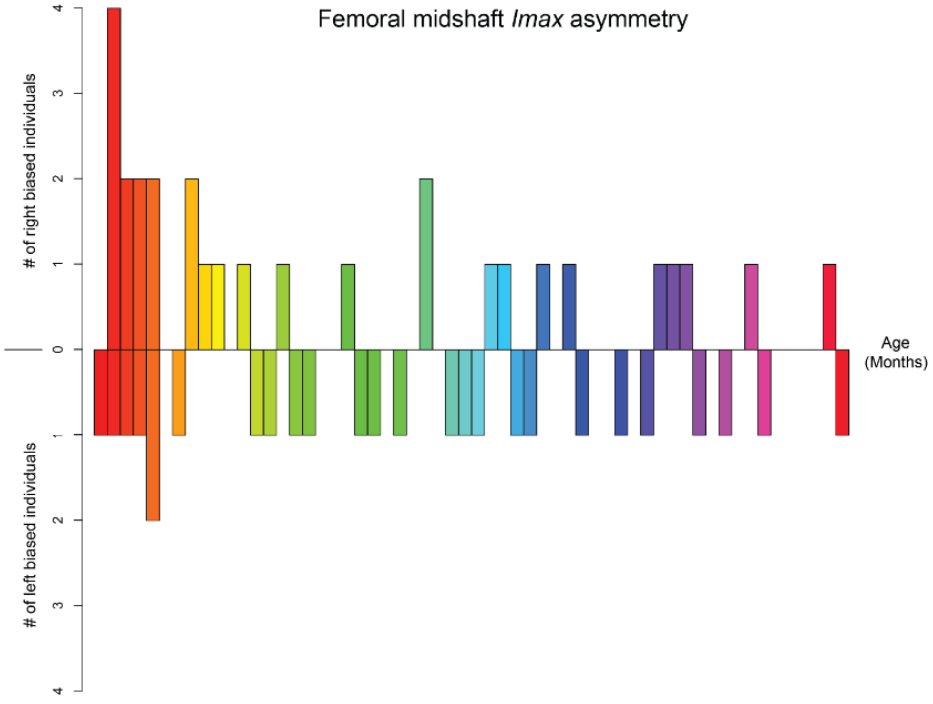


Figure 5.22. Femur midshaft I_{max} bar plot showing the number of individuals of each age (in months) with right-side and left-side biases.



Figure 5.23. Directional asymmetry in femur midshaft *J* (%). Positive values indicate a right-side bias (right measurement is larger), negative values indicate a left-side bias (left measurement is larger).

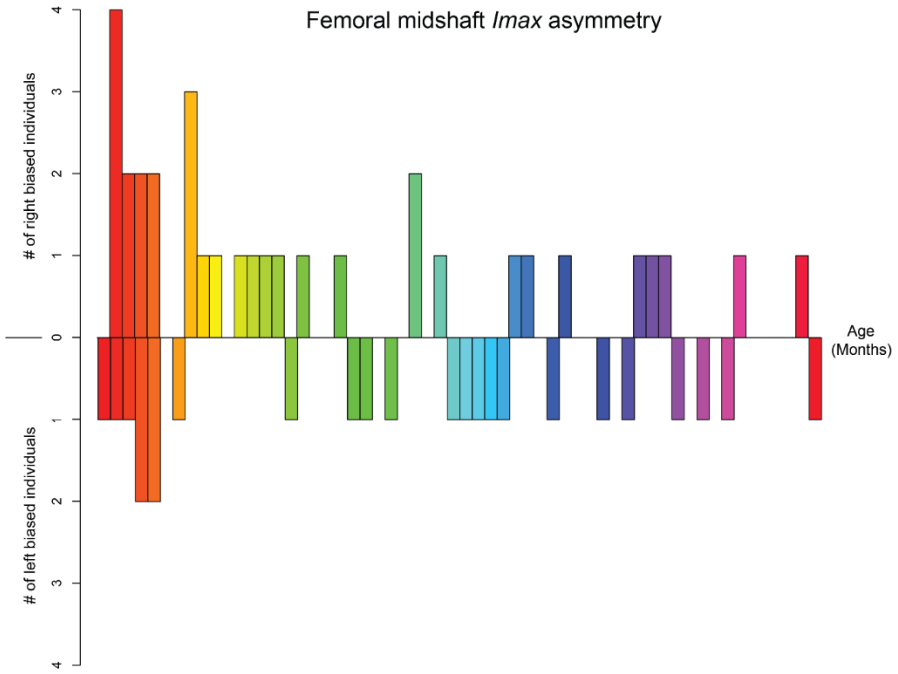


Figure 5.24. Femur midshaft *J* (%). bar plot showing the number of individuals of each age (in months) with right-side and left-side biases.

Chapter 6: Conclusions

6.1 | Introduction

My broad research program is aimed at identifying the evolutionary origins of crawling in humans. This dissertation is an important first step in this larger mission. The work herein was designed to provide an understanding how long bone growth correlates with the onset of crawling, walking, and the timing of the development of hand preference in human infants and children. Each chapter of this dissertation explored two or three questions, Chapter 3 about intra-element growth, Chapter 4 about inter-element growth, and Chapter 5 about bilateral asymmetry. Data for this cross-sectional ontogenetic study were collected from the medical CT scans of 100 infants and children from the New Mexico Decedent Imaging Database (NMDID; Edgar et al., 2019).

Results of this research provide foundational knowledge about how patterns of growth in long bones correlate with locomotor developments in human children. There are several notable results discussed below, including the role of endosteal bone formation in cortical bone growth, the changes in growth patterns correlating to the onset of crawling and walking, and the changes in patterns of bilateral asymmetry throughout ontogeny. Future research using similar methods can be applied to understanding ontogeny of other extant and extinct primates.

Conclusions from each chapter are briefly summarized below, followed by a discussion of limitations and an outline of future directions for research.

6.2 | Context

Previous research on the relationship between ontogenetic locomotion, hand preference, and skeletal properties suggests that changes in biomechanical loading patterns from crawling, walking, and preferentially using one hand more than the other can be detected in skeletal elements (see Chapter 1 for an in-depth discussion of previous research). This dissertation has built on the work of Ruff (2003b), Cowgill (2008), and Sumner & Andriacchi (1996) by using a relatively large sample of infants and children of known ages to investigate patterns of growth in long bones.

6.3 | Chapter 3: Intra-element growth and development

Chapter 3 explored intra-element growth and development in the humerus and femur of human infants and children. Questions about intra-element growth were investigated by comparing the growth rates and patterns of growth in bone length and cross-sectional properties at different measurement positions along the humerus and femur. This chapter examined three different questions, with results briefly summarized below.

6.3.1 | *Question 1.* Are there measurable differences in cortical properties in the portions of the humerus and femur that contribute the most to longitudinal growth?

In short, the answer to this question is yes. Results showed much overlap in the growth rates of the proximal, midshaft, and distal aspects of the humerus and femur, but also capture interesting patterns in bone growth. I discuss the results for the humerus first, and then address the femur.

Based on the individuals analyzed in this study, the proximal humerus grows significantly faster in I_{max} and J, and has a different pattern of growth in relative medullary area than the midshaft

and distal portions (Chapter 3, Figure 3.5). Focusing more closely on the proximal humerus, I found that the relative size of the medullary cavity increases very slowly during early childhood, and enlarges in size more slowly than the bone grows in length. The pattern of growth in medullary area (MA) could be an effect of the bone's relatively rapid increase in length, primarily due to growth from the proximal growth plate, though the precise mechanism for this relationship is unclear.

At all three humeral measurement positions, cortical area and total circumference increase relatively quickly in the first ~10 months of life. At the proximal humerus, but not the midshaft and distal humerus, the percentage of the subperiosteal area that is taken up by the medullary cavity stays relatively the same. This can be accomplished in two different ways – either the entire cross-section is getting larger at the same rate, such that the relative size of the medullary cavity stays the same, or cortical bone is being deposited more quickly than the medullary cavity is expanding. Because the same pattern of MA growth is not seen in the midshaft and distal portions of the humerus, but the rates of growth in circumference and total cortical area are relatively similar, the main difference in the proximal humerus may be the growth rate of the medullary cavity.

The distal femur is responsible for the majority of growth in femoral length. In contrast to the proximal humerus, there are no statistically significant differences in the distal aspect of the femur. Though the distal femur has the highest overall resistance to bending and resistance to torsion, the overlap with midshaft and distal values is important and should not be disregarded, as it may be an effect of sampling.

Considering the results of the proximal humerus and distal femur together, I hypothesize that the influence of loading from shoulder musculature is affecting cortical bone growth in the proximal humerus. Since only the proximal humerus shows this pattern, and not the distal femur as well, it is clear that there is another reason for this pattern beyond contribution to longitudinal growth. Since most infants begin propping themselves up with their arms well before they support their body weight with their legs, it is possible that the significant results from the proximal humerus reflect early locomotor behaviors such as army-crawling and use of the arms to prop oneself up when laying prone.

6.3.2 | *Question 2.* Is there evidence from cross-sectional properties that endosteal bone formation is contributing to cortical growth?

Yes, there is evidence that endosteal bone formation contributes to cortical growth in the proximal humerus. The growth patterns in cortical area, circumference, and medullary area compared with the midshaft and distal humerus suggest that endosteal bone formation is taking place in the proximal humerus. As described above, the growth pattern of MA compared to cortical area and total circumference suggests that the medullary cavity in the proximal humerus is staying relatively the same size while cortical area and circumference are both increasing. This is likely due to either endosteal formation or lack of endosteal resorption in the proximal humerus.

While it is not possible to discern if bone is actively being deposited, or just not being resorbed on the endosteal surface, this pattern suggests that the endosteum is responsible for some portion of cortical growth. This supports the results from Maggiano et al. (2016), who found that endosteal primary tissue (responsible for bone formation) is present on nearly the entire

endosteal surface of the proximal humerus, but not the midshaft or distal humerus. These results suggest that the increased endosteal bone deposition or decreased endosteal bone resorption is affected by loading from the shoulder musculature, because the pattern of growth in the proximal humerus changes around the onset of walking.

6.3.3 | *Question 3.* Are there any sex differences in the growth of the humerus and femur along the diaphysis?

The only significant difference between males and females is absolute length of the femur perinatally. This dimorphism disappears after ~7 months and may be an effect of sampling (n = 10 newborns, 2 of whom were assigned female at birth). Although there are very few perinatal females included in this study, this result suggests that there may be significant size dimorphism in neonates. Some studies have found significant size dimorphism in fetuses as early as 8 weeks post-conception (e.g., Bukowski et al., 2007). The conclusions of such studies are supported by the results presented here, though larger sample sizes would be helpful in determining the validity of this observation.

6.4 | Chapter 4: Inter-element growth and development

Chapter 4 explored the relationship between humeral growth and femoral growth. This was accomplished by comparing growth rates and patterns in homologous parts of the two limb elements (e.g., the proximal humerus and the proximal femur). This chapter addressed two different questions, whose results are discussed below.

6.4.1 | *Question 1.* Are there statistically significant differences between humeral and femoral growth throughout infancy and childhood?

Yes. Growth rates differ between the humerus and femur and the relationship between the two changes throughout ontogeny. During the first 6 months of life, the humerus grows significantly faster than the femur cortical thickness, I_{max}, and J at all three measurement positions. In the Group 3 and Group 4 individuals (11 months and older), this pattern is reversed, as growth rates of these traits in the femur are higher than that of the humerus. In Group 2 individuals, 7-10 months of age, there is a large amount of variation. This is an especially interesting developmental period during which most babies begin locomoting independently. Whereas the amount of variation obscures any conclusive patterns in this sample, future research focusing on this developmental period with better sampling and smaller time bins would increase clarity on growth patterns within this developmental period.

6.4.2 | *Question 2.* Do the observed growth patterns broadly correlate with the onset of crawling and walking?

Yes, growth patterns in the humerus and femur broadly correlate with locomotor milestones during the first few years of life. By the end of the 6^{th} postnatal month, 50% of babies are crawling on their stomachs and supporting bodyweight with their arms. By the end of the 9^{th} month, 50% of babies are able to walk bipedally with sufficient support and are primarily using some form of intermediate locomotion (crawling, scooting, etc.; Malina, 2004; Adolph et al., 2011). There is a shift in growth rates in the humerus and femur that occurs between months 7 and 10. In babies 6 months and under, when most infants are using their hands to explore their environment and some have the ability to support their bodyweight with their arms, the humerus is growing in strength relatively faster than the femur.

In individuals 11 months and older, when most babies are walking bipedally some or most of the time, femoral strength grows more quickly than humeral strength. While growth rates for both the humerus and the femur are greater in the first 6 months than later in life, the relative rate of humeral to femoral growth correlates with locomotor milestones like crawling and walking. Thus, the effect of changes in loading pattern during locomotor ontogeny are evident. Sample sizes for Group 2, who are the most likely to be crawling, are small and thus any conclusion about growth patterns in this developmental stage are tentative. Despite some uncertainty within the Group 2 developmental period, the changes in growth rates in the humerus and femur show that there are significant differences and changes in growth patterns as individuals transition from pre-locomotion, to intermediate locomotion, and finally to obligate bipedality.

6.5 | Chapter 5: Bilateral Asymmetry

Chapter 5 focused on bilateral asymmetry of the clavicle, humerus, and femur throughout ontogeny. Asymmetry is very common in biology, and can be caused by normal developmental differences between right and left elements, or can be influenced by repetitive behavior. The majority of humans have a right-hand preference, where the right forelimb has superior motor skills and is preferentially used for complex manual tasks. Up to 90% of humans are right-handed, and archaeologists and paleontologists have used bilateral asymmetries in skeletal elements to interpret hand preference in past populations. This chapter focuses on understanding the typical growth pattern of bilateral asymmetries in human infants and children by answering two questions:

6.5.1 | *Question 1.* Are there statistically significant differences between the lengths and cross-sectional properties of the clavicle, humerus, and femur in infants and children?

There are very few statistically significant differences between paired right and left elements in human infants and children. There is quite a bit of variation observed between right and left elements, most of which is not statistically significant. The femur exhibits the fewest differences between right and left sides. The lack of statistical significance does not indicate a lack of a pattern, but does show that differences between right and left elements are usually quite small. The lack of a clear pattern and statistical significance in the femur also suggest that the results from the humerus and clavicle are not a product of fluctuating asymmetry in older individuals.

6.5.2 | *Question 2.* Does the pattern of asymmetry change throughout ontogeny?

Despite the lack of statistical significance in most traits measured, there are some suggestive patterns. First, humans are born with asymmetries. Results show that individuals have about a 50:50 chance at birth of having a right side or left side bias in most traits studied, which suggests that asymmetry at birth is the result of gestational development that results in fluctuating asymmetry, rather than bilateral asymmetry that is seen in adults with an established hand preference. However, as age increases, individuals are more likely to have a pattern of bilateral asymmetry that mirrors what one would expect from right-handed individuals (i.e., a shorter, thicker, and stronger right forelimb than left forelimb). Older individuals are more likely to have shorter humeri on the right side (Figures 5.5 and 5.6), as well as a larger humeral circumference and thicker cortical bone on their right side (Figures 5.7-5.10). This pattern is much weaker in the clavicle, and absent in the femur. Femoral asymmetry is about 50:50 in infants, which remains mostly stable throughout ontogeny. The combined pattern of clavicular and humeral asymmetry correlates with the expected outcome based on hand preference. While asymmetry in

the humerus and clavicle do not reach the 90% right side bias of adult hand preference, the shift to right-side bias as individuals get older is notable.

This interesting shift from infants with fluctuating asymmetry to older children with directional asymmetry suggests that the effects of hand preference on skeletal anatomy are not present at birth, or even in the first few years of life. This mirrors behavioral data from Jacobsohn et al. (2012), who found that the group-level right-bias in hand use is not present in newborns and young infants, but begins to develop slowly over time. In this sample, it is not until around 100 months of age that the pattern of humeral and clavicular asymmetry begins to approach what would be expected from a largely right-handed sample. This could be because older individuals have more developed motor skills that allows them to perform tasks one-handed that younger individuals would use two hands for. This also indicates that any attempts to assess hand preference from juvenile skeletal remains may be misleading, as infants and young children do not exhibit the same patterns of bilateral asymmetry as older adults.

6.6 | Variability throughout ontogeny

An important result of this dissertation is the amount of variation in human ontogenetic growth and how skeletal variability changes throughout ontogeny. Change point analyses show a change in variability in this sample that occurs around 70 months of age in nearly every trait measured (description of analyses are included in Chapters 3 and 4). Thus, individuals younger than ~70 months of age are expected to have similar levels of variance. Variability throughout ontogeny is a complex topic, and isolating the driving forces affecting it is difficult. For example, variance in fluctuating asymmetry of human skeletons tends to increase throughout ontogeny (Hallgrímsson, 1999), and variance in height increases during puberty, but variance in body size decreases by the end of the pubertal growth spurt (Dickinson, 1960; Zelditch, 2005; Johnson et al., 2012). The decrease in variance in body size is likely driven by the tendency of juvenile skeletons to undergo catch-up growth in the event of illness or developmental stress that prevents normal growth from occurring. While the variation seen in younger individuals may be an effect of sampling or measurement error, it is also possible that the pattern seen in this sample is reflecting increased fluctuating asymmetry in younger individuals.

The change in variance detected by change point analyses occurs around 70 months of age. This correlates broadly with adrenarche, which typically occurs around 6 years of age in humans (Auchus & Rainey, 2003; Witchel, Pinto, Burghard, & Oberfeld, 2021). Adrenarche refers to the initial increase in endogenous concentrations dehydroepiandrosterone sulfate (DHEA) and is generally recognized as the first step towards puberty (Sato & Iemitsu, 2018). DHEA is a precursor to sex hormones and is converted to testosterone and estradiol during puberty. While it is possible that the change in variance in this sample is a result of sampling, it is also possible that the change in variance reflects variation in the onset of adrenarche. Future studies should investigate the correlation between skeletal growth and onset of adrenarche in a longitudinal *in vivo* study.

6.7 | Limitations

The results of this dissertation demonstrate a need for more research on the topic of ontogenetic long bone growth. More data should be collected from the NMDID and other data sources. Initially, an analysis on inter-observer repeatability will help elucidate the effects of error and the strength of methods used in this dissertation. The relatively small sample sizes, especially in the

7–10-month-old age group, result in ambiguity of some conclusions within this age group. The quality of medical CT scans of smaller individuals introduced methodological limitations that may bias the results of this study. Despite the limitations imposed by the study of very small individuals, some clear growth patterns are present, and conclusions may be strengthened by increasing sample sizes.

Including more individuals, especially in the 7–10-month age group, will help to increase understanding of the patterns and ranges of variation in the skeletal traits investigated in this dissertation. Babies between 7-10 months of age exhibit much variation in their motor development, type(s) of intermediate locomotion utilized, and timing of onset of different locomotor milestones, as well as a plethora of other sources of variation such as nutrition and environmental stressors. Such a large amount of variation during a short developmental period necessitates large sample sizes to accurately identify any significant patterns.

6.8 | Future Directions

The big picture aim of this dissertation was to provide a foundational understanding of how the development of crawling, walking, and hand preference correlates with developmental patterns in the clavicle, humerus, and femur. While there are several interesting patterns resulting from this research, future examinations of bone growth and locomotion in infants and children should also include more distal elements of the forelimb and hindlimb. Including the radius and tibia would help infer patterns of pre-walking locomotion. If infants are rarely supporting their body weight with their tibiae prior to bipedal standing and walking, the growth patterns in the tibia may be different than those of the femur, which is undergoing loading during hands-and-knees crawling. Perhaps, with additional research, identification of individuals who were in a pre-walking or pre-locomotion phase would be possible with long bone cross-sectional investigation.

Any investigation of muscular strength and/or bone properties in living individuals at known locomotor milestones would provide obvious insight. In this vein, more research should be done on the role of individual muscles and muscle groups in the different stages of locomotor development. This would allow for targeted data collection on muscles or muscle groups of interest and how their use affects bone properties.

Although the aim of this dissertation was to understand bone growth and development in infants and children, a better understanding of how cross-sectional properties examined here change with pubertal and post-pubertal growth would be interesting. This research provides a basis for future studies on pubertal and post pubertal growth that would build on the data presented here. Adding more older individuals and increasing the upper age limit to ~18-20 years would aid understanding in pubertal bone growth and its effects on the cross-sectional properties of long bones.

A top priority for my future research is to expand the foundational dataset for humans that I have discussed in this dissertation to include comparable data from non-human primates. The work of Sarringhaus et al. (2005; 2016) and Ruff (2013) investigated the correlations between ontogeny and long bone cross-sectional properties and ontogeny and asymmetry in chimpanzees and gorillas, but sample sizes were small, and methods are not conducive to comparison with the data presented here. Examination of ontogenetic bone growth and locomotor changes in non-human primates would provide important context for understanding the patterns discussed here in an evolutionary framework. Future studies should use similar methods to scan and measure the long

bones of non-human primates. If non-human, quadrupedal primates have similar growth patterns to those described in this dissertation, then obviously the correlations between the growth rates of humeral and femoral strength and onset of locomotor milestones would be falsified. Results from non-human primate studies could provide evidence that the locomotor-related changes in long bone strength described here are (or are not) correlated with human-specific locomotor patterns like crawling and obligatory bipedality.

While chimpanzees and gorillas do not exhibit an intermediate locomotor behavior like crawling, juveniles are often more arboreal than adults (Ruff, 2013; Sarringhaus et al., 2016). Thus, investigation of arboreal primate locomotor ontogeny and long bone growth is warranted as a comparison. If long bone cross-sectional growth patterns are reflective of locomotor ontogeny in non-human primates, I hypothesize that juvenile chimpanzees and gorillas would have growth patterns and biomechanical loading somewhat similar to orangutans, and that adult chimpanzees and gorillas would have cross sectional properties somewhat similar to crawling humans in relative humeral to femoral properties.

Investigating bone growth in non-human primates will not only add context to the conclusions of this dissertation, but might also be significant to the understanding of fossil hominids. With a baseline understanding of the long bone growth patterns in humans and extant non-human primates, inferences about hominid locomotor development could be made. If, hypothetically, great ape long bone ontogeny was quite different from that of humans discussed in this dissertation, comparisons with juvenile fossil hominids could help estimate the growth patterns of extinct hominids and provide insight into their ontogeny. Because the evolutionary origins of crawling are not yet understood, the first step to understanding when and why this uniquely human behavior arose should be based on a solid comprehension of extant human and non-human primate growth patterns and variation. This study lays a foundation to work towards addressing these evolutionary questions.

Finally, there are several methodological studies that merit undertaking. Using the methodology used in this dissertation, analyses of inter-observer error and repeatability would elucidate the reliability of conclusions reached here. Additional research should also be done on different methodologies for measuring second moments of area from medical CT scans of small individuals. Furthermore, research comparing cross-sectional measurements from medical CT scans, micro-CT scans, and measurements from dry bone would help to establish more reliable, accurate, and repeatable measurement methodologies.

6.9 | Conclusions

This dissertation explored the growth and development of long bones in human infants and children. Several patterns were detected in the results, supporting the hypothesis that locomotor ontogeny and hand preference affect long bone development in the clavicle, humerus, and femur. This investigation of long bone growth in human infants and children provides a foundational data set for future work. This work establishes baseline knowledge that will be built upon by including older individuals, non-human primates, and evolutionary perspective in future work.

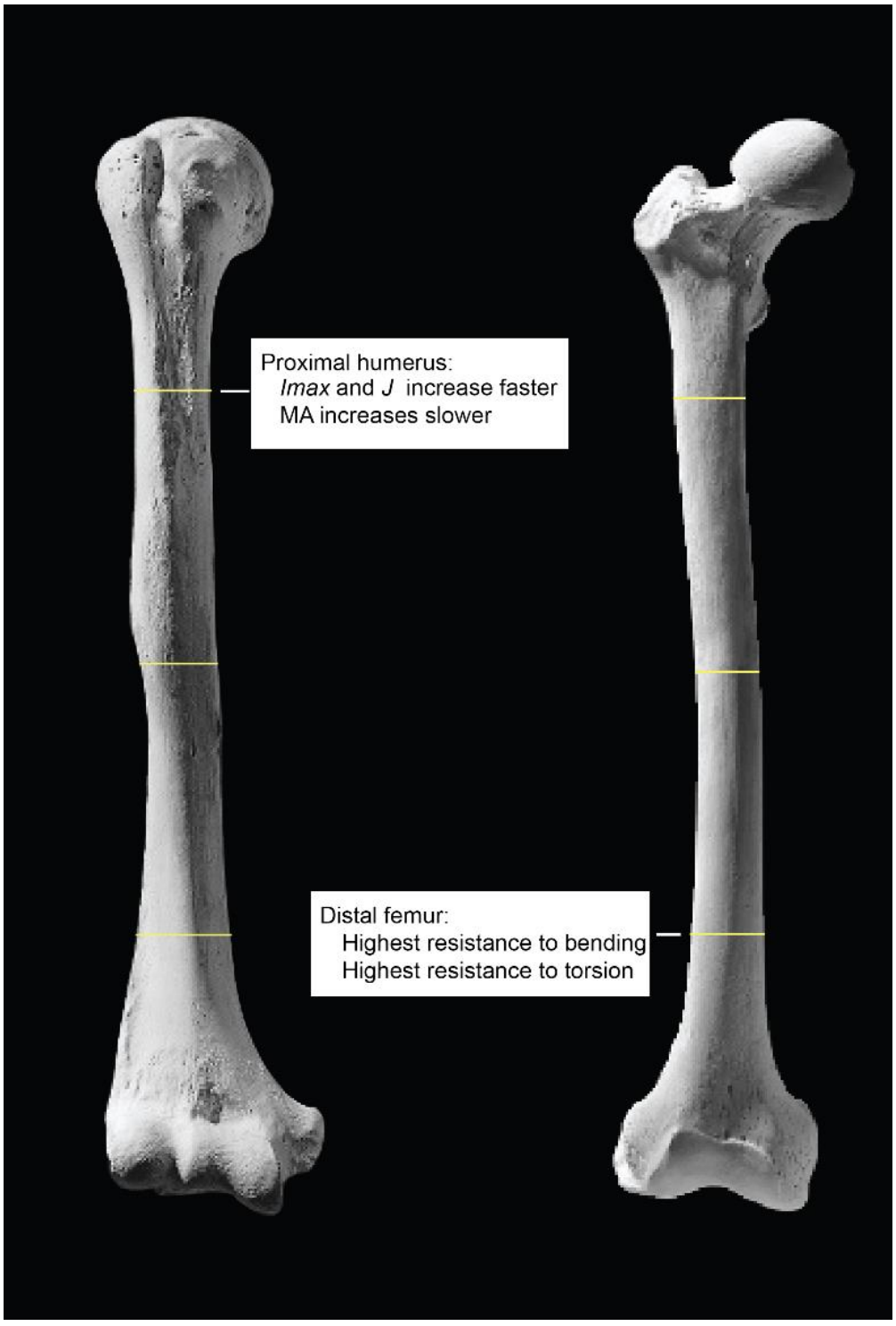


Figure 6.1. Summary figure depicting notable results from Chapter 3 in the humerus (left) and femur (right). Images modified from White et al. (2016).

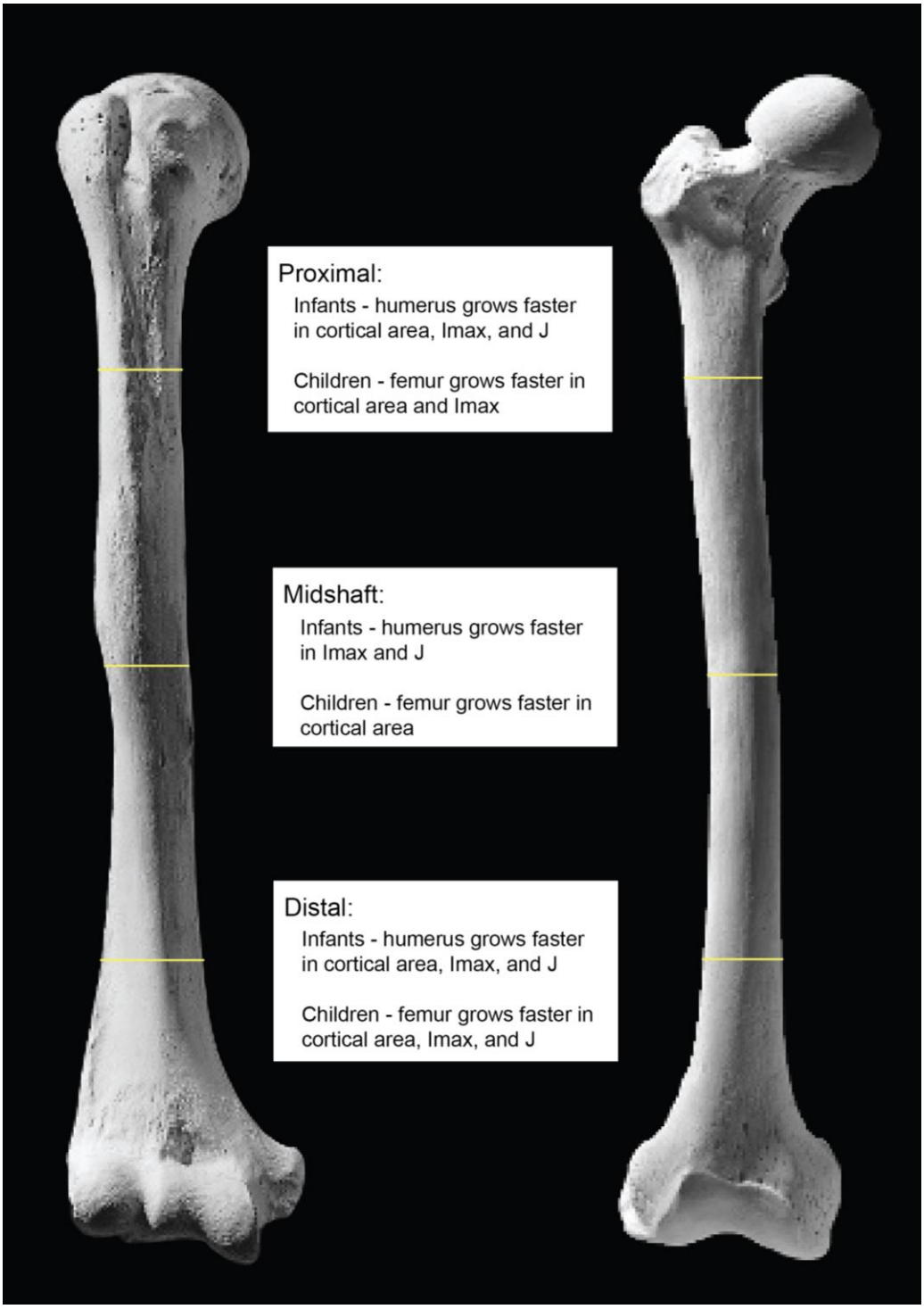


Figure 6.2. Summary figure depicting notable results from Chapter 4 in the humerus (left) and femur (right). Images modified from White et al. (2016).

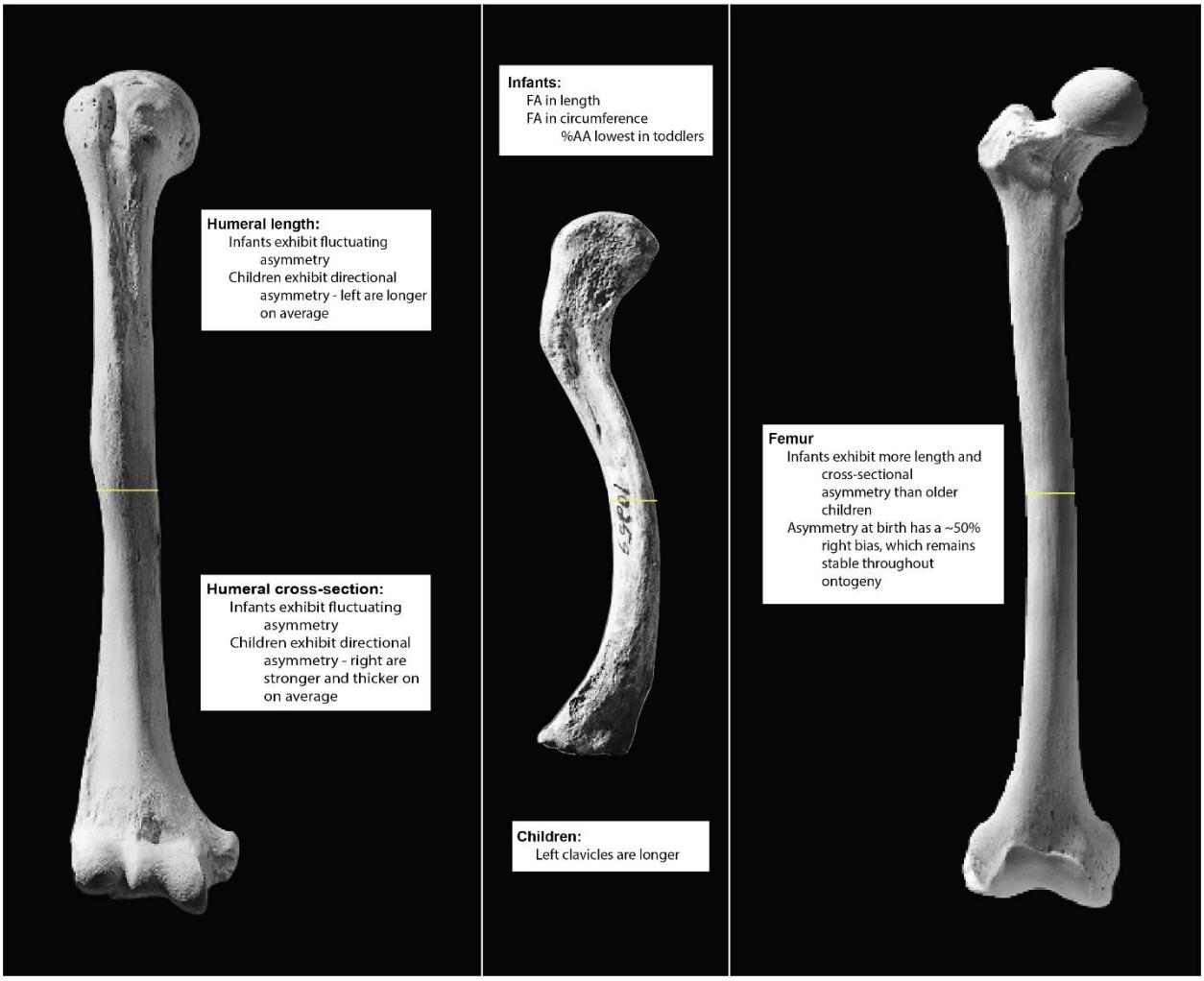


Figure 6.3. Summary figure depicting notable results from Chapter 5 in the humerus (left), clavicle (center) and femur (right). Images modified from White et al. (2016).

References

Adobe Inc. (2019). *Adobe Illustrator*. Retrieved from https://adobe.com/products/illustrator

Adolph, K. E., Bertenthal, B. I., Boker, S. M., Goldfield, E. C., & Gibson, E. J. (1997). Learning in the development of infant locomotion. *Monographs of the society for research in child development*, i-162.

Adolph, K. E., Vereijken, B., & Denny, M. A. (1998). Learning to crawl. *Child development*, *69*(5), 1299-1312.

Adolph, K. E., Berger, S. E., & Leo, A. J. (2011). Developmental continuity? Crawling, cruising, and walking. *Developmental science*, *14*(2), 306-318.

Adolph, K. E., & Hoch, J. E. (2019). Motor development: Embodied, embedded, enculturated, and enabling. *Annual review of psychology*, *70*, 141-164.

Ainsworth, M. D. S. (1967). Infancy in Uganda: Infant care and the growth of love.

Aiello, L. C., Montgomery, C., & Dean, C. (1991). The natural history of deciduous tooth attrition in hominoids. *Journal of Human Evolution*, *21*(5), 397-412.

Alexander, R. M., & Vernon, A. (1975). The mechanics of hopping by kangaroos (Macropodidae). *Journal of Zoology*, *177*(2), 265-303.

Alliston, T., & Derynck, R. (2002). Interfering with bone remodelling. *Nature*, *416*(6882), 686-687.

de Albuquerque Maia, L., Lisboa, P. C., De Oliveira, E., da Silva Lima, N., Da Costa, C. A. S., & De Moura, E. G. (2013). Two models of early weaning decreases bone structure by different changes in hormonal regulation of bone metabolism in neonate rat. *Hormone and Metabolic Research*, *45*(05), 332-337.

Akhter, M. P., Cullen, D. M., Pedersen, E. A., Kimmel, D. B., & Recker, R. R. (1998). Bone response to in vivo mechanical loading in two breeds of mice. *Calcified tissue international*, *63*(5), 442-449.

Albert, A. M., & Greene, D. L. (1999). Bilateral asymmetry in skeletal growth and maturation as an indicator of environmental stress. *American Journal of Physical Anthropology: The Official Publication of the American Association of Physical Anthropologists*, *110*(3), 341-349.

Alemseged, Z., Spoor, F., Kimbel, W. H., Bobe, R., Geraads, D., Reed, D., & Wynn, J. G. (2006). A juvenile early hominin skeleton from Dikika, Ethiopia. *Nature*, *443*(7109), 296-301.

Allen, M. C., & Capute, A. J. (1986). The evolution of primitive reflexes in extremely premature infants. *Pediatric research*, *20*(12), 1284-1289.

Amugongo, S. K., & Hlusko, L. J. (2014). Impact of maternal prenatal stress on growth of the offspring. *Aging and disease*, *5*(1), 1.

Angulo-Barroso, R. M., Schapiro, L., Liang, W., Rodrigues, O., Shafir, T., Kaciroti, N., ... & Lozoff, B. (2011). Motor development in 9-month-old infants in relation to cultural differences and iron status. *Developmental psychobiology*, *53*(2), 196-210.

Archer, C. W., & Francis-West, P. (2003). The chondrocyte. *The international journal of biochemistry & cell biology*, *35*(4), 401-404.

Argüello, D., Acevedo, H. S., & González-Estrada, O. A. (2019, November). Comparison of segmentation tools for structural analysis of bone tissues by finite elements. In *Journal of Physics: Conference Series* (Vol. 1386, No. 1, p. 012113). IOP Publishing.

Arsuaga, J. L., Martinez, I., Gracia, A., Carretero, J. M., & Carbonell, E. (1993). Three new human skulls from the Sima de los Huesos Middle Pleistocene site in Sierra de Atapuerca, Spain. *Nature*, *362*(6420), 534-537.

Atun-Einy, O., Cohen, D., Samuel, M., & Scher, A. (2013). Season of birth, crawling onset, and motor development in 7-month-old infants. *Journal of reproductive and infant psychology*, *31*(4), 342-351.

Auchus, R. J., & Rainey, W. E. (2004). Adrenarche–physiology, biochemistry and human disease. *Clinical endocrinology*, *60*(3), 288-296.

Auerbach, B. M., & Raxter, M. H. (2008). Patterns of clavicular bilateral asymmetry in relation to the humerus: variation among humans. *Journal of human evolution*, *54*(5), 663-674.

Auerbach, B. M., & Ruff, C. B. (2006). Limb bone bilateral asymmetry: variability and commonality among modern humans. *Journal of human evolution*, *50*(2), 203-218.

Austin, C., Smith, T. M., Bradman, A., Hinde, K., Joannes-Boyau, R., Bishop, D., ... & Arora, M. (2013). Barium distributions in teeth reveal early-life dietary transitions in primates. *Nature*, *498*(7453), 216-219.

Balzeau, A., Turq, A., Talamo, S., Daujeard, C., Guérin, G., Welker, F., ... & Gómez-Olivencia, A. (2020). Pluridisciplinary evidence for burial for the La Ferrassie 8 Neandertal child. *Scientific reports*, *10*(1), 1-10.

Bareggi, R., Grill, V., Zweyer, M., Sandrucci, M. A., Narducci, P., & Forabosco, A. (1994). The growth of long bones in human embryological and fetal upper limbs and its relationship to other developmental patterns. *Anatomy and embryology*, *189*(1), 19-24.

Bareggi, R., Grill, V., Zweyer, M., Sandrucci, M. A., Martelli, A. M., Narducci, P., & Forabosco, A. (1996). On the assessment of the growth patterns in human fetal limbs: longitudinal measurements and allometric analysis. *Early human development*, *45*(1-2), 11-25.

Baron, R., & Rawadi, G. (2007). Targeting the Wnt/β-catenin pathway to regulate bone formation in the adult skeleton. *Endocrinology*, *148*(6), 2635-2643.

Bass, S. L., Saxon, L., Daly, R. M., Turner, C. H., Robling, A. G., Seeman, E., & Stuckey, S. (2002). The effect of mechanical loading on the size and shape of bone in pre-, peri-, and postpubertal girls: a study in tennis players. *Journal of bone and mineral research*, *17*(12), 2274-2280.

Battles, H. T. (2009). Long bone bilateral asymmetry in the nineteenth-century Stirrup Court Cemetery collection from London, Ontario. *Nexus: The Canadian Student Journal of Anthropology*, *21*(1).

Beck, B. B. (1984). The birth of a lowland gorilla in captivity. *Primates*, *25*(3), 378-383.

Behrensmeyer, A. K. (2008). Paleoenvironmental context of the Pliocene AL 333 "first family" hominin locality, Hadar Formation, Ethiopia. *Geological Society of America Special Papers*, *446*, 203-214.

Besier, T. F., Lloyd, D. G., Cochrane, J. L., & Ackland, T. R. (2001). External loading of the knee joint during running and cutting maneuvers. *Medicine and science in sports and exercise*, *33*(7), 1168-1175.

Bellisari, A., Newman, T. K., Greenberg, C., Rogers, J., & Towne, B. (2001). Individual variation in the growth of captive infant gorillas. *American Journal of Physical Anthropology: The Official Publication of the American Association of Physical Anthropologists*, *115*(2), 110-132.

Bellido, T. (2014). Osteocyte-driven bone remodeling. *Calcified tissue international*, *94*(1), 25-34.

Bermúdez de Castro, J. B., Bromage, T. G., & Jalvo, Y. F. (1988). Buccal striations on fossil human anterior teeth: evidence of handedness in the middle and early Upper Pleistocene. *Journal of Human Evolution*, *17*(4), 403-412.

Bermúdez de Castro, J. M. B., Martinón-Torres, M., Prado, L., Gómez-Robles, A., Rosell, J., López-Polín, L., ... & Carbonell, E. (2010). New immature hominin fossil from European Lower Pleistocene shows the earliest evidence of a modern human dental development pattern. *Proceedings of the National Academy of Sciences*, *107*(26), 11739-11744.

Bermúdez de Castro, J. M., Martinón-Torres, M., Arsuaga, J. L., & Carbonell, E. (2017). Twentieth anniversary of Homo antecessor (1997-2017): a review. *Evolutionary Anthropology: Issues, News, and Reviews*, *26*(4), 157-171.

Bermúdez de Castro, J. M. B., de Pinillos, M. M., López-Polín, L., Martín-Francés, L., García-Campos, C., Modesto-Mata, M., ... & Martinón-Torres, M. (2020). A descriptive and comparative study of two Early Pleistocene immature scapulae from the TD6. 2 level of the Gran Dolina cave site (Sierra de Atapuerca, Spain). *Journal of Human Evolution*, *139*, 102689.

Bhattacharyya, K. B. (2016). Godfrey Newbold Hounsfield (1919–2004): The man who revolutionized neuroimaging. *Annals of Indian Academy of Neurology*, *19*(4), 448.

Bi, W., Deng, J. M., Zhang, Z., Behringer, R. R., & De Crombrugghe, B. (1999). Sox9 is required for cartilage formation. *Nature genetics*, *22*(1), 85-89.

Bi, W., Huang, W., Whitworth, D. J., Deng, J. M., Zhang, Z., Behringer, R. R., & De Crombrugghe, B. (2001). Haploinsufficiency of Sox9 results in defective cartilage primordia and premature skeletal mineralization. *Proceedings of the National Academy of Sciences*, *98*(12), 6698-6703.

Blackburn, A. (2011). Bilateral asymmetry of the humerus during growth and development. *American journal of physical anthropology*, *145*(4), 639-646.

Boeyer, M. E., Sherwood, R. J., Deroche, C. B., & Duren, D. L. (2018). Early maturity as the new normal: a century-long study of bone age. *Clinical Orthopaedics and Related Research*, *476*(11), 2112.

Bock, R. D. (2004). Multiple prepubertal growth spurts in children of the Fels Longitudinal Study: comparison with results from the Edinburgh Growth Study. *Annals of Human Biology*, *31*(1), 59-74.

Bonewald, L. F. (2011). The amazing osteocyte. *Journal of bone and mineral research*, *26*(2), 229-238.

Boreham, C. A., & McKay, H. A. (2011). Physical activity in childhood and bone health. *British Journal of Sports Medicine*, *45*(11), 877-879.

Boschetto, C., Ceriani, F., & Kustermann, A. (2010). Localized Movements. In *Development of Normal Fetal Movements* (pp. 59-75). Springer, Milano.

Bottos, M., Barba, B. D., Stefani, D., Pettenā, G., Tonin, C., & D'Este, A. (1989). Locomotor strategies preceding independent walking: prospective study of neurological and language development in 424 cases. *Developmental Medicine & Child Neurology*, *31*(1), 25-34.

Boyle, W. J., Simonet, W. S., & Lacey, D. L. (2003). Osteoclast differentiation and activation. *Nature*, *423*(6937), 337-342.

Bozzetti, V., & Tagliabue, P. (2009). Metabolic bone disease in preterm newborn: an update on nutritional issues. *Italian journal of pediatrics*, *35*(1), 1-8.

Bourguignon, J. P. (1988). Linear growth as a function of age at onset of puberty and sex steroid dosage: therapeutic implications. *Endocrine Reviews*, *9*(4), 467-488. https://doi.org/10.1210/edrv-9-4-467

Brash, J. C. (1934). Some problems in the growth and developmental mechanics of bone. *Edinburgh medical journal*, *41*(6), 363.

Brown, T., & Grave, K. C. (1976). Skeletal maturation in Australian aborigines. *Journal of Paediatrics and Child Health*, *12*(1), 24-30.

Bruder, S. P., & Caplan, A. I. (1989). Cellular and molecular events during embryonic bone development. Connective tissue research, 20(1-4), 65-71.

Berge, C., Orban-Segebarth, R., & Schmid, P. (1984). Obstetrical interpretation of the australopithecine pelvic cavity. *Journal of Human Evolution*, *13*(7), 573-587.

Berger, L. R., De Ruiter, D. J., Churchill, S. E., Schmid, P., Carlson, K. J., Dirks, P. H., & Kibii, J. M. (2010). Australopithecus sediba: a new species of Homo-like australopith from South Africa. *Science*, *328*(5975), 195-204.

Budd, A., & Smith, L. G. (1943, June). On the Birth and Upbringing of the Female Chimpanzee "Jacqueline"(born 28/11/37 in the Zoological Gardens, London). In *Proceedings of the Zoological Society of London* (Vol. 113, No. 1-2, pp. 1-20). Oxford, UK: Blackwell Publishing Ltd.

Bufalino, A., Paranaíba, L. M. R., Gouvêa, A. F., Gueiros, L. A., Martelli-Júnior, H., Junior, J. J., ... & Coletta, R. D. (2012). Cleidocranial dysplasia: oral features and genetic analysis of 11 patients. *Oral diseases*, *18*(2), 184-190.

Bukowski, R., Smith, G. C., Malone, F. D., Ball, R. H., Nyberg, D. A., Comstock, C. H., ... & D'Alton, M. E. (2007). Human sexual size dimorphism in early pregnancy. *American journal of epidemiology*, *165*(10), 1216-1218.

Burr, D. B., & Organ, J. M. (2017). Postcranial skeletal development and its evolutionary implications. *Building Bones: Bone Formation and Development in Anthropology*, *77*, 148.

Buschang, P. H. (1982). Differential long bone growth of children between two months and eleven years of age. *American Journal of Physical Anthropology*, *58*(3), 291-295.

Butler, G. E., McKie, M., & Ratcliffe, S. G. (1990). The cyclical nature of prepubertal growth. *Annals of Human Biology*, *17*(3), 177-198.

Caino, S., Kelmansky, D., Adamo, P., & Lejarraga, H. (2010). Short-term growth in head circumference and its relationship with supine length in healthy infants. *Annals of Human Biology*, *37*(1), 108-116.

Cao, X., & Chen, D. (2005). The BMP signaling and in vivo bone formation. *Gene*, *357*(1), 1-8.

Cambra-Moo, O., Meneses, C. N., Barbero, M. Á. R., Gil, O. G., Pérez, J. R., Rello-Varona, S., ... & Martín, A. G. (2012). Mapping human long bone compartmentalisation during ontogeny: A new methodological approach. *Journal of Structural Biology*, *178*(3), 338-

349.
Cameron, N., Bogin, B., Bolter, D., & Berger, L. R. (2017). The postcranial skeletal maturation of Australopithecus sediba. *American Journal of Physical Anthropology*, *163*(3), 633-640.
Caplan, A. I., & Correa, D. (2011). PDGF in bone formation and regeneration: new insights into a novel mechanism involving MSCs. *Journal of Orthopaedic Research*, *29*(12), 1795-1803.
Cardoso, H. F. (2007). Environmental effects on skeletal versus dental development: using a documented subadult skeletal sample to test a basic assumption in human osteological research. *American journal of physical anthropology*, *132*(2), 223-233.
Carmichael, L., Kraus, M. B., & Reed, T. (1962). The Washington National Zoological Park gorilla infant, Tomoko. *International Zoo Yearbook*, *3*(1), 88-93.
Carpes, F. P., Mota, C. B., & Faria, I. E. (2010). On the bilateral asymmetry during running and cycling–A review considering leg preference. *Physical therapy in sport*, *11*(4), 136-142.
Carretero, J. M., Arsuaga, J. L., & Lorenzo, C. (1997). Clavicles, scapulae and humeri from the Sima de los Huesos site (Sierra de Atapuerca, Spain). *Journal of human evolution*, *33*(2-3), 357-408.
Carretero, J. M., Lorenzo, C., & Arsuaga, J. L. (1999). Axial and appendicular skeleton of Homo antecessor. *Journal of Human Evolution*, *37*(3-4), 459-499.
Cashmore, L., Uomini, N., & Chapelain, A. (2008). The evolution of handedness in humans and great apes: a review and current issues. *Journal of Anthropological Sciences*, *86*(2008), 7-35.
Cashmore, L., & Zakrzewski, S. R. (2009). The expression of asymmetry in hand bones from the medieval cemetery at Écija, Spain.
Cavanagh, T., Berbesque, J. C., Wood, B., & Marlowe, F. (2016). Hadza handedness: Lateralized behaviors in a contemporary hunter–gatherer population. *Evolution and Human Behavior*, *37*(3), 202-209.
CDC (2022) – National Center for Health Statistics – https://www.cdc.gov/ncbddd/actearly/milestones/index.html
Chen, X., Hastings, P. D., Rubin, K. H., Chen, H., Cen, G., & Stewart, S. L. (1998). Child-rearing attitudes and behavioral inhibition in Chinese and Canadian toddlers: a cross-cultural study. *Developmental psychology*, *34*(4), 677.
Chen, B., Dodge, M. E., Tang, W., Lu, J., Ma, Z., Fan, C. W., ... & Lum, L. (2009). Small molecule–mediated disruption of Wnt-dependent signaling in tissue regeneration and cancer. *Nature chemical biology*, *5*(2), 100-107.
Chen, H. L., Tseng, H. I., Lu, C. C., Yang, S. N., & Yang, R. C. (2010). 1021 Bone Strength Measured by Quantitative Ultrasound in Newborn Infants in Taiwan. *Pediatric Research*, *68*(1), 508-508.
Chi, J. G., Dooling, E. C., & Gilles, F. H. (1977). Gyral development of the human brain. *Annals of Neurology: Official Journal of the American Neurological Association and the Child Neurology Society*, *1*(1), 86-93.
Cho, G. J., Park, H. T., Shin, J. H., Hur, J. Y., Kim, Y. T., Kim, S. H., ... & Kim, T. (2010). Age at menarche in a Korean population: secular trends and influencing factors. *European journal of pediatrics*, *169*(1), 89-94.
Chapelle, L., Rommers, N., Clarys, P., & D'Hondt, E. (2021). Whole-body morphological asymmetries in high-level female tennis players: A cross-sectional study. *Journal of*

sports sciences, *39*(7), 777-782.
Chevalley, T., Bonjour, J. P., Ferrari, S., & Rizzoli, R. (2008). Influence of age at menarche on forearm bone microstructure in healthy young women. *The Journal of Clinical Endocrinology & Metabolism*, *93*(7), 2594-2601.
Churchill, J. A., Igna, E., & Senf, R. (1962). The association of position at birth and handedness. *Pediatrics*, *29*(2), 307-309.
Cintas, H. M. (1989). Cross-cultural variation in infant motor development. *Physical & Occupational Therapy in Pediatrics*, *8*(4), 1-20.
Cinque, L., Forrester, A., Bartolomeo, R., Svelto, M., Venditti, R., Montefusco, S., ... & Settembre, C. (2015). FGF signalling regulates bone growth through autophagy. *Nature*, *528*(7581), 272-275.
Claxton, A. G., Hammond, A. S., Romano, J., Oleinik, E., & DeSilva, J. M. (2016). Virtual reconstruction of the Australopithecus africanus pelvis Sts 65 with implications for

obstetrics and locomotion. *Journal of Human Evolution*, *99*, 10-24.
Coe, C. L., Connolly, A. C., Kraemer, H. C., & Levine, S. (1979). Reproductive development and behavior of captive female chimpanzees. *Primates*, *20*(4), 571-582.
Cole, W. G., Lingeman, J. M., & Adolph, K. E. (2012). Go naked: Diapers affect infant walking. *Developmental science*, *15*(6), 783-790.
Craik, E. (2008). Hippocrates on Embryology. *Hippokrates, Über die Natur des Kindes (De genitura und De natura pueri. 58*(2), 367-369.
Crane, J. L., Zhao, L., Frye, J. S., Xian, L., Qiu, T., & Cao, X. (2013). IGF-1 signaling is essential for differentiation of mesenchymal stem cells for peak bone mass. *Bone research*, *1*(1), 186-194.
Crane, J. L., & Cao, X. (2014). Function of matrix IGF-1 in coupling bone resorption and formation. *Journal of molecular medicine*, *92*(2), 107-115.
Crevecoeur, I., Bayle, P., Rougier, H., Maureille, B., Higham, T., van der Plicht, J., ... & Semal, P. (2010). The Spy VI child: A newly discovered Neandertal infant. *Journal of Human Evolution*, *59*(6), 641-656.
Compere, E. L., & Adams, C. O. (1937). Studies of longitudinal growth of long bones: I. The influence of trauma to the diaphysis. *JBJS*, *19*(4), 922-936.
Cooper, C., Cawley, M., Bhalla, A., Egger, P., Ring, F., Morton, L., & Barker, D. (1995). Childhood growth, physical activity, and peak bone mass in women. *Journal of Bone and Mineral Research*, *10*(6), 940-947.
Cooper, S. C., Flaitz, C. M., Johnston, D. A., Lee, B., & Hecht, J. T. (2001). A natural history of cleidocranial dysplasia. *American journal of medical genetics*, *104*(1), 1-6.
Cooper, C., Javaid, K., Westlake, S., Harvey, N., & Dennison, E. (2005). Developmental origins of osteoporotic fracture: the role of maternal vitamin D insufficiency. *The Journal of nutrition*, *135*(11), 2728S-2734S.
Corballis, M. C. (2003). From mouth to hand: gesture, speech, and the evolution of right-handedness. *Behavioral and brain sciences*, *26*(2), 199-208.
Cowgill, L. W. (2010). The ontogeny of Holocene and Late Pleistocene human postcranial strength. *American Journal of Physical Anthropology: The Official Publication of the American Association of Physical Anthropologists*, *141*(1), 16-37.
Cowgill, L. W., Warrener, A., Pontzer, H., & Ocobock, C. (2010). Waddling and toddling: the biomechanical effects of an immature gait. *American journal of physical*

anthropology, *143*(1), 52-61.
Cowgill, L. W., & Rob'yn, A. J. (2018). Biomechanical implications of the onset of walking. *Journal of Human Evolution*, *122*, 133-145.
Cowin, S. C., Moss-Salentijn, L., & Moss, M. L. (1991). Candidates for the mechanosensory system in bone. *Journal of biomechanical engineering*, *113*(2), 191-197.
Cullen, D. M., Smith, R. T., & Akhter, M. P. (2001). Bone-loading response varies with strain magnitude and cycle number. *Journal of applied physiology*, *91*(5), 1971-1976.
Cunningham, C., Scheuer, L., & Black, S. (2016). *Developmental juvenile osteology*. Academic press.
Currey, J. D., & Butler, G. (1975). The mechanical properties of bone tissue in children. *The Journal of bone and joint surgery. American volume*, *57*(6), 810-814.
Currey, J. D. (2012). The structure and mechanics of bone. *Journal of Materials Science*, *47*(1), 41-54.
Cutler Jr, G. B. (1997). The role of estrogen in bone growth and maturation during childhood and adolescence. *The Journal of steroid biochemistry and molecular biology*, *61*(3-6), 141-144.
De Beer, F. C., Prevec, R., Cisneros, J., & Abdala, F. (2006, September). Hidden structure of fossils revealed by neutron and X-ray tomography. In *Proceedings of the 8th World Conference on Neutron Radiography (WCNR-8) held at NIST, Gaithersburg, USA* (Vol. 452).
da Silva Madaleno, C., Jatzlau, J., & Knaus, P. (2020). BMP signalling in a mechanical context–Implications for bone biology. *Bone*, *137*, 115416.
Dallas, S. L., Prideaux, M., & Bonewald, L. F. (2013). The osteocyte: an endocrine cell… and more. *Endocrine reviews*, *34*(5), 658-690.
Dandurand, F., & Shultz, T. R. (2010). Automatic detection and quantification of growth spurts. *Behavior research methods*, *42*(3), 809-823.
Danilovic, D. L. S., Correa, P. H. S., Costa, E. M. F., Melo, K. F. S., Mendonca, B. B., & Arnhold, I. J. P. (2007). Height and bone mineral density in androgen insensitivity syndrome with mutations in the androgen receptor gene. *Osteoporosis International*, *18*(3), 369-374.
Dean, C., Leakey, M. G., Reid, D., Schrenk, F., Schwartz, G. T., Stringer, C., & Walker, A. (2001). Growth processes in teeth distinguish modern humans from Homo erectus and earlier hominins. *Nature*, *414*(6864), 628-631.
Dean, C. & Wood, B. A. Digital radiographic atlas of the great apes skull and dentition. (2003) in *Digital Archives of Human Paleobiology* (eds Bondioli, L. & Machiarelli, R.) CD-ROM Vol. 3 (Museo Nazionale Preistorico Etnografico “L. Pigorini”, Rome, 2003)
Dean, C. (2007). Growing up slowly 160,000 years ago. *Proceedings of the National Academy of Sciences*, *104*(15), 6093-6094.
Dean, M. C., & Smith, B. H. (2009). Growth and development of the Nariokotome youth, KNM-WT 15000. In *The first humans–origin and early evolution of the genus Homo* (pp. 101-120). Springer, Dordrecht.
de León, M. S. P., Koesbardiati, T., Weissmann, J. D., Milella, M., Reyna-Blanco, C. S., Suwa, G., ... & Zollikofer, C. P. (2018). Human bony labyrinth is an indicator of population history and dispersal from Africa. *Proceedings of the National Academy of Sciences*, *115*(16), 4128-4133.
DeSilva, J. M., Gill, C. M., Prang, T. C., Bredella, M. A., & Alemseged, Z. (2018). A nearly

complete foot from Dikika, Ethiopia and its implications for the ontogeny and function of Australopithecus afarensis. *Science Advances*, *4*(7), eaar7723.
DeSilva, J. M., & Lesnik, J. J. (2008). Brain size at birth throughout human evolution: a new method for estimating neonatal brain size in hominins. *Journal of human evolution*, *55*(6), 1064-1074.
DeSilva, J. M. (2011). A shift toward birthing relatively large infants early in human evolution. *Proceedings of the National Academy of Sciences*, *108*(3), 1022-1027.
DeSilva, J. M., Laudicina, N. M., Rosenberg, K. R., & Trevathan, W. R. (2017). Neonatal shoulder width suggests a semirotational, oblique birth mechanism in Australopithecus afarensis. *The Anatomical Record*, *300*(5), 890-899.
DeSilva, J. M. (2022). Childbirth and infant care in early human ancestors: what the bones tell us. In *Evolutionary Perspectives on Infancy* (pp. 59-81). Springer, Cham.
De Souza, R. L., Matsuura, M., Eckstein, F., Rawlinson, S. C., Lanyon, L. E., & Pitsillides, A. A. (2005). Non-invasive axial loading of mouse tibiae increases cortical bone formation and modifies trabecular organization: a new model to study cortical and cancellous compartments in a single loaded element. *Bone*, *37*(6), 810-818.
Dennis, W., & Dennis, M. G. (1991). The effect of cradling practices upon the onset of walking in Hopi children. *The Journal of genetic psychology*, *152*(4), 563-572.
Dettwyler, K. A. (2017). A Time to Wean: The Hominid Blueprint for the Natural Age of Weaning. *Breastfeeding: biocultural perspectives*, 39.
DeVries, J. I. P., Wimmers, R. H., Ververs, I. A. P., Hopkins, B., Savelsbergh, G. J. P., & Van Geijn, H. P.(2001). Fetal handedness and head position preference: A developmental study. *Developmental Psychobiology: The Journal of the International Society for Developmental Psychobiology*, *39*(3), 171-178.
DeVries, N. A., Gassman, E. E., Kallemeyn, N. A., Shivanna, K. H., Magnotta, V. A., & Grosland, N. M. (2008). Validation of phalanx bone three-dimensional surface segmentation from computed tomography images using laser scanning. *Skeletal radiology*, *37*(1), 35-42.
DiCaglio, S. (2017). Staging embryos: Pregnancy, temporality and the history of the Carnegie stages of embryo development. *Body & Society*, *23*(2), 3-24.
Dickinson, A. G. (1960). Some genetic implications of maternal effects—an hypothesis of mammalian growth. *The Journal of Agricultural Science*, 54(3), 378-390.
Dixon, A. F. (1896). Ossification of the third trochanter in man. *Journal of Anatomy and Physiology*, *30*(Pt 4), 502.
Doran, D. M. (1992). The ontogeny of chimpanzee and pygmy chimpanzee locomotor behavior: a case study of paedomorphism and its behavioral correlates. *Journal of Human Evolution*, *23*(2), 139-157.
Dragonfly 2020.2 [Computer software]. Object Research Systems (ORS) Inc, Montreal, Canada, 2020; software available at http://www.theobjects.com/dragonfly.
Ducher, G., Prouteau, S., Courteix, D., & Benhamou, C. L. (2004). Cortical and trabecular bone at the forearm show different adaptation patterns in response to tennis playing. *Journal of Clinical Densitometry*, *7*(4), 399-405.
Ducher, G., Bass, S. L., Saxon, L., & Daly, R. M. (2011). Effects of repetitive loading on the growth-induced changes in bone mass and cortical bone geometry: A 12-month study in pre/peri-and postmenarcheal tennis players. *Journal of bone and mineral research*, *26*(6), 1321-1329.

Ducy, P., Zhang, R., Geoffroy, V., Ridall, A. L., & Karsenty, G. (1997). Osf2/Cbfa1: a transcriptional activator of osteoblast differentiation. *cell*, *89*(5), 747-754.

Dunn, P. M. (1993). Hippocrates (460-c 356 BC) and the founding of perinatal medicine. *Archives of disease in childhood*, *69*(5 Spec No), 540.

Dunsworth, H. M., Warrener, A. G., Deacon, T., Ellison, P. T., & Pontzer, H. (2012). Metabolic hypothesis for human altriciality. *Proceedings of the National Academy of Sciences*, *109*(38), 15212-15216. https://doi.org/10.1073/pnas.1205282109

Dunsworth, H. M. (2018). There is no" obstetrical dilemma": Towards a braver medicine with fewer childbirth interventions. *Perspectives in Biology and Medicine*, *61*(2), 249-263.

Edgar, HJH; Daneshvari Berry, S; Moes, E; Adolphi, NL; Bridges, P; Nolte, KB (2020). New Mexico Decedent Image Database. Office of the Medical Investigator, University of New Mexico.

Edwards, W. B., Gillette, J. C., Thomas, J. M., & Derrick, T. R. (2008). Internal femoral forces and moments during running: implications for stress fracture development. *Clinical Biomechanics*, *23*(10), 1269-1278.

Eliakim, A., Nemet, D., Friedland, O., Dolfin, T., & Regev, R. H. (2002). Spontaneous activity in premature infants affects bone strength. *Journal of Perinatology*, *22*(8), 650-652.

Ellwanger, K., Saito, H., Clément-Lacroix, P., Maltry, N., Niedermeyer, J., Lee, W. K., ... & Niehrs, C.(2008). Targeted disruption of the Wnt regulator Kremen induces limb defects and high bonedensity. *Molecular and cellular biology*, *28*(15), 4875-4882.

Eriksen, A. B., & von Cramon-Taubadel, N. (2020). The effect of hand preference on skeletal asymmetry in human limbs. *The FASEB Journal*, *34*(S1), 1-1.

Estalrrich, A., & Rosas, A. (2013). Handedness in Neandertals from the El Sidrón (Asturias, Spain): evidence from instrumental striations with ontogenetic inferences. *PloS one*, *8*(5), e62797.

Farrow, E., Nicot, R., Wiss, A., Laborde, A., & Ferri, J. (2018). Cleidocranial dysplasia: a review of clinical, radiological, genetic implications and a guidelines proposal. *Journal of Craniofacial Surgery*, *29*(2), 382-389.

Ferber, R., Noehren, B., Hamill, J., & Davis, I. (2010). Competitive female runners with a history of iliotibial band syndrome demonstrate atypical hip and knee kinematics. *journal of orthopaedic & sports physical therapy*, *40*(2), 52-58.

Fiorentino, M. R. (2014). *Normal and abnormal development: the influence of primitive reflexes on motor development*. Charles C Thomas Publisher.

Fiscaletti, M., Stewart, P., & Munns, C. F. (2017). The importance of vitamin D in maternal and child health: a global perspective. *Public health reviews*, *38*(1), 1-17.

Fisher, L. E. (1972). The birth of a Lowland gorilla (Gorilla g. gorilla) at Lincoln Park Zoo, Chicago. *International Zoo Yearbook*, *12*(1), 106-108.

Forwood, M. R., Owan, I. C. H. I. R. O., Takano, Y. U. I. C. H. I., & Turner, C. H. (1996). Increased bone formation in rat tibiae after a single short period of dynamic loading in vivo. *American Journal ofPhysiology-Endocrinology and Metabolism*, *270*(3), E419-E423.

Forwood, M. R., Kelly, W. L., & Worth, N. F. (1998). Localisation of prostaglandin endoperoxide H synthase (PGHS)-1 and PGHS-2 in bone following mechanical loading in vivo. *The Anatomical Record: An Official Publication of the American Association of Anatomists*, *252*(4), 580-586.

Fox, K. M., Kimura, S., Plato, C. C., & Kitagawa, T. (1995). Bilateral asymmetry in bone weight at variousskeletal sites of the rat. *The Anatomical Record*, *241*(2), 284-287.

Fox, A. T., Palmer, R. D., & Davies, P. (2002). Do "Shufflebottoms" bottom shuffle?. *Archives of disease in childhood*, *87*(6), 552-554. http://dx.doi.org/10.1136/adc.87.6.552

Frank, G. R. (2003). Role of estrogen and androgen in pubertal skeletal physiology. *Medical and pediatric oncology*, *41*(3), 217-221.

Franz-Odendaal, T. A., Hall, B. K., & Witten, P. E. (2006). Buried alive: how osteoblasts become osteocytes. *Developmental dynamics: an official publication of the American Association of Anatomists*, *235*(1), 176-190.

Frasnelli, E., Vallortigara, G., & Rogers, L. J. (2012). Left–right asymmetries of behaviour and nervous system in invertebrates. *Neuroscience & Biobehavioral Reviews*, *36*(4), 1273-1291.

Frayer, D. W., Lozano, M., Bermudez de Castro, J. M., Carbonell, E., Arsuaga, J. L., Radovčić, J., ... & Bondioli, L. (2012). More than 500,000 years of right-handedness in Europe. *Laterality: Asymmetries of Body, Brain and Cognition*, *17*(1), 51-69.

Frayer, D. W., Clarke, R. J., Fiore, I., Blumenschine, R. J., Pérez-Pérez, A., Martinez, L. M., ... & Bondioli, L. (2016). OH-65: The earliest evidence for right-handedness in the fossil record. *Journal of Human Evolution*, *100*, 65-72.

Forssberg, H. (1985). Ontogeny of human locomotor control I. Infant stepping, supported locomotion and transition to independent locomotion. *Experimental Brain Research*, *57*(3), 480-493.

Futagi, Y., Toribe, Y., & Suzuki, Y. (2012). The grasp reflex and moro reflex in infants: hierarchy of primitive reflex responses. *International journal of pediatrics*, 2012.

Galea, G. L., Lanyon, L. E., & Price, J. S. (2017). Sclerostin's role in bone's adaptive response to mechanical loading. *Bone*, *96*, 38-44.

García-González, R., Carretero, J. M., Rodríguez, L., Gómez-Olivencia, A., Arsuaga, J. L., de Castro, J. M. B., ... & Lorenzo, C. (2009). Étude analytique d'une clavicule complète de subadulte d'Homo antecessor (site de Gran Dolina, Sierra d'Atapuerca, Burgos, Espagne). *L'Anthropologie*, *113*(1), 222-232.

García-Martínez, D., Green, D. J., & Bermúdez de Castro, J. M. (2021). Evolutionary development of the Homo antecessor scapulae (Gran Dolina site, Atapuerca) suggests a modern-like development for Lower Pleistocene Homo. *Scientific reports*, *11*(1), 1-12.

Gardner, E. (1968). 2 The Embryology of the Clavicle. *Clinical Orthopaedics and Related Research (1976-2007)*, *58*, 9-16.

Gardner, E., & Gray, D. J. (1970). The prenatal development of the human femur. *American Journal of Anatomy*, *129*(2), 121-140.

Garn, S. M., Rohmann, C. G., Wagner, B., & Ascoli, W. (1967). Continuing bone growth throughout life: a general phenomenon. *American Journal of Physical Anthropology*, *26*(3), 313-317.

Garn, S. M. (1970). The early gain and later loss of cortical bone. *Nutritional perspective*.

Gassman, E. E., Powell, S. M., Kallemeyn, N. A., DeVries, N. A., Shivanna, K. H., Magnotta, V. A., ... & Grosland, N. M. (2008). Automated bony region identification using artificial neural networks: reliability and validation measurements. *Skeletal radiology*, *37*(4), 313-319.

Gluckman, P. D., & Hanson, M. A. (2006). Evolution, development and timing of puberty. *Trends in Endocrinology & Metabolism*, 17(1), 7-12.

Gluckman, P. D., Hanson, M. A., Cooper, C., & Thornburg, K. L. (2008). Effect of in utero and early-life conditions on adult health and disease. *New England Journal of Medicine*, *359*(1), 61-73.

Goldberg, S. (1972). Infant care and growth in urban Zambia. *Human Development*, *15*(2), 77-89.

Goldman, H. M., Mcfarlin, S. C., Cooper, D. M., Thomas, C. D. L., & Clement, J. G. (2009). Ontogenetic patterning of cortical bone microstructure and geometry at the human mid-shaft femur. *The Anatomical Record: Advances in Integrative Anatomy and Evolutionary Biology: Advances inIntegrative Anatomy and Evolutionary Biology*, *292*(1), 48-64.

Gómez-Olivencia, A., Crevecoeur, I., & Balzeau, A. (2015). La Ferrassie 8 Neandertal child reloaded: New remains and re-assessment of the original collection. *Journal of Human Evolution*, *82*, 107-126.

Goodall, J. (1967). Mother-offspring relationships in free-ranging chimpanzees.Goodall, J. (1977). Infant killing and cannibalism in free-living chimpanzees. *Folia primatologica*, *28*(4),

Goodall, J., & Athumani, J. (1980). An observed birth in a free-living chimpanzee (Pan troglodytes schweinfurthii) in Gombe National Park, Tanzania. *Primates*, *21*(4), 545-549.

Goodwin, R. S., & Michel, G. F. (1981). Head orientation position during birth and in infant neonatal period, and hand preference at nineteen weeks. *Child Development*, 819-826.

Gosman, J. H., Hubbell, Z. R., Shaw, C. N., & Ryan, T. M. (2013). Development of cortical bone geometry in the human femoral and tibial diaphysis. *The Anatomical Record*, *296*(5), 774-787.

Grattan, M. P., De Vos, E., Levy, J., & McClintock, M. K. (1992). Asymmetric action in the human newborn: Sex differences in patterns of organization. *Child Development*, *63*(2), 273-289.

Güntürkün, O., Ströckens, F., & Ocklenburg, S. (2020). Brain lateralization: a comparative perspective. *Physiological reviews*, *100*(3), 1019-1063.

Gunz, P., Neubauer, S., Falk, D., Tafforeau, P., Le Cabec, A., Smith, T. M., ... & Alemseged, Z. (2020). Australopithecus afarensis endocasts suggest ape-like brain organization and prolonged brain growth. *Science Advances*, *6*(14), eaaz4729.

Hägg, U., & Taranger, J. (1982). Maturation indicators and the pubertal growth spurt. *American Journal of Orthodontics*, *82*(4), 299-309.

Hales, S. (1733). Statical Essays.. (Vol. 2). W. Innys and R. Manby...; T. Woodward... and J. Peele.

Hall, B. K., & Miyake, T. (2000). All for one and one for all: condensations and the initiation of skeletal development. *Bioessays*, *22*(2), 138-147.

Hallgrímsson, B. (1999). Ontogenetic patterning of skeletal fluctuating asymmetry in rhesus macaques and humans: evolutionary and developmental implications. *International Journal of Primatology*, *20*(1), 121-151.

Hamada, Y., & Udono, T. (2002). Longitudinal analysis of length growth in the chimpanzee (Pan troglodytes). *American Journal of Physical Anthropology: The Official Publication of the American Association of Physical Anthropologists*, *118*(3), 268-284.

Harris, M. A., Prior, J. C., & Koehoorn, M. (2008). Age at menarche in the Canadian population: secular trends and relationship to adulthood BMI. *Journal of Adolescent Health*, *43*(6), 548-554.

Harrison, C. M., & Gibson, A. T. (2013). Osteopenia in preterm infants. *Archives of Disease in Childhood-Fetal and Neonatal Edition*, *98*(3), F272-F275.
Haeusler, M., Grunstra, N. D., Martin, R. D., Krenn, V. A., Fornai, C., & Webb, N. M. (2021). The obstetrical dilemma hypothesis: there's life in the old dog yet. *Biological Reviews*, *96*(5), 2031-2057.
Hayashi, M., & Matsuzawa, T. (2017). Mother–infant interactions in captive and wild chimpanzees. *InfantBehavior and Development*, *48*, 20-29.
Heim, J. L. (1976). Les Hommes Fossiles de La Ferrassie, Tomo I. *Archives de l'Institut de paléontologie humaine*, *35*.
Heim, J. L. (1982). Les hommes fossiles de La Ferrassie II. *Archives de l'Institut de Paléontologie Humaine*, *38*, 1-272.
Helmkamp, R. C., & Falk, D. (1990). Age-and sex-associated variations in the directional asymmetry of rhesus macaque forelimb bones. *American Journal of Physical Anthropology*, *83*(2), 211-218.
Henriksen, K., Neutzsky-Wulff, A. V., Bonewald, L. F., & Karsdal, M. A. (2009). Local communication on and within bone controls bone remodeling. *Bone*, *44*(6), 1026-1033.
Hepper, P. G., Shahidullah, S., & White, R. (1991). Handedness in the human fetus. *Neuropsychologia*, *29*(11), 1107-1111.
Hepper, P. G., Wells, D. L., & Lynch, C. (2005). Prenatal thumb sucking is related to postnatal handedness. *Neuropsychologia*, *43*(3), 313-315.
Hepper, P. G. (2013). The developmental origins of laterality: Fetal handedness. *Developmental psychobiology*, *55*(6), 588-595.
Hering-Hanit, R., Achiron, R., Lipitz, S., & Achiron, A. (2001). Asymmetry of fetal cerebral hemispheres: in utero ultrasound study. *Archives of Disease in Childhood-Fetal and Neonatal Edition*, *85*(3), F194-F196.
Hermanussen, M. (1998). The analysis of short-term growth. *Hormone Research in Pædiatrics*, *49*(2), 53-64.
Hernandez, C. J., Majeska, R. J., & Schaffler, M. B. (2004). Osteocyte density in woven bone. *Bone*, *35*(5), 1095-1099.
Hillenbrand, H. A. (2009). *An Australopithecus afarensis infant first metatarsal from Hadar, Ethiopia* (Bachelors dissertation, Miami University).
Hinojosa, T., Sheu, C. F., & Michel, G. F. (2003). Infant hand-use preferences for grasping objects contributes to the development of a hand-use preference for manipulating objects. *Developmental Psychobiology: The Journal of the International Society for Developmental Psychobiology*, *43*(4), 328-334.
Hita-Contreras, F., Sánchez-Montesinos, I., Martínez-Amat, A., Cruz-Díaz, D., Barranco, R. J., & Roda, O. (2018). Development of the human shoulder joint during the embryonic and early fetal stages: anatomical considerations for clinical practice. *Journal of anatomy*, *232*(3), 422-430.
Hopkins, B., & Westra, T. (1989). Maternal expectations of their infants 'development: some cultural differences. *Developmental Medicine & Child Neurology*, *31*(3), 384-390.
Hopkins, B., & Westra, T. (1990). Motor development, maternal expectations, and the role of handling. *Infant Behavior and Development*, *13*(1), 117-122.
Hublin, J. J., Ben-Ncer, A., Bailey, S. E., Freidline, S. E., Neubauer, S., Skinner, M. M., ... & Gunz, P. (2017). New fossils from Jebel Irhoud, Morocco and the pan-African origin of Homo sapiens. *Nature*, *546*(7657), 289-292.

Hrdy, S. B., & Burkart, J. M. (2022). How Reliance on Allomaternal Care Shapes Primate Development with Special Reference to the Genus Homo. In *Evolutionary Perspectives on Infancy* (pp. 161-188). Springer, Cham.

Hvidt, J. J., Brix, N., Ernst, A., Lauridsen, L. L. B., & Ramlau-Hansen, C. H. (2019). Size at birth, infant growth, and age at pubertal development in boys and girls. *Clinical epidemiology*, *11*, 873.

Ireland, A., Maden-Wilkinson, T., Ganse, B., Degens, H., & Rittweger, J. (2014). Effects of age and starting age upon side asymmetry in the arms of veteran tennis players: a cross-sectional study. *Osteoporosis International*, *25*(4), 1389-1400.

Iuliano-Burns, S., Hopper, J., & Seeman, E. (2009). The age of puberty determines sexual dimorphism in bone structure: a male/female co-twin control study. *The Journal of Clinical Endocrinology & Metabolism*, *94*(5), 1638-1643.

Jacobsohn, L., Rodrigues, P., Vasconcelos, O., Corbetta, D., & Barreiros, J. (2014). Lateral manual asymmetries: A longitudinal study from birth to 24 months. *Developmental Psychobiology*, *56*(1), 58-72.

Jia, Z., Zhang, J., Trindade, D. et al. Physical Activity Patterns and Correlates of 9-Month-Old Chinese Infants in the Macau Population. Matern Child Health J 22, 1526–1533 (2018).

Javaid, M. K., & Cooper, C. (2002). Prenatal and childhood influences on osteoporosis. *Best practice & research Clinical endocrinology & metabolism*, *16*(2), 349-367.

Javaid, M. K., Lekamwasam, S., Clark, J., Dennison, E. M., Syddall, H. E., Loveridge, N., ... & Cooper, C. (2006). Infant growth influences proximal femoral geometry in adulthood. *Journal of Bone and Mineral Research*, *21*(4), 508-512.

Jilka, R. L. (2013). The relevance of mouse models for investigating age-related bone loss in humans. *Journals of Gerontology Series A: Biomedical Sciences and Medical Sciences*, *68*(10), 1209-1217.

Jones, M. E., Boon, W. C., McInnes, K., Maffei, L., Carani, C., & Simpson, E. R. (2007). Recognizing rare disorders: aromatase deficiency. *Nature clinical practice Endocrinology & metabolism*, *3*(5), 414-421.

Johnson, W., Stovitz, S., Choh, A. *et al.* Patterns of linear growth and skeletal maturation from birth to 18 years of age in overweight young adults. *Int J Obes* **36,** 535–541 (2012).

Kaneko, T. S., Pejcic, M. R., Tehranzadeh, J., & Keyak, J. H. (2003). Relationships between material properties and CT scan data of cortical bone with and without metastatic lesions. *Medical engineering & physics*, *25*(6), 445-454.

Karagüzel, G., Aktürk, F. A., Okur, E., Gümele, H. R., Gedik, Y., & Ökten, A. (2010). Cleidocranial dysplasia: a case report. *Journal of Clinical Research in Pediatric Endocrinology*, *2*(3), 134.

Karasik, L. B., Adolph, K. E., Tamis-LeMonda, C. S., & Bornstein, M. H. (2010). WEIRD walking: Cross-cultural research on motor development. *The Behavioral and brain sciences*, *33*(2-3), 95.

Karasik, L. B., Tamis-LeMonda, C. S., Adolph, K. E., & Bornstein, M. H. (2015). Places and postures: A cross-cultural comparison of sitting in 5-month-olds. *Journal of Cross-Cultural Psychology*, *46*(8), 1023-1038.

Karlberg, J. (1990). The infancy–childhood growth spurt. *Acta paediatrica*, *79*, 111-118.

Karlberg, J., Kwan, C. W., Gelander, L., & Albertsson-Wikland, K. (2003). Pubertal growth assessment. *Hormone Research in Paediatrics*, *60*(Suppl. 1), 27-35.

Karp, S. J., Schipani, E., St-Jacques, B., Hunzelman, J., Kronenberg, H., & McMahon, A. P.

(2000). Indian hedgehog coordinates endochondral bone growth and morphogenesis via parathyroid hormone related-protein-dependent and-independent pathways. *Development*, *127*(3), 543-548.
Karsenty, G. (2003). The complexities of skeletal biology. *Nature*, *423*(6937), 316-318.
Karsenty, G., & Wagner, E. F. (2002). Reaching a genetic and molecular understanding of skeletal development. *Developmental cell*, *2*(4), 389-406.
Kasprian, G., Langs, G., Brugger, P. C., Bittner, M., Weber, M., Arantes, M., & Prayer, D. (2011). The prenatal origin of hemispheric asymmetry: an in utero neuroimaging study. *Cerebral cortex*, *21*(5), 1076-1083. https://doi.org/10.1093/cercor/bhq179
Killick R, Eckley IA (2014). "changepoint: An R Package for Changepoint Analysis." Journal of Statistical Software, 58(3), 1–19.
Kim, J. H., Liu, X., Wang, J., Chen, X., Zhang, H., Kim, S. H., ... & He, T. C. (2013). Wnt signaling in bone formation and its therapeutic potential for bone diseases. *Therapeutic advances inmusculoskeletal disease*, *5*(1), 13-31.
Kimbel, W. H., & Rak, Y. (2017). Australopithecus sediba and the emergence of Homo: Questionable evidence from the cranium of the juvenile holotype MH 1. *Journal of Human Evolution*, *107*, 94-106.
Klein-Nulend, J., & Bonewald, L. F. (2020). The osteocyte. In *Principles of bone biology* (pp. 133-162). Academic press.
Kono, R. T., Zhang, Y., Jin, C., Takai, M., & Suwa, G. (2014). A 3-dimensional assessment of molar enamel thickness and distribution pattern in Gigantopithecus blacki. *Quaternary International*, *354*, 46-51.
Komori, T., Yagi, H., Nomura, S., Yamaguchi, A., Sasaki, K., Deguchi, K., ... & Kishimoto, T. (1997). Targeted disruption of Cbfa1 results in a complete lack of bone formation owing to maturational arrest of osteoblasts. *Cell*, *89*(5), 755-764.
Komori, T. Regulation of bone development and extracellular matrix protein genes by RUNX2. *Cell Tissue Res* 339, 189 (2010).
Kontulainen, S. A., Macdonald, H. M., Khan, K. M., & McKay, H. A. (2005). Examining bone surfaces across puberty: a 20-month pQCT trial. *Journal of bone and mineral research*, *20*(7), 1202-1207.
Kuchirko, Y. A., & Tamis-LeMonda, C. S. (2019). The cultural context of infant development: Variability, specificity, and universality. In *Advances in child development and behavior* (Vol. 57, pp. 27-63). JAI.
Lampl, M. (1993). Evidence of saltatory growth in infancy. *American Journal of Human Biology*, *5*(6), 641-652.
Largo, R. H., Molinari, L., Weber, M., Pinto, L. C., & Duc, G. (1985). Early development of locomotion: significance of prematurity, cerebral palsy and sex. *Developmental Medicine & Child Neurology*, *27*(2), 183-191.
Lawson, L. Y., Brodt, M. D., Migotsky, N., Chermside-Scabbo, C. J., Palaniappan, R., & Silva, M. J. (2022). Osteoblast-Specific Wnt Secretion Is Required for Skeletal Homeostasis and Loading-Induced Bone Formation in Adult Mice. *Journal of Bone and Mineral Research*, *37*(1), 108-120.
Lazenby, R. A. (2002). Skeletal biology, functional asymmetry and the origins of "handedness". *Journal of theoretical Biology*, *218*(1), 129-138.
Lee, P. C. (1996). The meanings of weaning: growth, lactation, and life history. *Evolutionary Anthropology: Issues, News, and Reviews: Issues, News, and Reviews*, *5*(3), 87-98.

Lee, B., Thirunavukkarasu, K., Zhou, L., Pastore, L., Baldini, A., Hecht, J., ... & Karsenty, G. (1997). Missense mutations abolishing DNA binding of the osteoblast-specific transcription factor OSF2/CBFA1 in cleidocranial dysplasia. *Nature genetics*, *16*(3), 307-310.

Lewis, W. H. (1902). The development of the arm in man. *American Journal of Anatomy*, *1*(2), 145-183.

Lee, K. C. L., Maxwell, A., & Lanyon, L. E. (2002). Validation of a technique for studying functional adaptation of the mouse ulna in response to mechanical loading. *Bone*, *31*(3), 407-412.

Lefebvre, V., Huang, W., Harley, V. R., Goodfellow, P. N., & De Crombrugghe, B. (1997). SOX9 is a potent activator of the chondrocyte-specific enhancer of the pro alpha1 (II) collagen gene. *Molecular and cellular biology*, *17*(4), 2336-2346.

Lefebvre, V., & Dvir-Ginzberg, M. (2017). SOX9 and the many facets of its regulation in the chondrocyte lineage. *Connective tissue research*, *58*(1), 2-14.

Lefebvre, V., Angelozzi, M., & Haseeb, A. (2019). SOX9 in cartilage development and disease. *Current opinion in cell biology*, *61*, 39-47. https://doi.org/10.1016/j.ceb.2019.07.008

Leigh, S. R., & Shea, B. T. (1995). Ontogeny and the evolution of adult body size dimorphism in apes. *American Journal of Primatology*, *36*(1), 37-60.

Leigh, S. R. (2001). Evolution of human growth. *Evolutionary Anthropology: Issues, News, and Reviews: Issues, News, and Reviews*, *10*(6), 223-236. https://doi.org/10.1002/evan.20002

Lejarraga, H. (2002). Growth in infancy and childhood: A pediatric approach. *Human growth and development*, *2*.

Lewis, W. H. (1902). The development of the arm in man. *American Journal of Anatomy*, *1*(2), 145-183.

Lewis, K. J., Frikha-Benayed, D., Louie, J., Stephen, S., Spray, D. C., Thi, M. M., ... & Schaffler, M. B. (2017). Osteocyte calcium signals encode strain magnitude and loading frequency in vivo. *Proceedings of the National Academy of Sciences*, *114*(44), 11775-11780.

Levenston, M. E., Beaupré, G. S., & van der Meulen, M. C. (1994). Improved method for analysis of whole bone torsion tests. *Journal of Bone and Mineral Research*, *9*(9), 1459-1465.

Limony, Y., Kozieł, S., & Friger, M. (2015). Age of onset of a normally timed pubertal growth spurt affects the final height of children. *Pediatric research*, *78*(3), 351-355.

Litmanovitz, I., Dolfin, T., Friedland, O., Arnon, S., Regev, R., Shainkin-Kestenbaum, R., ... & Eliakim, A. (2003). Early physical activity intervention prevents decrease of bone strength in very low birth weight infants. *Pediatrics*, *112*(1), 15-19.

Litmanovitz, I., Erez, H., Eliakim, A., Bauer-Rusek, S., Arnon, S., Regev, R. H., ... & Nemet, D. (2016). The effect of assisted exercise frequency on bone strength in very low birth weight preterm infants: a randomized control trial. *Calcified tissue international*, *99*(3), 237-242.

Lobo, M. A., & Galloway, J. C. (2012). Enhanced handling and positioning in early infancy advances development throughout the first year. *Child Development*, *83*(4), 1290-1302.

Locatelli, V., & Bianchi, V. E. (2014). Effect of GH/IGF-1 on bone metabolism and osteoporsosis. *International journal of endocrinology*, *2014*.

Locke, J. L., & Bogin, B. (2022). An Unusually Human Time: Effects of the Most Social Stage

on the Most Social Species. In *Evolutionary Perspectives on Infancy* (pp. 107-133). Springer, Cham.
Long, F., & Ornitz, D. M. (2013). Development of the endochondral skeleton. *Cold Spring Harbor perspectives in biology*, *5*(1), a008334.
Lotshaw, R. (1971). Births of two lowland gorillas at Cincinnati Zoo. *International Zoo Yearbook*, *11*(1), 84-87.
Lovejoy, C. O., Johanson, D. C., & Coppens, Y. (1982). Hominid lower limb bones recovered from the Hadar Formation: 1974–1977 collections. *American Journal of Physical Anthropology*, *57*(4), 679-700.
Lovejoy, C. O., Cohn, M. J., & White, T. D. (1999). Morphological analysis of the mammalian postcranium: a developmental perspective. *Proceedings of the National Academy of Sciences*, *96*(23), 13247-13252.
Lovejoy, C. O., Suwa, G., Spurlock, L., Asfaw, B., & White, T. D. (2009). The pelvis and femur of Ardipithecus ramidus: the emergence of upright walking. *Science*, *326*(5949), 71-71e6.
Lozano, M., Mosquera, M., De Castro, J. M. B., Arsuaga, J. L., & Carbonell, E. (2009). Right handedness of Homo heidelbergensis from Sima de los Huesos (Atapuerca, Spain) 500,000 years ago. *Evolution and Human Behavior*, *30*(5), 369-376.
Lozano-Ruiz, M., De Castro, J. B., Martinón-Torres, M., & Sarmiento, S. (2004). Cutmarks on fossil human anterior teeth of the Sima de los Huesos site (Atapuerca, Spain). *Journal of Archaeological Science*, *31*(8), 1127-1135.
Lozano-Ruiz, M., Estalrrich, A., Bondioli, L., Fiore, I., Bermúdez de Castro, J. M., Arsuaga, J. L., ... & Frayer, D. (2017). Right-handed fossil humans.
Maggiano, I. S., Schultz, M., Kierdorf, H., Sosa, T. S., Maggiano, C. M., & Tiesler Blos, V. (2008). Cross-sectional analysis of long bones, occupational activities and long-distance trade of the Classic Maya from Xcambó—Archaeological and osteological evidence. *American Journal of Physical Anthropology: The Official Publication of the American Association of Physical Anthropologists*, *136*(4), 470-477.
Maggiano, I. S., Maggiano, C. M., Tiesler, V. G., Chi-Keb, J. R., & Stout, S. D. (2015). Drifting diaphyses: asymmetry in diametric growth and adaptation along the humeral and femoral length. *The Anatomical Record*, *298*(10), 1689-1699.
Maggiano, C. M., Maggiano, I. S., Tiesler, V. G., Chi-Keb, J. R., & Stout, S. D. (2016). Methods and theory in bone modeling drift: comparing spatial analyses of primary bone distributions in the human humerus. *Journal of anatomy*, *228*(1), 190-202.
Mak, K. K., Chen, M. H., Day, T. F., Chuang, P. T., & Yang, Y. (2006). Wnt/β-catenin signaling interacts differentially with Ihh signaling in controlling endochondral bone and synovial joint formation
Malina, R. M. (2004). Motor development during infancy and early childhood: Overview and suggested directions for research. *International journal of sport and health science*, *2*, 50-66.
Marshall, W. A., & Tanner, J. M. (1986). Puberty. In *Postnatal growth neurobiology* (pp. 171-209). Springer, Boston, MA.
Marván, M. L., Catillo-López, R. L., Alcalá-Herrera, V., & Del Callejo, D. (2016). The decreasing age at menarche in Mexico. *Journal of pediatric and adolescent gynecology*, *29*(5), 454-457.
Matsuoka, T., Ahlberg, P. E., Kessaris, N., Iannarelli, P., Dennehy, U., Richardson, W. D., ... & Koentges, G. (2005). Neural crest origins of the neck and shoulder. *Nature*, *436*(7049),

347-355.
Mays, S. A. (1985). The relationship between Harris line formation and bone growth and development. *Journal of archaeological science*, *12*(3), 207-220.
Mays, S., Steele, J., & Ford, M. (1999). Directional asymmetry in the human clavicle. *International Journal of Osteoarchaeology*, *9*(1), 18-28.
Mays, S. A. (2002). Asymmetry in metacarpal cortical bone in a collection of British post-mediaeval human skeletons. *Journal of Archaeological Science*, *29*(4), 435-441.
McDowell, G., Rajadurai, S., & Levin, M. (2016). From cytoskeletal dynamics to organ asymmetry: a nonlinear, regulative pathway underlies left–right patterning. *Philosophical Transactions of the Royal Society B: Biological Sciences*, *371*(1710), 20150409.
Mc Grew, W. C., & Marchant, L. F. (1992). Chimpanzees, tools, and termites: Hand preference or handedness?. *Current Anthropology*, *33*(1), 114-119.
McCartney, G., & Hepper, P. (1999). Development of lateralized behaviour in the human fetus from 12 to 27 weeks' gestation. *Developmental Medicine and Child Neurology*, *41*(2), 83-86.
McCollough, C. H., Bushberg, J. T., Fletcher, J. G., & Eckel, L. J. (2015, October). Answers to common questions about the use and safety of CT scans. In *Mayo Clinic Proceedings* (Vol. 90, No. 10, pp. 1380-1392). Elsevier.
McManus, C. (2019). Half a century of handedness research: Myths, truths; fictions, facts; backwards, but mostly forwards. *Brain and Neuroscience Advances*, *3*, 2398212818820513.
McNeilly, A. S. (1979). Effects of lactation on fertility. *British Medical Bulletin*, *35*(2), 151-154.
Meade, J. B., Cowin, S. C., Klawitter, J. J., Van Buskirk, W. C., & Skinner, H. B. (1984). Bone remodeling due to continuously applied loads. *Calcified Tissue International*, *36*(1), S25-S30.
Miller, M. E. (2005). Hypothesis: fetal movement influences fetal and infant bone strength. *Medical hypotheses*, *65*(5), 880-886.
Milovanovic, P., Djonic, D., Hahn, M., Amling, M., Busse, B., & Djuric, M. (2017). Region-dependent patterns of trabecular bone growth in the human proximal femur: A study of 3D bone microarchitecture from early postnatal to late childhood period. *American journal of physical anthropology*, *164*(2), 281-291.
Molinari, L., Largo, R. H., & Prader, A. (1980). Analysis of the growth spurt at age seven (mid-growth spurt). *Helvetica Paediatrica Acta*, *35*(4), 325-334.
Monroe, D. G., McGee-Lawrence, M. E., Oursler, M. J., & Westendorf, J. J. (2012). Update on Wnt signaling in bone cell biology and bone disease. *Gene*, *492*(1), 1-18.
Morimoto, N., Kunimatsu, Y., Nakatsukasa, M., Ponce de Leon, M. S., Zollikofer, C. P., Ishida, H., ... & Suwa, G. (2020). Variation of bony labyrinthine morphology in Mio− Plio− Pleistocene and modern anthropoids. *American journal of physical anthropology*, *173*(2), 276-292.
Mooney, M. P., Siegel, M. I., & Gest, T. R. (1985). Prenatal stress and increased fluctuating asymmetry in the parietal bones of neonatal rats. *American Journal of Physical Anthropology*, *68*(1), 131-134.
Moss, M. L., Noback, C. R., & Robertson, G. G. (1955). Critical developmental horizons in human fetal long bones. Correlated quantitative and histological criteria. *American Journal of Anatomy*, *97*(1), 155-175.
Motaei, J., Salmaninejad, A., Jamali, E., Khorsand, I., Ahmadvand, M., Shabani, S., ... &

Naqipour, F. (2021). Molecular genetics of cleidocranial dysplasia. *Fetal and pediatric pathology*, *40*(5), 442-454.
Moyer-Mileur, L. J., Brunstetter, V., McNaught, T. P., Gill, G., & Chan, G. M. (2000). Daily physical activity program increases bone mineralization and growth in preterm very low birth weight infants. *Pediatrics*, *106*(5), 1088-1092.
Mundlos, S., Otto, F., Mundlos, C., Mulliken, J. B., Aylsworth, A. S., Albright, S., ... & Olsen, B. R. (1997). Mutations involving the transcription factor CBFA1 cause cleidocranial dysplasia. *Cell*, *89*(5), 773-779.
Namgung, R., & Tsang, R. C. (2003). Bone in the pregnant mother and newborn at birth. *Clinica Chimica Acta*, *333*(1), 1-11.
Nauer, C. B., Rieke, A., Zubler, C., Candreia, C., Arnold, A., & Senn, P. (2011). Low-dose temporal bone CT in infants and young children: effective dose and image quality. *American journal of neuroradiology*, *32*(8), 1375-1380.
Noble, B. S. (2008). The osteocyte lineage. *Archives of biochemistry and biophysics*, *473*(2), 106-111.
Ocklenburg, S., Beste, C., Arning, L., Peterburs, J., & Güntürkün, O. (2014). The ontogenesis of language lateralization and its relation to handedness. *Neuroscience & Biobehavioral Reviews*, *43*, 191-198.
Ogata, S., & Uhthoff, H. K. (1990). The early development and ossification of the human clavicle—an embryologic study. *Acta Orthopaedica Scandinavica*, *61*(4), 330-334.
Ogden, J. A., Conlogue, G. J., & Jensen, P. (1978). Radiology of postnatal skeletal development: the proximal humerus. *Skeletal Radiology*, *2*(3), 153-160.
Ogden, J. A. (1984). Growth slowdown and arrest lines. *Journal of pediatric orthopedics*, *4*(4), 409-415.
Olsen, F. R., & Whitmore Jr, F. C. (1944). Machine for serial sectioning of fossils. *Journal of Paleontology*, 210-215.
Ollier, L. X. E. L.: Traité expérimental et clinique de la régénération des os et de la production artificielle du tissu osseux , Paris, V. Masson et fils, 1867, vol. 1.
Ooki, A., Onodera, S., Saito, A., Oguchi, A., Murakawa, Y., Sakamoto, T., ... & Azuma, T. (2020). CAGE-seq analysis of osteoblast derived from cleidocranial dysplasia human induced pluripotent stem cells. *Bone*, 141, 115582.
O'Neill, M. C., & Ruff, C. B. (2004). Estimating human long bone cross-sectional geometric properties: a comparison of noninvasive methods. *Journal of human evolution*, *47*(4), 221-235.
O'Rahilly, R., & Gardner, E. (1975). The timing and sequence of events in the development of the limbs in the human embryo. *Anatomy and embryology*, *148*(1), 1-
O'Rahilly, R., & Müller, F. (2007). The development of the neural crest in the human. *Journal of anatomy*, *211*(3), 335-351.
Osborn, M. L., & Homberger, D. G. (2015). The human shoulder suspension apparatus: a causal explanation for bilateral asymmetry and a fresh look at the evolution of human bipedality. *The Anatomical Record*, *298*(9), 1572-1588. https://doi.org/10.1002/ar.23178
Otto, F., Thornell, A. P., Crompton, T., Denzel, A., Gilmour, K. C., Rosewell, I. R., & Owen, M. J. (1997). Cbfa1, a candidate gene for cleidocranial dysplasia syndrome, is essential for osteoblast differentiation and bone development. *Cell*, *89*(5), 765-771.
Ozonoff, M. B. (1979). *Pediatric orthopedic radiology* (Vol. 15). WB Saunders Company.

Pablos, A., Gómez-Olivencia, A., García-Pérez, A., Martínez, I., Lorenzo, C., & Arsuaga, J. L. \ (2013). From toe to head: Use of robust regression methods in stature estimation based on foot remains. *Forensic Science International*, *226*(1-3), 299-e1.
Pablos, A., Martínez, I., Lorenzo, C., Sala, N., Gracia-Téllez, A., & Arsuaga, J. L. (2014). Human calcaneifrom the Middle Pleistocene site of Sima de los Huesos (sierra de Atapuerca, Burgos, Spain). *Journal of human evolution*, *76*, 63-76.
Palaiothodorou, D., Antoniou, T., & Vagenas, G. (2020). Bone asymmetries in the limbs of children tennis players: testing the combined effects of age, sex, training time, and maturity status. *Journal of Sports Sciences*, *38*(20), 2298-2306.
Palmer, A. R. (2004). Symmetry breaking and the evolution of development. *Science*, *306*(5697), 828-833.
Pan, C. Y., Tseng, Y. C., Lan, T. H., & Chang, H. P. (2017). Craniofacial features of cleidocranial dysplasia. *Journal of Dental Sciences*, *12*(4), 313-318.
Patel, N. H. (2009). Asymmetry with a twist. *Nature*, *462*(7274), 727-728.
Patrick, S. K., Noah, J. A., & Yang, J. F. (2012). Developmental constraints of quadrupedal coordination across crawling styles in human infants. *Journal of Neurophysiology*, *107*(11), 3050-3061.
Pearson, O. M., & Lieberman, D. E. (2004). The aging of Wolff's "law": ontogeny and responses to mechanical loading in cortical bone. *American journal of physical anthropology*, *125*(S39), 63-99.
Pérez, P. J., Gracia, A., Martínez, I., & Arsuaga, J. L. (1997). Paleopathological evidence of the cranial remains from the Sima de los Huesos Middle Pleistocene site (Sierra de Atapuerca, Spain). Description and preliminary inferences. *Journal of human evolution*, *33*(2-3), 409-421.
Pickering, T. R., & Hensley-Marschand, B. (2008). Cutmarks and hominid handedness. *Journal of Archaeological Science*, *35*(2), 310-315.
Pneumaticos, S. G., Christofides, A., Gkioka, E., Kalogeropoulos, T., Msaouel, P., & Koutsilieris, M. (2013). Osteoprotegerin expression during the micro-and macrometastatic phases of the osteoblastic metastasis in prostate cancer: therapeutic implications. *Expert Opinion on Therapeutic Targets*, *17*(12), 1395-1403.
Portmann, A. (1969). Biologische Fragmente zu einer Lehre vom Menschen [A Zoologist Looks at Humankind](Schwabe, Basel, Germany); trans Schaefer J (1990).
Pritchett, J. W. (1991). Growth plate activity in the upper extremity. *Clinical orthopaedics and related research*, (268), 235-242.
Provot, S., & Schipani, E. (2005). Molecular mechanisms of endochondral bone development. *Biochemical and biophysical research communications*, *328*(3), 658-665.
Quam, R. M., Arsuaga, J. L., de Castro, J. M. B., Díez, C. J., Lorenzo, C., Carretero, M., ... & Ortega, A. I. (2001). Human remains from Valdegoba Cave (Huérmeces, Burgos, Spain). *Journal of Human Evolution*, *41*(5), 385-435.
R Core Team (2021). R: A language and environment for statistical computing. R Foundation for Statistical Computing, Vienna, Austria. https://www.R-project.org/.
Raab-Cullen, D. M., Akhter, M. P., Kimmel, D. B., & Recker, R. R. (1994). Bone response to alternate-day mechanical loading of the rat tibia. Journal of Bone and Mineral Research, 9(2), 203-211.
Rahman, M. S., Akhtar, N., Jamil, H. M., Banik, R. S., & Asaduzzaman, S. M. (2015). TGF-β/BMP signaling and other molecular events: regulation of osteoblastogenesis and bone

formation. *Bone research*, *3*(1), 1-20.
Rak, Y., Kimbel, W. H., & Hovers, E. (1994). A Neandertal infant from Amud cave, Israel. *Journal of human evolution*, *26*(4), 313-324.
Ramirez Rozzi, F. V., & Bermúdez de Castro, J. M. (2004). Surprisingly rapid growth in Neanderthals. *Nature*, *428*(6986), 936-939.
Rathnayaka, K., Sahama, T., Schuetz, M. A., & Schmutz, B. (2011). Effects of CT image segmentation methods on the accuracy of long bone 3D reconstructions. *Medical engineering & physics*, *33*(2), 226-233.
Raymond, M., & Pontier, D. (2004). Is there geographical variation in human handedness?. *Laterality: Asymmetries of body, brain and cognition*, *9*(1), 35-51.
Reddi, A. H. (1981). Cell biology and biochemistry of endochondral bone development. *Collagen and related research*, *1*(2), 209-226.
Reed, T. H., & Gallagher, B. F. (1963). Gorilla birth at National Zoological Park Washington. *Der Zool. Garten (NF)*, *27*, 279-292.
Rehman, M. U., & Narchi, H. (2015). Metabolic bone disease in the preterm infant: Current state and future directions. *World journal of methodology*, *5*(3), 115.
Righetti, L., Nylén, A., Rosander, K., & Ijspeert, A. J. (2015). Kinematic and gait similarities between crawling human infants and other quadruped mammals. *Frontiers in neurology*, *6*, 17.
Robbins, M. M., & Robbins, A. M. (2021). Variability of weaning age in mountain gorillas (Gorilla beringei beringei). *American Journal of Physical Anthropology*, *174*(4), 776-
Roche, A. F. (1992). *Growth, maturation, and body composition: the Fels Longitudinal Study 1929-1991* (No. 9). Cambridge University Press.
Robling, A. G., Castillo, A. B., & Turner, C. H. (2006). Biomechanical and molecular regulation of bone remodeling. *Annu. Rev. Biomed. Eng.*, *8*, 455-498.
Rodríguez, J. I., Palacios, J., García-Alix, A., Pastor, I., & Paniagua, R. (1988). Effects of immobilization on fetal bone development. A morphometric study in newborns with congenital neuromuscular diseases with intrauterine onset. *Calcified tissue international*, *43*(6), 335-339.
Robson, P. (1970). Shuffling, hitching, scooting or sliding: some observations in 30 otherwise normal children. *Developmental Medicine & Child Neurology*, *12*(5), 608-617.
Robson, P. (1984). Prewalking locomotor movements and their use in predicting standing and walking. *Child: care, health and development*, *10*(5), 317-330.
Robson, S. L., & Wood, B. (2008). Hominin life history: reconstruction and evolution. *Journal of Anatomy*, *212*(4), 394-425.
Rosas, A., Ríos, L., Estalrrich, A., Liversidge, H., García-Tabernero, A., Huguet, R., ... & Dean, C. (2017). The growth pattern of Neandertals, reconstructed from a juvenile skeleton from El Sidrón (Spain). *Science*, *357*(6357), 1282-1287.
Rosenberg, K., & Trevathan, W. (2002). Birth, obstetrics and human evolution. *BJOG: An International Journal of Obstetrics & Gynaecology*, *109*(11), 1199-1206.
Ruff, C. B., & Hayes, W. C. (1982). Subperiosteal expansion and cortical remodeling of the human femur and tibia with aging. *Science*, *217*(4563), 945-948.
Ruff, C. B., & Hayes, W. C. (1983). Cross-sectional geometry of Pecos Pueblo femora and tibiae—A biomechanical investigation: I. Method and general patterns of variation. *American journal of physical anthropology*, *60*(3), 359-381.
Ruff, C. B. (1989). New approaches to structural evolution of limb bones in primates. *Folia*

Primatologica, *53*(1-4), 142-159.
Ruff, C. B., Walker, A., & Trinkaus, E. (1994). Postcranial robusticity in Homo. III: ontogeny. *American journal of physical anthropology*, *93*(1), 35-54.
Ruff, C. (2003a). Ontogenetic adaptation to bipedalism: age changes in femoral to humeral length and strength proportions in humans, with a comparison to baboons. *Journal of human evolution*, *45*(4), 317-349.
Ruff, C. (2003b). Growth in bone strength, body size, and muscle size in a juvenile longitudinal sample. *Bone*, *33*(3), 317-329.
Ruff, C. B., Burgess, M. L., Bromage, T. G., Mudakikwa, A., & McFarlin, S. C. (2013). Ontogenetic b changes in limb bone structural proportions in mountain gorillas (Gorilla beringei beringei). *Journal of Human Evolution*, *65*(6), 693-703.
Runestad, J. A., Ruff, C. B., Nieh, J. C., Thorington Jr, R. W., & Teaford, M. F. (1993). Radiographic estimation of long bone cross-sectional geometric properties. *American Journal of Physical Anthropology*, *90*(2), 207-213.
Sarringhaus, L. A., Stock, J. T., Marchant, L. F., & McGrew, W. C. (2005). Bilateral asymmetry in the limb bones of the chimpanzee (Pan troglodytes). *American Journal of Physical Anthropology: The Official Publication of the American Association of Physical Anthropologists*, *128*(4), 840-845.
Sarringhaus, L. A., MacLatchy, L. M., & Mitani, J. C. (2014). Locomotor and postural development of wild chimpanzees. *Journal of human evolution*, *66*, 29-38.
Sarringhaus, L. A., MacLatchy, L. M., & Mitani, J. C. (2016). Long bone cross-sectional properties reflect changes in locomotor behavior in developing chimpanzees. *American Journal of Physical Anthropology*, *160*(1), 16-29.
Sato, K., & Iemitsu, M. (2018). The role of dehydroepiandrosterone (DHEA) in skeletal muscle. *Vitamins and hormones*, *108*, 205-221.
Saunders, S. R. (2008). Juvenile skeletons and growth-related studies. *Biological anthropology of the human skeleton*, 115-147.
Schneider, H., & Brueckner, M. (2000). Of mice and men: dissecting the genetic pathway that controls left-right asymmetry in mice and humans. *American journal of medical genetics*, *97*(4), 258-270.
Schreiber, A. M. (2013). Flatfish: an asymmetric perspective on metamorphosis. *Current topics in developmental biology*, *103*, 167-194.
Schwartz, G. T. (2012). Growth, development, and life history throughout the evolution of Homo. *Current Anthropology*, *53*(S6), S395-S408.
Schoenau, E., Neu, C. M., Rauch, F., & Manz, F. (2001). The development of bone strength at the proximal radius during childhood and adolescence. *The Journal of Clinical Endocrinology & Metabolism*, *86*(2), 613-618.
Shahi, M., Peymani, A., & Sahmani, M. (2017). Regulation of bone metabolism. *Reports of biochemistry & molecular biology*, *5*(2), 73.
Shaw, C. N. (2011). Is 'hand preference'coded in the hominin skeleton? An in-vivo study of bilateral morphological variation. *Journal of human evolution*, *61*(4), 480-487.
Sheridan, M. D., Sharma, A., & Frost, M. (2002). *From birth to five years: children's developmental progress*. Routledge.
Simpson, S. W., Quade, J., Levin, N. E., Butler, R., Dupont-Nivet, G., Everett, M., & Semaw, S. (2008). A female Homo erectus pelvis from Gona, Ethiopia. *Science*, *322*(5904), 1089-1092.

Sissons, H. A., & Kember, N. F. (1977). Longitudinal bone growth of the human femur. *Postgraduate Medical Journal*, *53*(622), 433-437.
Smit, T. H., & Burger, E. H. (2000). Is BMU-coupling a strain-regulated phenomenon? A finite element analysis. *Journal of Bone and Mineral Research*, *15*(2), 301-307.
Smith, B. H. (1993). The physiological age of KNM-WT 15000. *The Nariokotome Homo erectus skeleton*, 195-220.
Smith, S. L., & Buschang, P. H. (2005). Longitudinal models of long bone growth during adolescence. *American Journal of Human Biology*, *17*(6), 731-745.
Smith, T. M., Toussaint, M., Reid, D. J., Olejniczak, A. J., & Hublin, J. J. (2007a). Rapid dental development in a middle Paleolithic Belgian Neanderthal. *Proceedings of the National Academy of Sciences*, *104*(51), 20220-20225.
Smith, T. M., Tafforeau, P., Reid, D. J., Grün, R., Eggins, S., Boutakiout, M., & Hublin, J. J. (2007b). Earliest evidence of modern human life history in North African early Homo sapiens. *Proceedings of the National Academy of Sciences*, *104*(15), 6128-6133.
Smith, T. M., Austin, C., Hinde, K., Vogel, E. R., & Arora, M. (2017). Cyclical nursing patterns in wild orangutans. *Science Advances*, *3*(5), e1601517.
Smith, T. M., Austin, C., Green, D. R., Joannes-Boyau, R., Bailey, S., Dumitriu, D., ... & Arora, M. (2018). Wintertime stress, nursing, and lead exposure in Neanderthal children. *Science Advances*, *4*(10), eaau9483.
Sohn, K. (2015). The trend in age at menarche in Indonesia: Birth cohorts 1944–1988. *Journal of biosocial science*, *47*(3), 407-412.
Song, H., & Park, K. H. (2020, December). Regulation and function of SOX9 during cartilage development and regeneration. In *Seminars in cancer biology* (Vol. 67, pp. 12-23). Academic Press.
Specker, B. L., Brazerol, W., Tsang, R. C., Levin, R., Searcy, J., & Steichen, J. (1987). Bone mineral content in children 1 to 6 years of age: detectable sex differences after 4 years of age. *American Journal of Diseases of Children*, *141*(3), 343-344.
Srinivasan, S., & Peh, W. C. (2013). Radiography in osteoporosis. In *Osteoporosis and bone densitometry measurements* (pp. 15-30). Springer, Berlin, Heidelberg.
Steele, J., & Mays, S. (1995). Handedness and directional asymmetry in the long bones of the human upper limb. *International Journal of Osteoarchaeology*, *5*(1), 39-49.
Stewart, K. J. (1977). The birth of a wild mountain gorilla (Gorilla gorilla beringei). *Primates*, *18*(4), 965-976.
Stock, J. T., & Pfeiffer, S. K. (2004). Long bone robusticity and subsistence behaviour among Later Stone Age foragers of the forest and fynbos biomes of South Africa. *Journal of Archaeological science*, *31*(7), 999-1013.
Størvold, G. V., Aarethun, K., & Bratberg, G. H. (2013). Age for onset of walking and prewalking strategies. *Early human development*, *89*(9), 655-659.
St-Jacques, B., Hammerschmidt, M., & McMahon, A. P. (1999). Indian hedgehog signaling regulates proliferation and differentiation of chondrocytes and is essential for bone formation. *Genes & development*, *13*(16), 2072-2086.
Sugiyama, T., Price, J. S., & Lanyon, L. E. (2010). Functional adaptation to mechanical loading in both cortical and cancellous bone is controlled locally and is confined to the loaded bones. *Bone*, *46*(2), 314-321.
Sumner, D. R., & Andriacchi, T. P. (1996). Adaptation to differential loading: comparison of growth-related changes in cross-sectional properties of the human femur and

humerus. *Bone*, *19*(2), 121-126.
Sun, T., Patoine, C., Abu-Khalil, A., Visvader, J., Sum, E., Cherry, T. J., ... & Walsh, C. A. (2005). Early asymmetry of gene transcription in embryonic human left and right cerebral cortex. *Science*, *308*(5729), 1794-1798.
Super, C. M. (1976). Environmental effects on motor development: The case of 'African infant precocity'. *Developmental medicine & child neurology*, *18*(5), 561-567.
Tacail, T., Thivichon-Prince, B., Martin, J. E., Charles, C., Viriot, L., & Balter, V. (2017). Assessing human weaning practices with calcium isotopes in tooth enamel. *Proceedings of the National Academy of Sciences*, *114*(24), 6268-6273.
Tacail, T., Martin, J. E., Arnaud-Godet, F., Thackeray, J. F., Cerling, T. E., Braga, J., & Balter, V. (2019). Calcium isotopic patterns in enamel reflect different nursing behaviors among South African early hominins. *Science advances*, *5*(8), eaax3250.
Tague, R. G., & Lovejoy, C. O. (1986). The obstetric pelvis of AL 288-1 (Lucy). *Journal of Human Evolution*, *15*(4), 237-255.
Tan, U., & Tan, M. (1999). Incidences of asymmetries for the palmar grasp reflex in neonates and hand preference in adults. *Neuroreport*, *10*(16), 3253-3256.
Tanaka, T., Komatsy, K., Takada, G., Miyashita, M., & Ohno, T. (1998). Probability estimation of final height. *Endocrine journal*, *45*(Suppl), S145-S149.
Taranger, J., & Hägg, U. (1980). The timing and duration of adolescent growth. *Acta Odontologica Scandinavica*, *38*(1), 57-67.
Tardieu, C. (1998). Short adolescence in early hominids: infantile and adolescent growth of the human femur. *American Journal of Physical Anthropology: The Official Publication of the American Association of Physical Anthropologists*, *107*(2), 163-178.
Taylor, A. B. (1995). Effects of ontogeny and sexual dimorphism on scapula morphology in the mountain gorilla (Gorilla gorilla beringel). *American journal of physical anthropology*, *98*(4), 431-445.
Testi, D., Zannoni, C., Cappello, A., & Viceconti, M. (2001). Border-tracing algorithm implementation for the femoral geometry reconstruction. *Computer methods and programs in biomedicine*, *65*(3), 175-182.
Teti, A. (2011). Bone development: overview of bone cells and signaling. *Current osteoporosis reports*, *9*(4), 264-273.
Thalange, N. K., Foster, P. J., Gill, M. S., Price, D. A., & Clayton, P. E. (1996). Model of normal prepubertal growth. *Archives of disease in childhood*, *75*(5), 427-431.
Thigpen, L. W. (1941). Further notes on preparing paraffin sections of bone. *American Journal of Clinical Pathology*, *11*(ts5_4), 119-120.
Toth, N. (1985). Archaeological evidence for preferential right-handedness in the Lower and Middle Pleistocene, and its possible implications. *Journal of Human Evolution*, *14*(6), 607-614.
Tracer, D. P., & Wyckoff, S. L. (2020). Determinants of infant carrying behavior in rural Papua New Guinea. *American Journal of Human Biology*, *32*(6), e23429.
Treece, G. M., Gee, A. H., Mayhew, P. M., & Poole, K. E. (2010). High resolution cortical bone thickness measurement from clinical CT data. *Medical image analysis*, *14*(3), 276-290.
Trevarthen, C. (1996). Lateral asymmetries in infancy: Implications for the development of the hemispheres. *Neuroscience & Biobehavioral Reviews*, *20*(4), 571-586.
Trinkaus, E., Churchill, S. E., & Ruff, C. B. (1994). Postcranial robusticity in Homo. II: Humeral bilateral asymmetry and bone plasticity. *American journal of physical*

anthropology, *93*(1), 1-34.
Trinkaus, E., & Ruff, C. B. (1999). Diaphyseal cross-sectional geometry of Near Eastern Middle Palaeolithic humans: the femur. *Journal of Archaeological Science*, *26*(4), 409-424.
Tseng, Z. J., & Flynn, J. J. (2015). Are cranial biomechanical simulation data linked to known diets in extant taxa? A method for applying diet-biomechanics linkage models to infer feeding capability of extinct species. *PLoS One*, *10*(4), e0124020.
Tseng, Z. J., & Flynn, J. J. (2018). Structure-function covariation with nonfeeding ecological variables influences evolution of feeding specialization in Carnivora. *Science advances*, *4*(2), eaao5441.
Turner, C. H., Forwood, M. R., Rho, J. Y., & Yoshikawa, T. (1994). Mechanical loading thresholds for lamellar and woven bone formation. *Journal of bone and mineral research*, *9*(1), 87-97.
Turner, C. H., & Robling, A. G. (2005). Mechanisms by which exercise improves bone strength. *Journal of bone and mineral metabolism*, *23*(1), 16-22.
Turnquist, J. E., & Wells, J. P. (1994). Ontogeny of locomotion in rhesus macaques (Macaca mulatta): I. Early postnatal ontogeny of the musculoskeletal system. *Journal of Human Evolution*, *26*(5-6), 487-499.
Ubelaker, D. H., & Zarenko, K. M. (2012). Can handedness be determined from skeletal remains? A chronological review of the literature. *Journal of Forensic Sciences*, *57*(6), 1421-1426.
Uda, Y., Azab, E., Sun, N., Shi, C., & Pajevic, P. D. (2017). Osteocyte mechanobiology. *Current osteoporosis reports*, *15*(4), 318-325.
Ueno, A., & Matsuzawa, T. (2004). Food transfer between chimpanzee mothers and their infants. *Primates*, *45*(4), 231-239. https://doi.org/10.1007/s10329-004-0085-9
Uomini, N. T. (2011). Handedness in neanderthals. In *Neanderthal lifeways, subsistence and technology* (pp. 139-154). Springer, Dordrecht.
Uomini, N. T., & Ruck, L. (2018). Manual laterality and cognition through evolution: An archeological perspective. *Progress in brain research*, *238*, 295-323.
Vaananen, H. K., Zhao, H., Mulari, M., & Halleen, J. M. (2000). The cell biology of osteoclast function. *Journal of cell science*, *113*(3), 377-381.
Van der Meer, A. L. H., Van der Weel, F. R., & Lee, D. N. (1995). The functional significance of arm movements in neonates. *Science*, *267*(5198), 693-695.
Van Eijnatten, M., van Dijk, R., Dobbe, J., Streekstra, G., Koivisto, J., & Wolff, J. (2018). CT image segmentation methods for bone used in medical additive manufacturing. *Medical engineering & physics*, *51*, 6-16.
Van Noordwijk, M. A., Kuzawa, C. W., & Van Schaik, C. P. (2013). The evolution of the patterning of human lactation: A comparative perspective. *Evolutionary Anthropology: Issues, News, and Reviews*, *22*(5), 202-212.
Vizmanos, B., Martí-Henneberg, C., Clivillé, R., Moreno, A., & Fernández-Ballart, J. (2001). Age of pubertal onset affects the intensity and duration of pubertal growth peak but not final height. *American Journal of Human Biology: The Official Journal of the Human Biology Association*, *13*(3), 409-416.
Volpato, V., Macchiarelli, R., Guatelli-Steinberg, D., Fiore, I., Bondioli, L., & Frayer, D. W. (2012). Hand to mouth in a Neandertal: right-handedness in Regourdou 1. *PLoS One* 7(8): e43949.
Wada, J. A., Clarke, R., & Hamm, A. (1975). Cerebral hemispheric asymmetry in humans:

Cortical speech zones in 100 adult and 100 infant brains. *Archives of neurology*, *32*(4), 239-246.
Waidhofer, M., & Kirchengast, S. (2015). Sexual dimorphism in directional asymmetry of the upper limb bones among Khoe-San skeletons. *Homo*, *66*(6), 508-519.
Walker, R., Hill, K., Burger, O., & Hurtado, A. M. (2006). Life in the slow lane revisited: Ontogenetic separation between chimpanzees and humans. *American Journal of Physical Anthropology: The Official Publication of the American Association of Physical Anthropologists*, *129*(4), 577-583.
Wall-Scheffler, C. M., Geiger, K., & Steudel-Numbers, K. L. (2007). Infant carrying: the role of increased locomotory costs in early tool development. *American Journal of Physical Anthropology: The Official Publication of the American Association of Physical Anthropologists*, *133*(2), 841-846.
Wall-Scheffler, C. M. (2012). Energetics, locomotion, and female reproduction: implications for human evolution. *Annual review of anthropology*, *41*, 71-85.
Warrener, A. G. (2017). Hominin hip biomechanics: changing perspectives. *The Anatomical Record*, *300*(5), 932-945.
Wang, R. N., Green, J., Wang, Z., Deng, Y., Qiao, M., Peabody, M., ... & Shi, L. L. (2014). Bone Morphogenetic Protein (BMP) signaling in development and human diseases. *Genes & diseases*, *1*(1), 87-105.
Weinmann, J. P., & Sicher, H. (1955). Bone and bones. Fundamentals of bone biology. *Bone and bones. Fundamentals of bone biology.*, (2nd ed).
Wescott, D. J., & Cunningham, D. L. (2006). Temporal changes in Arikara humeral and femoral cross-sectional geometry associated with horticultural intensification. *Journal of Archaeological Science*, *33*(7), 1022-1036.
Wesseling-Perry, K. (2010). FGF-23 in bone biology. *Pediatric Nephrology*, *25*(4), 603-608.
Westergaard, G. C., & Suomi, S. J. (1996). Hand preference for a bimanual task in tufted capuchins (Cebus apella) and rhesus macaques (Macaca mulatta). *Journal of Comparative Psychology*, *110*(4), 406.
Weinert, L. S., & Silveiro, S. P. (2015). Maternal–fetal impact of vitamin D deficiency: a critical review. *Maternal and child health journal*, *19*(1), 94-101.
Weise, M., De-Levi, S., Barnes, K. M., Gafni, R. I., Abad, V., & Baron, J. (2001). Effects of estrogen on growth plate senescence and epiphyseal fusion. *Proceedings of the National Academy of Sciences*, *98*(12), 6871-6876.
Whitcome, K. K., Miller, E. E., & Burns, J. L. (2017). Pelvic rotation effect on human stride length: Releasing the constraint of obstetric selection. *The Anatomical Record*, *300*(4), 752-763.
White, T. D., Black, M. T., & Folkens, P. A. (2011). *Human osteology*. Academic press.
Wickham H (2016). ggplot2: Elegant Graphics for Data Analysis. Springer-Verlag New York. ISBN 978-3-319-24277-4, https://ggplot2.tidyverse.org.
Witchel, S. F., Pinto, B., Burghard, A. C., & Oberfield, S. E. (2020). Update on adrenarche. *Current opinion in pediatrics*, *32*(4), 574.
Wolff J. 1892. Das Gesetz der Transformation der Knochen. Ber-lin: A. Hirchwild.
Wu, M., Chen, G., & Li, Y. P. (2016). TGF-β and BMP signaling in osteoblast, skeletal development, and bone formation, homeostasis and disease. *Bone research*, *4*(1), 1-21.
Xiong, J., Piemontese, M., Onal, M., Campbell, J., Goellner, J. J., Dusevich, V., ... & O'Brien, C. A. (2015). Osteocytes, not osteoblasts or lining cells, are the main source of the RANKL

required for osteoclast formation in remodeling bone. *PloS one*, *10*(9), e0138189.
Yang, J., Andre, P., Ye, L., & Yang, Y. Z. (2015). The Hedgehog signalling pathway in bone formation. *International journal of oral science*, *7*(2), 73-79.
Yavropoulou, M. P., & Yovos, J. G. (2016). The molecular basis of bone mechanotransduction. *Journal of musculoskeletal & neuronal interactions*, *16*(3), 221.
Yerkes, R. M., & Elder, J. H. (1937). Concerning reproduction in the chimpanzee. *The Yale Journal of Biology and Medicine*, *10*(1), 41.
You, L. D., Weinbaum, S., Cowin, S. C., & Schaffler, M. B. (2004). Ultrastructure of the osteocyte process and its pericellular matrix. *The Anatomical Record Part A: Discoveries in Molecular, Cellular, and Evolutionary Biology: An Official Publication of the American Association of Anatomists*, *278*(2), 505-513.
Zachmann, M., Prader, A., Sobel, E. H., Crigler Jr, J. F., Ritzén, E. M., Atarés, M., & Ferrandez, A. (1986). Pubertal growth in patients with androgen insensitivity: indirect evidence for the importance of estrogens in pubertal growth of girls. *The Journal of pediatrics*, *108*(5), 694-697.
Zelazo, P. R., Zelazo, N. A., & Kolb, S. (1972). " Walking" in the Newborn. *Science*, *176*(4032), 314-315.
Zelditch, M. L. (2005). Developmental regulation of variability. In V*ariation* (pp. 249-276). Academic Press.
Zhan, T., Rindtorff, N., & Boutros, M. (2017). Wnt signaling in cancer. *Oncogene*, *36*(11), 1461-1473.
Zhang, Y., & Wang, X. (2020). Targeting the Wnt/β-catenin signaling pathway in cancer. *Journal of hematology & oncology*, *13*(1), 1-16.
Zhang, N., Lo, C. W., Utsunomiya, T., Maruyama, M., Huang, E., Rhee, C., ... & Goodman, S. B. (2021). PDGF-BB and IL-4 co-overexpression is a potential strategy to enhance mesenchymal stem cell-based bone regeneration. *Stem Cell Research & Therapy*, *12*(1), 1-11.
Zollikofer, C. P., & de León, M. S. P. (2010, June). The evolution of hominin ontogenies. In *Seminars in cell & developmental biology* (Vol. 21, No. 4, pp. 441-452). Academic Press.

Appendix 1. List of individuals included in this study

ID #	Age (months)	Sex
135456	0	Female
101875	1	Female
105462	1	Female
113077	1	Female
138917	1	Female
103540	2	Female
108524	2	Female
111347	3	Female
101011	4	Female
102564	5	Female
114468	6	Female
119597	6	Female
137166	6	Female
160711	6	Female
161486	7	Female
100861	9	Female
137620	10	Female
131842	11	Female
112200	13	Female
165073	14	Female
168770	14	Female
198895	15	Female
110385	18	Female
137511	20	Female
143463	20	Female
152863	23	Female
192861	24	Female
108023	32	Female
140856	46	Female
119553	50	Female
119851	50	Female
149066	53	Female
116077	57	Female
114998	61	Female
187924	93	Female
142005	101	Female
121316	137	Female
112356	140	Female
105007	158	Female
113544	Stillborn	Female
102101	0	Male

113974	0	Male
137807	0	Male
139054	0	Male
159714	0	Male
159749	0	Male
160095	0	Male
160802	0	Male
104862	1	Male
137170	1	Male
160416	1	Male
113360	2	Male
134873	2	Male
105785	3	Male
107495	3	Male
111866	3	Male
112442	3	Male
105699	6	Male
109194	7	Male
195524	7	Male
125004	8	Male
101226	10	Male
109364	10	Male
165056	12	Male
131353	14	Male
106672	15	Male
118016	17	Male
140258	17	Male
110360	18	Male
113028	19	Male
113518	20	Male
136759	22	Male
147587	23	Male
155970	25	Male
137990	26	Male
137990	26	Male
191553	33	Male
164044	34	Male
109893	40	Male
134483	40	Male
148956	43	Male
106974	48	Male
112307	51	Male
175526	63	Male
104676	72	Male

193766	84	Male
193766	84	Male
165123	101	Male
140440	104	Male
179579	106	Male
107776	113	Male
129915	122	Male
103435	129	Male
150492	131	Male
183811	133	Male
136645	136	Male
135142	142	Male
111920	145	Male
133875	149	Male
106485	174	Male